ME280B

Finite Element Methods for Non-linear Continua

Panos Papadopoulos

Department of Mechanical Engineering
University of California, Berkeley

2019 edition

Introduction

This is a set of notes written as part of teaching ME280B, a graduate course on non-linear finite elements in the Department of Mechanical Engineering at the University of California, Berkeley.

Berkeley, California
January 2019

P. P.

Contents

List of Figures

Chapter 1

Review of Continuum Mechanics

1.1 Kinematics of Deformation

Define a body $\mathscr{B}$ as a collection of material points and identify a typical material point with P, as in Figure 1.1.

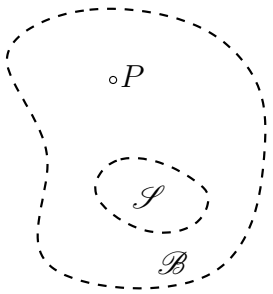

Figure 1.1. *A body $\mathscr{B}$ and its subset $\mathscr{S}$.*

At some time t, define the configuration of $\mathscr{B}$ as the region in the three-dimensional Euclidean point space $\mathcal{E}^3$ occupied by $\mathscr{B}$, and denote this configuration $\mathcal{R}$ and its boundary $\partial\mathcal{R}$. The material point P in the configuration of $\mathscr{B}$ at time t is identified with a vector $\mathbf{x}$ in three-dimensional Euclidean vector space E^3 drawn from any fixed origin o, see Figure 1.2. Let $\mathbf{x}$ be resolved with respect to a fixed orthonormal basis $\{\mathbf{e}_i\}$ as

$$\mathbf{x} \;=\; x_i\mathbf{e}_i \quad ; \quad x_i \;=\; \mathbf{x}\cdot\mathbf{e}_i \;, \tag{1.1}$$

where "$\cdot$" denotes dot-product between two vectors and the Einsteinian summation convention in enforced on repeated indices. The configuration of $\mathscr{B}$ at time t will be referred to as the *current* or *present* configuration.

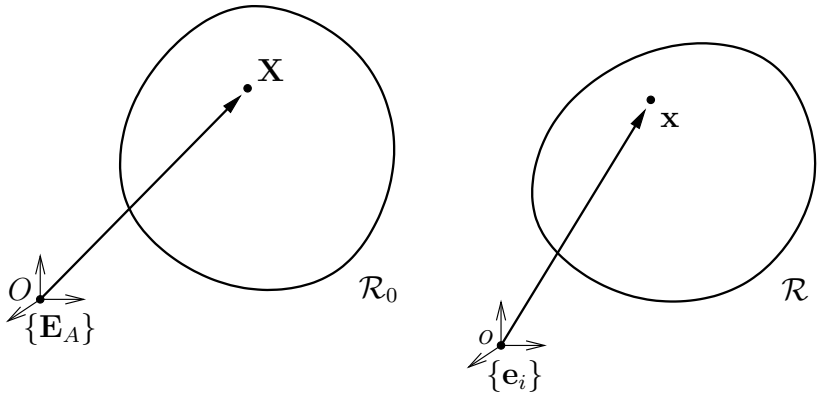

Figure 1.2. *Reference and current configurations of a body $\mathscr{B}$ at times t_0 and t, respectively.*

Let the same body $\mathscr{B}$ occupy at some other time $t = t_0$ (often set, without loss of generality, to $t_0 = 0$) the region $\mathcal{R}_0$ in $\mathcal{E}^3$ with boundary $\partial\mathcal{R}_0$. The material point P at time t_0 is identified with another vector $\mathbf{X}$ in E^3 drawn, in general, from another fixed origin O, see Figure 1.2. Let $\mathbf{X}$ be now resolved with respect to a fixed orthonormal basis $\{\mathbf{E}_A\}$ as

$$\mathbf{X} \;=\; X_A \mathbf{E}_A \quad ; \quad X_A \;=\; \mathbf{X}\cdot\mathbf{E}_A \;. \tag{1.2}$$

The configuration of $\mathscr{B}$ at time t_0 will be referred to as the *reference* configuration.

The motion $\boldsymbol{\chi} : \mathcal{E}^3 \times \mathbb{R} \to \mathcal{E}^3$ is a mapping of points $\mathbf{X}$ in the reference configuration to points in the current configuration $\mathbf{x}$ at given time t, that is,

$$\mathbf{x} \;=\; \boldsymbol{\chi}\,(\mathbf{X}, t) \quad ; \quad x_i \;=\; \chi_i\,(X_A, t) \;. \tag{1.3}$$

The *velocity* and *acceleration* fields are respectively defined at time t as

$$\mathbf{v} \;=\; \dot{\boldsymbol{\chi}}\,(\mathbf{X}, t) \;=\; \frac{\partial \boldsymbol{\chi}\,(\mathbf{X}, t)}{\partial t} \quad ; \quad v_i \;=\; \dot{\chi}_i \;=\; \frac{\partial \chi_i\,(X_A, t)}{\partial t} \tag{1.4}$$

and

$$\mathbf{a} \;=\; \ddot{\boldsymbol{\chi}}\,(\mathbf{X}, t) \;=\; \frac{\partial^2 \boldsymbol{\chi}\,(\mathbf{X}, t)}{\partial t^2} \quad ; \quad a_i \;=\; \ddot{\chi}_i \;=\; \frac{\partial^2 \chi_i\,(X_A, t)}{\partial t^2} \;. \tag{1.5}$$

where $\dot{(\,)}$ denotes the material time derivative, that is, the time derivative of a quantity for a fixed material point.

The fundamental measure of relative deformation is the deformation gradient tensor $\mathbf{F}$ which may be viewed as a linear mapping of an infinitesimal material line element $d\mathbf{X}$ of the reference configuration to an infinitesimal line element $d\mathbf{x}$ in the current configuration, that is,

$$d\mathbf{x} \;=\; \mathbf{F}\, d\mathbf{X} \quad ; \quad dx_i \;=\; F_{iA}\, dX_A \;, \tag{1.6}$$

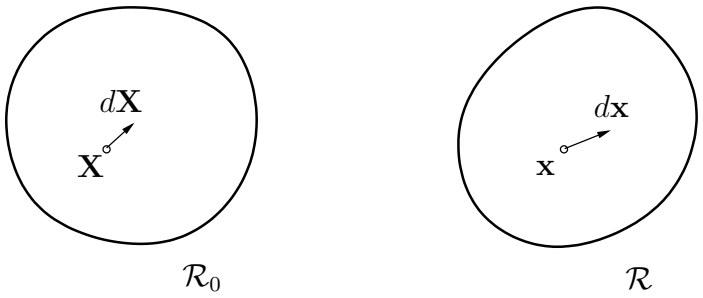

Figure 1.3. *Mapping of an infinitesimal material line element $d\mathbf{X}$ from the reference to the current configuration.*

see Figure 1.3. Assuming that there is a *motion* $\boldsymbol{\chi}$, where

$$\boldsymbol{\chi} \ : \ (\mathbf{X}, t) \to \mathbf{x} = \boldsymbol{\chi}(\mathbf{X}, t) \ , \tag{1.7}$$

one readily concludes from (1.6) that

$$\mathbf{F} \ = \ \frac{\partial \boldsymbol{\chi}}{\partial \mathbf{X}} \ . \tag{1.8}$$

The deformation gradient is a *two-point tensor*, in the sense that

$$\mathbf{F} \ = \ F_{iA} \mathbf{e}_i \otimes \mathbf{E}_A \ , \tag{1.9}$$

where "$\otimes$" denotes tensor product of two vectors. As seen from (1.8), the deformation gradient $\mathbf{F}$ has one "leg" (the first) in the current configuration and the other "leg" in the reference configuration.

An infinitesimal material volume element dV in the reference configuration is likewise mapped to an infinitesimal volume element dv in the current configuration, such that

$$dv \ = \ J dV \ , \tag{1.10}$$

where $J = \det \mathbf{F}$ is the *Jacobian* of the motion. Appealing to the *inverse function theorem* of calculus, it can be established that a continuously differentiable (in $\mathbf{X}$) motion $\boldsymbol{\chi}$ is invertible at a given time t if, and only if,

$$\det \mathbf{F} \ = \ \det \frac{\partial \boldsymbol{\chi}}{\partial \mathbf{X}} \ \neq \ 0 \ , \tag{1.11}$$

for all $\mathbf{X} \in \mathcal{R}_0$. Upon assuming, on physical grounds, that the sign of a given material volume should be always preserved, it can be concluded from (1.10) that invertibility of $\boldsymbol{\chi}$ necessitates that $J > 0$.

An infinitesimal material area element dA in the reference configuration is mapped to an infinitesimal area element da in the current configuration according to *Nanson's formula*, which states that

$$\mathbf{n}\, da \;=\; J\mathbf{F}^{-T}\mathbf{N}\, dA\;, \tag{1.12}$$

where $\mathbf{N}$ (resp. $\mathbf{n}$) is a unit vector normal to the surface dA (resp. da), see Figure 1.4.

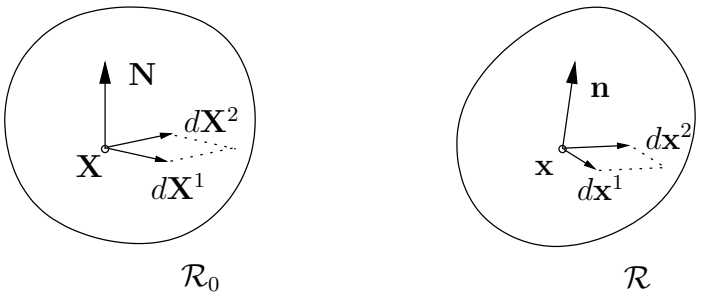

Figure 1.4. *Mapping of an infinitesimal material surface element dA to its image da in the current configuration.*

Other useful measures of deformation are the *right* and *left Cauchy-Green deformation tensors* $\mathbf{C}$ and $\mathbf{B}$ defined, respectively, as

$$\mathbf{C} \;=\; \mathbf{F}^T\mathbf{F} \quad ; \quad C_{AB} \;=\; F_{iA}F_{iB} \tag{1.13}$$

and

$$\mathbf{B} \;=\; \mathbf{F}\mathbf{F}^T \quad ; \quad B_{ij} \;=\; F_{iA}F_{jA}\;. \tag{1.14}$$

It is clear from the preceding component representations that $\mathbf{C}$ is a *referential tensor*, while $\mathbf{B}$ is a *spatial* tensor. Both tensors are *symmetric*, which means that their components form can be represented in the form of symmetric matrices.

Let $\mathbf{M}$ and $\mathbf{m}$ be unit vectors in the direction of $d\mathbf{X}$ and $d\mathbf{x}$, respectively, such that

$$d\mathbf{X} \;=\; \mathbf{M}dS \quad , \quad d\mathbf{x} \;=\; \mathbf{m}ds\;, \tag{1.15}$$

and define the ratio

$$\lambda \;=\; \frac{ds}{dS} \tag{1.16}$$

as the *stretch* of the material line element $d\mathbf{X}$. It can be easily established with the aid of (1.8), (1.15), and (1.16) that

$$\lambda\mathbf{m} \;=\; \mathbf{F}\mathbf{M} \tag{1.17}$$

and, upon also using (1.13), that

$$\lambda^2 \;=\; \mathbf{M}\cdot\mathbf{C}\mathbf{M} \quad ; \quad \lambda^2 \;=\; M_A C_{AB} M_B \;. \tag{1.18}$$

Likewise, (1.17) can be alternatively expressed as

$$\frac{1}{\lambda}\mathbf{M} \;=\; \mathbf{F}^{-1}\mathbf{m}\;, \tag{1.19}$$

hence, with the aid of (1.14), it follows that

$$\frac{1}{\lambda^2} \;=\; \mathbf{m}\cdot\mathbf{B}^{-1}\mathbf{m} \quad ; \quad \frac{1}{\lambda^2} \;=\; m_i B^{-1}_{ij} m_j \;. \tag{1.20}$$

Two important measures of strain can be obtained by resolving the difference $ds^2 - dS^2$ as

$$\begin{aligned} ds^2 - dS^2 \;&=\; d\mathbf{x}\cdot d\mathbf{x} - d\mathbf{X}\cdot d\mathbf{X} \\ &=\; (\mathbf{F}d\mathbf{X})\cdot(\mathbf{F}d\mathbf{X}) - d\mathbf{X}\cdot d\mathbf{X} \\ &=\; d\mathbf{X}\cdot(\mathbf{C}d\mathbf{X}) - d\mathbf{X}\cdot d\mathbf{X} \;=\; d\mathbf{X}\cdot(\mathbf{C}-\mathbf{I})\,d\mathbf{X} \\ &=\; d\mathbf{X}\cdot 2\mathbf{E}d\mathbf{X} \end{aligned} \tag{1.21}$$

or, alternatively,

$$\begin{aligned} ds^2 - dS^2 \;&=\; d\mathbf{x}\cdot d\mathbf{x} - d\mathbf{X}\cdot d\mathbf{X} \\ &=\; d\mathbf{x}\cdot d\mathbf{x} - \left(\mathbf{F}^{-1}d\mathbf{x}\right)\cdot\left(\mathbf{F}^{-1}d\mathbf{x}\right) \\ &=\; d\mathbf{x}\cdot d\mathbf{x} - d\mathbf{x}\cdot\mathbf{B}^{-1}d\mathbf{x} \;=\; d\mathbf{x}\cdot\left(\mathbf{i}-\mathbf{B}^{-1}\right)d\mathbf{x} \\ &=\; d\mathbf{x}\cdot 2\mathbf{e}d\mathbf{x}\;, \end{aligned} \tag{1.22}$$

where $\mathbf{I}$ and $\mathbf{i}$ are the *referential* and *spatial identity tensors*, respectively. These measures are the (relative) *Lagrangian strain tensor* $\mathbf{E}$, given with the aid of (1.21) by

$$\mathbf{E} \;=\; \frac{1}{2}\left(\mathbf{C}-\mathbf{I}\right) \quad ; \quad E_{AB} \;=\; \frac{1}{2}\left(C_{AB}-\delta_{AB}\right) \;. \tag{1.23}$$

and the (relative) *Eulerian* (or *Almansi*) *strain tensor* $\mathbf{e}$, defined from (1.22) as

$$\mathbf{e} \;=\; \frac{1}{2}\left(\mathbf{i}-\mathbf{B}^{-1}\right) \quad ; \quad e_{ij} \;=\; \frac{1}{2}\left(\delta_{ij}-B^{-1}_{ij}\right) \;. \tag{1.24}$$

The *polar decomposition theorem* states that $\mathbf{F}$, being non-singular by virtue of $J = \det\mathbf{F} > 0$, can be uniquely resolved into

$$\mathbf{F} \;=\; \mathbf{R}\mathbf{U} \;=\; \mathbf{V}\mathbf{R} \quad ; \quad F_{iA} = R_{iB}U_{BA} = V_{ij}R_{jA} \;. \tag{1.25}$$

Clearly, $\mathbf{R}$ is a two-point tensor, $\mathbf{U}$ is a referential tensor, and $\mathbf{V}$ is a spatial tensor. More specifically, $\mathbf{R}$ is a *proper-orthogonal* (or indexrotation—seealsotensor!proper orthogonal*rotation*) *tensor*, that is, one which satisfies $\mathbf{R}^T\mathbf{R} = \mathbf{I}$, $\mathbf{R}\mathbf{R}^T = \mathbf{i}$, and $\det \mathbf{R} = +1$. In addition, $\mathbf{U}$ and $\mathbf{V}$ are symmetric positive-definite tensors referred to as the *right* and *left stretch tensors*, respectively. In light of these definitions, equations $(1.25)_{1,2}$ are correspondingly referred to as the *right* and *left polar decompositions* of $\mathbf{F}$.

Starting from (1.17) it can be seen that

$$d\mathbf{x} \;=\; \mathbf{R}\,(\mathbf{U}d\mathbf{X}) \;, \tag{1.26}$$

which implies that $d\mathbf{X}$ is first stretched and rotated by $\mathbf{U}$, and is subsequently further rotated by $\mathbf{R}$, see Figure 1.5. A corresponding interpretation may be readily formulated for the left

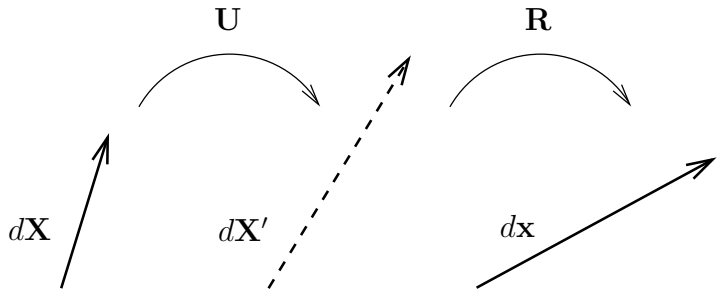

Figure 1.5. *Interpretation of the right polar decomposition.*

polar decomposition.

Along its *principal directions*, $\mathbf{U}$ effects stretch without any rotation, which implies that, if $d\mathbf{X}$ lies along such a principal direction, then

$$\mathbf{U}d\mathbf{X} \;=\; \lambda d\mathbf{X} \tag{1.27}$$

or, upon recalling $(1.15)_1$,

$$\mathbf{U}\mathbf{M} \;=\; \lambda\mathbf{M} \;. \tag{1.28}$$

With reference to the principal stretches $\lambda_I,\ I = 1,2,3$ and the associated principal directions $\mathbf{M}_I,\ I = 1,2,3$[1] of the preceding linear eigenvalue problem, one may use the *spectral representation theorem* to write

$$\mathbf{U} \;=\; \sum_{I=1}^{3} \lambda_I \mathbf{M}_I \otimes \mathbf{M}_I \;, \tag{1.29}$$

[1]The set of eigenvectors $\{\mathbf{M}_I\}$ may be taken to be orthonormal without loss of generality.

from which it follows that

$$\mathbf{F} \;=\; \mathbf{RU} \;=\; \sum_{I=1}^{3} \lambda_I \, (\mathbf{R}\mathbf{M}_I) \otimes \mathbf{M}_I \tag{1.30}$$

and also, given the definition of $\mathbf{C}$ and the orthogonality of $\mathbf{R}$, that

$$\mathbf{C} \;=\; \mathbf{F}^T\mathbf{F} \;=\; (\mathbf{RU})^T \, (\mathbf{RU}) \;=\; \mathbf{U}^2 \;=\; \sum_{I=1}^{3} \lambda_I^2 \mathbf{M}_I \otimes \mathbf{M}_I \; . \tag{1.31}$$

Generalized referential measures of deformation can be introduced in the form

$$\mathbf{C}^m \;=\; \sum_{I=1}^{3} \lambda_I^{2m} \mathbf{M}_I \otimes \mathbf{M}_I \qquad m \neq 0 \tag{1.32}$$

$$\log \mathbf{C} \;=\; \sum_{I=1}^{3} \log \lambda_I^2 \mathbf{M}_I \otimes \mathbf{M}_I \qquad (\textit{Hencky strain}) \tag{1.33}$$

with associated measures of generalized referential strain

$$\mathbf{E}^{(m)} = \begin{cases} \frac{1}{m} \left(\mathbf{C}^{m/2} - \mathbf{I} \right) & \text{if } m \neq 0 \\ \frac{1}{2} \ln \mathbf{C} & \text{if } m = 0 \end{cases} \; . \tag{1.34}$$

Note that $m = 2$ in (1.34) recovers the Lagrangian strain tensor.

It is readily concluded from (1.25) and (1.29) that

$$\mathbf{V} \;=\; \sum_{I=1}^{3} \lambda_I \, (\mathbf{R}\mathbf{M}_I) \otimes (\mathbf{R}\mathbf{M}_I) \tag{1.35}$$

and also, given the definition of $\mathbf{B}$ and the orthogonality of $\mathbf{R}$, that

$$\mathbf{B} \;=\; \mathbf{F}\mathbf{F}^T \;=\; (\mathbf{VR}) \, (\mathbf{VR})^T \;=\; \mathbf{V}^2 \;=\; \sum_{I=1}^{3} \lambda_I^2 \, (\mathbf{R}\mathbf{M}_I) \otimes (\mathbf{R}\mathbf{M}_I) \; . \tag{1.36}$$

There exist several ways to extract the polar factors of $\mathbf{F}$. In particular, focusing attention to the right polar decomposition, one may:

(a) Extract the stretch $\mathbf{U}$ directly from $\mathbf{F}$ in closed form[2], and subsequently obtain $\mathbf{R}$ as

$$\mathbf{R} \;=\; \mathbf{F}\mathbf{U}^{-1} \; . \tag{1.37}$$

[2] A. Hoger and D.E. Carlson, "Determination of the stretch and rotation in the polar decomposition of the deformation gradient", *Q. Appl. Math.*, 42:113–117, (1984).

(b) Extract the rotation $\mathbf{R}$ directly from $\mathbf{F}$ in closed form[3], and subsequently obtain $\mathbf{U}$ as

$$\mathbf{U} \;=\; \mathbf{R}^T\mathbf{F}\;. \tag{1.38}$$

(c) Use a numerical method to solve the matrix equation

$$[C_{AB}] \;=\; [F_{iA}F_{iB}] \;=\; [U_{AC}U_{CB}] \tag{1.39}$$

for the components $[U_{AB}]$ of $\mathbf{U}$ to within the required tolerance, then evaluate $\mathbf{R}$ as in (a). A computationally efficient algorithm for solving this matrix equation employs the Newton-Raphson method, according to which

$$\mathbf{U}^{(i+1)} \;=\; \frac{1}{2}\left(\mathbf{U}^{(i)} + \mathbf{C}\mathbf{U}^{(i)-1}\right)\;, \tag{1.40}$$

with initial guess

$$\mathbf{U}^{(0)} \;=\; \mathbf{I} \qquad (\text{or } m\mathbf{I},\; m>0)\;. \tag{1.41}$$

It can be shown that with this choice of $\mathbf{U}^{(0)}$, all $\mathbf{U}^{(i)}$ are positive-definite and also $\mathbf{U}^{(i)}$ converges to $\mathbf{U}$ at a quadratic rate[4]

(d) Solve the linear eigenvalue problem (1.31) for the eigenpairs $\{(\lambda_I^2, \mathbf{M}_I)\}$, form $\mathbf{U}$ using (1.29), and then calculate $\mathbf{R}$ as $\mathbf{R} = \mathbf{F}\mathbf{U}^{-1}$.

Lastly, attention is focused on mixed space-time derivatives of the motion, which give rise to measures of deformation rate. Invoking the chain rule, write

$$\dot{\mathbf{F}} \;=\; \frac{d}{dt}\frac{\partial \boldsymbol{\chi}}{\mathbf{X}} \;=\; \frac{\partial}{\partial \mathbf{X}}\frac{d\boldsymbol{\chi}}{dt} \;=\; \frac{\partial \mathbf{v}}{\partial \mathbf{X}} \;=\; \frac{\partial \mathbf{v}}{\partial \mathbf{x}}\frac{\partial \mathbf{x}}{\partial \mathbf{X}} \;=\; \mathbf{L}\mathbf{F}\;. \tag{1.42}$$

In (1.42), $\mathbf{L}$ is the *spatial velocity gradient*, defined as

$$\mathbf{L} \;=\; \frac{\partial \mathbf{v}}{\partial \mathbf{x}} \quad ; \quad L_{ij} \;=\; \frac{\partial v_i}{\partial x_j} \tag{1.43}$$

The tensor $\mathbf{L}$ may be uniquely decomposed into a symmetric tensor $\mathbf{D}$, termed the *rate-of-deformation tensor*, and a skew-symmetric tensor $\mathbf{W}$, termed the *vorticity* or indexspin tensor—seealsovorticity tensor*spin tensor*, such that

$$\mathbf{L} \;=\; \mathbf{D} + \mathbf{W}\;. \tag{1.44}$$

[3] P. Papadopoulos and J. Lu, "On the direct determination of the rotation tensor from the deformation gradient", *Math. Mech. Solids.*, 2:17–26, (1997).

[4] N.J. Higham, "Newton's method for the matrix square root", *Math. Comp.*, 46:537–549, (1986).

The physical meaning of $\mathbf{D}$ can be established by observing that (1.17), (1.42), and (1.44) imply that

$$\overline{\dot{\ln \lambda}} \;=\; \frac{\dot{\lambda}}{\lambda} \;=\; \mathbf{m}\cdot\mathbf{D}\mathbf{m}\;. \tag{1.45}$$

Regarding $\mathbf{W}$, first note that owing to its skew-symmetry, it can be put into a one-to-one correspondence with a vector $\mathbf{w}$ of E^3, such that for any vector $\mathbf{z}$ in E^3,

$$\mathbf{W}\mathbf{z} \;=\; \mathbf{w}\times\mathbf{z}\;. \tag{1.46}$$

The vector $\mathbf{w}$ is called the *axial vector* of $\mathbf{W}$. Then, considering a unit vector $\overline{\mathbf{m}}$ along a principal direction of $\mathbf{D}$, it can be established with the aid of (1.17), (1.42), (1.44), and (1.45) that

$$\dot{\overline{\mathbf{m}}} \;=\mathbf{W}\overline{\mathbf{m}} \;=\; \mathbf{w}\times\overline{\mathbf{m}}\;. \tag{1.47}$$

This shows that the axial vector of $\mathbf{W}$ can be thought of as the angular velocity of a line element positioned along a principal direction of $\mathbf{D}$.

Using (1.42), as well as the earlier definitions of the deformation and strain tensors, it can be readily concluded that

$$\dot{\mathbf{C}} \;=\overline{\dot{\mathbf{F}^T\mathbf{F}}} \;=\; 2\mathbf{F}^T\mathbf{D}\mathbf{F} \quad;\quad \dot{C}_{AB} \;=\; 2F_{iA}D_{ij}F_{jB}\;, \tag{1.48}$$

$$\dot{\mathbf{E}} \;=\; \mathbf{F}^T\mathbf{D}\mathbf{F} \quad;\quad \dot{E}_{AB} \;=\; F_{iA}D_{ij}F_{jB}\;, \tag{1.49}$$

and also

$$\dot{\mathbf{B}} \;=\overline{\dot{\mathbf{F}\mathbf{F}^T}} \;=\; \mathbf{L}\mathbf{B}+\mathbf{B}\mathbf{L}^T \quad;\quad \dot{B}_{ij} \;=\; L_{ik}B_{kj}+B_{ik}L_{jk}\;, \tag{1.50}$$

$$\dot{\mathbf{e}} \;=\; \frac{1}{2}\left(\mathbf{B}^{-1}\mathbf{L}+\mathbf{L}^T\mathbf{B}^{-1}\right) \quad;\quad \dot{e}_{ij} \;=\; \frac{1}{2}\left(B^{-1}_{ik}L_{kj}+L_{ki}B^{-1}_{kj}\right)\;. \tag{1.51}$$

It is also easy to show that

$$\frac{dJ}{dt} \;=\; J\,\mathrm{div}\,\mathbf{v} \;=\; J\,\mathrm{tr}\,\mathbf{L}\;. \tag{1.52}$$

1.2 Balance Laws

The underlying physical principal of continuum mechanics are the conservation of mass, the balance of linear and angular momentum, and the balance of energy. There are briefly reviewed in this section.

Preliminary to the introduction of the balance laws, three important results from calculus and real analysis are stated without proof. The first is the *divergence theorem*, according to which, given a continuously differentiable real-valued function $\phi = \tilde{\phi}(\mathbf{x}, t) : \mathcal{P} \times \mathbb{R} \to \mathbb{R}$ defined at time t on some subset $\mathcal{P}$ of $\mathcal{E}^3$ with boundary $\partial\mathcal{P}$, then

$$\int_{\mathcal{P}} \operatorname{grad} \phi \, dv \;=\; \int_{\partial\mathcal{P}} \phi \mathbf{n} \, da \;, \tag{1.53}$$

where $\operatorname{grad} \phi$ is the *gradient* of the function ϕ, defined as

$$\operatorname{grad} \phi \;=\; \frac{\partial \tilde{\phi}}{\partial x_i} \mathbf{e}_i \;. \tag{1.54}$$

Versions of this theorem may be easily deduced from the above for vector and tensor functions. The second result is known as the *Reynolds' transport theorem*, and states that if ϕ is differentiable in both of its variables, then

$$\frac{d}{dt} \int_{\mathcal{P}} \phi \, dv \;=\; \int_{\mathcal{P}} (\dot{\phi} + \phi \operatorname{div} \mathbf{v}) \, dv \;, \tag{1.55}$$

where

$$\dot{\phi} \;=\; \frac{\partial \tilde{\phi}}{\partial t} + \frac{\partial \tilde{\phi}}{\partial \mathbf{x}} \cdot \mathbf{v} \;. \tag{1.56}$$

Using 1.56 and the divergence theorem, it is easy to show that (1.55) may be recast as

$$\frac{d}{dt} \int_{\mathcal{P}} \phi \, dv \;=\; \int_{\mathcal{P}} \left[\frac{\partial \tilde{\phi}}{\partial t} + \operatorname{div}(\phi \mathbf{v}) \right] dv \;=\; \int_{\mathcal{P}} \frac{\partial \tilde{\phi}}{\partial t} \, dv + \int_{\partial\mathcal{P}} \phi \mathbf{v} \cdot \mathbf{n} \, da \;. \tag{1.57}$$

Lastly, the *localization theorem* states that if ϕ is continuous in $\mathbf{x}$ and

$$\int_{\mathcal{P}} \phi \, dv \;=\; 0 \;, \tag{1.58}$$

for all subsets $\mathcal{P}$ of $\mathcal{R}$ at a given time t, then $\phi = 0$ everywhere in $\mathcal{R}$ at time t.

Extensive use of these three important results will be made henceforth.

1.2.1 Conservation of Mass

Start by axiomatically admitting the existence of a measure of *mass* $m(\mathscr{S})$ for every subset $\mathscr{S}$ of the body $\mathscr{B}$. Upon assuming certain regularity conditions for this measure, it can be established that there exists a *mass density* $\rho(\mathbf{x}, t)$ such that

$$\int_{\mathscr{S}} dm \;=\; \int_{\mathcal{P}} \rho \, dv \tag{1.59}$$

for the region $\mathcal{P} \subset \mathcal{R}$ that occupies the part $\mathscr{S}$ at time t.

Likewise, there exists a mass density function $\rho_0(\mathbf{X})$ at time t_0, such that

$$\int_{\mathscr{S}} dm \;=\; \int_{\mathcal{P}_0} \rho_0 \, dV \tag{1.60}$$

for the region $\mathcal{P}_0 \subset \mathcal{R}_0$ that occupies the part $\mathscr{S}$ at time t_0. The preceding two statements reflect the conservation of mass between the configurations occupied by the body at times t and t_0. Equating the right-hand sides of these statements and recalling (1.10) leads to the integral statement

$$\int_{\mathcal{P}_0} \rho_0 \, dV \;=\; \int_{\mathcal{P}} \rho \, dv \;=\; \int_{\mathcal{P}_0} \rho J \, dV \tag{1.61}$$

or

$$\int_{\mathcal{P}_0} (\rho_0 - \rho J) \, dV \;=\; 0 \; . \tag{1.62}$$

Invoking the localization theorem, this implies that

$$\rho_0 \;=\; \rho J \; . \tag{1.63}$$

This is a local statement of mass conservation between the two configurations.

Alternatively, conservation of mass may be stated in integral form as

$$\frac{d}{dt} \int_{\mathcal{P}} \rho \, dv \;=\; 0 \; . \tag{1.64}$$

Applying Reynolds' transport theorem in the form of (1.55) implies that

$$\int_{\mathcal{P}} (\dot{\rho} + \rho \, \mathrm{div}\, \mathbf{v}) \, dv \;=\; 0 \; . \tag{1.65}$$

Appealing to the localization theorem, this leads to a local statement of mass conservation in the form

$$\dot{\rho} + \rho \, \mathrm{div}\, \mathbf{v} \;=\; 0 \; . \tag{1.66}$$

1.2.2 Balance of Linear Momentum

The linear momentum of the material which occupies the region $\mathcal{P}$ at time t is $\int_{\mathcal{P}} \rho \mathbf{v} \, dv$.

Admit the existence of two types of external forces, both of which quantify the interaction of $\mathcal{P}$ with its surrounding environment. Specifically, consider: (a) body forces per unit mass $\mathbf{b} = \mathbf{b}(\mathbf{X}, t)$ acting on the material particles the region $\mathscr{S}$ which occupies $\mathcal{P}$ at time t and (b) contact forces per unit area $\mathbf{t} = \mathbf{t}(\mathbf{x}, t; \mathbf{n})$ acting on the boundary surface $\partial\mathcal{P}$ and depending

on the orientation $\mathbf{n}$ of the surface. The integral statement of linear momentum balance for the continuum occupying $\mathcal{P}$ at time t takes the form

$$\frac{d}{dt}\int_{\mathcal{P}} \rho\mathbf{v}\,dv \;=\; \int_{\mathcal{P}} \rho\mathbf{b}\,dv + \int_{\partial\mathcal{P}} \mathbf{t}\,da\;. \tag{1.67}$$

Using linear momentum balance in the preceding primitive form it can be shown that

$$\mathbf{t}(\mathbf{x},t;\mathbf{n}) \;=\; -\mathbf{t}(\mathbf{x},t;-\mathbf{n})\;. \tag{1.68}$$

This result is known as *Cauchy's lemma*, and asserts that contact forces acting at a point $\mathbf{x}$ on opposite sides of the same surface are equal and opposite.

Applying balance of linear momentum to a right-angled tetrahedral region (the *Cauchy tetrahedron*) in conjunction with Cauchy's lemma, it can be shown that there exists a tensor $\mathbf{T}$, appropriately termed the *Cauchy stress tensor*, such that

$$\mathbf{t} \;=\; \mathbf{T}\mathbf{n} \quad ; \quad t_i \;=\; T_{ij}n_j\;. \tag{1.69}$$

Upon using mass conservation, (1.68), and the divergence theorem, it can be concluded from the linear momentum balance statement (1.67) that

$$\begin{aligned}\frac{d}{dt}\int_{\mathcal{P}} \rho\mathbf{v}\,dv \;&=\; \int_{\mathcal{P}} \rho\mathbf{a}\,dv\\ &=\; \int_{\mathcal{P}} \rho\mathbf{b}\,dv + \int_{\mathcal{P}} \mathbf{T}\mathbf{n}\,da\\ &=\; \int_{\mathcal{P}} \rho\mathbf{b}\,dv + \int_{\mathcal{P}} \operatorname{div}\mathbf{T}\,dv\;.\end{aligned} \tag{1.70}$$

Upon invoking the localization theorem, this results in

$$\operatorname{div}\mathbf{T} + \rho\mathbf{b} \;=\; \rho\mathbf{a} \quad ; \quad T_{ij,j} + \rho b_i \;=\; \rho a_i\;. \tag{1.71}$$

The preceding statement of linear momentum balance can be also resolved on the geometry of the reference configuration, where, upon again using mass conservation, Cauchy's lemma

and the divergence theorem, in conjunction with Nanson's formula (1.12), one finds that

$$\begin{aligned}\frac{d}{dt}\int_{\mathcal{P}}\rho\mathbf{v}\,dv &= \frac{d}{dt}\int_{\mathcal{P}_0}\rho_0\mathbf{v}\,dV\\ &= \int_{\mathcal{P}}\rho\mathbf{b}\,dv+\int_{\partial\mathcal{P}}\mathbf{T}\mathbf{n}\,da\\ &= \int_{\mathcal{P}_0}\rho_0\mathbf{b}\,dV+\int_{\partial\mathcal{P}_0}\mathbf{T}J\mathbf{F}^{-T}\mathbf{N}\,dA\\ &= \int_{\mathcal{P}_0}\rho_0\mathbf{b}\,dV+\int_{\partial\mathcal{P}_0}\mathbf{P}\mathbf{N}\,dA\\ &= \int_{\mathcal{P}_0}\rho_0\mathbf{b}\,dV+\int_{\partial\mathcal{P}_0}\mathrm{Div}\,\mathbf{P}\,dV\ ,\end{aligned}\tag{1.72}$$

where $\mathbf{P}$, defined as

$$\mathbf{P} \;=\; J\mathbf{T}\mathbf{F}^{-T} \quad ; \quad P_{iA} \;=\; JT_{ij}F^{-1}_{Aj}\ ,\tag{1.73}$$

is the *first Piola-Kirchhoff stress tensor*. Upon again invoking the localization theorem, it follows that the local statement of linear momentum balance may be expressed in referential form as

$$\mathrm{Div}\,\mathbf{P}+\rho_0\mathbf{b} \;=\; \rho_0\mathbf{a} \quad ; \quad P_{iA,A}+\rho_0 b_i \;=\; \rho_0 a_i\ .\tag{1.74}$$

Recalling (1.76), one may define the traction $\mathbf{p}$ resolved on the geometry of the reference configuration as

$$\mathbf{p} \;=\; \mathbf{P}\mathbf{N} \quad ; \quad p_i \;=\; P_{iA}N_A\ .\tag{1.75}$$

where the (differential) force $d\mathbf{f}$ across a surface is given by

$$d\mathbf{f} \;=\; \mathbf{t}da \;=\; \mathbf{p}dA\ .\tag{1.76}$$

1.2.3 Balance of Angular Momentum

The angular momentum of the material which occupies the region $\mathcal{P}$ at time t is $\int_{\mathcal{P}}\mathbf{x}\times\rho\mathbf{v}\,dv$, see Figure 1.6.

The integral statement of angular momentum balance for the continuum occupying $\mathcal{P}$ at time t is

$$\frac{d}{dt}\int_{\mathcal{P}}\mathbf{x}\times\rho\mathbf{v}\,dv \;=\; \int_{\mathcal{P}}\mathbf{x}\times\rho\mathbf{b}\,dv+\int_{\partial\mathcal{P}}\mathbf{x}\times\mathbf{t}\,da\ .\tag{1.77}$$

Upon invoking mass conservation and linear momentum balance, as well as using the divergence and localization theorems, it follows from the above that

$$\mathbf{T} \;=\; \mathbf{T}^T \quad ; \quad T_{ij} \;=\; T_{ji}\ ,\tag{1.78}$$

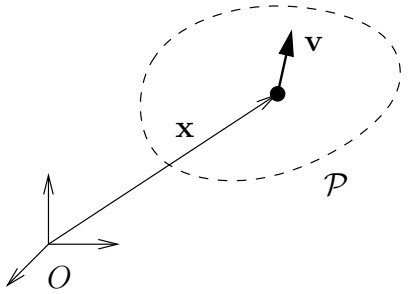

Figure 1.6. *Angular momentum of an infinitesimal volume element.*

namely angular momentum balance requires that $\mathbf{T}$ be symmetric. An equivalent local statement of angular momentum balance may be formulated in terms of the first Piola-Kirchhoff stress. Indeed, upon using (1.73), this takes the form

$$\mathbf{P}\mathbf{F}^T \;=\; \mathbf{F}\mathbf{P}^T \quad ; \quad P_{iA}F_{jA} \;=\; F_{iA}P_{jA} \;. \tag{1.79}$$

1.2.4 Balance of Energy

First, consider the *mechanical energy balance theorem*, which is a direct consequence of the preceding three balance laws. According to it,

$$\frac{d}{dt}\int_{\mathcal{P}} \frac{1}{2}\rho\mathbf{v}\cdot\mathbf{v}\,dv + \int_{\mathcal{P}} \mathbf{T}\cdot\mathbf{D}\,dv \;=\; \int_{\mathcal{P}} \rho\mathbf{b}\cdot\mathbf{v}\,dv + \int_{\partial\mathcal{P}} \mathbf{t}\cdot\mathbf{v}\,da \;, \tag{1.80}$$

where

$$\mathscr{K}(\mathcal{P}) \;=\; \int_{\mathcal{P}} \frac{1}{2}\rho\mathbf{v}\cdot\mathbf{v}\,dv \tag{1.81}$$

is the *kinetic energy* of the continuum in $\mathcal{P}$,

$$\mathscr{S}(\mathcal{P}) \;=\; \int_{\mathcal{P}} \mathbf{T}\cdot\mathbf{D}\,dv \tag{1.82}$$

is the *stress power*, and

$$\mathscr{R}(\mathcal{P}) \;=\; \int_{\mathcal{P}} \rho\mathbf{b}\cdot\mathbf{v}\,dv + \int_{\partial\mathcal{P}} \mathbf{t}\cdot\mathbf{v}\,da \tag{1.83}$$

is the rate at which the external forces do work in $\mathcal{P}$. In words, the theorem asserts that the rate of change of the kinetic energy and the stress power of the material in $\mathcal{P}$ are equal to the rate at which work is done by the external forces acting on $\mathcal{R}$.

Note that the stress power can be expressed as

$$\int_{\mathcal{P}} \mathbf{T}\cdot\mathbf{D}\,dv \;=\; \int_{\mathcal{P}_0} \mathbf{P}\cdot\dot{\mathbf{F}}\,dV \;=\; \int_{\mathcal{P}_0} \mathbf{S}\cdot\dot{\mathbf{E}}\,dV \;, \tag{1.84}$$

where $\mathbf{S}$ is the *second Piola-Kirchhoff stress tensor*. Given (1.42) and (1.73), it can be easily concluded from (1.84) that

$$\mathbf{S} \;=\; \mathbf{F}^{-1}\mathbf{P} \;=\; J\mathbf{F}^{-1}\mathbf{T}\mathbf{F}^{-T} \quad ; \quad S_{AB} \;=\; F^{-1}_{Ai}P_{iB} \;=\; JF^{-1}_{Ai}T_{ij}F^{-1}_{Bj} \tag{1.85}$$

or

$$\mathbf{T} \;=\; \frac{1}{J}\mathbf{P}\mathbf{F}^{T} \;=\frac{1}{J}\mathbf{F}\mathbf{S}\mathbf{F}^{T} \quad ; \quad T_{ij} \;=\; \frac{1}{J}P_{iA}F_{iA} \;=\; \frac{1}{J}F_{iA}S_{AB}F_{jB} \;. \tag{1.86}$$

It is immediately concluded from the above that $\mathbf{S}$ is a symmetric tensor.

Next, admit the existence of a scalar *heat supply* $r = r(\mathbf{x}, t)$ per unit mass, which quantifies the rate at which heat is supplied (or absorbed) by the body. Also, introduce a scalar *heat flux* $h = h(\mathbf{x}, t; \mathbf{n})$ per unit area across a surface ∂P with outward unit normal $\mathbf{n}$. In addition, assume that there exists a scalar function $\varepsilon = \varepsilon(\mathbf{x}, t)$ per unit mass, called the *internal energy* which quantifies all forms of energy stored in the body other than kinetic energy.

Now the principle of energy balance is postulated in the form

$$\frac{d}{dt}\int_{\mathcal{P}}\left[\frac{1}{2}\rho\mathbf{v}\cdot\mathbf{v} + \rho\varepsilon\right]\,dv \;=\; \int_{\mathcal{P}}\rho\mathbf{b}\cdot\mathbf{v}\,dv + \int_{\partial\mathcal{P}}\mathbf{t}\cdot\mathbf{v}\,da + \int_{\mathcal{P}}\rho r\,dv - \int_{\partial\mathcal{P}}h\,da \;. \tag{1.87}$$

This is a statement of the first law of thermodynamics. Using a standard procedure akin to the one used to deduce (1.68), it can be established that

$$h(\mathbf{x}, t; \mathbf{n}) \;=\; -h(\mathbf{x}, t; -\mathbf{n}) \;. \tag{1.88}$$

Likewise, using (1.88), the Cauchy tetrahedron argument can be repeated for the balance of energy to show that there exists a *heat flux vector* $\mathbf{q}$, such that

$$h \;=\; \mathbf{q}\cdot\mathbf{n} \;. \tag{1.89}$$

Now, using the divergence and localization theorems, along with the previously deduced local forms of mass, linear momentum, and angular momentum balance, a local statement of energy balance can be obtained from (1.87) as

$$\rho\dot{\varepsilon} \;=\; \rho r - \operatorname{div}\mathbf{q} + \mathbf{T}\cdot\mathbf{D} \quad ; \quad \rho\dot{\varepsilon} \;=\; \rho r - q_{i,i} + T_{ij}D_{ij} \;. \tag{1.90}$$

An equivalent referential local statement of energy balance may be readily deduced from (1.90) as

$$\rho_0\dot{\epsilon} \;=\; \rho_0 r - \operatorname{Div}\mathbf{q}_0 + \mathbf{P}\cdot\dot{\mathbf{F}} \quad ; \quad \rho_0\dot{\varepsilon} \;=\; \rho_0 r - q_{0\,A,A} + P_{iA}F_{iA} \;, \tag{1.91}$$

where $\mathbf{q}_0 = J\mathbf{F}^{-1}\mathbf{q}$.

1.3 Invariance under Superposed Rigid-body Motions

Consider two motions $\boldsymbol{\chi}$ and $\boldsymbol{\chi}^+$ which map points of the same reference configuration to points of two current configuration which at time t differ from each other by a superposed rigid motion $\overline{\boldsymbol{\chi}}^+$, as in Figure 1.7.

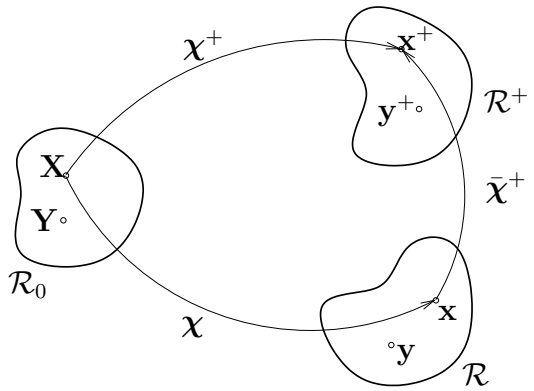

Figure 1.7. *Configurations associated with motions $\boldsymbol{\chi}$ and $\boldsymbol{\chi}^+$ differing by a superposed rigid-body motion $\bar{\boldsymbol{\chi}}^+$.*

It can be shown using a standard procedure that

$$\mathbf{x}^+ \;=\; \overline{\boldsymbol{\chi}}^+(\mathbf{x},t) \;=\; \mathbf{Q}(t)\mathbf{x}+\mathbf{c}(t) \tag{1.92}$$

where $\mathbf{Q}$ is a proper orthogonal tensor and $\mathbf{c}$ a vector, both functions of time t only.

It follows easily from chain rule that

$$\mathbf{F}^+ \;=\; \frac{\partial \boldsymbol{\chi}^+}{\partial \mathbf{X}} \;=\; \frac{\partial \boldsymbol{\chi}^+}{\partial \mathbf{x}}\frac{\partial \mathbf{x}}{\partial \mathbf{X}} \;=\; \mathbf{Q}\mathbf{F}\;, \tag{1.93}$$

This can be used to establish the relations

$$\mathbf{R}^+ \;=\; \mathbf{Q}\mathbf{R} \quad,\quad \mathbf{U}^+ \;=\; \mathbf{U} \quad,\quad \mathbf{V}^+ \;=\; \mathbf{Q}\mathbf{V}\mathbf{Q}^T \tag{1.94}$$

and also

$$\mathbf{C}^+ \;=\; \mathbf{C} \quad,\quad \mathbf{E}^+ \;=\; \mathbf{E} \quad,\quad \mathbf{B}^+ \;=\; \mathbf{Q}\mathbf{B}\mathbf{Q}^T \quad,\quad \mathbf{e}^+ \;=\; \mathbf{Q}\mathbf{e}\mathbf{Q}^T\;. \tag{1.95}$$

In addition, it is easy to show that

$$\mathbf{n}^+ \;=\; \mathbf{Q}\mathbf{n} \quad,\quad \mathbf{m}^+ \;=\; \mathbf{Q}\mathbf{m} \quad,\quad ds^+ \;=\; ds \quad,\quad da^+ \;=\; da \quad,\quad dv^+ \;=\; dv\;. \tag{1.96}$$

Also, taking the material time derivative of (1.92), it follows that

$$\begin{aligned}\mathbf{v}^+ \;=\; \dot{\mathbf{x}}^+ \;&=\; \dot{\mathbf{Q}}\mathbf{x} + \mathbf{Q}\mathbf{v} + \dot{\mathbf{c}} \\ &=\; \boldsymbol{\Omega}\mathbf{Q}\mathbf{x} + \mathbf{Q}\mathbf{v} + \dot{\mathbf{c}} \qquad \left(\dot{\mathbf{Q}}\mathbf{Q}^T = \boldsymbol{\Omega}\right) \\ &=\; \boldsymbol{\Omega}(\mathbf{x}^+ - \mathbf{c}) + \mathbf{Q}\mathbf{v} + \dot{\mathbf{c}} \;=\; \boldsymbol{\omega} \times (\mathbf{x}^+ - \mathbf{c}) + \mathbf{Q}\mathbf{v} + \dot{\mathbf{c}}\end{aligned} \tag{1.97}$$

Using the above, it can be readily establish that

$$\mathbf{L}^+ \;=\; \mathbf{Q}\mathbf{L}\mathbf{Q}^T + \boldsymbol{\Omega} \quad , \quad \mathbf{D}^+ \;=\; \mathbf{Q}\mathbf{D}\mathbf{Q}^T \quad , \quad \mathbf{W}^+ \;=\; \mathbf{Q}\mathbf{W}\mathbf{Q}^T + \boldsymbol{\Omega}\;. \tag{1.98}$$

A physically plausible assumption is made about the transformation of the stress vector $\mathbf{t}$ under a superposed rigid-body motion. Indeed, recalling that

$$\mathbf{t} \;=\; \mathbf{T}\mathbf{n}, \tag{1.99}$$

namely that $\mathbf{t}$ is linear in $\mathbf{n}$, assume that

$$\mathbf{t}^+ \;=\; \mathbf{Q}\mathbf{t} \tag{1.100}$$

which immediately implies that

$$\mathbf{T}^+ \;=\; \mathbf{Q}\mathbf{T}\mathbf{Q}^T\;. \tag{1.101}$$

From the above, it follows easily that

$$\mathbf{P}^+ \;=\; \mathbf{Q}\mathbf{P} \quad , \quad \mathbf{S}^+ \;=\; \mathbf{S}\;. \tag{1.102}$$

Invariance under superposed rigid-body motions is a physically motivated postulate in continuum mechanics, according to which the stress response remains unaltered when a rigid motion is superposed onto the actual motion of interest. Following this postulate, assume that

$$\mathbf{T} \;=\; \hat{\mathbf{T}}\left(\mathbf{F}, \dot{\mathbf{F}}, \cdots, \operatorname{Grad}\mathbf{F}, \cdots, \rho, \cdots\right) \tag{1.103}$$

then invariance under superposed rigid-body motion implies

$$\mathbf{T}^+ \;=\; \hat{\mathbf{T}}\left(\mathbf{F}^+, \dot{\mathbf{F}}^+, \cdots, \operatorname{Grad}\mathbf{F}^+, \cdots, \rho^+, \cdots\right)\;, \tag{1.104}$$

namely $\hat{\mathbf{T}}$ remains unaltered by the superposed rigid motion.

Regarding invariance, it is also postulated that

$$r^+ \;=\; r \quad , \quad \varepsilon^+ \;=\; \varepsilon \quad , \quad \mathbf{q}^+ \;=\; \mathbf{Q}\mathbf{q}\;. \tag{1.105}$$

The last relation implies

$$h^+ \;=\; h\;. \tag{1.106}$$

1.4 Closure of the Theory

It is instructive to summarize the governing equations of continuum mechanics in the context of a thermomechanical theory. There are a total of 8 equations stemming from the balance laws, that is,

1. 1 equation from balance of mass, see (1.63) or (1.66),
2. 3 equations from balance of linear momentum, see (1.71) or (1.74),
3. 3 equations from balance of angular momentum, see (1.78) or (1.79)
4. 1 equation from balance of energy, see (1.90) or (1.91).

The unknowns of the problem are the position $\mathbf{x}$ (or velocity $\mathbf{v}$), the mass density ρ, the stress $\mathbf{T}$, the heat flux $\mathbf{q}$, and the temperature θ, which is a total of 3+1+9+3+1=17.

Closure is provided in the theory by constitutive laws for the stress (6 unknowns) and heat flux (3 unknowns).

Chapter 2

Consistent Linearization

2.1 Sources of Non-linearity

The consistent linearization of the kinematic and kinetic variables, as well as of the balance laws themselves is of importance in two ways. First, in deriving "linearized" theories consistent with general non-linear theories of continuum mechanics. For instance, consistent linearization may be used to derive the classical theory of linear elasticity from non-linear elasticity or a theory of infinitesimal deformations superposed on pre-existing finite deformations ("small-on-large" theories). The latter has an important application spectral analysis of non-linear systems at a given time.

A second application of consistent linearization, which is especially relevant to finite element analysis, is in obtaining the solution to boundary- and initial- value problem of continuum mechanics using iterative methods methods that rely on instantaneous approximation of the non-linear system by a linear counterpart.

There are three distinct sources of non-linearity when solving problems in continuum mechanics. Each of them is briefly discussed here.

2.1.1 Geometric non-linearity

The measures of deformation may be non-linear functions of $\mathbf{x}$ (or $\mathbf{v}$) and its gradients. For instance, consider the (relative) Lagrangian strain tensor $\mathbf{E}$ defined in (1.23), and recall that its components E_{AB} may be expressed in terms of the components x_i of the position vector $\mathbf{x}$ as

$$E_{AB} \;=\; \frac{1}{2}\left(\frac{\partial x_i}{\partial X_A}\frac{\partial x_i}{\partial X_B} - \delta_{AB}\right) \;. \tag{2.1}$$

This is clearly a non-linear function of x_i through its derivative with respect to the referential position $\mathbf{X}$. This form of non-linearity is referred to as *geometric*.

Geometric non-linearity can be present even when the strains are "infinitesimal" (that is, when they can be accurately approximated as linear in $\mathbf{x}$). This could be the case when the rotations are large.

2.1.2 Material non-linearity

The constitutive equation of the stress or heat flux may be a non-linear function of its arguments (which are themselves generally functions of the unknowns of the problem). This form of non-linearity is referred to as *material* or *physical*.

Material non-linearity would exist in a general isotropic non-linear elastic solid, for which the constitutive law is of the form

$$\mathbf{T} \;=\; \alpha_0\mathbf{i} + \alpha_1\mathbf{B} + \alpha_2\mathbf{B}^2 \;, \tag{2.2}$$

where α_0, α_1, and α_2 are functions of the scalar invariants of $\mathbf{B}$. Likewise, material non-linearity exists in a general Reiner-Rivlin fluid, for which

$$\mathbf{T} \;=\; \beta_0\mathbf{i} + \beta_1\mathbf{D} + \beta_2\mathbf{D}^2 \;, \tag{2.3}$$

where β_1, β_2, and β_3 are functions of the scalar invariants of $\mathbf{D}$.

2.1.3 Non-linearity in the balance laws

The equation of linear momentum balance can exhibit non-linearity due to the convective term in the acceleration term. Indeed, recalling (1.71) and also taking into account that $\mathbf{v} = \tilde{\mathbf{v}}(\mathbf{x}, t)$, it follows that

$$\operatorname{div}\mathbf{T} + \rho\mathbf{b} \;=\; \rho\dot{\mathbf{v}} \;=\; \rho\left(\frac{\partial\tilde{\mathbf{v}}}{\partial t} + \frac{\partial\tilde{\mathbf{v}}}{\partial\mathbf{x}}\cdot\tilde{\mathbf{v}}\right) \tag{2.4}$$

The second term on the right-hand side of (2.4) is clearly non-linear in $\mathbf{v}$.

Note that this form of non-linearity vanishes when linear momentum balance is written in the referential form of (1.74), since, in this case $\mathbf{v} = \hat{\mathbf{v}}(\mathbf{X}, t)$ and

$$\operatorname{Div}\mathbf{P} + \rho_0\mathbf{b} \;=\; \rho_0\dot{\mathbf{v}} \;=\; \rho_0\frac{\partial\hat{\mathbf{v}}}{\partial t} \;. \tag{2.5}$$

2.2 Gâteaux and Fréchet Differentials

In this section, the Gâteaux and Fréchet differentials are introduced in the context of a non-linear operator F mapping elements from a Banach space $\mathscr{U}$ to another Banach space $\mathscr{V}$, as in Figure 2.1.[1] As a special case, one may $\mathscr{U} = \mathscr{V} = \mathbb{R}^n$, where $\mathbb{R}^n$ is equipped with the

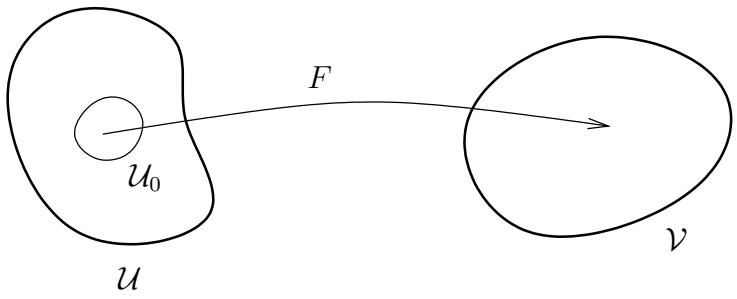

Figure 2.1. *Non-linear mapping between Banach spaces*

usual Euclidean norm.[2]

Let $F : \mathscr{U}_0 \subset \mathscr{U} \to \mathscr{V}$ be a non-linear mapping, where $\mathscr{U}_0$ is an open set, and take $x \in \mathscr{U}_0$, $v \in \mathscr{U}_0$ and $\omega \in \mathbb{R}$. The *Gâteaux differential* $D_G F(x, v)$ of the operator F at x in the direction v is formally defined as

$$D_G F(x, v) \;=\; \lim_{\omega \to 0} \frac{F(x + \omega v) - F(x)}{\omega} \;. \tag{2.6}$$

Equivalently, the Gâteaux differential may be defined as

$$D_G F(x, v) \;=\; \left[\frac{d}{d\omega} F(x + \omega v) \right]_{\omega = 0} \;, \tag{2.7}$$

since

$$\begin{aligned} \left[\frac{d}{d\omega} F(x + \omega v) \right]_{\omega = 0} &= \left[\lim_{\Delta\omega \to 0} \frac{F(x + \{\omega + \Delta\omega\} v) - F(x + \omega v)}{\Delta\omega} \right]_{\omega = 0} \\ &= \lim_{\Delta\omega \to 0} \left[\frac{F(x + \omega v + \Delta\omega v) - F(x + \omega v)}{\Delta\omega} \right]_{\omega = 0} \\ &= \lim_{\Delta\omega \to 0} \frac{F(x + \Delta\omega v) - F(x)}{\Delta\omega} \;=\; D_G F(x, v) \;, \end{aligned} \tag{2.8}$$

where continuity of F is invoked for fixed x and v.

[1] The treatment in this section follows closely the presentation in M.M. Vainberg, *Variational Methods for the Study of Non-linear Operators*(English translation from Russian), Hold-Day, San Francisco, 1964.

[2] It is easy to show that all finite-dimensional normed vector spaces are complete.

The Gâteaux differential $D_G F(x, v)$ is not necessarily linear in v. However, $D_G F(x, v)$ is necessarily homogeneous in v, that is, for any $\alpha \in \mathbb{R}$, $\alpha \neq 0$,

$$\begin{aligned} D_G F(x, \alpha v) &= \lim_{\omega \to 0} \frac{F(x + \alpha\omega v) - F(x)}{\omega} \\ &= \alpha \lim_{\alpha\omega \to 0} \frac{F(x + \alpha\omega v) - F(x)}{\alpha\omega} = \alpha D_G F(x, v) \ . \end{aligned} \tag{2.9}$$

It can be shown that if:

(a) $D_G F(x, v)$ exists in some open neighborhood $\mathcal{U}_0$ of x_0 and is continuous in x at $x = x_0$,

(b) $D_G F(x_0, v)$ is continuous in v at $v = 0$,

then the Gâteaux differential $D_G F(x_0, v)$ is actually linear in v and one may write

$$D_G F(x_0, v) = \left[D_G F(x_0)\right](v) \ , \tag{2.10}$$

where the function $D_G F(x_0)$ is called the *Gâteaux derivative* of F at $x = x_0$. The Gâteaux derivative is a linear operator on the Banach space $\mathscr{U}$, since for a given $x = x_0$ it maps $v \in \mathscr{U}$ to $\left[D_G F(x_0)\right](v) \in \mathscr{V}$, that is,

$$D_G F(x_0) \ : \ v \ \to \ \left[D_G F(x_0)\right](v) \ . \tag{2.11}$$

Example 2.2.1: Gâteaux differential and derivative of a function in $\mathbb{R}$
Let $\mathscr{U} = \mathscr{V} = \mathbb{R}$ and define F according to $F(x) = x^2$. Then, use the definition (2.6) to write

$$D_G F(x, v) = \lim_{\omega \to 0} \frac{F(x + \omega v) - F(x)}{\omega} = \lim_{\omega \to 0} \frac{(x + \omega v)^2 - x^2}{\omega} = \lim_{\omega \to 0} \left[2xv + \omega v^2\right] = 2xv \ .$$

Clearly, in this case the Gâteaux differential is linear in v, therefore the Gâteaux derivative $D_G F(x)$ is a linear operator defined as

$$D_G F(x) \ : \ v \in \mathbb{R} \ \to \ \left[D_G F(x)\right](v) = 2xv \ , \tag{2.12}$$

for any given $x \in \mathbb{R}$.

Note that the differential is not necessarily "infinitesimal" in magnitude. For a given x, this depends on the magnitude of v.

Let F be again a non-linear mapping from the Banach space $\mathscr{U}$ to the Banach space $\mathscr{V}$. Also, assume that at a given point $x \in \mathscr{U}$,

$$F(x + v) = F(x) + D_F F(x, v) + O(x, v) \ , \tag{2.13}$$

for all $v \in \mathscr{U}$, where $D_F F(x,v)$ is a linear mapping in $v \in \mathscr{U}$ and

$$\lim_{\|v\|_{\mathcal{U}} \to 0} \frac{\|O(x,v)\|_{\mathcal{V}}}{\|v\|_{\mathcal{U}}} \;=\; 0 \;. \tag{2.14}$$

Then, $D_F F(x,v)$ is called the *Fréchet differential* of F at x and $O(x,v)$ is the *remainder* of F at x. The *Fréchet derivative* $D_F F(x_0)$ at a given point $x = x_0$ is defined as the linear operator on $\mathscr{U}$ which takes any $v \in \mathscr{U}$ and maps it to $[D_F F(x_0)]\,(v) = D_F F(x_0, v)$, that is,

$$D_F F(x_0) \;:\; u \in \mathscr{U} \;\to\; [D_F F(x_0)]\,(v) \;. \tag{2.15}$$

In view of (2.13) and the properties of its constituent parts, one may define *the linear part* of F at x as

$$\mathcal{L}[F; v]_x \;=\; F(x) + D_F F(x,v) \;. \tag{2.16}$$

A corollary of the above definition and the property of the remainder in (2.14) is that if $v \neq 0$ is fixed and $\alpha > 0$, then

$$\lim_{\|\alpha v\|_{\mathcal{U}} \to 0} \frac{\|O(x,\alpha v)\|_{\mathcal{V}}}{\|\alpha v\|_{\mathcal{U}}} \;=\; 0 \tag{2.17}$$

implies

$$\lim_{\alpha \to 0} \frac{\|O(x,\alpha v)\|_{\mathcal{V}}}{\alpha} \;=\; 0 \;. \tag{2.18}$$

Note that $D_F F(x,v)$ is unique as defined in (2.13). To argue this, let, by contradiction,

$$F(x+v) \;=\; F(x) + D_F F(x,v) + O(x,v) \;=\; F(x) + D'_F F(x,v) + O'(x,v) \;. \tag{2.19}$$

Then, clearly,

$$D_F F(x,v) - D'_F F(x,v) \;=\; O'(x,v) - O(x,v) \;. \tag{2.20}$$

If one now replaces in the above v with αv, $\alpha \neq 0$, it follows that

$$\alpha\,[D_F F(x,v) - D'_F F(x,v)] \;=\; O'(x,\alpha v) - O(x,\alpha v) \tag{2.21}$$

or

$$D_F F(x,v) - D'_F F(x,v) \;=\; \frac{O'(x,\alpha v) - O(x,\alpha v)}{\alpha} \tag{2.22}$$

Now, taking norms of both sides and then considering the limit $\alpha \to 0$ and recalling (2.18), it follows that $D'_F F(x,v) = D_F F(x,v)$.

Example 2.2.2: Fréchet differential and derivative of a function in $\mathbb{R}$
Take, again, $F(x) = x^2$ and write

$$F(x+v) \;=\; (x+v)^2 \;=\; x^2 + 2xv + v^2 \;=\; F(x) + D_F F(x,v) + O(x,v) \;,$$

where, clearly,

$$D_F F(x,v) \;=\; 2xv \;,$$

which is linear in v, and also

$$O(x,v) \;=\; v^2 \;,$$

such that

$$\lim_{|v|\to 0} \frac{|v|^2}{|v|} \;=\; 0 \;.$$

Thus, the Fréchet differential of F at x is given in this case by

$$D_F F(x,v) \;=\; 2xv$$

and the Fréchet derivative $D_F F(x)$ is

$$D_F F(x) \;:\; v \in \mathbb{R} \;\to\; [D_F F(x)]\,(v) \;=\; 2xv \;.$$

From the definition of the Gâteaux and Fréchet derivatives, it follows that if the Fréchet derivative of F exists at a point $x = x_0$, then so does the Gâteaux derivative and, furthermore, the two derivatives coincide. Indeed, if the Fréchet derivative exists at x_0, then, by definition, one may write

$$F(x_0 + \omega v) \;=\; F(x_0) + [D_F F(x_0)]\,(\omega v) + O(x, \omega v) \;, \tag{2.23}$$

therefore,

$$\lim_{\omega\to 0} \frac{F(x_0+\omega v) - F(x_0)}{\omega} \;=\; [D_G F(x_0)]\,(v) + \lim_{\omega\to 0} \frac{O(x,\omega v)}{\omega} \;=\; [D_G F(x_0)]\,(v) \;, \tag{2.24}$$

in view of the property (2.18) of the remainder. The inverse of the above assertion does not hold, namely the Gâteaux derivative is weaker than the Fréchet derivative. However, it can be shown that if $D_G F(x)$ exists and is continuous at x, then $D_F F(x)$ exists and coincides with $D_G F(x)$.

Note that continuity of an operator such as $D_G F(x)$ at a point $x = x_0$ is defined using the natural norm induced with the mapping F, namely $D_G F(x)$ is continuous at $x = x_0$ if for every $\varepsilon > 0$ there is a $\delta = \delta(x_0, \varepsilon)$ such that

$$\|D_G F(x) - D_G F(x_0)\|_{\mathcal{UV}} \;<\; \varepsilon \;, \tag{2.25}$$

whenever

$$\|x - x_0\|_{\mathcal{U}} \;<\; \delta \;. \tag{2.26}$$

Here, the natural norm is defined as

$$\|D_G F(x)\|_{\mathcal{U}\mathcal{V}} \;=\; \sup_{y\in\mathcal{U}} \frac{\|D_G(x,y)\|_{\mathcal{V}}}{\|y\|_{\mathcal{U}}} \;, \tag{2.27}$$

where "sup" denotes least upper bound.

2.3 Consistent Linearization in Continuum Mechanics

In this section, linearization will be considered for quantities defined in the current configuration $\mathcal{R}$ with respect to another configuration of a body associated with a region $\overline{\mathcal{R}}$.

To this end, start with the region $\mathcal{R}_0$ occupied by the body in the reference configuration, and define a motion $\overline{\boldsymbol{\chi}}$, such that

$$\overline{\boldsymbol{\chi}}:\; (\mathbf{X},t) \;\to\; \overline{\mathbf{x}} \;=\; \overline{\boldsymbol{\chi}}(\mathbf{X},t) \;=\; \overline{\boldsymbol{\chi}}_t(\mathbf{X}) \;, \tag{2.28}$$

so that at time t the body occupies the region $\overline{\mathcal{R}}$. In addition, define another motion $\boldsymbol{\chi}$ as in (1.7), that is,

$$\boldsymbol{\chi}:\; (\mathbf{X},t) \;\to\; \mathbf{x} \;=\; \boldsymbol{\chi}(\mathbf{X},t) \;=\; \boldsymbol{\chi}_t(\mathbf{X}) \;, \tag{2.29}$$

where the body ends up in the region $\mathcal{R}$ at time t, see Figure 2.2. Both motions are assumed

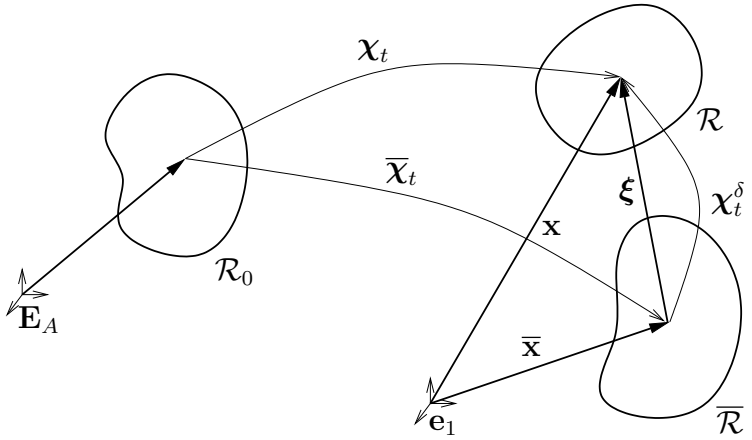

Figure 2.2. *Configurations of the body for consistent linearization*

invertible at any fixed t, that is both mappings $\overline{\boldsymbol{\chi}}_t$ and $\boldsymbol{\chi}_t$ are invertible.

One may now write

$$\mathbf{x} \;=\; \boldsymbol{\chi}_t(\mathbf{X}) \;=\; \boldsymbol{\chi}_t(\overline{\boldsymbol{\chi}}_t^{-1}(\overline{\mathbf{x}})) \;=\; \boldsymbol{\chi}_t^{\delta}(\overline{\mathbf{x}}) \tag{2.30}$$

where $\boldsymbol{\chi}_t^{\delta}$ is a motion superposed on $\overline{\mathcal{R}}$, see, again, Figure 2.2. Symbolically, one may write

$$\boldsymbol{\chi}_t \;=\; \boldsymbol{\chi}_t^{\delta} \circ \overline{\boldsymbol{\chi}}_t \;, \tag{2.31}$$

where "$\circ$" denotes functional composition, hence

$$\left(\boldsymbol{\chi}_t^{\delta} \circ \overline{\boldsymbol{\chi}}_t\right)(\mathbf{X}) \;=\; \boldsymbol{\chi}_t^{\delta}(\overline{\boldsymbol{\chi}}_t(\mathbf{X})) \;=\; \boldsymbol{\chi}_t^{\delta}(\overline{\mathbf{x}}) \;=\; \mathbf{x} \;=\; \boldsymbol{\chi}_t^{-1}(\mathbf{X}) \tag{2.32}$$

Next, define a vector field $\boldsymbol{\xi} = \hat{\boldsymbol{\xi}}(\mathbf{X}, t)$, such that

$$\boldsymbol{\xi} \;=\; \mathbf{x} - \overline{\mathbf{x}} \;=\; \boldsymbol{\chi}(\mathbf{X}, t) - \overline{\boldsymbol{\chi}}(\mathbf{X}, t) \quad ; \quad \boldsymbol{\xi} \;=\; \xi_i \mathbf{e}_i \;. \tag{2.33}$$

The vector $\boldsymbol{\xi}$ is called the *tangent vector field* on $\overline{\mathcal{R}}$.

The consistent linearization of kinematic and kinetic fields, as well as balance laws with respect to the configuration associated with the region $\overline{\mathcal{R}}$ is achieved by application of Gâteaux differentiation to each field (or balance law) at $\overline{\mathcal{R}}$ in the direction of the tangent vector field $\boldsymbol{\xi}$. In what follows, all involved functions will be assumed as smooth as necessary to make their Gâteaux and Fréchet derivatives coincide. For this reason, the common notation $DF(\overline{\mathbf{x}}, \boldsymbol{\xi})$ and $DF(\overline{\mathbf{x}})$ will be employed henceforth for differentials and derivatives, respectively.

Note that the tangent vector field $\boldsymbol{\xi}$ is not the usual displacement field $\mathbf{u}$, given by

$$\mathbf{u} \;=\; \mathbf{x} - \mathbf{X} \;=\; \boldsymbol{\chi}(\mathbf{X}, t) - \mathbf{X} \;. \tag{2.34}$$

However, in the special case

$$\overline{\boldsymbol{\chi}}(\mathbf{X}, t) \;=\; \mathbf{X} \;, \tag{2.35}$$

for which $\overline{\mathcal{R}} \equiv \mathcal{R}_0$, the displacement and tangent vectors coincide. In this case, all linearizations are taken with respect to the reference configuration[3]

Start with the deformation gradient $\mathbf{F}$ and note that, by (1.8) and (2.7),

$$D\mathbf{F}(\overline{\mathbf{x}}, \boldsymbol{\xi}) \;=\; \left[\frac{d}{dw}\mathbf{F}(\overline{\mathbf{x}} + w\boldsymbol{\xi})\right]_{w=0} \;=\; \left[\frac{d}{dw}\frac{\partial(\overline{\mathbf{x}} + w\boldsymbol{\xi})}{\partial \mathbf{X}}\right]_{w=0} \;=\; \frac{\partial \hat{\boldsymbol{\xi}}}{\partial \mathbf{X}} \;, \tag{2.36}$$

[3] See J. Casey, "On infinitesimal deformation measures", *J. Elast.*, 28:257-269, (1992), for derivations of linearized kinematic quantities relative to the reference configuration.

where $\boldsymbol{\xi} = \hat{\boldsymbol{\xi}}(\mathbf{X}, t)$. This implies that

$$\mathcal{L}\left[\mathbf{F}; \boldsymbol{\xi}\right]_{\overline{\mathbf{x}}} \;=\; \overline{\mathbf{F}} + \frac{\partial \hat{\boldsymbol{\xi}}}{\partial \mathbf{X}} \;=\; \mathbf{F} \quad , \quad \overline{\mathbf{F}} \;=\; \frac{\partial \overline{\mathbf{x}}}{\partial \mathbf{X}} \; , \tag{2.37}$$

that is, $\mathbf{F}$ is itself linear in $\boldsymbol{\xi}$.

Observe that

$$\boldsymbol{\xi} \;=\; \hat{\boldsymbol{\xi}}(\mathbf{X}, t) \;=\; \hat{\boldsymbol{\xi}}\left(\overline{\boldsymbol{\chi}}_t^{-1}(\overline{\mathbf{x}}), t\right) \;=\; \overline{\boldsymbol{\xi}}(\overline{\mathbf{x}}, t) \; , \tag{2.38}$$

therefore, by the chain rule,

$$\frac{\partial \hat{\boldsymbol{\xi}}}{\partial \mathbf{X}} \;=\; \frac{\partial \overline{\boldsymbol{\xi}}}{\partial \overline{\mathbf{x}}} \frac{\partial \overline{\mathbf{x}}}{\partial \mathbf{X}} \;=\; \frac{\partial \overline{\boldsymbol{\xi}}}{\partial \overline{\mathbf{x}}} \overline{\mathbf{F}} \tag{2.39}$$

and the linear part of $\mathbf{F}$ can be alternatively written as

$$\mathcal{L}\left[\mathbf{F}; \boldsymbol{\xi}\right]_{\overline{\mathbf{x}}} \;=\; \overline{\mathbf{F}} + \frac{\partial \overline{\boldsymbol{\xi}}}{\partial \overline{\mathbf{x}}} \overline{\mathbf{F}} \; . \tag{2.40}$$

Consider next the linearization of the Lagrangian strain tensor $\mathbf{E}$ defined in (1.23). Here, employing again the definition (2.7), it follows that

$$\begin{aligned} D\mathbf{E}(\overline{\mathbf{x}}, \boldsymbol{\xi}) \;&=\; \left[\frac{d}{dw}\left\{\frac{1}{2}\left(\mathbf{F}^T(\overline{\mathbf{x}} + w\boldsymbol{\xi})\mathbf{F}(\overline{\mathbf{x}} + w\boldsymbol{\xi}) - \mathbf{I}\right)\right\}\right]_{w=0} \\ &=\; \frac{1}{2}\left\{\left[\frac{d}{dw}\mathbf{F}^T(\overline{\mathbf{x}} + w\boldsymbol{\xi})\right]_{w=0} \overline{\mathbf{F}} + \overline{\mathbf{F}}^T \left[\frac{d}{dw}\mathbf{F}(\overline{\mathbf{x}} + w\boldsymbol{\xi})\right]_{w=0}\right\} \\ &=\; \frac{1}{2}\left[\left(\frac{\partial \boldsymbol{\xi}}{\partial \mathbf{X}}\right)^T \overline{\mathbf{F}} + \overline{\mathbf{F}}^T \frac{\partial \boldsymbol{\xi}}{\partial \mathbf{X}}\right] \; . \end{aligned} \tag{2.41}$$

Alternatively, in view of (2.39),

$$D\mathbf{E}(\overline{\mathbf{x}}, \boldsymbol{\xi}) \;=\; \frac{1}{2}\left[\overline{\mathbf{F}}^T \left(\frac{\partial \boldsymbol{\xi}}{\partial \overline{\mathbf{x}}}\right)^T \overline{\mathbf{F}} + \overline{\mathbf{F}}^T \frac{\partial \boldsymbol{\xi}}{\partial \overline{\mathbf{x}}} \overline{\mathbf{F}}\right] \;=\; \overline{\mathbf{F}}^T \left(\frac{\partial \boldsymbol{\xi}}{\partial \overline{\mathbf{x}}}\right)^S \overline{\mathbf{F}} \; , \tag{2.42}$$

where

$$\left(\frac{\partial \boldsymbol{\xi}}{\partial \overline{\mathbf{x}}}\right)^S \;=\; \frac{1}{2}\left[\frac{\partial \boldsymbol{\xi}}{\partial \overline{\mathbf{x}}} + \left(\frac{\partial \boldsymbol{\xi}}{\partial \overline{\mathbf{x}}}\right)^T\right] \; . \tag{2.43}$$

Therefore,

$$\mathcal{L}\left[\mathbf{E}; \boldsymbol{\xi}\right]_{\overline{\mathbf{x}}} \;=\; \overline{\mathbf{E}} + \overline{\mathbf{F}}^T \left(\frac{\partial \boldsymbol{\xi}}{\partial \overline{\mathbf{x}}}\right)^S \overline{\mathbf{F}} \tag{2.44}$$

and the linear part of $\mathbf{E}$ remains symmetric, as expected. Likewise, given (1.13) and (2.42), it is immediately clear that

$$\mathcal{L}\left[\mathbf{C}; \boldsymbol{\xi}\right]_{\overline{\mathbf{x}}} \;=\; \overline{\mathbf{C}} + 2\overline{\mathbf{F}}^T \left(\frac{\partial \boldsymbol{\xi}}{\partial \overline{\mathbf{x}}}\right)^S \overline{\mathbf{F}} \; . \tag{2.45}$$

Similarly, it is simple to conclude from (1.14) and (2.40) that

$$\mathcal{L}\left[\mathbf{B};\boldsymbol{\xi}\right]_{\overline{\mathbf{x}}} \;=\; \overline{\mathbf{B}} + \frac{\partial \boldsymbol{\xi}}{\partial \overline{\mathbf{x}}}\,\overline{\mathbf{B}} + \overline{\mathbf{B}}\left(\frac{\partial \boldsymbol{\xi}}{\partial \overline{\mathbf{x}}}\right)^{T} \;. \tag{2.46}$$

In the special case when the linearization is performed with respect to the reference configuration, where

$$\overline{\mathbf{x}} \;=\; \mathbf{X} \quad , \quad \boldsymbol{\xi} = \mathbf{u} \quad , \quad \overline{\mathbf{F}} \;=\; \mathbf{I}\,, \tag{2.47}$$

it is easy to see that, given (2.39),

$$\frac{\partial \hat{\boldsymbol{\xi}}}{\partial \mathbf{X}} \;=\; \frac{\partial \overline{\boldsymbol{\xi}}}{\partial \overline{\mathbf{x}}}\overline{\mathbf{F}} \;=\; \frac{\partial \overline{\boldsymbol{\xi}}}{\partial \overline{\mathbf{x}}}\,. \tag{2.48}$$

Hence, once may conclude from (2.42) that

$$D\mathbf{E}(\overline{\mathbf{x}},\boldsymbol{\xi}) \;=\; \overline{\mathbf{F}}^{T}\left(\frac{\partial \overline{\boldsymbol{\xi}}}{\partial \overline{\mathbf{x}}}\right)^{S}\overline{\mathbf{F}} \;=\; \left(\frac{\partial \overline{\boldsymbol{\xi}}}{\partial \overline{\mathbf{x}}}\right)^{S} \;=\; \left(\frac{\partial \hat{\boldsymbol{\xi}}}{\partial \mathbf{X}}\right)^{S} \tag{2.49}$$

and

$$\mathcal{L}\left[\mathbf{E};\boldsymbol{\xi}\right]_{\mathbf{X}} \;=\; \overline{\mathbf{E}} + \frac{1}{2}\left[\frac{\partial \hat{\boldsymbol{\xi}}}{\partial \mathbf{X}} + \left(\frac{\partial \hat{\boldsymbol{\xi}}}{\partial \mathbf{X}}\right)^{T}\right] \;=\; \boldsymbol{\varepsilon}(\boldsymbol{\xi})\,, \tag{2.50}$$

where

$$\boldsymbol{\varepsilon}(\boldsymbol{\xi}) \;=\; \frac{1}{2}\left(\xi_{A,B} + \xi_{B,A}\right)\mathbf{E}_A \otimes \mathbf{E}_B \tag{2.51}$$

and since, in view of $(2.47)_3$, $\overline{\mathbf{E}} = \mathbf{0}$. Given $(2.47)_2$ and (2.50), one may also conclude that

$$\mathcal{L}\left[\mathbf{E};\boldsymbol{\xi}\right]_{\mathbf{X}} \;=\; \mathcal{L}\left[\mathbf{E};\mathbf{u}\right]_{\mathbf{X}} \;=\; \boldsymbol{\varepsilon}(\mathbf{u}) \;=\; \frac{1}{2}\left(u_{A,B} + u_{B,A}\right)\mathbf{E}_A \otimes \mathbf{E}_B\,, \tag{2.52}$$

which is the usual measure of strain at infinitesimal deformations. In addition, it follows from (2.45) and (2.45) that

$$\mathcal{L}\left[\mathbf{C};\boldsymbol{\xi}\right]_{\mathbf{X}} \;=\; \mathcal{L}\left[\mathbf{C};\mathbf{u}\right]_{\mathbf{X}} \;=\; 2\boldsymbol{\varepsilon}(\mathbf{u})\,. \tag{2.53}$$

and

$$\mathcal{L}\left[\mathbf{B};\boldsymbol{\xi}\right]_{\mathbf{X}} \;=\; \mathcal{L}\left[\mathbf{B};\mathbf{u}\right]_{\mathbf{X}} \;=\; 2\boldsymbol{\varepsilon}(\mathbf{u})\,. \tag{2.54}$$

Next, consider the linearization of $J = \det \mathbf{F}$ with respect to the configuration $\overline{\mathcal{R}}$. Starting once more with the definition (2.7),

$$\begin{aligned}
DJ(\overline{\mathbf{x}}, \boldsymbol{\xi}) &= \left[\frac{d}{dw} \det \mathbf{F}(\overline{\mathbf{x}} + w\boldsymbol{\xi})\right]_{w=0} \\
&= \left[\frac{d}{dw} \det \left(\overline{\mathbf{F}} + w \frac{\partial \hat{\boldsymbol{\xi}}}{\partial \mathbf{X}}\right)\right]_{w=0} \\
&= \left[\frac{d}{dw} \det \left(\overline{\mathbf{F}} + w\mathbf{G}\right)\right]_{w=0} \quad ; \quad \mathbf{G} = \frac{\partial \hat{\boldsymbol{\xi}}}{\partial \mathbf{X}} \\
&= \left[\frac{d}{dw} \det \left\{w\overline{\mathbf{F}} \left[\overline{\mathbf{F}}^{-1}\mathbf{G} - \left(-\frac{1}{w}\right)\mathbf{I}\right]\right\}\right]_{w=0} \\
&= \left[\frac{d}{dw} \left\{w^3 \det \overline{\mathbf{F}} \left[-\left(-\frac{1}{w}\right)^3 + \left(\frac{1}{w}\right)^2 \mathrm{I}_{\overline{\mathbf{F}}^{-1}\mathbf{G}} - \left(-\frac{1}{w}\right) \mathrm{II}_{\overline{\mathbf{F}}^{-1}\mathbf{G}} + \mathrm{III}_{\overline{\mathbf{F}}^{-1}\mathbf{G}}\right]\right\}\right]_{w=0} \\
&= \left[\frac{d}{dw} \left\{\det \overline{\mathbf{F}} \left[1 + w\mathrm{I}_{\overline{\mathbf{F}}^{-1}\mathbf{G}} + w^2 \mathrm{II}_{\overline{\mathbf{F}}^{-1}\mathbf{G}} + w^3 \mathrm{III}_{\overline{\mathbf{F}}^{-1}\mathbf{G}}\right]\right\}\right]_{w=0} \\
&= \det \overline{\mathbf{F}}\ \mathrm{I}_{\overline{\mathbf{F}}^{-1}\mathbf{G}}
\end{aligned} \tag{2.55}$$

where it is recalled that for any second-order tensor, say $\mathbf{T}$,

$$\det(\mathbf{T} - \lambda\mathbf{I}) = -\lambda^3 + \lambda^2 \mathrm{I}_{\mathbf{T}} - \lambda \mathrm{II}_{\mathbf{T}} + \mathrm{III}_{\mathbf{T}} \ . \tag{2.56}$$

In the above, $\mathrm{I}_{\mathbf{T}}$, $\mathrm{II}_{\mathbf{T}}$, and $\mathrm{III}_{\mathbf{T}}$ are the principal invariants of $\mathbf{T}$, defined as

$$\mathrm{I}_{\mathbf{T}} = \operatorname{tr} \mathbf{T} \tag{2.57}$$

$$\mathrm{II}_{\mathbf{T}} = \frac{1}{2}\left[(\operatorname{tr} \mathbf{T})^2 - \operatorname{tr} \mathbf{T}^2\right] \tag{2.58}$$

$$\mathrm{III}_{\mathbf{T}} = \det \mathbf{T} = \frac{1}{6}\left[(\operatorname{tr} \mathbf{T})^3 - 3\,(\operatorname{tr} \mathbf{T})\left(\operatorname{tr} \mathbf{T}^2\right) + 2\ \operatorname{tr} \mathbf{T}^3\right] \ . \tag{2.59}$$

Equation (2.55) may be expressed as

$$\left[\frac{d}{dw} \det \mathbf{F}(\overline{\mathbf{x}} + w\boldsymbol{\xi})\right]_{w=0} = \overline{J} \operatorname{tr}\left(\overline{\mathbf{F}}^{-1} \frac{\partial \hat{\boldsymbol{\xi}}}{\partial \mathbf{X}}\right) \tag{2.60}$$

where $\overline{J} = \det \overline{\mathbf{F}}$, and the linear part of $\det \mathbf{F}$ relative to the configuration $\overline{\mathcal{R}}$ takes the form

$$\mathcal{L}\left[\det \mathbf{F}; \boldsymbol{\xi}\right]_{\overline{\mathbf{x}}} = \overline{J} + \overline{J} \operatorname{tr}\left(\overline{\mathbf{F}}^{-1} \frac{\partial \hat{\boldsymbol{\xi}}}{\partial \mathbf{X}}\right) = \overline{J}\left[1 + \operatorname{tr}\left(\overline{\mathbf{F}}^{-1} \frac{\partial \hat{\boldsymbol{\xi}}}{\partial \mathbf{X}}\right)\right] \ . \tag{2.61}$$

Alternatively, taking into account (2.39), one may obtain an Eulerian form of the above linearization by rewriting (2.60) as

$$\begin{aligned} DJ(\overline{\mathbf{x}},\boldsymbol{\xi}) \;=\; \overline{J}\;\mathrm{tr}\left(\overline{\mathbf{F}}^{-1}\frac{\partial\hat{\boldsymbol{\xi}}}{\partial\mathbf{X}}\right) \;&=\; \overline{J}\;\mathrm{tr}\left[\overline{\mathbf{F}}^{-1}\left(\frac{\partial\overline{\boldsymbol{\xi}}}{\partial\overline{\mathbf{x}}}\overline{\mathbf{F}}\right)\right] \\ &=\; \overline{J}\;\mathrm{tr}\left[\overline{\mathbf{F}}\overline{\mathbf{F}}^{-1}\frac{\partial\overline{\boldsymbol{\xi}}}{\partial\overline{\mathbf{x}}}\right] \quad ; \quad (\mathrm{tr}\,[\mathbf{AB}] \;=\; \mathrm{tr}\,[\mathbf{BA}]) \\ &=\; \overline{J}\;\mathrm{tr}\left(\frac{\partial\overline{\boldsymbol{\xi}}}{\partial\overline{\mathbf{x}}}\right) \;=\; \overline{J}\,\mathrm{div}\,\boldsymbol{\xi}\;, \end{aligned} \tag{2.62}$$

where $\mathrm{div}\,\boldsymbol{\xi} = \frac{\partial\overline{\xi}_i}{\partial\overline{\mathbf{x}}_i}$[4], therefore

$$\mathcal{L}\,[J;\boldsymbol{\xi}]_{\overline{\mathbf{x}}} \;=\; \overline{J} + \overline{J}\,\mathrm{div}\,\boldsymbol{\xi} \;=\; \overline{J}(1+\mathrm{div}\,\boldsymbol{\xi})\;. \tag{2.63}$$

For the special case of linearization with respect to the reference configuration, equations (2.47) and (2.51) imply that

$$\mathcal{L}\,[J;\boldsymbol{\xi}]_{\mathbf{X}} \;=\; 1+\mathrm{Div}\,\boldsymbol{\xi} \;=\; 1+\mathrm{tr}\,\boldsymbol{\varepsilon}(\boldsymbol{\xi}) \;=\; 1+\mathrm{tr}\,\boldsymbol{\varepsilon}(\mathbf{u})\;. \tag{2.64}$$

Also, consider the linearization of $\dfrac{da}{dA}$, namely the ratio of the surface element areas of the current over the reference configuration. To this end, start with Nanson's formula (1.12), from where it follows that

$$\frac{da}{dA}\mathbf{n} \;=\; J\mathbf{F}^{-T}\mathbf{N} \;=\; \mathbf{F}^{*}\mathbf{N}\;, \tag{2.65}$$

where

$$\mathbf{F}^{*} \;=\; J\mathbf{F}^{-T} \tag{2.66}$$

is the *adjugate* of $\mathbf{F}$. Upon taking the dot-product of each side of (2.65) with itself, one finds that

$$\begin{aligned} \left(\frac{da}{dA}\right)^2 \;&=\; (\mathbf{F}^{*}\mathbf{N})\cdot(\mathbf{F}^{*}\mathbf{N}) \\ &=\; \mathbf{N}\cdot(\mathbf{F}^{*T}\mathbf{F}^{*}\mathbf{N}) \;=\; \mathbf{N}\cdot(\mathbf{C}^{*}\mathbf{N})\;, \end{aligned} \tag{2.67}$$

where

$$\mathbf{C}^{*} \;=\; \mathbf{F}^{*T}\mathbf{F}^{*} \;=\; J^2\mathbf{C}^{-1}\;. \tag{2.68}$$

[4] In strict terms, one should use the notation $\overline{\mathrm{div}}\boldsymbol{\xi}$ for this term, but the extra overbar is neglected here.

It now follows from the usual definition (2.7) that

$$D\left[\left(\frac{da}{dA}\right)^2\right](\overline{\mathbf{x}},\boldsymbol{\xi}) \;=\; \left[\frac{d}{dw}\left\{\mathbf{N}\cdot\mathbf{C}^*(\overline{\mathbf{x}}+w\boldsymbol{\xi})\mathbf{N}\right\}\right]_{w=0}\,, \tag{2.69}$$

where

$$\begin{aligned}\left[\frac{d}{dw}\mathbf{C}^*(\overline{\mathbf{x}}+w\boldsymbol{\xi})\right]_{w=0} &= \left[\frac{d}{dw}\left\{J^2(\overline{\mathbf{x}}+w\boldsymbol{\xi})\mathbf{C}^{-1}(\overline{\mathbf{x}}+w\boldsymbol{\xi})\right\}\right]_{w=0}\\ &= 2\overline{J}\left[\frac{d}{dw}J(\overline{\mathbf{x}}+w\boldsymbol{\xi})\right]_{w=0}\overline{\mathbf{C}}^{-1}+\overline{J}^2\left[\frac{d}{dw}\mathbf{C}^{-1}(\overline{\mathbf{x}}+w\boldsymbol{\xi})\right]_{w=0}\,.\end{aligned} \tag{2.70}$$

Since $\mathbf{C}\mathbf{C}^{-1}=\mathbf{I}$,

$$\left[\frac{d}{dw}\left\{\mathbf{C}(\overline{\mathbf{x}}+w\boldsymbol{\xi})\mathbf{C}^{-1}(\overline{\mathbf{x}}+w\boldsymbol{\xi})\right\}\right]_{w=0} \;=\; D\mathbf{C}(\overline{\mathbf{x}},\boldsymbol{\xi})\overline{\mathbf{C}}^{-1}+\overline{\mathbf{C}}D\mathbf{C}^{-1}(\overline{\mathbf{x}},\boldsymbol{\xi}) \;=\; \mathbf{0}\,, \tag{2.71}$$

therefore

$$D\mathbf{C}^{-1}(\overline{\mathbf{x}},\boldsymbol{\xi}) \;=\; \left[\frac{d}{dw}\mathbf{C}^{-1}(\overline{\mathbf{x}}+w\boldsymbol{\xi})\right]_{w=0} \;=\; -\overline{\mathbf{C}}^{-1}D\mathbf{C}(\overline{\mathbf{x}},\boldsymbol{\xi})\overline{\mathbf{C}}^{-1} \tag{2.72}$$

or, in light of (2.45),

$$D\mathbf{C}^{-1}(\overline{\mathbf{x}},\boldsymbol{\xi}) \;=\; -\overline{\mathbf{F}}^{-1}\overline{\mathbf{F}}^{-T}\left[2\overline{\mathbf{F}}^T\left(\frac{\partial\boldsymbol{\xi}}{\partial\overline{\mathbf{x}}}\right)^S\overline{\mathbf{F}}\right]\overline{\mathbf{F}}^{-1}\overline{\mathbf{F}}^{-T} \;=\; -2\overline{\mathbf{F}}^{-1}\left(\frac{\partial\boldsymbol{\xi}}{\partial\overline{\mathbf{x}}}\right)^S\overline{\mathbf{F}}^{-T}\,. \tag{2.73}$$

Return to (2.70) and substituting in it (2.62) and (2.45), it follows that

$$\begin{aligned}\left[\frac{d}{dw}\mathbf{C}^*(\overline{\mathbf{x}}+w\boldsymbol{\xi})\right]_{w=0} &= 2\overline{J}\left[\overline{J}\,\mathrm{div}\,\boldsymbol{\xi}\right]\overline{\mathbf{C}}^{-1}+\overline{J}^2\left[-2\overline{\mathbf{F}}^{-1}\left(\frac{\partial\boldsymbol{\xi}}{\partial\overline{\mathbf{x}}}\right)^S\overline{\mathbf{F}}^{-T}\right]\\ &= 2\overline{J}^2\left[\mathrm{div}\,\boldsymbol{\xi}\,\overline{\mathbf{C}}^{-1}-\overline{\mathbf{F}}^{-1}\left(\frac{\partial\boldsymbol{\xi}}{\partial\overline{\mathbf{x}}}\right)^S\overline{\mathbf{F}}^{-T}\right]\,.\end{aligned} \tag{2.74}$$

This means that (2.69) takes the form

$$\begin{aligned}D\left[\left(\frac{da}{dA}\right)^2\right](\overline{\mathbf{x}},\boldsymbol{\xi}) &= 2\overline{\left(\frac{da}{dA}\right)}D\left[\frac{da}{dA}\right](\overline{\mathbf{x}},\boldsymbol{\xi})\\ &= \mathbf{N}\cdot 2\overline{J}^2\left[\mathrm{div}\,\boldsymbol{\xi}\overline{\mathbf{C}}^{-1}-\overline{\mathbf{F}}^{-1}\left(\frac{\partial\boldsymbol{\xi}}{\partial\overline{\mathbf{x}}}\right)^S\overline{\mathbf{F}}^{-T}\right]\mathbf{N}\,,\end{aligned} \tag{2.75}$$

hence

$$D\left[\frac{da}{dA}\right](\overline{\mathbf{x}},\boldsymbol{\xi}) \;=\; \overline{\left(\frac{dA}{da}\right)}\mathbf{N}\cdot\overline{J}^2\left[\mathrm{div}\,\boldsymbol{\xi}\overline{\mathbf{C}}^{-1}-\overline{\mathbf{F}}^{-1}\left(\frac{\partial\boldsymbol{\xi}}{\partial\overline{\mathbf{x}}}\right)^S\overline{\mathbf{F}}^{-T}\right]\mathbf{N} \tag{2.76}$$

and, accordingly,

$$\mathcal{L}\left[\frac{da}{dA};\boldsymbol{\xi}\right]_{\overline{\mathbf{x}}} \;=\; \overline{\left(\frac{da}{dA}\right)} + D\left[\frac{da}{dA}\right](\overline{\mathbf{x}},\boldsymbol{\xi})\;. \tag{2.77}$$

When the linearization is performed with respect to the reference configuration, it follows from (2.47) and (2.51) that (2.76) reduces to

$$\begin{aligned} D\left[\frac{da}{dA}\right](\mathbf{X},\boldsymbol{\xi}) \;&=\; \mathbf{N}\cdot\left[\operatorname{div}\boldsymbol{\xi}\mathbf{I} - \left(\frac{\partial\boldsymbol{\xi}}{\partial\overline{\mathbf{x}}}\right)^{S}\right]\mathbf{N} \\ &=\; \mathbf{N}\cdot\left[\operatorname{Div}\boldsymbol{\xi}\mathbf{I} - \left(\frac{\partial\boldsymbol{\xi}}{\partial\mathbf{X}}\right)^{S}\right]\mathbf{N} \\ &=\; \mathbf{N}\cdot\left[\operatorname{tr}\boldsymbol{\varepsilon}(\boldsymbol{\xi})\mathbf{I} - \boldsymbol{\varepsilon}(\boldsymbol{\xi})\right]\mathbf{N} \\ &=\; \operatorname{tr}\boldsymbol{\varepsilon}(\mathbf{u}) - \mathbf{N}\cdot\boldsymbol{\varepsilon}(\mathbf{u})\mathbf{N} \end{aligned} \tag{2.78}$$

and

$$\mathcal{L}\left[\frac{da}{dA};\boldsymbol{\xi}\right]_{\mathbf{X}} \;=\; 1 + \operatorname{tr}\boldsymbol{\varepsilon}(\mathbf{u}) - \mathbf{N}\cdot\boldsymbol{\varepsilon}(\mathbf{u})\mathbf{N}\;. \tag{2.79}$$

The balance laws are also subject to linearization. For instance, consider the balance of mass in the form (1.63) and linearize it relative to the configuration $\overline{\mathcal{R}}$, that is, write

$$\mathcal{L}\left[\rho_0;\boldsymbol{\xi}\right]_{\overline{\mathbf{x}}} \;=\; \mathcal{L}\left[\rho J;\boldsymbol{\xi}\right]_{\overline{\mathbf{x}}} \quad\Rightarrow \tag{2.80}$$

which leads, with the aid of (2.62) to

$$\begin{aligned} \rho_0 \;&=\; \overline{\rho}\,\overline{J} + D[\rho J](\overline{\mathbf{x}},\boldsymbol{\xi}) \\ &=\; \overline{\rho}\,\overline{J} + D\rho(\overline{\mathbf{x}},\boldsymbol{\xi})\overline{J} + \overline{\rho}DJ(\overline{\mathbf{x}},\boldsymbol{\xi}) \\ &=\; \overline{\rho}\,\overline{J} + D\rho(\overline{\mathbf{x}},\boldsymbol{\xi})\overline{J} + \overline{\rho}\,\overline{J}\operatorname{div}\boldsymbol{\xi}\;. \end{aligned} \tag{2.81}$$

Assuming that conservation of mass holds in $\overline{\mathcal{R}}$ (which is tantamount to letting $\overline{\rho}$ be such that $\rho_0 = \overline{\rho}\,\overline{J}$), it follows from the above that

$$D\rho(\overline{\mathbf{x}},\boldsymbol{\xi}) \;=\; -\overline{\rho}\operatorname{div}\boldsymbol{\xi}\;, \tag{2.82}$$

so that

$$\mathcal{L}\left[\rho;\boldsymbol{\xi}\right]_{\overline{\mathbf{x}}} \;=\; \overline{\rho} + (-\overline{\rho}\operatorname{div}\boldsymbol{\xi}) \;=\; \overline{\rho}(1-\operatorname{div}\boldsymbol{\xi})\;. \tag{2.83}$$

In view of (2.82), the special case of linearization with respect to $\mathcal{R}_0$ readily yields

$$\mathcal{L}\left[\rho;\boldsymbol{\xi}\right]_{\mathbf{X}} \;=\; \rho_0(1-\operatorname{div}\boldsymbol{\xi}) \;=\; \rho_0(1-\operatorname{Div}\boldsymbol{\xi}) \;=\; \rho_0(1-\operatorname{tr}\boldsymbol{\varepsilon}(\boldsymbol{\xi})) \;=\; \rho_0(1-\operatorname{tr}\boldsymbol{\varepsilon}(\mathbf{u}))\;, \tag{2.84}$$

which implies that conservation of mass may be expressed as

$$\rho \;=\; \rho_0(1-\operatorname{tr}\boldsymbol{\varepsilon}(\mathbf{u})) \tag{2.85}$$

Note that ρ is not equal to ρ_0 when linearized with respect to $\mathcal{R}_0$.

Lastly, consider the balance of linear momentum (1.71) in spatial form and take its linear part with respect to $\overline{\mathcal{R}}$, which is

$$\mathcal{L}\left[\operatorname{div}\mathbf{T};\boldsymbol{\xi}\right]_{\overline{\mathbf{x}}}+\mathcal{L}\left[\rho\mathbf{b};\boldsymbol{\xi}\right]_{\overline{\mathbf{x}}} \;=\; \mathcal{L}\left[\rho\ddot{\mathbf{u}};\boldsymbol{\xi}\right]_{\overline{\mathbf{x}}} \tag{2.86}$$

The differential of each of the three terms in the preceding equation is considered separately. First, write the acceleration term as

$$D\left[\rho\ddot{\mathbf{u}}\right](\overline{\mathbf{x}},\boldsymbol{\xi}) \;=\; \left[\frac{d}{dw}\left\{\rho(\overline{\mathbf{x}}+w\boldsymbol{\xi})\ddot{\mathbf{u}}(\overline{\mathbf{x}}+w\boldsymbol{\xi})\right\}\right]_{w=0} \;=\; -\overline{\rho}\operatorname{div}\boldsymbol{\xi}\ddot{\overline{\mathbf{u}}}+\overline{\rho}\ddot{\boldsymbol{\xi}} \tag{2.87}$$

with the use of (2.82) and the fact that $\ddot{\mathbf{u}}(\mathbf{x})=\ddot{\mathbf{x}}$. Next, the body force term becomes

$$D\left[\rho\mathbf{b}\right](\overline{\mathbf{x}},\boldsymbol{\xi}) \;=\; \left[\frac{d}{dw}\left\{\rho(\overline{\mathbf{x}}+w\boldsymbol{\xi})\mathbf{b}(\overline{\mathbf{x}}+w\boldsymbol{\xi})\right\}\right]_{w=0} \;=\; -\overline{\rho}\operatorname{div}\boldsymbol{\xi}\overline{\mathbf{b}}+\overline{\rho}D\mathbf{b}(\overline{\mathbf{x}},\boldsymbol{\xi}) \tag{2.88}$$

where, again, use is made of (2.82) and also of the definition

$$\mathcal{L}\left[\mathbf{b};\boldsymbol{\xi}\right]_{\overline{\mathbf{x}}} \;=\; \overline{\mathbf{b}}+D\mathbf{b}(\overline{\mathbf{x}},\boldsymbol{\xi})\;. \tag{2.89}$$

For the stress-divergence term, it can be shown that

$$\begin{aligned} D\left[\operatorname{div}\mathbf{T}\right](\overline{\mathbf{x}},\boldsymbol{\xi}) \;&=\; \left[\frac{d}{dw}\left\{\operatorname{div}\mathbf{T}(\overline{\mathbf{x}}+w\boldsymbol{\xi})\right\}\right]_{w=0} \\ &=\; \operatorname{div}\left[\frac{d}{dw}\mathbf{T}(\overline{\mathbf{x}}+w\boldsymbol{\xi})\right]_{w=0}-\overline{T}_{ij,k}\xi_{k,j}\mathbf{e}_i \\ &=\; \operatorname{div}\left[D\mathbf{T}(\overline{\mathbf{x}},\boldsymbol{\xi})\right]-\operatorname{grad}\overline{\mathbf{T}}\cdot\operatorname{grad}^T\boldsymbol{\xi}\;. \end{aligned} \tag{2.90}$$

Note that a constitutive equation for $\mathbf{T}$ is required in order to evaluate the first term on the right-hand side of $(2.90)_3$. To derive (2.90), it is best to resort to component representation, as follows:

$$\begin{aligned} D\left[\operatorname{div}\mathbf{T}\right](\overline{\mathbf{x}},\boldsymbol{\xi}) \;&=\; \left[\frac{d}{dw}\left\{\operatorname{div}\mathbf{T}(\overline{\mathbf{x}}+w\boldsymbol{\xi})\right\}\right]_{w=0} \\ &=\; \left[\frac{d}{dw}\frac{\partial T_{ij}(\overline{\mathbf{x}}+w\boldsymbol{\xi})}{\partial(\overline{x}_j+w\xi_j)}\right]_{w=0}\mathbf{e}_i \\ &=\; \left[\frac{d}{dw}\left\{\frac{\partial T_{ij}(\overline{\mathbf{x}}+w\boldsymbol{\xi})}{\partial\overline{x}_k}\frac{\partial\overline{x}_k}{\partial(\overline{x}_j+w\xi_j)}\right\}\right]_{w=0}\mathbf{e}_i \\ &=\; \left[\frac{d}{dw}\left\{\frac{\partial T_{ij}(\overline{\mathbf{x}}+w\boldsymbol{\xi})}{\partial\overline{x}_k}\right\}\right]_{w=0}\frac{\partial\overline{x}_k}{\partial\overline{x}_j}\mathbf{e}_i+\frac{\partial\overline{T}_{ij}}{\partial\overline{x}_k}\left[\frac{d}{dw}\left\{\frac{\partial\overline{x}_k}{\partial(\overline{x}_j+w\xi_j)}\right\}\right]_{w=0}\mathbf{e}_i\;. \end{aligned} \tag{2.91}$$

Note that it is not possible to switch the order of the differential operators $\frac{d}{dw}$ and $\frac{\partial}{\partial \mathbf{x}}$ in $(2.91)_2$ as the latter is explicitly dependent on ω.[5] To evaluate the second term on the right-hand side of $(2.91)_4$, observe that

$$\left[\frac{d}{dw}\left\{\frac{\partial(\overline{x}_k + w\xi_k)}{\partial \overline{x}_l}\frac{\partial \overline{x}_l}{\partial(\overline{x}_j + w\xi_j)}\right\}\right]_{w=0} = \left[\frac{d}{dw}\{\delta_{kj}\}\right]_{w=0} = 0\ , \tag{2.92}$$

therefore,

$$\left[\frac{d}{dw}\left\{\frac{\partial(\overline{x}_k + w\xi_k)}{\partial \overline{x}_l}\right\}\right]_{w=0}\delta_{lj} + \delta_{kl}\left[\frac{d}{dw}\left\{\frac{\partial \overline{x}_l}{\partial(\overline{x}_j + w\xi_j)}\right\}\right]_{w=0} = 0\ , \tag{2.93}$$

hence

$$\left[\frac{d}{dw}\left\{\frac{\partial \overline{x}_k}{\partial(\overline{x}_j + w\xi_j)}\right\}\right]_{w=0} = -\xi_{k,j}\ . \tag{2.94}$$

Equation (2.90) follows upon substituting (2.94) into $(2.91)_4$.

Return to the linearized statement of linear momentum balance (2.86) and taking into account (2.87), (2.88) and (2.90), it follows that

$$\begin{aligned}\overline{\operatorname{div}\mathbf{T}} + \operatorname{div}[D\mathbf{T}(\overline{\mathbf{x}},\boldsymbol{\xi})] - \operatorname{grad}\overline{\mathbf{T}}\cdot\operatorname{grad}^T\boldsymbol{\xi} + \overline{\rho\mathbf{b}} + \left\{-\overline{\rho}\operatorname{div}\boldsymbol{\xi}\overline{\mathbf{b}} + \overline{\rho}D\mathbf{b}(\overline{\mathbf{x}},\boldsymbol{\xi})\right\} \\ = \overline{\rho}\ddot{\overline{\mathbf{u}}} + \left\{-\overline{\rho}\operatorname{div}\boldsymbol{\xi}\ddot{\overline{\mathbf{u}}} + \overline{\rho}\ddot{\boldsymbol{\xi}}\right\}\ .\end{aligned} \tag{2.95}$$

Assuming that linear momentum balance holds in $\overline{\mathcal{R}}$, the preceding equation reduces to

$$\operatorname{div}[D\mathbf{T}(\overline{\mathbf{x}},\boldsymbol{\xi})] - \operatorname{grad}\overline{\mathbf{T}}\cdot\operatorname{grad}^T\boldsymbol{\xi} + \overline{\rho}\operatorname{div}\boldsymbol{\xi}(\ddot{\overline{\mathbf{u}}} - \overline{\mathbf{b}}) + \overline{\rho}D\mathbf{b}(\overline{\mathbf{x}},\boldsymbol{\xi}) = \overline{\rho}\ddot{\boldsymbol{\xi}} \tag{2.96}$$

or, equivalently,

$$\operatorname{div}[D\mathbf{T}(\overline{\mathbf{x}},\boldsymbol{\xi})] - \operatorname{grad}\overline{\mathbf{T}}\cdot\operatorname{grad}^T\boldsymbol{\xi} + \operatorname{div}\overline{\mathbf{T}}\operatorname{div}\boldsymbol{\xi} + \overline{\rho}D\mathbf{b}(\overline{\mathbf{x}},\boldsymbol{\xi}) = \overline{\rho}\ddot{\boldsymbol{\xi}}\ . \tag{2.97}$$

Assuming that the refefence configuration $\mathcal{R}_0$ is initial stress- and initial acceleration-free, it is immediately obvious from linear momentum balance that the body force vanishes as well in this configuration. As a result,

$$\mathcal{L}[\mathbf{T};\boldsymbol{\xi}]_{\mathbf{X}} = D\mathbf{T}(\mathbf{X},\boldsymbol{\xi}) = \boldsymbol{\sigma}\ , \tag{2.98}$$

$$\mathcal{L}[\ddot{\mathbf{u}};\boldsymbol{\xi}]_{\mathbf{X}} = D\ddot{\mathbf{u}}(\mathbf{X},\boldsymbol{\xi}) = \mathbf{a}\ , \tag{2.99}$$

[5] This point appears to have been overlooked in T.J.R. Hughes and K.S. Pister, "Consistent linearization in mechanics of solids and structures", *Comp. Struct.*, 8:391–397, (1978).

and

$$\mathcal{L}\left[\mathbf{b};\boldsymbol{\xi}\right]_{\mathbf{X}} \;=\; D\mathbf{b}(\overline{\mathbf{x}},\boldsymbol{\xi}) \;=\; \mathbf{b}\;. \tag{2.100}$$

It follows from (2.97) and the above three equations that the linearized statement of linear momentum balance with respect to $\mathcal{R}_0$ reduces to

$$\mathrm{Div}\,\boldsymbol{\sigma} + \rho_0\mathbf{b} \;=\; \rho_0\mathbf{a}\;. \tag{2.101}$$

Chapter 3

Incremental Formulations

A typical procedure for the solution of continuum mechanics problems using the finite element method starts with the derivation of a weak (*e.g.*, Galerkin) form of the governing (balance) equations from the original strong form. In general, the weak form comprises a set of integro-differential equations in space and time. Next, these equations are considered in a given time domain (real or implied by the application of the external loads). The solution of these equations is now performed by partitioning the time into time increments and deducing the solution from the beginning of the first time increment (where this solution is assumed to be given) to the end of the first time increment, and so on up to the end of the last increment. This process gives rise to the term *incremental formulation* for the solution of the continuum mechanics equations.

Each incremental solution requires that dependent variables of the problem be interpolated in space. This reduces the original integro-differential equations in space-time to merely differential equations in time. Upon observing that the incrementation in time induces a natural discretization, it follows that the preceding differential equations in time are further reduced to either implicit (generally, non-linear) algebraic equations or merely explicit equations. The solution to the former requires some iterative approach (*e.g.*, Newton-Raphson method or its variants), while the latter does not.

3.1 Strong and Weak Form of the Balance Laws

Consider a motion $\boldsymbol{\chi} : \mathcal{R}_0 \times \mathbb{R} \mapsto \mathcal{R} \subset \mathcal{E}^3$ of a body, as in (1.3), which is due to externally applied loads. Note that the preceding definition of this motion is predicated on the existence

of a reference configuration $\mathcal{R}_0$. In this case, recall that the displacement field $\mathbf{u}$ is defined as in (2.34), see also Figure 3.1. If a reference configuration is not available, then one needs to formulate the strong and weak forms of the initial/boundary-value problem without using (explicitly or implicitly) such a configuration.

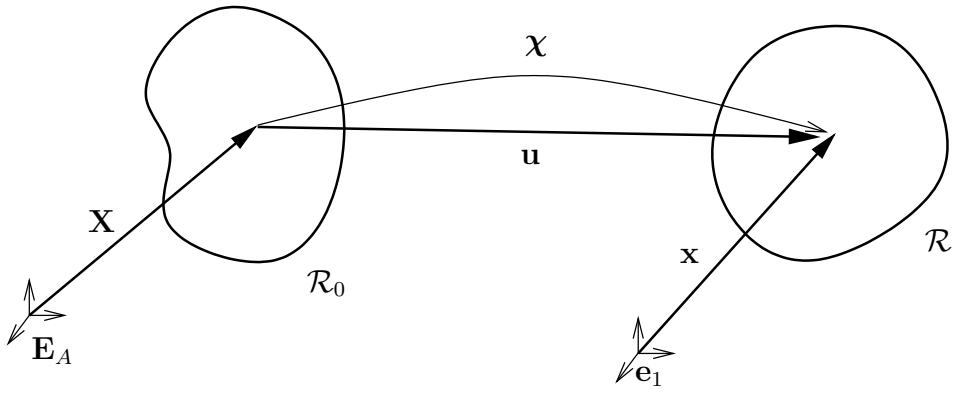

Figure 3.1. *Reference and current configuration*

Let the boundary $\partial\mathcal{R}$ of $\mathcal{R}$ be smooth enough for a unique outward unit normal $\mathbf{n}$ defined everywhere on $\partial\mathcal{R}$, as in Figure 3.2. Assume further that the boundary $\partial\mathcal{R}$ is decomposed into parts Γ_u and Γ_q such that at any time t

$$\partial\mathcal{R} \;=\; \overline{\Gamma_u \cup \Gamma_q}\,. \tag{3.1}$$

These two parts are defined as

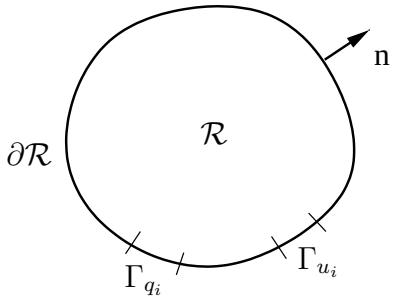

Figure 3.2. *Partition of boundary $\partial\mathcal{R}$ of $\mathcal{R}$*

$$\Gamma_u \;=\; \overline{\cup_{i=1}^{3}\Gamma_{u_i}} \qquad , \qquad \Gamma_q \;=\; \overline{\cup_{j=1}^{3}\Gamma_{q_j}}\,, \tag{3.2}$$

such that

$$u_i \;=\; \overline{u}_i(\mathbf{x},t) \text{ on } \Gamma_{u_i} \quad \text{(Dirichlet boundary conditions in solids)} \tag{3.3}$$

or

$$v_i \;=\; \overline{v}_i(\mathbf{x},t) \text{ on } \Gamma_{u_i} \quad \text{(Dirichlet boundary conditions in fluids)} \tag{3.4}$$

and

$$t_j \;=\; \bar{t}_j(\mathbf{x},t) \text{ on } \Gamma_{q_j} \quad \text{(Neumann boundary conditions)} \tag{3.5}$$

where $\overline{\mathbf{u}}$ (resp., $\overline{\mathbf{v}}$) and $\bar{\mathbf{t}}$ are the prescribed displacements (resp., velocities) and tractions on $\partial\mathcal{R}$ and

$$\Gamma_{u_i} \cap \Gamma_{q_i} \;=\; \emptyset \; . \tag{3.6}$$

Note that the components in (3.3-3.5) do not need to be those resolved on the basis vectors $\{\mathbf{e}_i\}$ associated with the current configuration.

The *strong form* of the general initial/boundary-value problem in continuum mechanics can be stated as follows: given the external forces and prescribed displacements (resp., velocities) $\mathbf{b}$, $\bar{\mathbf{t}}$, $\overline{\mathbf{u}}$ (resp., $\overline{\mathbf{v}}$) defined as above, the initial velocity and density fields $\mathbf{v}_0$ and ρ_0, and a constitutive law for the Cauchy stress tensor $\mathbf{T}$, such that $\mathbf{T} = \mathbf{T}^T$, determine the displacement field $\mathbf{u}$ such that $\det \dfrac{\partial(\mathbf{X}+\mathbf{u})}{\partial \mathbf{X}} > 0$ (or the velocity field $\mathbf{v}$) and the mass density $\rho > 0$, such that, for all t, linear momentum holds in the form (1.71) or (1.74) and mass balance holds in the form (1.66) or (1.63), subject to the boundary conditions (3.3) (or (3.4)) and (3.5), and the initial conditions

$$\mathbf{u}(\mathbf{X},0) \;=\; \mathbf{0} \quad , \quad \dot{\mathbf{u}}(\mathbf{X},0) \;=\; \mathbf{v}_0 \quad \text{in } \mathcal{R}_0 \tag{3.7}$$

for solids and

$$\mathbf{v}(\mathbf{x},0) \;=\; \mathbf{v}_0 \quad \text{in } \mathcal{R} \tag{3.8}$$

for fluids.

At every point $\mathbf{x}$ of the current configuration, define a *tangent vector* $\boldsymbol{\xi} = \tilde{\boldsymbol{\xi}}(\mathbf{x},t)$, that is any vector which originates at $\mathbf{x}$, as in Figure 3.3. Define the space of admissible tangent vector field $\mathcal{W}$ as

$$\mathcal{W} \;=\; \left\{ \boldsymbol{\xi} : \mathcal{R}\times\mathbb{R} \longrightarrow \mathcal{E}^3 \quad , \quad \tilde{\xi}_i(\mathbf{x},t) \;=\; 0 \text{ on } \Gamma_{u_i} \right\} \; , \tag{3.9}$$

that is, such that $\boldsymbol{\xi}$ vanishes identically where a displacement or velocity boundary condition is enforced.

Now define the weighted residual form

$$R \;=\; \int_{\mathcal{R}\times I} \boldsymbol{\xi}\cdot(\rho\ddot{\mathbf{u}} - \rho\mathbf{b} - \operatorname{div}\mathbf{T})\, dvdt + \int_{\Gamma_q\times I} \boldsymbol{\xi}\cdot(\mathbf{t}-\bar{\mathbf{t}})\, dadt \; , \tag{3.10}$$

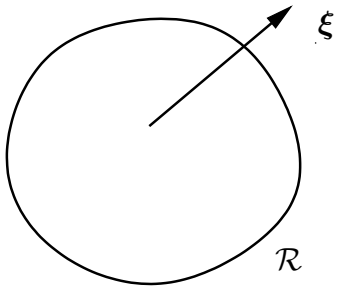

Figure 3.3. *Tangent vector at a point in the current configuration*

where $I = (t_0, T)$ is the time domain of the analysis. Note that the second integral on the right-hand side of (3.10) is understood as being a short-hand for $\sum_i \int_{\Gamma_{q,i}} \xi_i(t_i - \bar{t}_i)\, dadt$, that is, it includes the contributions of all the components of the prescribed traction in all of their directions.

The *weak form* of the general initial/boundary-value problem in continuum mechanics reads as follows: given the external forces $\mathbf{b}$ and $\bar{\mathbf{t}}$, a constitutive law for $\mathbf{T}$, such that $\mathbf{T}^T = \mathbf{T}$, find the displacement field $\mathbf{u} \in \mathcal{U}$ (or the velocity field $\mathbf{v} \in \mathcal{V}$), such that

$$R \;=\; 0 \tag{3.11}$$

for all $\boldsymbol{\xi} \in \mathcal{W}$. Here,

$$\mathcal{U} \;=\; \left\{ \mathbf{u} : \mathcal{R}_0 \times \mathbb{R} \to \mathcal{E}^3 \;|\; \det\left(\mathbf{I} + \frac{\partial \mathbf{u}}{\partial \mathbf{X}}\right) > 0 \;,\; u_i(\mathbf{X}, t) \;=\; \overline{u}_i \text{ on } \Gamma_{u_i} \;, \right.$$
$$\left. \mathbf{u}(\mathbf{X}, 0) \;=\; \mathbf{0} \;,\; \dot{\mathbf{u}}(\mathbf{X}, 0) \;=\; \mathbf{v}_0 \right\} \tag{3.12}$$

for solids and

$$\mathcal{V} \;=\; \left\{ \mathbf{v} : \mathcal{R} \times \mathbb{R} \to \mathcal{E}^3 \;|\; v_i(\mathbf{x}, t) \;=\; \overline{v}_i \text{ on } \Gamma_{u_i} \;,\; \mathbf{v}(\mathbf{x}, 0) = \mathbf{v}_0 \right\} \tag{3.13}$$

for fluids. In the solids problem, mass conservation is enforced trivially, in the sense that, given $\rho_0 > 0$ at time t_0, one may find ρ as a function of ρ_0 and the deformation, according to (1.63). Therefore, there is no need for mass conservation to be enforced through the weak form. On the contrary, in fluid mechanics, one needs to additionally enforce mass conservation according to (1.66). To achieve this, the weighted residual R of (3.10) must be amended by an additional term as

$$R \;=\; \int_{\mathcal{R}\times I} \boldsymbol{\xi} \cdot (\rho \ddot{\mathbf{u}} - \rho \mathbf{b} - \operatorname{div} \mathbf{T})\, dvdt + \int_{\Gamma_q \times I} \boldsymbol{\xi} \cdot (\mathbf{t} - \bar{\mathbf{t}})\, dadt + \int_{\mathcal{R}\times I} \sigma(\dot{\rho} + \rho \operatorname{div} \mathbf{v})\, dvdt \;, \tag{3.14}$$

such that a solution $(\mathbf{v}, p) \in \mathcal{V} \times \mathcal{Z}^+$ is sought by enforcing (3.11) for all $(\boldsymbol{\xi}, \sigma) \in \mathcal{W} \times \mathcal{Z}$, where

$$\mathcal{Z} \;=\; \{\sigma : \mathcal{R} \times \mathbb{R} \to \mathbb{R}\} \quad , \quad \mathcal{Z}^+ \;=\; \{\sigma : \mathcal{R} \times \mathbb{R} \to \mathbb{R} \mid \sigma > 0\} \;. \tag{3.15}$$

Additional assumptions on smoothness are required for the functions in $\mathcal{U}$, $\mathcal{V}$,$\mathcal{W}$,$\mathcal{Z}$ in order to guarantee the existence of the integrals which comprise R in (3.14). These requirements will be discussed when introducing finite element counterparts of these spaces.

It is worth observing here that the balance of linear momentum (as well as the mass balance in fluids) and the traction boundary conditions are enforced through the weighted residual form. On the other hand, the displacement (or velocity) boundary conditions and initial conditions are satisfied from the outset by the choice of admissible fields $\mathcal{U}$ or $\mathcal{V}$. In addition, balance of angular momentum is satisfied by the constitutive law for stress.

The above strong and weak form are equivalent (that is, derivable from each other) only under the assumption of continuity of all integrands in (3.10) or (3.14). This is a fairly severe assumption, which, when violated, leads to solutions obtained from the weak form (termed *weak solutions*) that may differ from the *strong solution* where/when discontinuities are encountered.

The complete proof of the preceding result may be found elsewhere. Here, only a sketch of the proof is provided, as follows: first, it is clear by inspection that the strong form implies the weak form. for the opposite, note that (3.10) (or (3.14)) applies for *any* $\xi \in \mathcal{W}$ (and, $\sigma \in \mathcal{Z}$, if applicable). Now fix a time t and choose $\boldsymbol{\xi}$ such that $\boldsymbol{\xi} = \mathbf{0}$ on Γ_q (and also $\sigma = 0$ on $\mathcal{R}$, if applicable). Next, argue, by contradiction, that if there is a point $\mathbf{x} \in \mathcal{R}$ where $\rho\mathbf{a} - \rho\mathbf{b} - \operatorname{div}\mathbf{T} \neq \mathbf{0}$, then one may choose $\boldsymbol{\xi}$ to vanish everywhere and every time except in a neighborhood $\mathcal{N}_\mathbf{x}$ of $\mathbf{x}$ in which $\boldsymbol{\xi} \cdot (\rho\mathbf{a} - \rho\mathbf{b} - \operatorname{div}\mathbf{T}) > \mathbf{0}$, which is always possible due to the continuity of the preceding scalar quantity. It follows that $\int_{\mathcal{R}\times I} \boldsymbol{\xi} \cdot (\rho\mathbf{a} - \rho\mathbf{b} - \operatorname{div}\mathbf{T})\, dvdt > 0$, which contradicts the original assumption, thus $\rho\mathbf{a} - \rho\mathbf{b} - \operatorname{div}\mathbf{T} = \mathbf{0}$ everywhere in $\mathcal{R}$ at all times t. Then, the same argument may be repeated on Γ_q (as well as on $\mathcal{R}$ for the continuity equation in (3.14), if applicable).

Proceed with separating the space from the time integrals in the weighted residual form (3.10), and consider first the spatial integrals (that is, "freeze" time). In particular, set

$$\int_\mathcal{R} \boldsymbol{\xi} \cdot (\rho\ddot{\mathbf{u}} - \rho\mathbf{b} - \operatorname{div}\mathbf{T})\, dv + \int_{\Gamma_q} \boldsymbol{\xi} \cdot (\mathbf{t} - \bar{\mathbf{t}})\, da \;=\; 0 \tag{3.16}$$

and note that, upon using integration by parts, the divergence theorem, and the property

of $\boldsymbol{\xi}$ specified in (3.9)

$$\begin{aligned}\int_{\mathcal{R}} \boldsymbol{\xi}\cdot\operatorname{div}\mathbf{T}\,dv &= \int_{\mathcal{R}} \xi_i T_{ij,j}\,dv = \int_{\mathcal{R}} \left[(\xi_i T_{ij})_{,j} - \xi_{i,j}T_{ij}\right]\,dv \\ &= \int_{\partial\mathcal{R}} \xi_i T_{ij} n_j\,da - \int_{\mathcal{R}} \xi_{i,j}T_{ij}\,dv \\ &= \int_{\overline{\Gamma_u\cup\Gamma_q}} \xi_i T_{ij} n_j\,da - \int_{\mathcal{R}} \xi_{i,j}T_{ij}\,dv \\ &= \int_{\Gamma_q} \xi_i t_i da - \int_{\mathcal{R}} \xi_{i,j}T_{ij}\,dv \\ &= \int_{\Gamma_q} \boldsymbol{\xi}\cdot\mathbf{t}\,da - \int_{\mathcal{R}} \frac{\partial\boldsymbol{\xi}}{\partial\mathbf{x}}\cdot\mathbf{T}\,dv\ . \end{aligned} \tag{3.17}$$

Substituting the preceding expression to the weighted-residual form (3.16), it follows that

$$\int_{\mathcal{R}} \boldsymbol{\xi}\cdot\rho\ddot{\mathbf{u}}\,dv + \int_{\mathcal{R}} \frac{\partial\boldsymbol{\xi}}{\partial\mathbf{x}}\cdot\mathbf{T}\,dv = \int_{\mathcal{R}} \boldsymbol{\xi}\cdot\rho\mathbf{b}\,dv + \int_{\Gamma_q} \boldsymbol{\xi}\cdot\bar{\mathbf{t}}\,da \tag{3.18}$$

The full space-time integral form can be easily reconstructed from the above. Observing the symmetry of $\mathbf{T}$, the second term on the left-hand side of (3.18) can be also written as $\int_{\mathcal{R}} \left(\frac{\partial\boldsymbol{\xi}}{\partial\mathbf{x}}\right)^s \cdot \mathbf{T}\,dv$ The above expression is computationally convenient, as it involves the term

$$\left(\frac{\partial\boldsymbol{\xi}}{\partial\mathbf{x}}\right)^s = \frac{1}{2}\left[\frac{\partial\boldsymbol{\xi}}{\partial\mathbf{x}} + \left(\frac{\partial\boldsymbol{\xi}}{\partial\mathbf{x}}\right)^T\right] \tag{3.19}$$

which resembles the infinitesimal strain tensor. This observation is important when attempting to extend finite element formulations originally developed for infinitesimal deformations to finite deformations.

If $\boldsymbol{\xi}$ is identified as the *variation* $\delta\mathbf{u}$[1] of $\mathbf{u}$, one obtains a *statement of virtual work*, according to which the virtual work done by the internal forces (inertial forces and stresses) is equal to the virtual work done by the external forces (body forces and surface tractions) over the whole body occupying the configuration $\mathcal{R}$. A corresponding *statement of virtual power* is obtained from (3.18) when $\boldsymbol{\xi}$ is substituted with a virtual velocity. It is instructive to contrast these statements to the mechanical energy balance equation for the whole body, see (1.80).

One may assume at the outset that the traction boundary conditions (3.5) are satisfied at the outset and do not need to be included in the weighted residual form (3.10). While

[1]Recall that, by definition, the variation of $\mathbf{u}$ vanishes where $\mathbf{u}$ is specified, which confirms that the space of admissible variations of $\mathbf{u}$ is precisely $\mathcal{W}$.

this goes against the premise of finite element modeling (where one may one directly impose boundary conditions on the dependent variables that enter the finite element approximation), it is instructive to consider this option, where the weighted-residual statement is reduced

$$\int_{\mathcal{R}} \boldsymbol{\xi} \cdot (\rho \mathbf{a} - \rho \mathbf{b} - \operatorname{div} \mathbf{T})\, dv \;=\; 0 \tag{3.20}$$

for all $\boldsymbol{\xi} \in \mathcal{W}$. Repeating the preceding procedure leads to:

$$\int_{\mathcal{R}} \boldsymbol{\xi} \cdot \rho \mathbf{a}\, dv + \int_{\mathcal{R}} \frac{\partial \boldsymbol{\xi}}{\partial \mathbf{x}} \cdot \mathbf{T}\, dv \;=\; \int_{\mathcal{R}} \boldsymbol{\xi} \cdot \rho \mathbf{b}\, dv + \int_{\Gamma_q} \boldsymbol{\xi} \cdot \mathbf{t}\, da \;. \tag{3.21}$$

Upon now enforcing (3.5), one immediately recovers the derived weighted-residual statement in (3.18).

A completely equivalent weighted-residual form can be derived based on the referential statement of linear momentum balance (1.74). In this case, one observes that the tangent vector $\boldsymbol{\xi}$ may be represented as

$$\boldsymbol{\xi} \;=\; \hat{\boldsymbol{\xi}}(\mathbf{X}, t) \;=\; \tilde{\boldsymbol{\xi}}(\mathbf{x}, t) \;. \tag{3.22}$$

Next, "freeze" again time and start from the weighted residual statement

$$R_0 \;=\; \int_{\mathcal{R}_0} \boldsymbol{\xi} \cdot (\rho_0 \mathbf{a} - \rho_0 \mathbf{b} - \operatorname{Div} \mathbf{P})\, dV + \int_{\Gamma_{q_0}} \boldsymbol{\xi} \cdot (\mathbf{p} - \overline{\mathbf{p}})\, dA \;=\; 0 \;, \tag{3.23}$$

for all $\boldsymbol{\xi} \in \mathcal{W}$, where $\mathbf{p} = \mathbf{P}\mathbf{N}$ is the traction vector on the boundary of the body in the current configuration, but resolved using the geometry of the reference configuration. Repeating the same procedure as with the spatial weak form, it is easy to show that

$$\int_{\mathcal{R}_0} \boldsymbol{\xi} \cdot \rho_0 \mathbf{a}\, dV + \int_{\mathcal{R}_0} \frac{\partial \boldsymbol{\xi}}{\partial \mathbf{X}} \cdot \mathbf{P}\, dV \;=\; \int_{\mathcal{R}_0} \boldsymbol{\xi} \cdot \rho_0 \mathbf{b}\, dV + \int_{\Gamma_{q_0}} \boldsymbol{\xi} \cdot \overline{\mathbf{p}}\, dA \;. \tag{3.24}$$

Recalling (2.36), it is concluded that the integrand of the second term on the left-hand side of (3.24) satisfies

$$\frac{\partial \boldsymbol{\xi}}{\partial \mathbf{X}} \cdot \mathbf{P} \;=\; D\mathbf{F}(\mathbf{X}, \boldsymbol{\xi}) \cdot \mathbf{P} \;. \tag{3.25}$$

Furthermore,

$$\begin{aligned} \frac{\partial \boldsymbol{\xi}}{\partial \mathbf{X}} \cdot \mathbf{P} \;=\; \frac{\partial \boldsymbol{\xi}}{\partial \mathbf{X}} \cdot (\mathbf{F}\mathbf{S}) \;&=\; \left(\mathbf{F}^T \frac{\partial \boldsymbol{\xi}}{\partial \mathbf{X}} \right) \cdot \mathbf{S} \\ &=\; \frac{1}{2} \left[\mathbf{F}^T \frac{\partial \boldsymbol{\xi}}{\partial \mathbf{X}} + \left(\frac{\partial \boldsymbol{\xi}}{\partial \mathbf{X}} \right)^T \mathbf{F} \right] \cdot \mathbf{S} \;=\; D\mathbf{E}(\mathbf{x}, \boldsymbol{\xi}) \cdot \mathbf{S} \;, \end{aligned} \tag{3.26}$$

where use is made of (1.85), (2.41), and the symmetry of $\mathbf{S}$.

3.2 Lagrangian and Eulerian Methods

Preliminary to the presentation of any specific finite element methods, it is essential to formally distinguish between Lagrangian and Eulerian computations. To this end, consider a body occupying the configuration $\mathcal{R}$ at time and define a surface $\mathcal{S}(t)$, as in Figure 3.4, which may be represented by the parametric equation

$$\mathbf{x}_s \;=\; \mathbf{x}_s(\xi, \eta, t) \;, \tag{3.27}$$

where ξ, η are surface parameters. These parameters may be eliminated to obtain an alter-

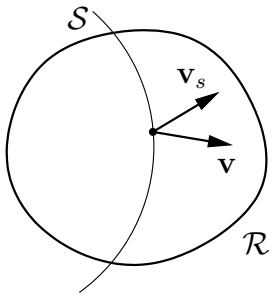

Figure 3.4. *A surface $\mathcal{S}$ traversing the configuration $\mathcal{R}$ at time t*

native representation of the surface as

$$f(\mathbf{x}_s, t) \;=\; 0 \;. \tag{3.28}$$

Taking the time derivative of the above equation, while following any given point on the surface, it follows that

$$\frac{\partial f}{\partial t} + \frac{\partial f}{\partial \mathbf{x}} \cdot \mathbf{v}_s \;=\; 0 \;, \tag{3.29}$$

where $\mathbf{v}_s$ is the velocity of the surface, see Figure (3.4), which can be readily obtained from (3.27). Alternatively, consider a material point which occupies a point $\mathbf{x} \in \mathcal{S}$ at time t. The material time derivative of f describes the rate of change of f for the given material point. This equals

$$\dot{f} \;=\; \frac{\partial f}{\partial t} + \frac{\partial f}{\partial \mathbf{x}} \cdot \mathbf{v} \;, \tag{3.30}$$

where $\mathbf{v} = \dot{\boldsymbol{\chi}}$ is the velocity of the particle, see, again, Figure 3.4. Generally, at the fixed time t, $\mathbf{v}_s \neq \mathbf{v}$. Hence, subtracting (3.29) from (3.30), it follows that

$$\dot{f} \;=\; \frac{\partial f}{\partial \mathbf{x}} \cdot (\mathbf{v} - \mathbf{v}_s) \tag{3.31}$$

and, since the unit normal $\mathbf{n}$ to the surface may be written as

$$\mathbf{n} \;=\; \frac{\frac{\partial f}{\partial \mathbf{x}}}{\left|\frac{\partial f}{\partial \mathbf{x}}\right|} \;, \tag{3.32}$$

it is concluded that the flux of mass through the surface $\mathcal{S}$ at time t is given by

$$\int_{\mathcal{S}} \rho(\mathbf{v}-\mathbf{v}_s)\cdot\mathbf{n}\, da \;=\; \int_{\mathcal{S}} \rho \dot{f} \left|\frac{\partial f}{\partial \mathbf{x}}\right|^{-1} da \;. \tag{3.33}$$

Upon invoking the localization theorem, it follows from the above that the necessary and sufficient condition for the flux of mass through $\mathcal{S}$ (or any part of it) to vanishes is $\dot{f}=0$, in which case

$$(\mathbf{v}-\mathbf{v}_s)\cdot\mathbf{n} \;=\; 0 \;. \tag{3.34}$$

This mandates that the surface $\mathcal{S}$ and the material particles on it travel with the same normal velocity to $\mathcal{S}$. In this case, the surface $\mathcal{S}$ is called a *material surface*. The necessary and sufficient condition

$$\dot{f} \;=\; 0 \tag{3.35}$$

is referred to as *Lagrange's criterion of materiality*.

Assume that at any given time t the region $\mathcal{R}$ is spatially discretized according to $\mathcal{R} \doteq \cup_e \Omega^e$, where Ω^e is the domain of the typical finite element e, such that all bound-

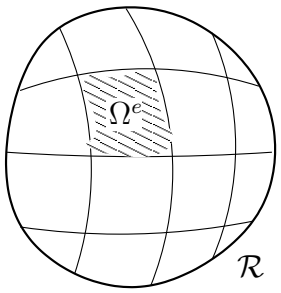

Figure 3.5. *Finite element mesh schematic*

ary surfaces (or edges) of each Ω^e are material. Lagrangian finite element computations are making use of finite elements with domains whose boundaries are material.

To understand how it can be guaranteed that the boundary of a finite element domain are material, note that in Lagrangian finite element computations the motion of the element is completely parametrized by the motion of its nodal points. Hence, the finite element system

is finite-dimensional, in the sense that the motion of the discretized body is fully determined at any given time t by a finite set of parameters.

Consider a typical surface $\mathcal{S}$ of a finite element domain Ω^e, in the context of classical isoparametric interpolations. For a typical point $\mathbf{X}$ on $\mathcal{S}$ in the reference configuration, one may write

$$\mathbf{X} \;=\; \sum_i N_i(\xi,\eta)\mathbf{X}_i \tag{3.36}$$

where (ξ,η) are the natural coordinates (which coincide, here, with the surface coordinates),

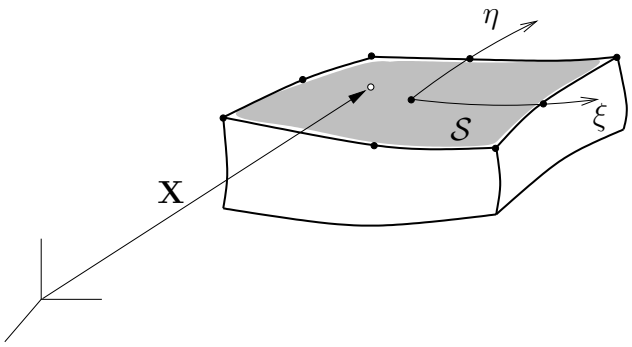

Figure 3.6. *Lagrangian finite element surface*

N_i are the isoparametric shape functions, and $\mathbf{X}_i$ the position vector of node i on $\mathcal{S}$, as in Figure 3.6. The point $\mathbf{X}$ is mapped in the current configuration to $\mathbf{x} = \boldsymbol{\chi}(\mathbf{X},t)$, such that

$$\begin{aligned}
\mathbf{x} \;&=\; \sum_i N_i(\xi,\eta)\mathbf{x}_i \\
&=\; \sum_i N_i(\xi,\eta)\boldsymbol{\chi}(\mathbf{X}_i,t) \\
&=\; \sum_i N_i(\xi,\eta)\,[\mathbf{X}_i + \mathbf{u}_i] \\
&=\; \sum_i N_i(\xi,\eta)\mathbf{X}_i + \sum_i N_i(\xi,\eta)\mathbf{u}_i \;=\; \mathbf{X} + \mathbf{u}\;.
\end{aligned} \tag{3.37}$$

The surface $\mathcal{S}$ is clearly material, since it consists of the same material points at all times with respect to the motion $\boldsymbol{\chi}$ of the nodal points i and the isoparametric interpolation. Put differently, all $\mathbf{x}_i$ are material points by definition, while any $\mathbf{x}$ on $\mathcal{S}$ is also material by construction of the motion in terms of the nodal motions and the isoparametric interpolation.

Alternatively, one may consider an Eulerian finite element formulation for which the mesh is stationary, that is $\mathbf{v}_s = \mathbf{0}$ on the boundary $\partial\Omega^e$ of any element element e. In this case, each element becomes a *control volume*. In view of (3.34) it is clear that the element

region Ω^e is not material. Thus, mass flux takes place across $\partial\Omega^e$, which necessitates that mass balance be enforced through the equation

$$\int_{\Omega^e} \sigma(\dot{\rho} + \rho \operatorname{div} \mathbf{v})\, dv \;=\; 0 \;, \tag{3.38}$$

for all admissible σ, as also argued earlier (see (3.14)).

Lagrangian and Eulerian methods have both advantages and disadvantages from an algorithmic standpoint. For instance, when Eulerian methods are used for solids or free-surface fluids, then

(a) A geometric detection algorithm is required to identify the "full" elements at each time t, see Figure 3.7.

(b) A special treatment is generally needed for "partial" element at each time t, see again Figure 3.7.

(c) The application of Dirichlet conditions on the physical boundary is not necessarily trivial.

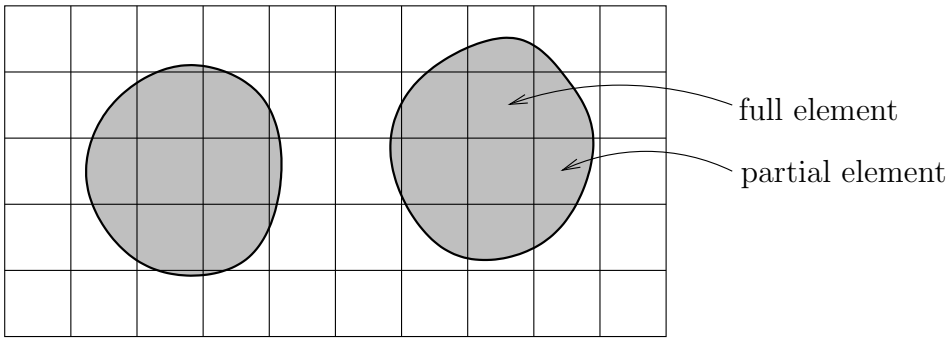

Figure 3.7. *Eulerian finite element mesh with a moving solid or fluid*

Moreover, the tracking of material-based history variables requires a special procedure, since such variables cannot be directly stored at nodal or integration points.

Lagrangian methods suffer from excessive mesh distortion, which may cause loss of uniqueness in the isoparametric mapping, as well as from inability to directly handle loss of materiality, as is the case, for instance, when modeling crack propagation or fragmentation.

3.3 Semi-discretization

As done earlier, it is customary (and practical) to separate the time from the space integrals in (3.14), which often referred to as *semi-discretization*. Assuming that the solution must be determined in the time domain $(t_0, T]$, perform a time discretization by introducing a finite sequence of distinct times $t_1, t_2, ..., t_N$, as in Figure 3.8. Here, $\Delta t_n = t_{n+1} - t_n$ is the discrete

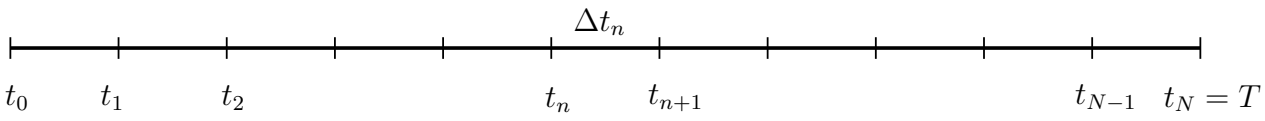

Figure 3.8. *Time discretization*

time step at time t_n and

$$\Delta t \;=\; \frac{\sum_{n=1}^{N} \Delta t_{n-1}}{N} \;=\; \frac{T - t_0}{N} \tag{3.39}$$

is the average step size, with the understanding that $\Delta t_n = O(\Delta t)$, $n = 0, 1, \ldots, N-1$.

The basic idea of incremental methods is to satisfy the equations of motion only at discrete time instances $t_1, t_2, ..., t_N$, where at each such t_{n+1}, the solution to these equations is known for all t_i, $i = 1, 2, \ldots, n$. In the limit as $N \to \infty$, incremental methods recover a solution in a dense subset of $(t_0, T]$.

Incremental methods make sense on two grounds. First, they recover the history of a deformation, which is oftentimes, in itself, useful to the analyst. Second, they are necessary when modeling continua made of path-dependent material or which are subject to path-dependent loading. In the latter case, iterative methods are essentially used to resolve the path-dependency.

A weighted-residual interpretation of semi-discretization can be obtained by starting from (3.10) (similarly, for (3.14)) and writing $\boldsymbol{\xi}(\mathbf{x}, \mathbf{t}) = \theta(t)\boldsymbol{\xi}(\mathbf{x})$, such that

$$R \;=\; \int_{t_0}^{T} \theta \left[\int_{\mathcal{R}} \boldsymbol{\xi} \cdot (\rho \mathbf{a} - \rho \mathbf{b} - \operatorname{div} \mathbf{T})\, dv + \int_{\Gamma_q} \boldsymbol{\xi} \cdot (\mathbf{t} - \overline{\mathbf{t}})\, da \right] dt \;= 0 \;, \tag{3.40}$$

where the time-dependent weighting function $\theta(t)$ is defined as $\theta(t) = \sum_{i=1}^{N} \theta_i \delta(t - t_i)$. This discretization leads naturally to the requirement that linear momentum balance and traction boundary conditions must be enforced at each of the times $t_1, t_2, ..., t_N$.

3.4 Total and Updated Lagrangian Methods

Consider an incremental Lagrangian method and assume that the balance laws have been already satisfied (in a weak form) and the motion $\boldsymbol{\chi}$ has been determined for times $t_1, t_2, ..., t_n$, see Figure 3.9. The objective is now to determine the position of all material particles (therefore, the configuration of the body) at $t = t_{n+1}$, such that

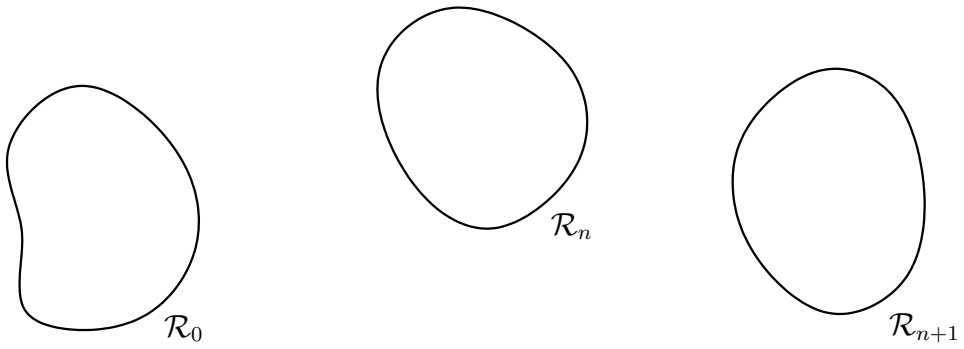

Figure 3.9. *Configurations at times t_0, t_n and t_{n+1}*

$$\int_{\mathcal{R}_{n+1}} \boldsymbol{\xi}_{n+1} \cdot \rho_{n+1} \mathbf{a}_{n+1}\, dv + \int_{\mathcal{R}_{n+1}} \left(\frac{\partial \boldsymbol{\xi}}{\partial \mathbf{x}}\right)^s_{n+1} \cdot \mathbf{T}_{n+1}\, dv = \int_{\mathcal{R}_{n+1}} \boldsymbol{\xi}_{n+1} \cdot \rho_{n+1} \mathbf{b}_{n+1}\, dv + \int_{\Gamma_{q_{n+1}}} \boldsymbol{\xi}_{n+1} \cdot \overline{\mathbf{t}}_{n+1}\, da\ , \quad (3.41)$$

for all $\boldsymbol{\xi}_{n+1} \in \mathcal{W}$. The preceding equation may be resolved iteratively for the displacement field $\mathbf{u}_{n+1} \in \mathcal{U}$ (or, equivalently, the relative displacement field $\mathbf{u}_{n+1} - \mathbf{u}_n$), assuming the data (that is, $\mathbf{b}$ and $\overline{\mathbf{t}}$) is known in $(t_n, t_{n+1}]$.

Alternatively, one may pull-back (3.41) to the reference configuration and write

$$\int_{\mathcal{R}_0} \boldsymbol{\xi}_{n+1} \cdot \rho_0 \mathbf{a}_{n+1}\, dV + \int_{\mathcal{R}_0} \frac{\partial \boldsymbol{\xi}_{n+1}}{\partial \mathbf{X}} \cdot \mathbf{P}_{n+1}\, dV = \int_{\mathcal{R}_0} \boldsymbol{\xi}_{n+1} \cdot \rho_0 \mathbf{b}_{n+1}\, dV + \int_{\Gamma_{q_0}} \boldsymbol{\xi}_{n+1} \cdot \overline{\mathbf{p}}_{n+1}\, dA\ , \quad (3.42)$$

for all $\boldsymbol{\xi}_{n+1} \in \mathcal{W}$. Note that, since, in general, Γ_q depends on time, by Γ_{q_0} in (3.42), one denotes the pull-back of $\Gamma_{q_{n+1}}$ to the reference configuration, rather than the traction boundary of the reference configuration itself.

Starting with the referential weak form (3.42), concentrate on a typical Lagrangian finite element e with domain Ω_0^e in the reference configuration. For this element, write at $t = t_{n+1}$

$$\begin{aligned}
\mathbf{u}(\mathbf{X}, t_{n+1})\big|_{\Omega_0^e} &= \mathbf{u}^e_{n+1}(\mathbf{X}) \doteq \sum_{i=1}^{\texttt{NEN}} N_i^e \mathbf{u}^e_{i\,n+1} \ , \\
\mathbf{a}_{n+1}(\mathbf{X}, t_{n+1})\big|_{\Omega_0^e} &= \mathbf{a}^e_{n+1}(\mathbf{X}) \doteq \sum_{i=1}^{\texttt{NEN}} N_i^e \mathbf{a}^e_{i\,n+1} \ , \\
\boldsymbol{\xi}_{n+1}(\mathbf{X}, t_{n+1})\big|_{\Omega_0^e} &= \boldsymbol{\xi}^e_{n+1}(\mathbf{X}) \doteq \sum_{i=1}^{\texttt{NEN}} N_i^e \boldsymbol{\xi}^e_{i\,n+1} \ ,
\end{aligned} \tag{3.43}$$

where the element is assumed isoparametric with NEN nodes and interpolation functions $N_i^e(\mathbf{X})$, $i = 1, 2 \ldots, \texttt{NEN}$. Special cases, such as those involving hierarchical, mixed or incompatible interpolations can be easily handled by extending the above definitions.

For ease of computer implementation, one may write the preceding interpolations in matrix form as

$$\begin{aligned}
\mathbf{u}^e_{n+1} &\doteq \sum_{i=1}^{\texttt{NEN}} N_i^e \mathbf{u}^e_{i\,n+1} \\
&= \underbrace{\Big[\underbrace{N_1^e \mathbf{1}_3}_{(3\times 3)} \quad N_2^e \mathbf{1}_3 \quad \cdots \quad N_{\texttt{NEN}}^e \mathbf{1}_3\Big]}_{3\times(3\times\texttt{NEN})} \underbrace{\begin{bmatrix} \mathbf{u}_1^e \\ \mathbf{u}_2^e \\ \vdots \\ \mathbf{u}_{\texttt{NEN}}^e \end{bmatrix}_{n+1}}_{(3\times\texttt{NEN})\times 1} = [\mathbf{N}^e][\hat{\mathbf{u}}^e_{n+1}] \ ,
\end{aligned} \tag{3.44}$$

where $[\hat{\mathbf{u}}^e_{n+1}]$ is a vector that contains all nodal displacements, while $\mathbf{1}_3$ denotes the 3×3 identity matrix. Similarly, one may write

$$\mathbf{a}^e_{n+1} \doteq [\mathbf{N}^e][\hat{\mathbf{a}}^e_{n+1}] \quad , \quad \boldsymbol{\xi}^e_{n+1} \doteq [\mathbf{N}^e][\hat{\boldsymbol{\xi}}^e_{n+1}] \ . \tag{3.45}$$

Also, to resolve in convenient matrix form the stress $\mathbf{P}_{n+1}$ and the derivative $\frac{\partial \boldsymbol{\xi}^e_{n+1}}{\partial \mathbf{X}}$ in (3.42),

write their 9 components as column vectors according to

$$\langle \mathbf{P}_{n+1} \rangle = \begin{bmatrix} P_{11} \\ P_{22} \\ P_{33} \\ P_{12} \\ P_{23} \\ P_{31} \\ P_{13} \\ P_{21} \\ P_{32} \end{bmatrix}_{n+1} , \quad \left\langle \frac{\partial \boldsymbol{\xi}^e_{n+1}}{\partial \mathbf{X}} \right\rangle = \begin{bmatrix} \xi^e_{1,1} \\ \xi^e_{2,2} \\ \xi^e_{3,3} \\ \xi^e_{1,2} \\ \xi^e_{2,3} \\ \xi^e_{3,1} \\ \xi^e_{1,3} \\ \xi^e_{2,1} \\ \xi^e_{3,2} \end{bmatrix}_{n+1} . \tag{3.46}$$

Thus, one may write

$$\underbrace{\left\langle \frac{\partial \boldsymbol{\xi}^e_{n+1}}{\partial \mathbf{X}} \right\rangle}_{(9\times 1)} = \underbrace{[\mathbf{B}^e]}_{9\times(3\times \mathtt{NEN})} \underbrace{[\hat{\boldsymbol{\xi}}^e_{n+1}]}_{(3\times \mathtt{NEN})\times 1} , \tag{3.47}$$

where

$$\underbrace{[\mathbf{B}^e]}_{9\times(3\times \mathtt{NEN})} = \Big[\underbrace{[\mathbf{B}^e_1]}_{(9\times 3)} \quad [\mathbf{B}^e_2] \quad \cdots \quad [\mathbf{B}^e_{\mathtt{NEN}}] \Big] \tag{3.48}$$

and $[\mathbf{B}^e_i]$ is such that

$$< \mathbf{B}^e_i \hat{\boldsymbol{\xi}}^e_{i_{n+1}} > = \begin{bmatrix} N^e_{i,1}\xi^e_{i_1} \\ N^e_{i,2}\xi^e_{i_2} \\ N^e_{i,3}\xi^e_{i_3} \\ N^e_{i,2}\xi^e_{i_1} \\ N^e_{i,3}\xi^e_{i_2} \\ N^e_{i,1}\xi^e_{i_3} \\ N^e_{i,3}\xi^e_{i_1} \\ N^e_{i,1}\xi^e_{i_2} \\ N^e_{i,2}\xi^e_{i_3} \end{bmatrix}_{n+1} \quad \text{(no summation on } i) , \tag{3.49}$$

consequently

$$\underbrace{[\mathbf{B}_i^e]}_{9\times 3} = \begin{bmatrix} N_{i,1}^e & & \\ & N_{i,2}^e & \\ & & N_{i,3}^e \\ N_{i,2}^e & & \\ & N_{i,3}^e & \\ & & N_{i,1}^e \\ N_{i,3}^e & & \\ & N_{i,1}^e & \\ & & N_{i,2}^e \end{bmatrix}, \tag{3.50}$$

where $N_{i,A}^e = \frac{\partial N_i^e}{\partial X_A}$.

Likewise, to express the spatial statement (3.41) in matrix form, one need to express the (symmetric) stress $\mathbf{T}_{n+1}$ and the derivative $\left(\frac{\partial \boldsymbol{\xi}_{n+1}^e}{\partial \mathbf{x}}\right)^s$ as 6-dimensional vectors according to

$$\langle \mathbf{T}_{n+1} \rangle = \begin{bmatrix} T_{11} \\ T_{22} \\ T_{33} \\ T_{12} \\ T_{23} \\ T_{31} \end{bmatrix}_{n+1}, \quad \left\langle \left(\frac{\partial \boldsymbol{\xi}^e}{\partial \mathbf{x}}\right)_{n+1}^s \right\rangle = \begin{bmatrix} \xi_{1,1}^e \\ \xi_{2,2}^e \\ \xi_{3,3}^e \\ \xi_{1,2}^e + \xi_{2,1}^e \\ \xi_{2,3}^e + \xi_{3,2}^e \\ \xi_{3,1}^e + \xi_{1,3}^e \end{bmatrix}_{n+1}. \tag{3.51}$$

It follows that

$$\begin{aligned} \underbrace{\left\langle \left(\frac{\partial \boldsymbol{\xi}^e}{\partial \mathbf{x}}\right)_{n+1}^s \right\rangle}_{6\times 1} &= \underbrace{[\mathbf{B}_{n+1}^e]}_{6\times(3\times \mathtt{NEN})} \underbrace{[\hat{\boldsymbol{\xi}}_{n+1}^e]}_{(3\times \mathtt{NEN})\times 1} \\ &= \left[\underbrace{[\mathbf{B}_{1,n+1}^e]}_{6\times 3} \quad [\mathbf{B}_{2,n+1}^e] \quad \cdots \quad [\mathbf{B}_{\mathtt{NEN},n+1}^e]\right] \begin{bmatrix} \boldsymbol{\xi}_1^e \\ \boldsymbol{\xi}_2^e \\ \vdots \\ \boldsymbol{\xi}_{\mathtt{NEN}}^e \end{bmatrix}_{n+1}, \end{aligned} \tag{3.52}$$

where

$$\underbrace{[\mathbf{B}^e_{i,n+1}]}_{6\times 3} = \begin{bmatrix} N^e_{i,1} & & \\ & N^e_{i,2} & \\ & & N^e_{i,3} \\ N^e_{i,2} & N^e_{i,1} & \\ & N^e_{i,3} & N^e_{i,2} \\ N^e_{i,3} & & N^e_{i,1} \end{bmatrix}_{n+1} \tag{3.53}$$

and $N^e_{i,j} = \frac{\partial N^e_i}{\partial x_j}$, where now it is understood that the element interpolation functions are functions of the current position of the element points, that is, $N^e_i = N^e_i(\mathbf{x})$.

Substituting the interpolations (3.44), (3.45) and (3.47), and the vectorial representation of stress from $(3.46)_1$ to the weak form (restricted to the domain Ω^e_0 of element e), one finds that

$$\begin{aligned} [\hat{\boldsymbol{\xi}}^e_{n+1}]^T \left(\int_{\Omega^e_0} [\mathbf{N}^e]^T \rho_0 [\mathbf{N}^e]\, dV \right) [\hat{\mathbf{a}}^e_{n+1}] + [\hat{\boldsymbol{\xi}}^e_{n+1}]^T \int_{\Omega^e_0} [\mathbf{B}^e]^T < \mathbf{P}_{n+1} > \, dV \\ = [\hat{\boldsymbol{\xi}}^e_{n+1}]^T \int_{\Omega^e_0} [\mathbf{N}^e]^T \rho_0 [\mathbf{b}_{n+1}]\, dV + [\hat{\boldsymbol{\xi}}^e_{n+1}]^T \int_{\partial\Omega^e_0 \cap \Gamma_{q_0}} [\mathbf{N}^e]^T [\overline{\mathbf{p}}_{n+1}]\, dA \\ + [\hat{\boldsymbol{\xi}}^e_{n+1}]^T \int_{\partial\Omega^e_0 \setminus \Gamma_{q_0}} [\mathbf{N}^e]^T \mathbf{p}_{n+1}\, dA \ , \end{aligned} \tag{3.54}$$

where $\partial\Omega^e_0 \cap \Gamma_{q_0}$ is the part of the element boundary which (potentially) intersects with the Neumann boundary Γ_{q_0} and $\partial\Omega^e_0 \setminus \Gamma_{q_0}$ is the rest of the element boundary, as in Figure 3.10.

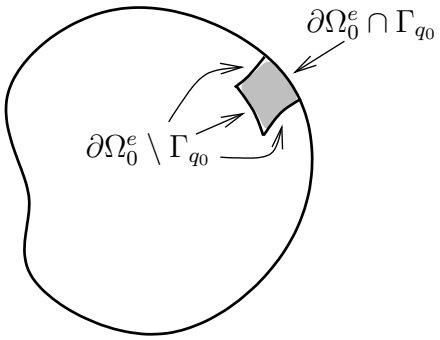

Figure 3.10. *Partition of element boundary* $\partial\Omega^e_0$

The preceding statement may be compactly rewritten as

$$[\hat{\boldsymbol{\xi}}^e_{n+1}]^T \left[[\mathbf{M}^e][\hat{\mathbf{a}}^e_{n+1}] + [\mathbf{R}^e(\hat{\mathbf{u}}^e_{n+1})] - [\mathbf{F}^e_{n+1}] \right] = [\hat{\boldsymbol{\xi}}^e_{n+1}]^T \int_{\partial\Omega^e_0 \setminus \Gamma_{q_0}} [\mathbf{N}^e]^T [\mathbf{p}_{n+1}]\, dA \tag{3.55}$$

where

$$\underbrace{[\mathbf{M}^e]}_{(3\times\texttt{NEN})\times(3\times\texttt{NEN})} = \int_{\Omega_0^e} [\mathbf{N}^e]^T \rho_0 [\mathbf{N}^e]\, dV \tag{3.56}$$

is the *element mass matrix*, which is clearly symmetric,

$$\underbrace{[\mathbf{R}^e_{n+1}]}_{(3\times\texttt{NEN})\times 1} = \int_{\Omega_0^e} [\mathbf{B}^e]^T < \mathbf{P}_{n+1} > \, dV \tag{3.57}$$

is the *element stress-divergence vector*, and

$$\underbrace{[\mathbf{F}^e_{n+1}]}_{(3\times\texttt{NEN})\times 1} = \int_{\Omega_0^e} [\mathbf{N}^e]^T \rho_0 [\mathbf{b}_{n+1}]\, dV + \int_{\partial\Omega_0^e\cap\Gamma_{q_0}} [\mathbf{N}^e]^T [\overline{\mathbf{p}}_{n+1}]\, dA \tag{3.58}$$

is the *element external force vector*.

Since $\boldsymbol{\xi}_{n+1}$ is an arbitrary tangent vector on the current configuration, it follows that

$$[\mathbf{M}^e][\hat{\mathbf{a}}^e_{n+1}] + [\mathbf{R}^e(\hat{\mathbf{u}}^e_{n+1})] = [\mathbf{F}^e_{n+1}] + \int_{\partial\Omega_0^e\setminus\Gamma_{q_0}} [\mathbf{N}^e]^T [\mathbf{p}_{n+1}]\, dA\ . \tag{3.59}$$

Under the action of the assembly operator $\mathop{\mathbf{A}}_{e}$, the above equation leads to

$$\mathop{\mathbf{A}}_{e} \left[[\mathbf{M}^e][\hat{\mathbf{a}}^e_{n+1}] + [\mathbf{R}^e(\hat{\mathbf{u}}^e_{n+1})] \right] = \mathop{\mathbf{A}}_{e} \left[[\mathbf{F}^e_{n+1}] + \int_{\partial\Omega_0^e\setminus\Gamma_{q_0}} [\mathbf{N}^e]^T [\mathbf{p}_{n+1}]\, dA \right]\ . \tag{3.60}$$

which, in turn, yields

$$[\mathbf{M}][\hat{\mathbf{a}}_{n+1}] + [\mathbf{R}(\hat{\mathbf{u}}_{n+1})] = [\mathbf{F}_{n+1}]\ , \tag{3.61}$$

where

$$[\mathbf{M}] = \mathop{\mathbf{A}}_{e} [\mathbf{M}^e] \tag{3.62}$$

is the *global mass matrix*, which is symmetric,

$$[\mathbf{R}_{n+1}] = \mathop{\mathbf{A}}_{e} [\mathbf{R}^e_{n+1}] \tag{3.63}$$

is the *global stress-divergence vector*, and

$$[\mathbf{F}_{n+1}] = \mathop{\mathbf{A}}_{e} [\mathbf{F}^e_{n+1}] \tag{3.64}$$

is the *global external force vector*. In (3.61), the term $\mathop{\mathbf{A}}_{e} \int_{\partial\Omega_0^e\setminus\Gamma_{q_0}} [\mathbf{N}^e]^T [\mathbf{p}_{n+1}]\, dA$, which quantifies the cumulative interelement jump in tractions is neglected, as is customary in finite

element approximations. This term is frequently used to quantify the error in the finite element analysis *a posteriori*. In addition, the global displacement and acceleration vectors are defined as

$$[\hat{\mathbf{u}}_{n+1}] = \begin{bmatrix} \hat{\mathbf{u}}^1_{n+1} \\ \hat{\mathbf{u}}^2_{n+1} \\ \cdots \\ \hat{\mathbf{u}}^{\texttt{NUMNP}}_{n+1} \end{bmatrix} \quad , \quad [\hat{\mathbf{a}}_{n+1}] = \begin{bmatrix} \hat{\mathbf{a}}^1_{n+1} \\ \hat{\mathbf{a}}^2_{n+1} \\ \cdots \\ \hat{\mathbf{a}}^{\texttt{NUMNP}}_{n+1} \end{bmatrix} , \tag{3.65}$$

where NUMNP is the total number of nodes in the mesh. Equations (3.61) constitute the *semi-discrete* form of linear momentum balance, that is, the approximate equations of motion obtained after spatial discretization. This is a (generally) non-linear system of second-order ordinary differential equations in time, with unknowns the nodal displacements $\hat{\mathbf{u}}_{n+1}$. Under *quasi-static* conditions (that is, when the inertia term can be neglected), the above system of equations becomes purely algebraic. Also, Dirichlet boundary conditions are readily accounted for by merely fixing the relevant displacement degrees-of-freedom on nodes which lie on Γ_u and, if desired, calculating the corresponding forces upon solution of the overall problem as reactions.

Note that the stress-divergence vector in (3.57) may well depend not only on $\hat{\mathbf{u}}_{n+1}$, but also on $\hat{\mathbf{v}}_{n+1}$. This would be the case when the stress response is rate-dependent. Also, the external force vector in (3.58) may be explicitly dependent on the motion, as would be the case, for instance, when the externally imposed traction is a *follower load* (*e.g.*, a pressure load). In this case, $\mathbf{F}_{n+1} = \mathbf{F}_{n+1}(\hat{\mathbf{u}}_{n+1})$, so the external force is itself a function of the solution.

If one chooses to start with the spatial statement of linear momentum balance in (3.41), an analogous procedure would ensue that would yield the element arrays

$$\underbrace{[\mathbf{M}^e]}_{(3\times\texttt{NEN})\times(3\times\texttt{NEN})} = \int_{\Omega^e} [\mathbf{N}^e]^T \rho [\mathbf{N}^e] \, dv \tag{3.66}$$

$$\underbrace{[\mathbf{R}^e_{n+1}]}_{(3\times\texttt{NEN})\times 1} = \int_{\Omega^e} [\mathbf{B}^e_{n+1}]^T < \mathbf{T}_{n+1} > \, dv \tag{3.67}$$

and

$$\underbrace{[\mathbf{F}^e_{n+1}]}_{(3\times\texttt{NEN})\times 1} = \int_{\Omega^e} [\mathbf{N}^e]^T \rho [\mathbf{b}_{n+1}] \, dv + \int_{\partial\Omega^e \cap \Gamma_{q_{n+1}}} [\mathbf{N}^e]^T [\overline{\mathbf{t}}_{n+1}] \, da \ . \tag{3.68}$$

The system of differential equations in (3.61) may be integrated in time using one of several standard integration methods. The most commonly used such time integrator in

solid mechanics is the *Newmark method*,[2] which is based on a time series expansion of $(\hat{\mathbf{u}}_{n+1}, \hat{\mathbf{v}}_{n+1})$, such as one may write in the time interval $(t_n, t_{n+1}]$

$$\begin{aligned} \hat{\mathbf{u}}_{n+1} &= \hat{\mathbf{u}}_n + \hat{\mathbf{v}}_n \Delta t_n + \frac{1}{2}\left[(1-2\beta)\hat{\mathbf{a}}_n + 2\beta \hat{\mathbf{a}}_{n+1}\right]\Delta t_n^2 \\ \hat{\mathbf{v}}_{n+1} &= \hat{\mathbf{v}}_n + \left[(1-\gamma)\hat{\mathbf{a}}_n + \gamma \hat{\mathbf{a}}_{n+1}\right]\Delta t_n \end{aligned} \quad , \tag{3.69}$$

where the parameters β and γ are chosen such that

$$0 \;<\; \gamma \;\leq\; 1 \qquad , \qquad 0 \;<\; \beta \;\leq\; \frac{1}{2} \, , \tag{3.70}$$

and the brackets around each of the matrix terms is dropped for brevity. It is easy to show that the special case $\beta = \frac{1}{4}, \gamma = \frac{1}{2}$ corresponds to the trapezoidal rule. Equation $(3.69)_1$ may be solved for the acceleration $\hat{\mathbf{a}}_{n+1}$ as

$$\hat{\mathbf{a}}_{n+1} \;=\; \frac{1}{\beta \Delta t_n^2}\left(\hat{\mathbf{u}}_{n+1} - \hat{\mathbf{u}}_n - \hat{\mathbf{v}}_n \Delta t_n\right) - \frac{1-2\beta}{2\beta}\hat{\mathbf{a}}_n \; . \tag{3.71}$$

Substituting the above to (3.61) yields

$$\frac{1}{\beta \Delta t_n^2}\mathbf{M}\hat{\mathbf{u}}_{n+1} + \mathbf{R}(\hat{\mathbf{u}}_{n+1}) \;=\; \underbrace{\mathbf{F}_{n+1} + \mathbf{M}\left\{\left(\hat{\mathbf{u}}_n + \hat{\mathbf{v}}_n \Delta t_n\right)\frac{1}{\beta \Delta t_n^2} + \frac{1-2\beta}{2\beta}\hat{\mathbf{a}}_n\right\}}_{\text{known quantities}} \; . \tag{3.72}$$

The preceding system of non-linear algebraic equations for $\hat{\mathbf{u}}_{n+1}$ can be solved using a standard iterative method (*e.g.*, the Newton-Raphson method or one of its variants). After $\hat{\mathbf{u}}_{n+1}$ is determined, $\hat{\mathbf{a}}_{n+1}$ and, then, $\hat{\mathbf{v}}_{n+1}$ are computed from (3.71) and $(3.69)_2$, respectively. An alternative solution sequence would entail substituting $(3.69)_1$ into (3.61), solving for the acceleration $\hat{\mathbf{a}}_{n+1}$, then substituting it back into $(3.69)_{1,2}$ to determine $\hat{\mathbf{u}}_{n+1}$ and $\hat{\mathbf{v}}_{n+1}$. In either approach, minor and straightforward modifications suffice to accommodate the case where $\mathbf{F}_{n+1}$ depends explicitly on $\hat{\mathbf{u}}_{n+1}$ or the case where $\mathbf{R}_{n+1}$ depends explicitly on both $\hat{\mathbf{u}}_{n+1}$ and $\hat{\mathbf{v}}_{n+1}$.

The above time integration scheme is *implicit*, in the sense that determining the state at time t_{n+1} requires the solution of a system of algebraic equations. A weighted-residual formalization in time can be easily formulated results in deriving the Newmark equation (3.69).[3]

[2] N.M. Newmark, "A Method of Computation in Structural Dynamics", *J. Engr. Mech. Div. ASCE*, 85:67-94, (1959).

[3] O.C. Zienkiewicz, "A New Look at the Newmark, Houbolt and other Stepping Formulas. A Weighted Residual Approach", *Earthquake Engin. Struct. Dyn.*, 5:413-418, (1977).

An *explicit* integration scheme may be obtained from the Newmark formulae by setting $\beta = 0$. This leads to the equations

$$\begin{aligned} \hat{\mathbf{u}}_{n+1} &= \hat{\mathbf{u}}_n + \hat{\mathbf{v}}_n \Delta t_n + \frac{1}{2}\hat{\mathbf{a}}_n \Delta t_n^2 \\ \hat{\mathbf{v}}_{n+1} &= \hat{\mathbf{v}}_n + [(1-\gamma)\hat{\mathbf{a}}_n + \gamma \hat{\mathbf{a}}_{n+1}]\, \Delta t_n \end{aligned} \quad . \tag{3.73}$$

It is again easy to show that in the special case $\gamma = 0.5$ one recovers the classical *centered-difference method*. The general explicit Newmark integrator is implemented as follows: starting from the semi-discrete form (3.61), one may substitute $\hat{\mathbf{u}}_{n+1}$ from $(3.73)_1$ to get

$$\mathbf{M}\hat{\mathbf{a}}_{n+1} \;=\; \mathbf{F}_{n+1} - \mathbf{R}(\hat{\mathbf{u}}_n + \hat{\mathbf{v}}_n \Delta t_n + \frac{1}{2}\hat{\mathbf{a}}_n \Delta t_n^2) \;. \tag{3.74}$$

If $\mathbf{M}$ is rendered diagonal,[4] then $\hat{\mathbf{a}}_{n+1}$ can be determined without solving equations. Subsequently, the velocity vector $\hat{\mathbf{v}}_{n+1}$ is computed from $(3.73)_2$. Note that the displacement vector $\hat{\mathbf{u}}_{n+1}$ is updated through $(3.73)_1$ without using $\hat{\mathbf{a}}_{n+1}$.

As with the implicit Newmark scheme, it is easy to accomodate the case where $\mathbf{F}_{n+1}$ depends on $\hat{\mathbf{u}}_{n+1}$. On the other hand, if $\mathbf{R}_{n+1}$ depends on $\hat{\mathbf{u}}_{n+1}$, then the explicit nature of the time-stepping may not be preserved unless one resorts to a time-shifting modification, in which the term $\mathbf{R}_{n+1}(\hat{\mathbf{u}}_{n+1}, \hat{\mathbf{v}}_{n+1})$ is replaced, at an error that depends on Δt_n, by $\mathbf{R}_{n+1}(\hat{\mathbf{u}}_{n+1}, \hat{\mathbf{v}}_n)$ or $\mathbf{R}_{n+1}(\hat{\mathbf{u}}_{n+1}, \hat{\mathbf{v}}_n + \hat{\mathbf{a}}_n \Delta t_n)$.

Explicit time integration is computationally inexpensive, as there is no need to compute gradients and solve coupled algebraic equations. However, explicit time integration can only be conditionally stable, that is, the step-size must be restricted (sometimes severely) to yield convergent solutions.

The preceding formulation is often referred to *total Lagrangian*. This means that the motion and deformation is always measured relative to the original fixed reference configuration regardless of its magnitude. Alternatively, one may choose to measure the motion and deformation at time t_{n+1} relative to any previously determined (and, therefore, *de facto* fixed) configuration at time $t = t_k$, where $k = 1, 2, \cdots, n$. The so-called *updated Lagrangian* formulation is specifically obtained by measuring the motion and deformation at $t = t_{n+1}$ relative to the configuration at time $t = t_n$.[5] To this end, consider again a motion $\boldsymbol{\chi} : \mathcal{R}_0 \times \mathbb{R} \to \mathcal{E}^3$, as in Figure 3.11.

[4] See Appendix H of O.C. Zienkiewicz, R.L. Taylor, and J.Z. Zhu, **The Finite Element Method: Its Basis & Fundamentals**, 7th edition, Butterworth-Heinemann, Boston, (2013), for full details on the theory and practice of mass matrix diagonalization.

[5] K.-J. Bathe, E. Ramm, and E.L. Wilson, "Finite element formulations for large deformation dynamic analysis", *Int. J. Num. Meth. Engr.*, 9:353–386, (1975).

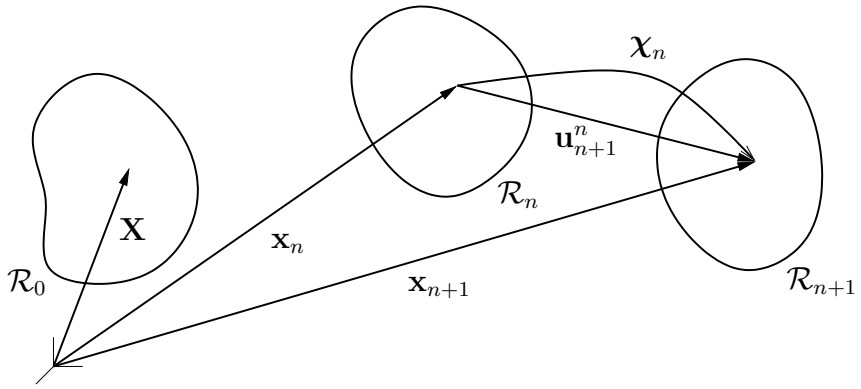

Figure 3.11. *Configurations for updated Lagrangian formulation*

Note that, by definition,

$$\mathbf{x}_n \;=\; \boldsymbol{\chi}(\mathbf{X}, t_n) \tag{3.75}$$

and

$$\mathbf{x}_{n+1} \;=\; \boldsymbol{\chi}(\mathbf{X}, t_{n+1}) \;, \tag{3.76}$$

so that a mapping $\boldsymbol{\chi}_n : \mathcal{R}_n \times \mathbb{R} \to \mathcal{E}^3$ is defined, such that for any time t

$$\mathbf{x} \;=\; \boldsymbol{\chi}(\mathbf{X}, t) \;=\; \boldsymbol{\chi}(\boldsymbol{\chi}_{t_n}^{-1}(\mathbf{x}_n), t) \;=\; \boldsymbol{\chi}_n(\mathbf{x}_n, t) \;. \tag{3.77}$$

Clearly, $\boldsymbol{\chi}_n$ is the relative motion with respect to the (generally deformed) configuration $\mathcal{R}_n$. It follows that the deformation gradient $\mathbf{F}^n_{n+1}$ at time $t = t_{n+1}$ relative to the configuration $\mathcal{R}_n$ is defined as

$$\mathbf{F}^n_{n+1} \;=\; \frac{\partial \boldsymbol{\chi}_n(\mathbf{x}_n, t_{n+1})}{\partial \mathbf{x}_n} \;=\; \frac{\partial \mathbf{x}_{n+1}}{\partial \mathbf{x}_n} = \frac{\partial (\mathbf{x}_n + \mathbf{u}^n_{n+1})}{\partial \mathbf{x}_n} \;=\; \mathbf{I} + \frac{\partial \mathbf{u}^n_{n+1}}{\partial \mathbf{x}_n} \;,$$

where $\mathbf{u}^n_{n+1} = \mathbf{x}_{n+1} - \mathbf{x}_n$ is the displacement at t_{n+1} relative to t_n, see Figure 3.11. Invoking the chain rule and recalling (3.77),

$$\frac{\partial \boldsymbol{\chi}(\mathbf{X}, t_{n+1})}{\partial \mathbf{X}} \;=\; \frac{\partial \boldsymbol{\chi}_n(\mathbf{x}_n, t_{n+1})}{\partial \mathbf{x}_n} \frac{\partial \boldsymbol{\chi}(\mathbf{X}, t_n)}{\partial \mathbf{X}} \tag{3.78}$$

or

$$\mathbf{F}_{n+1} \;=\; \mathbf{F}^n_{n+1} \mathbf{F}_n \;. \tag{3.79}$$

It follows from the above that, since $\det \mathbf{F} > 0$ for all $(\mathbf{X}, t)$, the same applies to $\mathbf{F}^n_{n+1}$ for all $(\mathbf{x}_n, t)$.

Starting from the spatial statement of the weak form in (3.41), one may "pull-back" to the configuration $\mathcal{R}_n$ to find that

$$\int_{\mathcal{R}_n} \boldsymbol{\xi}^n_{n+1} \cdot \rho_n \mathbf{a}^n_{n+1}\, dV_n + \int_{\mathcal{R}_n} \frac{\partial \boldsymbol{\xi}^n_{n+1}}{\partial \mathbf{x}_n} \cdot \mathbf{P}^n_{n+1}\, dV_n = \int_{\mathcal{R}_n} \boldsymbol{\xi}^n_{n+1} \cdot \rho_n \mathbf{b}^n_{n+1}\, dV_n + \int_{\Gamma_{q_n}} \boldsymbol{\xi}^n_{n+1} \cdot \overline{\mathbf{p}}^n_{n+1}\, dA_n \ , \quad (3.80)$$

where

$$\boldsymbol{\xi} \ = \ \tilde{\boldsymbol{\xi}}(\mathbf{x},t) \ = \ \tilde{\boldsymbol{\xi}}(\boldsymbol{\chi}_{n\,t}(\mathbf{x}_n),t) \ = \ \boldsymbol{\xi}^n(\mathbf{x}_n,t) \ , \quad (3.81)$$

hence

$$\boldsymbol{\xi}^n_{n+1} \ = \ \boldsymbol{\xi}^n(\mathbf{x}_n,t_{n+1}) \ . \quad (3.82)$$

Also, for the acceleration and body forces

$$\mathbf{a} \ = \ \tilde{\mathbf{a}}(\mathbf{x},t) \ = \ \tilde{\mathbf{a}}\left(\boldsymbol{\chi}_n(\mathbf{x}_n,t),t\right) \ = \ \mathbf{a}^n(\mathbf{x}_n,t) \quad (3.83)$$

$$\mathbf{b} \ = \ \tilde{\mathbf{b}}(\mathbf{x},t) \ = \ \tilde{\mathbf{b}}\left(\boldsymbol{\chi}_n(\mathbf{x}_n,t),t\right) \ = \ \mathbf{b}^n(\mathbf{x}_n,t) \ , \quad (3.84)$$

therefore

$$\mathbf{a}^n_{n+1} \ = \ \mathbf{a}^n(\mathbf{x}_n,t_{n+1}) \qquad , \qquad \mathbf{b}^n_{n+1} \ = \ \mathbf{b}^n(\mathbf{x}_n,t_{n+1}) \ . \quad (3.85)$$

In addition,

$$\rho_n \ = \ \rho_{n+1} J^n_{n+1} \ , \quad (3.86)$$

where $J^n_{n+1} = \det \mathbf{F}^n_{n+1}$, which confirms that ρ_n in (3.86) is precisely the mass density of the body at $t = t_n$. Likewise,

$$dV_n \ = \ \frac{1}{J^n_{n+1}}\, dv_{n+1} \quad (3.87)$$

and

$$\mathbf{n}_{n+1}\, da_{n+1} \ = \ J^n_{n+1} \left(\mathbf{F}^n_{n+1}\right)^{-T} \mathbf{n}_n\, dA_n \ , \quad (3.88)$$

where $\mathbf{n}_n$ and $\mathbf{n}_{n+1}$ are unit normals to the same material surface at times t_n and t_{n+1}, respectively.

Analogous definitions apply for the traction and stress. In particular, the traction vector $\overline{\mathbf{p}}^n_{n+1}$ is defined according to

$$\bar{\mathbf{t}}_{n+1}\, da_{n+1} \ = \ \overline{\mathbf{p}}^n_{n+1}\, dA_n \ , \quad (3.89)$$

while $\mathbf{P}^n_{n+1}$ is the first Piola-Kirchhoff stress tensor obtained by resolving tractions on the geometry of the configuration $\mathcal{R}_n$, that is,

$$\mathbf{P}^n_{n+1} \;=\; J^n_{n+1}\mathbf{T}_{n+1}\left(\mathbf{F}^n_{n+1}\right)^{-T} \;. \tag{3.90}$$

In view of the above and upon recalling (3.44), one may write for a typical Lagrangian element which at time $t = t_n$ occupies the region Ω^e_n

$$\mathbf{u}^n(\mathbf{x}_n, t_{n+1})\big|_{\Omega^e_n} \;=\; \mathbf{u}^{e\,n}_{n+1}(\mathbf{x}_n) \;\doteq\; \sum_{i=1}^{\texttt{NEN}} N^e_i \mathbf{u}^{e\,n}_{i\,n+1} \;=\; [\mathbf{N}^e][\hat{\mathbf{u}}^{e\,n}_{n+1}] \;, \tag{3.91}$$

and, likewise,

$$\mathbf{a}^{e\,n}_{n+1} \;\doteq\; [\mathbf{N}^e][\hat{\mathbf{a}}^{e\,n}_{n+1}] \quad , \quad \boldsymbol{\xi}^{e\,n}_{n+1} \;\doteq\; [\mathbf{N}^e][\hat{\boldsymbol{\xi}}^{e\,n}_{n+1}] \;. \tag{3.92}$$

Furthermore,

$$\underbrace{\left\langle \frac{\partial \boldsymbol{\xi}^{e\,n}_{n+1}}{\partial \mathbf{x}_n} \right\rangle}_{(9\times 1)} \;=\; \underbrace{[\mathbf{B}^{e\,n}]}_{9\times(3\times\texttt{NEN})}\;\underbrace{[\hat{\boldsymbol{\xi}}^{e\,n}_{n+1}]}_{(3\times\texttt{NEN})\times 1} \;, \tag{3.93}$$

where

$$\underbrace{[\mathbf{B}^{e\,n}]}_{9\times(3\times\texttt{NEN})} \;=\; \Big[\underbrace{[\mathbf{B}^{e\,n}_1]}_{(9\times 3)} \;\; [\mathbf{B}^{e\,n}_2] \;\; \cdots \;\; [\mathbf{B}^{e\,n}_{\texttt{NEN}}]\Big] \tag{3.94}$$

and

$$\underbrace{[\mathbf{B}^{e\,n}_i]}_{9\times 3} \;=\; \begin{bmatrix} N^e_{i,1} & & \\ & N^e_{i,2} & \\ & & N^e_{i,3} \\ N^e_{i,2} & & \\ & N^e_{i,3} & \\ & & N^e_{i,1} \\ N^e_{i,3} & & \\ & N^e_{i,1} & \\ & & N^e_{i,2} \end{bmatrix} \;. \tag{3.95}$$

Note that here $N^e_i = N^e_i(\mathbf{x}_n)$ and $N^e_{i,j} = \frac{\partial N^e_i}{\partial x_{n_j}} = \frac{\partial N^e_i}{\partial X_A} F^{-1}_{n\,Aj}$.

Substituting the interpolations in (3.91), (3.92) and (3.93) to the weak form (3.80) applied to element e yields

$$[\hat{\boldsymbol{\xi}}^{e\,n}_{n+1}]^T\left[[\mathbf{M}^e][\hat{\mathbf{a}}^{e\,n}_{n+1}] + [\mathbf{R}^{e\,n}(\hat{\mathbf{u}}^{e\,n}_{n+1})] - [\mathbf{F}^{e\,n}_{n+1}]\right] \;=\; [\hat{\boldsymbol{\xi}}^{e\,n}_{n+1}]^T \int_{\partial\Omega^e_n \setminus \Gamma_{q_n}} [\mathbf{N}^e]^T [\mathbf{p}^n_{n+1}]\, dA_n \;, \tag{3.96}$$

where

$$\underbrace{[\mathbf{M}^e]}_{(3\times\texttt{NEN})\times(3\times\texttt{NEN})} = \int_{\Omega_0^e} [\mathbf{N}^e]^T \rho_n [\mathbf{N}^e]\, dV_n \ , \tag{3.97}$$

$$\underbrace{[\mathbf{R}^{e\,n}_{n+1}]}_{(3\times\texttt{NEN})\times 1} = \int_{\Omega_n^e} [\mathbf{B}^{e\,n}]^T < \mathbf{P}^n_{n+1} > \, dV_n \tag{3.98}$$

and

$$\underbrace{[\mathbf{F}^{e\,n}_{n+1}]}_{(3\times\texttt{NEN})\times 1} = \int_{\Omega_n^e} [\mathbf{N}^e]^T \rho_n [\mathbf{b}^n_{n+1}]\, dV_n + \int_{\partial\Omega_n^e\cap\Gamma_{q_n}} [\mathbf{N}^e]^T [\overline{\mathbf{p}}^n_{n+1}]\, dA_n \ . \tag{3.99}$$

Under the action of the assembly operator $\mathop{\mathbf{A}}_{e}$ over all elements one recovers the semi-discrete form of the updated Lagrangian formulation as

$$\mathbf{M}\hat{\mathbf{a}}^n_{n+1} + \mathbf{R}^n(\hat{\mathbf{u}}^n_{n+1}) = \mathbf{F}^n_{n+1} \ , \tag{3.100}$$

where

$$[\hat{\mathbf{u}}^n_{n+1}] = \begin{bmatrix} \hat{\mathbf{u}}^{1\,n}_{n+1} \\ \hat{\mathbf{u}}^{2\,n}_{n+1} \\ \cdots \\ \hat{\mathbf{u}}^{\texttt{NUMNP}\,n}_{n+1} \end{bmatrix} \quad , \quad [\hat{\mathbf{a}}^n_{n+1}] = \begin{bmatrix} \hat{\mathbf{a}}^{1\,n}_{n+1} \\ \hat{\mathbf{a}}^{2\,n}_{n+1} \\ \cdots \\ \hat{\mathbf{a}}^{\texttt{NUMNP}\,n}_{n+1} \end{bmatrix} \ . \tag{3.101}$$

The solution of the above system of non-linear second-order differential equations in time is achieved as in the total Lagrangian formulation.

The total and updated Lagrangian formulations are completely equivalent, in the sense that, given the same finite element mesh, they yield the exact same solution. However, since they involve different unknown vectors ($[\hat{\mathbf{u}}_{n+1}]$ for the total Lagrangian and $[\hat{\mathbf{u}}^n_{n+1}]$ for the update Lagrangian method), this solution is obtained by solving two different non-linear algebraic systems. Therefore, it is conceivable that one of the two systems may be more easily (or, given the limitations of finite arithmetic, more accurately) solvable than the other. This would form a practical basis for selecting one of the two methods over the other.

3.5 Corotational Methods

When solving problems in solid mechanics, it is sometimes desirable to use coordinate systems which rotate together with a Lagrangian mesh. This is principally the case when using structural elements (*e.g.*, bars, beams). By way of motivation, contrast the cases of fixed *vs.* corotating coordinate systems for a two-dimensional bar element, as in Figure 3.12.

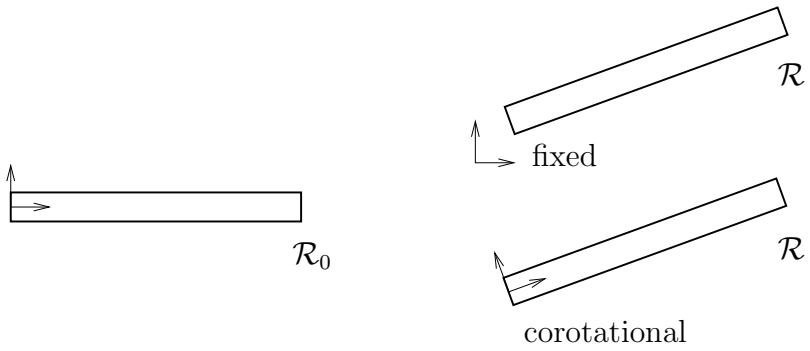

Figure 3.12. *Fixed* vs. *corotational coordinate system*

Consider the general case shown in Figure 3.13, where one may identify a rotation field $\bar{\mathbf{R}}(\mathbf{x}, t)$, such that the balance laws are expressed at any point $\mathbf{x}$ and time t in terms of the corotating right-hand orthonormal coordinate system $\{\mathbf{e}'_i\}$. This system is related to the fixed global coordinate system $\{\mathbf{e}_i\}$ according to

$$\mathbf{e}'_i \;=\; \bar{\mathbf{R}}\mathbf{e}_i \;, \tag{3.102}$$

for $i = 1, 2, 3$. Any spatial vector, say $\mathbf{v}$, is resolved relative to $\{\mathbf{e}_i\}$ and $\{\mathbf{e}'_i\}$ as

$$\mathbf{v} \;=\; v_i\mathbf{e}_i \;=\; v'_i\mathbf{e}'_i \;. \tag{3.103}$$

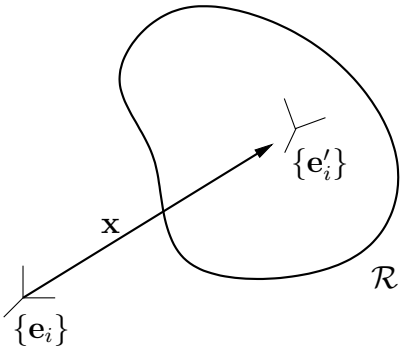

Figure 3.13. *General corotational coordinate system*

In view of (3.102) and (3.103), one may write

$$\begin{aligned} v'_i \;&= \mathbf{v}\cdot\mathbf{e}'_i \\ &= v_j\mathbf{e}_j\cdot\mathbf{e}'_i \;=\; v_j\mathbf{e}_j\cdot(\bar{\mathbf{R}}\mathbf{e}_i) \;=\; \bar{R}_{ji}v_j \;. \end{aligned} \tag{3.104}$$

In direct notation, equation (3.104) may be stated as

$$\mathbf{v}' \;=\; \bar{\mathbf{R}}^T\mathbf{v}\;, \tag{3.105}$$

where $\mathbf{v}' = v'_i\mathbf{e}_i$ is the vector with the corotational components of$\mathbf{v}$ on the global basis (hence, in general, $\mathbf{v}' \neq \mathbf{v}$).

Similarly, for a spatial tensor, say $\mathbf{T}$, one may write with the aid of (3.102)

$$\begin{aligned}\mathbf{T} \;=\; T_{ij}\mathbf{e}_i\otimes\mathbf{e}_j \;&= T'_{ij}\mathbf{e}'_i\otimes\mathbf{e}'_j\\ &= T'_{ij}(\bar{\mathbf{R}}\mathbf{e}_i)\otimes(\bar{\mathbf{R}}\mathbf{e}_j)\\ &= \bar{\mathbf{R}}(T'_{ij}\mathbf{e}_i\otimes\mathbf{e}_j)\bar{\mathbf{R}}^T\;,\end{aligned} \tag{3.106}$$

which implies that

$$\mathbf{T}' \;=\; \bar{\mathbf{R}}^T\mathbf{T}\bar{\mathbf{R}} \quad;\quad T'_{ij} = \bar{R}_{ki}T_{kl}\bar{R}_{lj}\;. \tag{3.107}$$

Of all terms in the weak form of linear momentum balance (3.41) typically only the stress-divergence term is resolved using the corotational system (the other terms are resolved directly in the global system). Ultimately, the stress-divergence term is also rotated back to the global system before the integration of the semi-discrete equations.

Taking into account (3.105) and (3.106), and using the chain rule, the stress-divergence term in (3.41) takes the form

$$\begin{aligned}\int_{\mathcal{R}}\left(\frac{\partial\boldsymbol{\xi}}{\partial\mathbf{x}}\right)^s\cdot\mathbf{T}\,dv \;&=\; \int_{\mathcal{R}}\left(\frac{\partial\boldsymbol{\xi}}{\partial\boldsymbol{\xi}'}\frac{\partial\boldsymbol{\xi}'}{\partial\mathbf{x}'}\frac{\partial\mathbf{x}'}{\partial\mathbf{x}}\right)^s\cdot(\bar{\mathbf{R}}\mathbf{T}\bar{\mathbf{R}}^T)\,dv\\ &=\; \int_{\mathcal{R}}\left(\bar{\mathbf{R}}\frac{\partial\boldsymbol{\xi}'}{\partial\mathbf{x}'}\bar{\mathbf{R}}^T\right)^s\cdot(\bar{\mathbf{R}}\mathbf{T}\bar{\mathbf{R}}^T)\,dv\\ &=\; \int_{\mathcal{R}}\left(\frac{\partial\boldsymbol{\xi}'}{\partial\mathbf{x}'}\right)^s\cdot\mathbf{T}'\,dv\;.\end{aligned} \tag{3.108}$$

It is important to emphasize that the coordinate system $\{\mathbf{e}'_i\}$ is not inertial. This means that if one needs to represent time-dependent effects (such as those of inertia) using a corotational frame, then one needs to explicitly account for the dynamics of the coordinate system.

3.6 Arbitrary Lagrangian-Eulerian Methods

Arbitrary Lagrangian-Eulerian (ALE) methods constitute a creative compromise between the classical Lagrangian and Eulerian methods. In ALE methods, the mesh undergoes a

motion which is generally different from the motion of the continuum. The mesh motion is specifically designed to preserve, to the extent possible, the quality of the mesh as the continuum undergoes significant deformation.

To set up a general ALE method, consider a body $\mathscr{B}$ with reference configuration $\mathcal{R}_0$ at time $t = 0$, and identify this configuration with an initial "mesh configuration" $\mathcal{M}_0$ at the same time, see Figure 3.14. Next, in addition to the usual body motion $\boldsymbol{\chi} : \mathcal{R}_0 \times \mathbb{R} \to \mathcal{E}^3$,

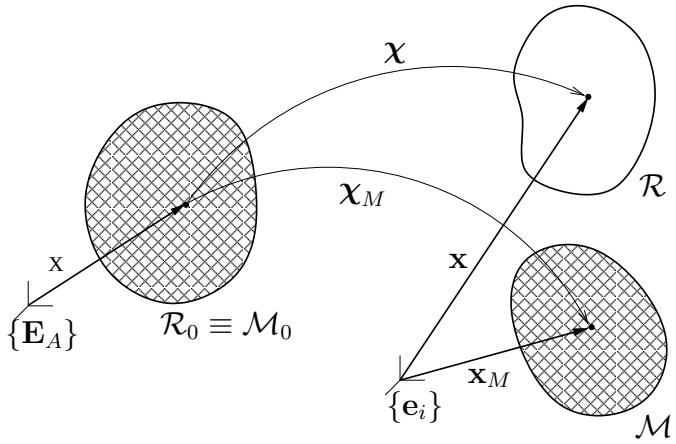

Figure 3.14. *Configurations of ALE method*

admit the existence of a "mesh motion" $\boldsymbol{\chi}_M : \mathcal{M}_0 \times \mathbb{R} \to \mathcal{E}^3$, such that

$$\mathbf{x}_M \;=\; \boldsymbol{\chi}_M(\mathbf{X}_M, t) \;, \tag{3.109}$$

where, in general, $\mathbf{x} \neq \mathbf{x}_M$ when $\mathbf{X} = \mathbf{X}_M$, as in Figure 3.14. This mesh motion is sometimes referred to as "arbitrary", in the sense that it is generally different from the motion of the body. The velocity $\mathbf{v}_m$ of the mesh is now defined as

$$\mathbf{v}_M \;=\; \frac{\partial \boldsymbol{\chi}_M(\mathbf{X}_M, t)}{\partial t} \;. \tag{3.110}$$

Two special cases arise naturally: (a) $\boldsymbol{\chi}_M = \boldsymbol{\chi}$, in which case the mesh motion is identical to body motion and the method is Lagrangian, and (b) $\boldsymbol{\chi}_M = \mathbf{i}$, hence $\mathbf{x}_M = \mathbf{X}$, in which case the mesh remains stationary, thereby rendering the method Eulerian.

Attention is focused henceforth to the case $\boldsymbol{\chi}_M \neq \boldsymbol{\chi}$ and $\boldsymbol{\chi}_M \neq \mathbf{i}$. Generally, creative choices for $\boldsymbol{\chi}_M$ can provide serious advantages over pure Lagrangian or Eulerian methods when the continuum undergoes significant non-homogeneous deformations. The mesh motion $\boldsymbol{\chi}_M$ is typically chosen to satisfy the following four conditions:

(i) The ALE mesh consists of elements with better aspect ratios and narrower size distribution than the corresponding Lagrangian mesh,

(ii) The element connectivities do not change (otherwise, the procedure yields a new mesh, and is referred to as *remeshing*),

(iii) The mesh motion $\boldsymbol{\chi}_M$ is assumed invertible at all times, that is,

$$J_M \;=\; \det \frac{\partial \boldsymbol{\chi}_M}{\partial \mathbf{X}_M} \;\neq\; 0 \;. \tag{3.111}$$

As argued in Section 1.1, the inverse function theorem enables the unique mapping of a mesh point $\mathbf{x}_M$ to its referential counterpart $\mathbf{X}_M$ and, through it, to a material point $\mathbf{x}$ with which $\mathbf{x}_M$ coincided at time $t = 0$. Actually, since $J_M(\mathbf{X}_M, 0) = 1$ and $\boldsymbol{\chi}_M$ is assumed smooth, it follows from (3.111) that $J_M(\mathbf{X}_M, t) > 0$ at all times.

Since the mesh motion is invertible, one may write

$$\mathbf{v}_M \;=\; \hat{\mathbf{v}}_M(\mathbf{X}_M, t) \;=\; \hat{\mathbf{v}}_M(\boldsymbol{\chi}_{M\,t}^{-1}(\mathbf{x}_M), t) \;=\; \tilde{\mathbf{v}}_M(\mathbf{x}_M, t) \;, \tag{3.112}$$

therefore the mesh velocity may be readily expressed in spatial form.

(iv) In certain classes of problems, the body motion and the mesh motion are chosen such that the normal components of their velocities coincide on the boundary of the body (or on part of it) at all times. This is generally the case with problems in solid Mechanics and in free-surface flow problems of fluid mechanics (at least along the free surface). This restriction is placed to avoid the flow of material outside the mesh, which would render it unavailable for approximation. At a given time t, let $\mathbf{x} = \mathbf{x}_M$ lie on the (common) boundary $\partial\mathcal{R} = \partial\mathcal{M}$, having outward unit normal $\mathbf{n}$, as in Figure 3.15.

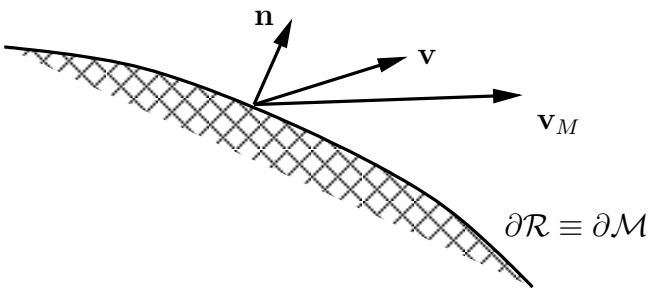

Figure 3.15. *Velocity constraint on the boundary of an ALE mesh*

The above constraint on the mesh motion implies that

$$(\mathbf{v} - \mathbf{v}_M) \cdot \mathbf{n} \;=\; 0 \tag{3.113}$$

on $\partial\mathcal{R} \equiv \partial\mathcal{M}$. Thus, the mesh motion $\boldsymbol{\chi}_M$ is such that it convects with the body along its boundary. Assuming that the constraint (3.113) is enforced on the whole (common) boundary of the mesh and body, the kinematic setting for the ALE method is now depicted in Figure 3.16.

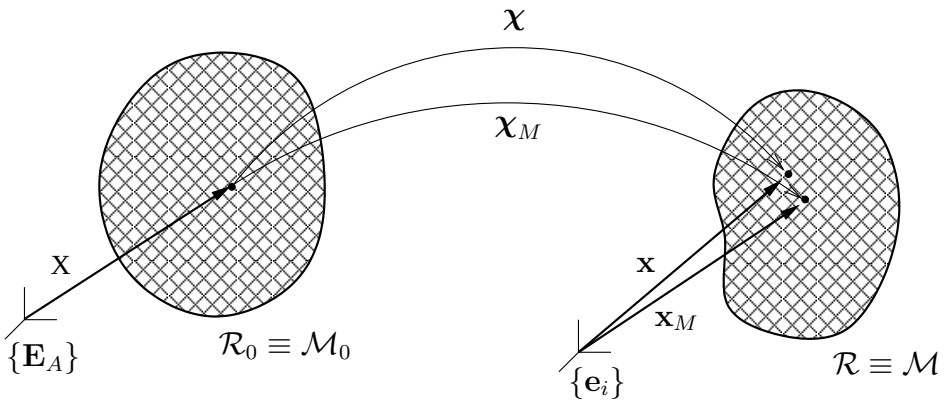

Figure 3.16. *Configurations of ALE method with coincident body and mesh boundaries*

The two main tasks in developing an ALE method are: (a) to formulate and enforce the balance laws on the ALE finite elements, and (b) to prescribe (in an automated fashion) an appropriate motion $\boldsymbol{\chi}_M$.

Consider the first of the above tasks and start with conservation of mass. Let $\mathcal{P} \subset \mathcal{R}$ be a region occupied by material in the current configuration an let $\mathcal{P}_M \subset \mathcal{M}$ be a mesh region, such that $\mathcal{P} \equiv \mathcal{P}_M$ at time t, as in Figure 3.17.

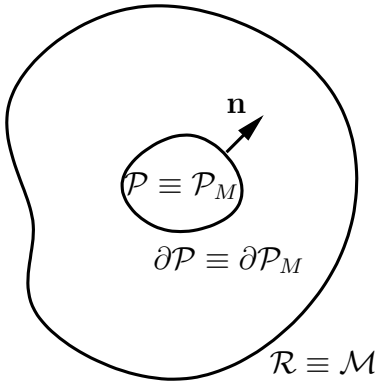

Figure 3.17. *Mesh region $\mathcal{P}_M$ in the current configuration*

Recall from 1.2.1 that, according to the principle of mass conservation, the rate of change of the mass of the particles which occupy the material region $\mathcal{P}$ at time t is equal to zero. Starting with the spatial statement of conservation of mass in (1.64), note that

$$\begin{aligned}
\frac{d}{dt}\int_{\mathcal{P}} \rho(\mathbf{x},t)dv \;&=\; \underbrace{\int_{\mathcal{P}} \frac{d\rho}{dt}\,dv}_{\substack{\text{rate of change of mass}\\ \text{for material particles in } \mathcal{P}}} \;+\; \underbrace{\int_{\mathcal{P}} \rho\frac{d(dv)}{dt}\,dt}_{\substack{\text{rate of change of mass}\\ \text{due to change in } \mathcal{P}}} \;=\; \int_{\mathcal{P}} (\dot{\rho} + \rho\,\mathrm{div}\,\mathbf{v})\,dv \\
&= \int_{\mathcal{P}} \left(\frac{\partial\rho}{\partial t} + \frac{\partial\rho}{\partial\mathbf{x}}\cdot\mathbf{v} + \rho\,\mathrm{div}\,\mathbf{v}\right) dv \\
&= \int_{\mathcal{P}} \left[\frac{\partial\rho}{\partial t} + \mathrm{div}(\rho\mathbf{v})\right] dv \\
&= \underbrace{\int_{\mathcal{P}} \frac{\partial\rho}{\partial t}\,dv}_{\substack{\text{rate of change of mass}\\ \text{in fixed region } \mathcal{P}}} \;+\; \underbrace{\int_{\partial\mathcal{P}} \rho\mathbf{v}\cdot\mathbf{n}\,da}_{\substack{\text{flux of mass}\\ \text{through boundary } \partial\mathcal{P}}} \;=\; 0\;,
\end{aligned} \tag{3.114}$$

where use is made of (1.10), (1.52), and the divergence theorem. Next, proceed with the derivation of an ALE statement of mass balance by defining the rate of change of the mass contained in a mesh region $\mathcal{P}_M$ at time t as

$$\frac{d_M}{dt}\int_{\mathcal{P}_M} \tilde{\rho}_M(\mathbf{x}_M,t)dv_M\;, \tag{3.115}$$

where $\dfrac{d_M}{dt}$ denotes the *mesh time derivative*, that is, the time derivative which keeps the mesh points fixed.

At this state, it is instructive to consider the different representations of a scalar function, say f, using material, spatial, or mesh coordinates. Specifically, one may write

$$f \;=\; \hat{f}(\mathbf{X},t) \;=\; \hat{f}_M(\mathbf{X}_M,t) \;=\; \tilde{f}(\mathbf{x},t) \;=\; \tilde{f}_M(\mathbf{x}_M,t)\;. \tag{3.116}$$

Here, it is clear that $\tilde{f}_M(\mathbf{x}_M,t) = \tilde{f}(\mathbf{x}_M,t)$ (which means that there is no distinction between the two spatial representations, hence, in principal, one may drop the subscript "M" from $\tilde{f}_M$),[6] $\hat{f}_M(\mathbf{X}_M,t) \neq \hat{f}(\mathbf{X}_M,t)$ (which is tantamount to observing that at time t the density of the mesh point which was at $\mathbf{X}_M$ at time t_0 is not equal to that of the material point that occupied $\mathbf{X}_M$ at t_0), and, also $\dfrac{d_M}{dt}\hat{f}_M(\mathbf{X}_M,t) = \dfrac{\partial\hat{f}_M}{\partial t}$. It is also clear from (3.116) that

$$\frac{d_M f}{dt} \;=\; \frac{\partial\hat{f}_M}{\partial t} \;=\; \frac{\partial\tilde{f}_M}{\partial t} + \frac{\partial\tilde{f}_M}{\partial\mathbf{x}_M}\cdot\mathbf{v}_M\;. \tag{3.117}$$

[6] It is important to emphasize, in connection to the different representations of a function in (3.116), that the mesh velocity $\mathbf{v}_M$ is *not* equal to the mesh-coordinate representation of the material velocity.

The variables $(\mathbf{x}_M, t)$ used in ALE methods are often referred to as the *mixed* variables.

Following the procedure above, one may also write

$$\begin{aligned}
\frac{d_M}{dt}\int_{\mathcal{P}_M}\tilde{\rho}_M(\mathbf{x}_M,t)\,dv_M &= \underbrace{\int_{\mathcal{P}_M}\frac{d_M\tilde{\rho}_M}{dt}\,dv_M}_{\substack{\text{rate of change of mass}\\ \text{for particles in } \mathcal{P}_M}} + \underbrace{\int_{\mathcal{P}_M}\rho\frac{d_M(dv_M)}{dt}}_{\substack{\text{rate of change of mass}\\ \text{because of change in } \mathcal{P}_M}} \\
&= \int_{\mathcal{P}_M}\left(\frac{d_M\tilde{\rho}_M}{dt}+\rho\,\mathrm{div}\,\mathbf{v}_M\right)dv_M \\
&= \int_{\mathcal{P}_M}\left(\frac{\partial\tilde{\rho}_M}{\partial t}+\frac{\partial\tilde{\rho}_M}{\partial\mathbf{x}_M}\cdot\mathbf{v}_M+\rho\,\mathrm{div}\,\mathbf{v}_M\right)dv_M \\
&= \int_{\mathcal{P}_M}\left[\frac{\partial\tilde{\rho}_M}{\partial t}+\mathrm{div}(\rho\mathbf{v}_M)\right]dv_M \\
&= \int_{\mathcal{P}_M}\frac{\partial\tilde{\rho}_M}{\partial t}\,dv_M+\int_{\partial\mathcal{P}_M}\rho\mathbf{v}_M\cdot\mathbf{n}\,da_M\ . \qquad (3.118)
\end{aligned}$$

Clearly, since $\dfrac{\partial\tilde{\rho}_M}{\partial t}$ above denotes the rate of change of ρ for *fixed* $\mathbf{x}_M$ in the (necessarily) fixed region $\mathcal{P}_M\equiv\mathcal{P}$, it follows from (3.118) that

$$\int_{\mathcal{P}_M}\frac{\partial\tilde{\rho}_M}{\partial t}dv_M = \int_{\mathcal{P}}\frac{\partial\rho}{\partial t}\,dv = -\int_{\partial\mathcal{P}}\rho\mathbf{v}\cdot\mathbf{n}\,da\ . \qquad (3.119)$$

Therefore, it is concluded from (3.118) and (3.119) that

$$\frac{d_M}{dt}\int_{\mathcal{P}_M}\tilde{\rho}_M(\mathbf{x}_M,t)\,dv_M = \int_{\partial\mathcal{P}_M}\rho(\mathbf{v}_M-\mathbf{v})\cdot\mathbf{n}\,da_M\ , \qquad (3.120)$$

which states that the rate of change of the mass contained in a mesh region equals to the rate at which mass flows through the boundary of the region. Using the divergence theorem, one may alternatively express (3.120) as

$$\frac{d_M}{dt}\int_{\mathcal{P}_M}\tilde{\rho}_M(\mathbf{x}_M,t)\,dv_M = \int_{\mathcal{P}_M}\mathrm{div}\left[\rho(\mathbf{v}_M-\mathbf{v})\right]dv_M\ . \qquad (3.121)$$

Upon combining $(3.118)_2$ and (3.121), it follows that

$$\int_{\mathcal{P}_M}\left(\frac{d_M\tilde{\rho}_M}{dt}+\rho\,\mathrm{div}\,\mathbf{v}_M\right)dv_M = \int_{\mathcal{P}_M}\rho\,\mathrm{div}(\mathbf{v}_M-\mathbf{v})\,dv_M+\int_{\mathcal{P}_M}\frac{\partial\tilde{\rho}_M}{\partial\mathbf{x}_M}\cdot(\mathbf{v}_M-\mathbf{v})\,dv_M\ , \qquad (3.122)$$

hence, appealing to the localization theorem,

$$\frac{d_M\tilde{\rho}_M}{dt}+\rho\,\mathrm{div}\,\mathbf{v} = \frac{\partial\tilde{\rho}_M}{\partial\mathbf{x}_M}\cdot(\mathbf{v}_M-\mathbf{v})\ . \qquad (3.123)$$

For consistency, it merits attention to check the two following two cases:

(a) $\mathbf{v}_M = \mathbf{v}$, where (3.123) reduces to the standard mass balance statement $\dfrac{d\rho}{dt} + \rho \operatorname{div} \mathbf{v} = 0$ (since, in this case, $\dfrac{d_M}{dt} = \dfrac{d}{dt}$),

(b) $\mathbf{v}_M = \mathbf{0}$, where (3.123) reduces to the standard mass balance statement $\dfrac{\partial \tilde{\rho}}{\partial t} + \operatorname{div}(\rho \mathbf{v}) = 0$ (since, in this case, $\dfrac{d_M}{dt} = \dfrac{\partial}{\partial t}$).

If $(\mathbf{v}_M - \mathbf{v}) \cdot \mathbf{n} = 0$ on $\partial\mathcal{M}$, then setting $\mathcal{P}_M = \mathcal{M}$ it is immediately concluded from (3.120) that

$$\frac{d_M}{dt} \int_{\mathcal{M}} \rho(\mathbf{x}_M, t)\, dv_M = 0 \,, \tag{3.124}$$

that is, the total mass of the body is conserved automatically by the ALE method.

The local statements of mass balance (1.66) (in the spatial frame) and (3.123) (in the mesh frame) jointly imply that

$$\dot{\rho} = -\rho \operatorname{div} \mathbf{v} = \frac{d_M \tilde{\rho}_M}{dt} - \frac{\partial \tilde{\rho}_M}{\partial \mathbf{x}_m} \cdot (\mathbf{v}_M - \mathbf{v}) \,. \tag{3.125}$$

The derivation of linear momentum balance in the mesh frame follows a similar procedure. First, define the rate of change of linear momentum in a mesh region $\mathcal{P}_M$ at time t as

$$\frac{d_M}{dt} \int_{\mathcal{P}_M} \rho \mathbf{v}\, dv_M \,, \tag{3.126}$$

and then evaluate the mesh time derivative to conclude that

$$\begin{aligned}
\frac{d_M}{dt} \int_{\mathcal{P}_M} \rho \mathbf{v} dv_M &= \int_{\mathcal{P}_M} \frac{d_M}{dt}(\rho \mathbf{v})\, dv_M + \int_{\mathcal{P}_M} \rho \mathbf{v} \frac{d_M (dv_M)}{dt} \\
&= \int_{\mathcal{P}_M} \frac{d_M}{dt}(\rho \mathbf{v})\, dv_M + \int_{\mathcal{P}_M} \rho \mathbf{v} \operatorname{div} \mathbf{v}_M\, dv_M \\
&= \int_{\mathcal{P}_M} \left[\frac{\partial}{\partial t}(\rho \mathbf{v}) + \frac{\partial (\rho \mathbf{v})}{\partial \mathbf{x}_M} \cdot \mathbf{v}_M + \rho \mathbf{v} \operatorname{div} \mathbf{v}_M \right] dv_M \\
&= \int_{\mathcal{P}_M} \frac{\partial}{\partial t}(\rho \mathbf{v})\, dv_M + \int_{\mathcal{P}_M} \operatorname{div}(\rho \mathbf{v} \otimes \mathbf{v}_M)\, dv_M \\
&= \int_{\mathcal{P}_M} \frac{\partial}{\partial t}(\rho \mathbf{v})\, dv_M + \int_{\partial \mathcal{P}_M} \rho \mathbf{v} (\mathbf{v}_M \cdot \mathbf{n})\, da_M \,.
\end{aligned} \tag{3.127}$$

Setting $\mathcal{P}_M \equiv \mathcal{P}$ and writing the linear momentum balance statement in Eulerian form as

$$\begin{aligned}
\frac{d}{dt}\int_{\mathcal{P}} \rho\mathbf{v}\, dv &= \int_{\mathcal{P}} \rho\mathbf{b}\, dv + \int_{\mathcal{P}} \mathbf{t}\, da \\
&= \int_{\mathcal{P}} \left(\dot{\overline{\rho}}\overline{\mathbf{v}} + \rho\mathbf{v}\,\mathrm{div}\,\mathbf{v}\right) dv \\
&= \int_{\mathcal{P}} \left[\frac{\partial}{\partial t}(\rho\mathbf{v}) + \frac{\partial(\rho\mathbf{v})}{\partial\mathbf{x}}\cdot\mathbf{v} + \rho\mathbf{v}\,\mathrm{div}\,\mathbf{v}\right] dv \\
&= \int_{\mathcal{P}} \frac{\partial}{\partial t}(\rho\mathbf{v})\, dv + \int_{\mathcal{P}} \mathrm{div}(\rho\mathbf{v}\otimes\mathbf{v})\, dv \\
&= \int_{\mathcal{P}} \frac{\partial}{\partial t}(\rho\mathbf{v})\, dv + \int_{\partial\mathcal{P}} \rho\mathbf{v}(\mathbf{v}\cdot\mathbf{n})\, da\ . \qquad (3.128)
\end{aligned}$$

As argued before for mass balance,

$$\int_{\mathcal{P}_M} \frac{\partial}{\partial t}(\rho\mathbf{v})\, dv_M = \int_{\mathcal{P}} \frac{\partial}{\partial t}(\rho\mathbf{v})\, dv = \int_{\mathcal{P}} \rho\mathbf{b}\, dv + \int_{\partial\mathcal{P}} \mathbf{t}\, da - \int_{\partial\mathcal{P}} \rho\mathbf{v}(\mathbf{v}\cdot\mathbf{n})\, da\ , \qquad (3.129)$$

where use is also made of (3.128). It follows from (3.127), (3.129), and the divergence theorem that

$$\begin{aligned}
\frac{d_M}{dt}\int_{\mathcal{P}_M} \rho\mathbf{v}\, dv_M &= \int_{\mathcal{P}_M} \rho\mathbf{b}\, dv_M + \int_{\partial\mathcal{P}_M} \mathbf{t}\, da_M + \int_{\partial\mathcal{P}_M} \rho\mathbf{v}\left[(\mathbf{v}_M - \mathbf{v})\cdot\mathbf{n}\right] da_M \\
&= \int_{\mathcal{P}_M} \rho\mathbf{b}\, dv_M + \int_{\mathcal{P}_M} \mathrm{div}\,\mathbf{T}\, dv_M + \int_{\mathcal{P}_M} \mathrm{div}\left[\rho\mathbf{v}\otimes(\mathbf{v}_M - \mathbf{v})\right] dv_M\ . \qquad (3.130)
\end{aligned}$$

Expanding the left- and the right-hand sides of the above leads to

$$\begin{aligned}
\int_{\mathcal{P}_M} \left(\frac{d_M\tilde{\rho}_M}{dt}\mathbf{v} + \rho\frac{d_M\tilde{\mathbf{v}}}{dt} + \rho\mathbf{v}\,\mathrm{div}\,\mathbf{v}_M\right) dv_M &= \int_{\mathcal{P}_M} \rho\mathbf{b} dv_M + \int_{\mathcal{P}_M} \mathrm{div}\,\mathbf{T} dv_M \\
+ \int_{\mathcal{P}_M} \mathbf{v}\left[\frac{\partial\tilde{\rho}_M}{\partial\mathbf{x}_M}\cdot(\mathbf{v}_M - \mathbf{v}) + \rho\,\mathrm{div}(\mathbf{v}_M - \mathbf{v})\right] dv_M + \int_{\mathcal{P}_M} \frac{\partial\tilde{\mathbf{v}}_M}{\partial\mathbf{x}_M}\rho(\mathbf{v}_M - \mathbf{v})\, dv_M \qquad (3.131)
\end{aligned}$$

or, upon imposing conservation of mass in the form (3.123),

$$\int_{\mathcal{P}_M} \rho\frac{d_M\tilde{\mathbf{v}}}{dt}\, dv = \int_{\mathcal{P}_M} \rho\mathbf{b}\, dv_M + \int_{\mathcal{P}_M} \mathrm{div}\,\mathbf{T}\, dv_M + \int_{\mathcal{P}_M} \frac{\partial\tilde{\mathbf{v}}_M}{\partial\mathbf{x}_M}\rho(\mathbf{v}_M - \mathbf{v})\, dv_M\ . \qquad (3.132)$$

Hence, the localization theorem, when applied to (3.132) results in the local form of linear momentum balance

$$\rho\frac{d_M\tilde{\mathbf{v}}}{dt} = \rho\mathbf{b} + \mathrm{div}\,\mathbf{T} + \frac{\partial\tilde{\mathbf{v}}}{\partial\mathbf{x}_M}\rho\left(\mathbf{v}_M - \mathbf{v}\right)\ . \qquad (3.133)$$

As with mass conservation, it is instructive to consider the two special cases:

(a) $\mathbf{v}_M = \mathbf{v}$, where (3.133) reduces to the standard linear momentum balance statement $\rho\mathbf{a} = \rho\mathbf{b} + \operatorname{div}\mathbf{T}$ (since, in this case, $\dfrac{d_M}{dt} = \dfrac{d}{dt}$),

(b) $\mathbf{v}_M = \mathbf{0}$, where (3.133) reduces to $\rho\left(\dfrac{\partial\mathbf{v}}{\partial t} + \dfrac{\partial\mathbf{v}}{\partial\mathbf{x}}\cdot\mathbf{v}\right) = \rho\mathbf{b} + \operatorname{div}\mathbf{T}$ (since, in this case, $\dfrac{d_M}{dt} = \dfrac{\partial}{\partial t}$).

Angular momentum balance in the mesh frame yields the symmetry of the Cauchy stress, as usual.

An alternative procedure for the derivation of the balance laws is possible without resorting to any integral statements.[7] Indeed, start by recalling (3.117) and use (1.66) to conclude that

$$\begin{aligned}\frac{d_M\rho_M}{dt} &= \frac{\partial\tilde{\rho}_M}{\partial t} + \frac{\partial\tilde{\rho}_M}{\partial\mathbf{x}_M}\cdot\mathbf{v}_M &&= \frac{\partial\tilde{\rho}}{\partial t} + \frac{\partial\tilde{\rho}_M}{\partial\mathbf{x}_M}\cdot\mathbf{v}_M \\ &&&= -\operatorname{div}(\rho\mathbf{v}) + \frac{\partial\tilde{\rho}_M}{\partial\mathbf{x}_M}\cdot\mathbf{v}_M \\ &&&= -\rho\operatorname{div}\mathbf{v} - \frac{\partial\tilde{\rho}}{\partial\mathbf{x}}\cdot\mathbf{v} + \frac{\partial\tilde{\rho}_M}{\partial\mathbf{x}_M}\cdot\mathbf{v}_M \\ &&&= -\rho\operatorname{div}\mathbf{v} - \frac{\partial\tilde{\rho}_M}{\partial\mathbf{x}_M}\cdot(\mathbf{v}-\mathbf{v}_M)\ , \end{aligned} \tag{3.134}$$

since $\tilde{\rho}(\mathbf{x}_M, t) = \tilde{\rho}_M(\mathbf{x}_M, t)$ implies that $\dfrac{\partial\tilde{\rho}}{\partial t} = \dfrac{\partial\tilde{\rho}_M}{\partial t}$ and also $\dfrac{\partial\tilde{\rho}}{\partial\mathbf{x}} = \dfrac{\partial\tilde{\rho}_M}{\partial\mathbf{x}}$. Therefore, (3.134) immediately implies (3.123). Linear momentum balance may be derived analogously.

To derive weak forms of the balance laws (3.123) and (3.133), $\sigma = \sigma_M(\mathbf{x}_M, t)$ and $\boldsymbol{\xi} = \tilde{\mathbf{x}}_M(\mathbf{x}_M, t)$ be a scalar and vector function at a point $\mathbf{x}_M$ of $\mathcal{M}$ at time t, respectively. The weak form of (3.123) amounts to finding $\rho \in \mathcal{Z}_M^+$, such that

$$\int_{\mathcal{M}} \sigma\left[\frac{d_M\tilde{\rho}}{dt} + \rho\operatorname{div}\mathbf{v} - \frac{\partial\tilde{\rho}}{\partial\mathbf{x}_M}\cdot(\mathbf{v}_M - \mathbf{v})\right] dv_M \ = \ 0\ , \tag{3.135}$$

for all $\sigma \in \mathcal{Z}_M$, where, in analogy to the definitions in (3.15),

$$\mathcal{Z}_M \ = \ \{\sigma : \mathcal{M}\times\mathbb{R}\to\mathbb{R}\} \quad , \quad \mathcal{Z}_M^+ \ = \ \{\sigma : \mathcal{M}\times\mathbb{R}\to\mathbb{R} \mid \sigma > 0\}\ . \tag{3.136}$$

[7] J. Donea, A. Huerta, J.-Ph. Ponthot, and A. Rodriguez-Ferran. Arbitrary Lagrangian-Eulerian methods. In E. Stein and R. De Borst and T.J.R. Hughes, editors, *Encyclopedia of Computational Mechanics, Volume 1: Fundamentals*, chapter 14. John Wiley, New York, 2004.

Likewise, the weighted-residual form of the linear momentum balance statement in (3.133) including the Neumann boundary conditions at a given time t requires that the displacement $\mathbf{u} \in \mathcal{U}_M$ (or velocity $\mathbf{v} \in \mathcal{V}_M$) be such that

$$\int_{\mathcal{M}} \boldsymbol{\xi} \cdot \left[\rho \frac{d_M \tilde{\mathbf{v}}}{dt} - \rho \mathbf{b} - \operatorname{div} \mathbf{T} - \frac{\partial \tilde{\mathbf{v}}}{\partial \mathbf{x}_M} \rho (\mathbf{v}_M - \mathbf{v}) \right] dv_M + \int_{\Gamma_{q_M}} \boldsymbol{\xi} \cdot (\mathbf{t} - \overline{\mathbf{t}}) \, da_M \;=\; 0 \;, \tag{3.137}$$

for all $\boldsymbol{\xi} \in \mathcal{W}_M$, where

$$\mathcal{U}_M \;=\; \left\{ \mathbf{u} : \mathcal{M}_0 \times \mathbb{R} \to \mathcal{E}^3 \mid \det \left(\mathbf{I} + \frac{\partial \mathbf{u}}{\mathbf{X}} \right) > 0 \;,\; u_i(\mathbf{X}, t) \;=\; \overline{u}_i \text{ on } \Gamma_{u_i} \;, \right.$$
$$\left. \mathbf{u}(\mathbf{X}, 0) \;=\; \mathbf{0} \;,\; \dot{\mathbf{u}}(\mathbf{X}, 0) \;=\; \mathbf{v}_0 \right\} \tag{3.138}$$

for solids,

$$\mathcal{V}_M \;=\; \left\{ \mathbf{v} : \mathcal{M} \times \mathbb{R} \to \mathcal{E}^3 \mid v_i(\mathbf{x}, t) \;=\; \overline{v}_i \text{ on } \Gamma_{u_i} \;,\; \mathbf{v}(\mathbf{x}, 0) = \mathbf{v}_0 \right\} \tag{3.139}$$

for fluids, and

$$\mathcal{W}_M \;=\; \left\{ \boldsymbol{\xi} : \mathcal{M} \times \mathbb{R} \longrightarrow \mathcal{E}^3 \quad , \quad \tilde{\xi}_i(\mathbf{x}, t) \;=\; 0 \text{ on } \Gamma_{u_i} \right\} \;. \tag{3.140}$$

Note that Γ_{q_M} in (3.137) is the part of the exterior boundary $\partial\mathcal{M}$ which *coincides* with the material boundary Γ_q at time t, as in Figure 3.18. Using integration by parts and the

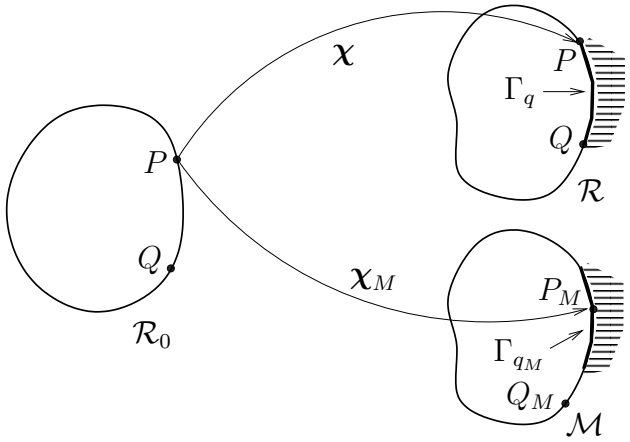

Figure 3.18. *Neumann boundary conditions in ALE methods ($\mathcal{R}$ and $\mathcal{M}$ are shown apart from each other for clarity)*

divergence theorem, as well as the definition of $\mathcal{W}_M$ in (3.140), it follows that

$$\int_{\mathcal{M}} \boldsymbol{\xi} \cdot \operatorname{div} \mathbf{T} \, dv_M \;=\; \int_{\Gamma_{q_M}} \boldsymbol{\xi} \cdot \mathbf{t} \, da_M - \int_{\mathcal{M}} \frac{\partial \tilde{\boldsymbol{\xi}}}{\partial \mathbf{x}_M} \cdot \mathbf{T} \, dv_M \;. \tag{3.141}$$

It follows from (3.137) and (3.141) that the weak form of linear momentum balance takes the form

$$\int_{\mathcal{M}} \boldsymbol{\xi} \cdot \rho \frac{d_M \tilde{\mathbf{v}}}{dt}\, dv_M + \int_{\mathcal{M}} \frac{\partial \tilde{\boldsymbol{\xi}}}{\partial \mathbf{x}_M} \cdot \mathbf{T}\, dv_M = \int_{\mathcal{M}} \boldsymbol{\xi} \cdot \rho \mathbf{b}\, dv_M + \int_{\Gamma_{q_M}} \boldsymbol{\xi} \cdot \overline{\mathbf{t}}\, da_M + \int_{\mathcal{M}} \boldsymbol{\xi} \cdot \rho \left[\frac{\partial \tilde{\mathbf{v}}}{\partial \mathbf{x}_M} (\mathbf{v}_M - \mathbf{v}) \right] dv_M \ . \quad (3.142)$$

There exist two general methodologies for the finite element approximation of (3.135) and (3.142) in an incremental formulation:

(a) Solve (3.135) and (3.142) simultaneaously at every time step,

(b) Use an *operator-split* procedure, where a typical ALE time step comprises two sub-steps:

(b.1) a purely Lagrangian step (where conservation of mass is automatic),

(b.2) if needed, a sub-step in which the mesh convects according to a specified mesh motion $\boldsymbol{\chi}_M$ (hence, mass balance should be enforced).

In both methodologies, it is important to emphasize that convection of any history variables (attached, by definition, to material points) requires an additional algorithmic procedure, since the mesh points are not material.

Starting with the first of the above methodologies, interpolate the relevant fields in an ALE finite element with domain Ω^e at time t_{n+1} as

$$\begin{aligned}
\mathbf{u}(\mathbf{x}_M, t_{n+1})\big|_{\Omega^e} &= \mathbf{u}^e_{n+1}(\mathbf{x}_M) \doteq \sum_{i=1}^{\texttt{NEN}} N^e_i \mathbf{u}^e_{i_{n+1}} = [\mathbf{N}^e][\hat{\mathbf{u}}^e_{n+1}] \ , \\
\mathbf{v}(\mathbf{x}_M, t_{n+1})\big|_{\Omega^e} &= \mathbf{v}^e_{n+1}(\mathbf{x}_M) \doteq \sum_{i=1}^{\texttt{NEN}} N^e_i \mathbf{v}^e_{i_{n+1}} = [\mathbf{N}^e][\hat{\mathbf{v}}^e_{n+1}] \ , \\
\frac{d_M \mathbf{v}}{dt}(\mathbf{x}_M, t_{n+1})\big|_{\Omega^e} &= \mathring{\mathbf{v}}^e_{n+1}(\mathbf{x}_M) \doteq \sum_{i=1}^{\texttt{NEN}} N^e_i \mathring{\mathbf{v}}^e_{i_{n+1}} = [\mathbf{N}^e][\hat{\mathring{\mathbf{v}}}^e_{n+1}] \ , \\
\mathbf{v}_M(\mathbf{x}_M, t_{n+1})\big|_{\Omega^e} &= \mathbf{v}^e_{M\, n+1}(\mathbf{x}_M) \doteq \sum_{i=1}^{\texttt{NEN}} N^e_i \mathbf{v}^e_{M\, i_{n+1}} = [\mathbf{N}^e][\hat{\mathbf{v}}^e_{M\, n+1}] \ , \\
\boldsymbol{\xi}(\mathbf{x}_M, t_{n+1})\big|_{\Omega^e} &= \boldsymbol{\xi}^e_{n+1}(\mathbf{x}_M) \doteq \sum_{i=1}^{\texttt{NEN}} N^e_i \boldsymbol{\xi}^e_{i_{n+1}} = [\mathbf{N}^e][\hat{\boldsymbol{\xi}}^e_{n+1}] \ ,
\end{aligned} \quad (3.143)$$

where $N_i^e = N_i^e(\mathbf{x}_M)$, $i = 1, 2, \ldots, \texttt{NEN}$. In addition,

$$\begin{aligned}
\rho(\mathbf{x}_M, t_{n+1})\big|_{\Omega^e} &= \rho^e_{n+1}(\mathbf{x}_M) \doteq \sum_{j=1}^{\texttt{NEM}} \bar{N}^e_j \rho^e_{j_{n+1}} = [\bar{\mathbf{N}}^e][\hat{\boldsymbol{\rho}}^e_{n+1}] \,, \\
\frac{d_M \rho}{dt}(\mathbf{x}_M, t_{n+1})\big|_{\Omega^e} &= \mathring{\rho}^e_{n+1}(\mathbf{x}_M) \doteq \sum_{j=1}^{\texttt{NEM}} \bar{N}^e_j \mathring{\rho}^e_{j_{n+1}} = [\bar{\mathbf{N}}^e][\hat{\mathring{\boldsymbol{\rho}}}^e_{n+1}] \,, \\
\sigma(\mathbf{x}_M, t_{n+1})\big|_{\Omega^e} &= \sigma^e_{n+1}(\mathbf{x}_M) \doteq \sum_{j=1}^{\texttt{NEM}} \bar{N}^e_j \sigma^e_{j_{n+1}} = [\bar{\mathbf{N}}^e][\hat{\boldsymbol{\sigma}}^e_{n+1}] \,,
\end{aligned} \tag{3.144}$$

where $\bar{N}^e_j = \bar{N}^e_j(\mathbf{x}_M)$, $j = 1, 2, \ldots \texttt{NEM}$, are the element interpolation function for density and its derivatives. These may, in general, be different from those used for the body motion and its derivatives.

Substituting the interpolations in (3.143) and (3.144) to (3.135), when the latter is restricted to the domain Ω^e of an ALE element, it follows that

$$\begin{aligned}
[\hat{\boldsymbol{\sigma}}^e_{n+1}]^T \int_{\Omega^e} [\bar{\mathbf{N}}^e]^T \Big\{ [\bar{\mathbf{N}}^e][\hat{\mathring{\boldsymbol{\rho}}}^e_{n+1}] + \left([\bar{\mathbf{N}}^e][\hat{\boldsymbol{\rho}}^e_{n+1}]\right) \left([\boldsymbol{\Delta}^e_{n+1}][\hat{\mathbf{v}}^e_{n+1}]\right) \\
- \left([\hat{\boldsymbol{\rho}}^e_{n+1}]^T [\boldsymbol{\Lambda}^e_{n+1}]^T\right) [\mathbf{N}^e] \left([\hat{\mathbf{v}}^e_{M_{n+1}}] - [\hat{\mathbf{v}}^e_{n+1}]\right) \Big\} \, dv_M = 0 \,,
\end{aligned} \tag{3.145}$$

where

$$[\boldsymbol{\Delta}^e_{n+1}] = \begin{bmatrix} N^e_{1,1} & N^e_{1,2} & N^e_{1,3} & \cdots & N^e_{I,1} & N^e_{I,2} & N^e_{I,3} & \cdots & N^e_{\texttt{NEN},1} & N^e_{\texttt{NEN},2} & N^e_{\texttt{NEN},3} \end{bmatrix} \tag{3.146}$$

and

$$[\boldsymbol{\Lambda}^e_{n+1}] = \begin{bmatrix} \bar{N}^e_{1,1} & \cdots & \bar{N}^e_{I,1} & \cdots & \bar{N}^e_{\texttt{NEM},1} \\ \bar{N}^e_{1,2} & \cdots & \bar{N}^e_{I,2} & \cdots & \bar{N}^e_{\texttt{NEM},2} \\ \bar{N}^e_{1,3} & \cdots & \bar{N}^e_{I,3} & \cdots & \bar{N}^e_{\texttt{NEM},3} \end{bmatrix} . \tag{3.147}$$

Similarly, substituting the interpolations in (3.143) and (3.144) to (3.142), when the latter is written for the domain Ω^e of an ALE element, it follows that

$$\begin{aligned}
[\hat{\boldsymbol{\xi}}^e_{n+1}]^T \Bigg[\int_{\Omega^e} [\mathbf{N}^e]^T \left([\mathbf{N}^e][\hat{\mathring{\mathbf{v}}}^e_{n+1}]\right) \left([\bar{\mathbf{N}}^e][\hat{\boldsymbol{\rho}}^e_{n+1}]\right) dv_M + \int_{\Omega^e} [\mathbf{B}^e_{n+1}]^T < \mathbf{T}_{n+1} > dv_M \\
- \int_{\Omega^e} [\mathbf{N}^e]^T [\mathbf{b}_{n+1}] \left([\bar{\mathbf{N}}^e][\hat{\boldsymbol{\rho}}^e_{n+1}]\right) dv_M - \int_{\partial\Omega^e} [\mathbf{N}^e]^T [\bar{\mathbf{t}}_{n+1}] da_M \\
- \int_{\partial\Omega^e} [\mathbf{N}^e]^T [\boldsymbol{\Gamma}^e_{n+1}][\mathbf{N}^e] [\left([\hat{\mathbf{v}}^e_{M_{n+1}}] - [\hat{\mathbf{v}}^e_{n+1}]\right) \left([\bar{\mathbf{N}}^e][\hat{\boldsymbol{\rho}}^e_{n+1}]\right) dv_M \Bigg] = 0 \,.
\end{aligned} \tag{3.148}$$

Here,

$$[\boldsymbol{\Gamma}^e_{n+1}] = \begin{bmatrix} [\mathbf{N}^e_{,1}][\hat{\mathbf{v}}^e_{n+1}] & [\mathbf{N}^e_{,2}][\hat{\mathbf{v}}^e_{n+1}] & [\mathbf{N}^e_{,3}][\hat{\mathbf{v}}^e_{n+1}] \end{bmatrix} , \tag{3.149}$$

and all derivatives in $[\mathbf{B}^e_{n+1}]$ and $[\mathbf{\Gamma}^e_{n+1}]$ are taken with respect to $\mathbf{x}_M$.

Recalling that $\hat{\boldsymbol{\sigma}}^e_{n+1}$ and $\hat{\boldsymbol{\xi}}^e_{n+1}$ are arbitrary and after assemblying the element equations, as usual, one recovers a system of coupled non-linear ordinary differential equations in time with unknowns $\hat{\mathbf{u}}_{n+1}$ (or $\hat{\mathbf{v}}_{n+1}$) and $\hat{\boldsymbol{\rho}}_{n+1}$. Note that the mesh motion $\boldsymbol{\chi}_M$ is assumed to be either prescribed or deduced (an extra task that will be discussed later in this section).

The two sets of equations can be integrated either by an implicit or an explicit method, along the lines of the corresponding discussion in Section 3.4. In the former case, one may use, *e.g.*, the Newmark method at the cost of repeated solving of coupled algebraic equations. In the latter case, one may use, *e.g.*, the centered-difference method, which, for the domain $(t_n, t_{n+1}]$, yields the equations

$$\boldsymbol{\rho}_{n+1} \;=\; \boldsymbol{\rho}_n + \mathring{\hat{\boldsymbol{\rho}}}_n \Delta t_n \tag{3.150}$$

and also

$$\hat{\mathbf{v}}_{n+1} \;=\; \hat{\mathbf{v}}_n + \frac{1}{2}\left(\mathring{\hat{\mathbf{v}}}_n + \mathring{\hat{\mathbf{v}}}_{n+1}\right)\Delta t_n \quad , \quad \hat{\mathbf{u}}_{n+1} \;=\; \hat{\mathbf{u}}_n + \hat{\mathbf{v}}_n \Delta t_n + \frac{1}{2}\mathring{\hat{\mathbf{v}}}_n \Delta t_n^2 \; . \tag{3.151}$$

For the centered-difference method to be free of equation-solving, it is necessary that the two global associated with the element matrices

$$[\bar{\mathbf{M}}^e_{n+1}] \;=\; \int_{\Omega^e} [\bar{\mathbf{N}}^e]^T [\bar{\mathbf{N}}^e]\, dv_M \quad , \quad [\mathbf{M}^e_{n+1}] \;=\; \int_{\Omega^e} \rho [\mathbf{N}^e]^T [\mathbf{N}^e]\, dv_M \tag{3.152}$$

to be rendered diagonal. In addition, it is readily seen from (3.145) and (3.148) that an explicit velocity estimate $\hat{\mathbf{v}}^{e,0}_{n+1}$ is needed to estimate the ALE-related flux terms before the velocity vector is updated using $(3.151)_1$.

Consider next the alternative operator-split algorithm, which consists of a purely Lagrangian step, followed, if needed, by an *advective* or *Eulerian remapping* sub-step, where the nodal/elemental variables are mapped from the previous Lagrangian mesh to the new ALE mesh, as dictated by the mesh motion. Most often in practice, there are multiple Lagrangian steps before a single remapping sub-step. Also, the operator-split algorithm facilitates the automatic determination of the mesh motion based on the distortion encountered in the Lagrangian mesh between two Eulerian remappings.

The advective remapping sub-step involves the following tasks:

(i) select the mesh regions to be remapped,

(ii) deduce a suitable mesh motion,

(iii) compute the advection of mass and linear momentum,

(iv) compute the advection of history variables.

By way of background, it is instructive to distinguish advective remapping from *adaptive remeshing* (or *mesh rezoning*). In the latter, a new mesh is generated at $t = t_{n+1}$ not necessarily with the same connectivities with the old mesh from $t = t_n$, and all variables are projected from the old mesh. In contrast, Eulerian remapping by the mesh motion $\boldsymbol{\chi}_M$ maps the mesh from $t = t_n$ to its new configuration at $t = t_{n+1}$, and updates all relevant variables to account for the transport of material. Hence, Eulerian remapping entails no change in the element connectivities.

Deferring momentarily the discussion of tasks (i) and (ii) above, concentrate on the last two tasks of Eulerian remapping. For task (iii), two distinct approaches may be adopted. In the first approach, the ALE equations are solved in $(t_n, t_{n+1}]$ for a fixed motion $\boldsymbol{\chi}$ (as computed from the Lagrangian step) and for prescribed mesh motion $\boldsymbol{\chi}_M$ to obtain updated values for $\hat{\rho}_{n+1}$, $\hat{\mathbf{u}}_{n+1}$, $\hat{\mathbf{v}}_{n+1}$, *etc.* Indeed, assume that the vectors $\hat{\rho}^L_{n+1}$, $\hat{\mathbf{u}}^L_{n+1}$, $\hat{\mathbf{v}}^L_{n+1}$, *etc.*, have been computed from the Lagrangian step. Also, assume that the mesh motion in $(t_n, t_{n+1}]$ has been somehow determined. The nodal and elemental quantities will change

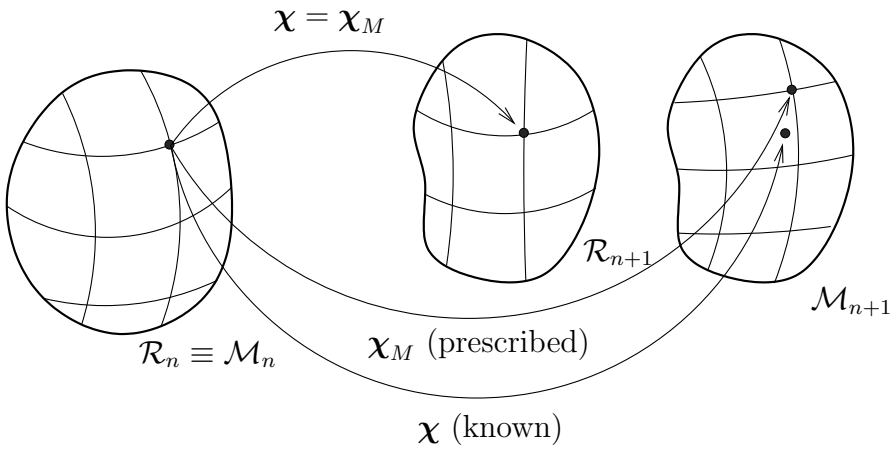

Figure 3.19. *Operator-split approach for ALE implementation ($\mathcal{R}_{n+1}$, resulting from Lagrangian step and $\mathcal{M}_{n+1}$, resulting from Eulerian remapping are shown apart from each other for clarity)*

during the remapping sub-step because the nodes are moving independently of the fixed body, as in Figure 3.19. The new nodal and elemental values can be computed separately for conservation of mass and balance of linear momentum, using the ALE weak forms introduced earlier, except that here the density and body motion are already known with reference to

the Lagrangian mesh and need only be calculated on the remapped mesh. In particular, the discrete counterpart of the mass conservation equation (3.135) becomes

$$\int_{\mathcal{M}} \sigma \left[\frac{d_M \tilde{\rho}}{dt} + \rho \operatorname{div} \mathbf{v}^L - \frac{\partial \tilde{\rho}}{\partial \mathbf{x}_M} \cdot (\mathbf{v}_M - \mathbf{v}^L) \right] dv_M \;=\; 0 \;, \tag{3.153}$$

and can be integrated in $(t_n, t_{n+1}]$ with given $\mathbf{v}^L$ and $\mathbf{v}_M$ for ρ_{n+1}. Likewise, one may obtain $\mathbf{v}_{n+1}$ by rewriting the discrete counterpart of (3.142) as

$$\begin{aligned} &\int_{\mathcal{M}} \boldsymbol{\xi} \cdot \rho^L \frac{d_M \tilde{\mathbf{v}}}{dt} \, dv_M + \int_{\mathcal{M}} \frac{\partial \tilde{\boldsymbol{\xi}}}{\partial \mathbf{x}_M} \cdot \mathbf{T} \, dv_M \\ &\qquad = \int_{\mathcal{M}} \boldsymbol{\xi} \cdot \rho^L \mathbf{b} \, dv_M + \int_{\Gamma_{q_M}} \boldsymbol{\xi} \cdot \bar{\mathbf{t}} \, da_M + \int_{\mathcal{M}} \boldsymbol{\xi} \cdot \rho^L \left[\frac{\partial \tilde{\mathbf{v}}}{\partial \mathbf{x}_M} (\mathbf{v}_M - \mathbf{v}) \right] dv_M \;, \end{aligned} \tag{3.154}$$

and integrating for $\mathbf{v}_{n+1}$ in $(t_n, t_{n+1}]$ with given ρ^L and $\mathbf{v}_M$. Note that the sets of equations resulting from (3.153) and (3.154) are uncoupled.

Projection methods are addressing the same problem in a purely geometric fashion, which is also applicable to the advection of history variables in task (iv) above. To introduce these methods, consider a scalar field f which must be remapped at a given time t_{n+1}. With

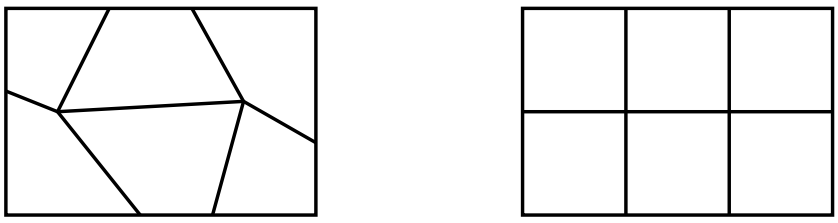

"-" mesh "+" mesh

Figure 3.20. *Projection method from one mesh (denoted "-") to another (denoted "+")*

reference to Figure 3.20, let the interpolation of f on the initial mesh (denoted here as the "-" mesh) be

$$f^- \;=\; \sum_I \varphi_I^- f_I^- \;, \tag{3.155}$$

where φ_I^- are global interporation functions. After remapping, the same function is interpolated on the new mesh (denoted here as the "+" mesh) as

$$f^+ \;=\; \sum_I \varphi_I^+ f_I^+ \;, \tag{3.156}$$

where φ_I^+ are the global interpolation functions on the new mesh. Assuming that f^- is given, the goal of a projection method is to determine the nodal values f_I^+, such that the error between f^- and f^+ be minimized in some way. This is generally accomplished by choosing f_I^+ such that

$$\int_{\mathcal{M}} \psi(f^+ - f^-)\, dv_M \;=\; 0\;. \tag{3.157}$$

Here, $\psi = \sum_I \alpha_I \psi_I$, where ψ_I are linearly independent weighting functions and α_I are arbitrary parameters. The projection condition (3.157) leads to the system of linear algebraic equations

$$\int_{\mathcal{M}} \psi_I(f^+ - f^-)\, dv_M \;=\; \int_{\mathcal{M}} \psi_I \left[\sum_J \varphi_J^+ f_J^+ - \sum_J \varphi_J^- f_J^-\right] dv_M \;=\; 0\;. \tag{3.158}$$

for all I. This system can be solved for f_J^+ assuming non-singularity of the matrix with components $\int_{\mathcal{M}} \psi_I \varphi_J^+ dv_M$. A typical choice for this projection is $\psi_I = \varphi_I^+$, which leads to a classical least-squares problem.

Attention is now turned to tasks (i) and (ii), which pertain to the definition of a suitable mesh motion. Preliminary to any developments, it is essential to stress that such for such a motion to be practical, it has to be defined in an automated manner as the ALE solution evolves. Start by considering a popular heuristic procedure employed for meshes with 4-node quadrilateral elements.[8] The idea here is to maintain a mesh which resembles as much as possible a uniform mesh, see Figure 3.21. With reference to Figure 3.21, consider a

ideal mesh patch actual mesh patch

Figure 3.21. *Volumetric and shear distortion indicators for a patch of 4-node quadrilaterals*

[8] D.J. Benson. An efficient, accurate, simple ALE method for nonlinear finite element programs. *Comp. Meth. Appl. Mech. Engr.*, 72:305–350, (1989).

typical node in a mesh of 4-node quadrilaterals, and define a scalar measure R_v of *volumetric distortion* around this node as

$$R_v \;=\; \frac{\min\limits_{I=1-4}(A_I)}{\max\limits_{I=1-4}(A_I)}\;, \tag{3.159}$$

where, generally, $0 < R_v \leq 1$ and $R_v = 1$ for the uniform mesh. A scalar measure R_s is shear distortion is likewise defined as

$$R_s \;=\; \min_{I=1-4}(\sin\theta_i)\;, \tag{3.160}$$

where, generally, $0 < R_s \leq 1$ and $R_s = 1$ for a uniform mesh. Note that R_s detects both acute and obtuse angles. Subsequently, define an empirical non-negative function $f(R_v, R_s)$, such that $f(1,1) = 0$ (optimal value), and a node I is "flagged" to move when $f > \bar{f}$, where $\bar{f} > 0$ is a user-specified constant.

The last outstanding task is to decuce a mesh motion. The simplest possible scheme would place node I in the coordinate-wise arithmetic mean of the locations of its immediately neighboring nodes. A more sophisticated (and better performing) scheme is based on the so-called *equipotential relaxation* originally propounded by A.M. Winslow for triangular meshes

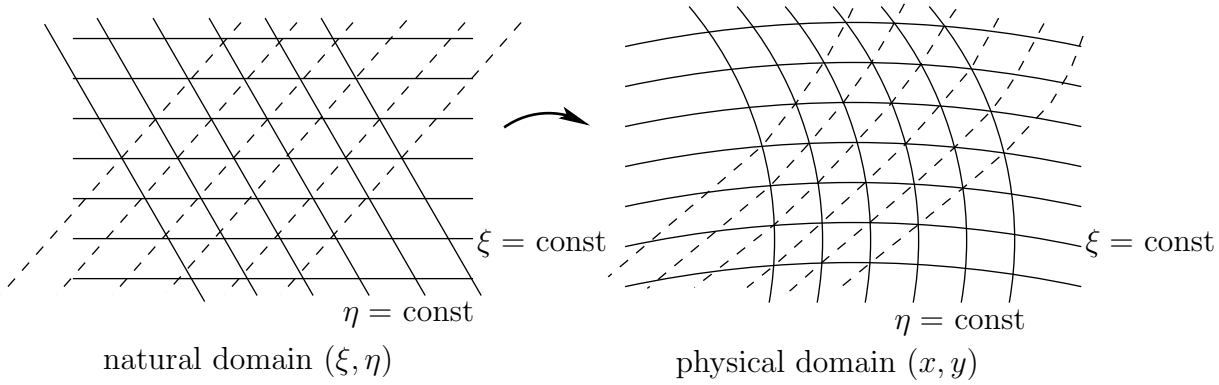

Figure 3.22. *Smooth map between equilateral triangles in the natural space* (ξ, η) *and general triangles in the physical space* (x, y)

used in hydrocodes.[9] Winslow argued that, since any triagular element domain can be mapped uniquely into a regular equilateral triangle (common for all elements of a mesh) in the space of natural coordinates (ξ, η), a high-quality mesh can be created by the intersections of equally-spaced lines of "potential" ξ = constant, η = constant, together with a third set

[9] A.M. Winslow. Numerical solution of the quasilinear Poisson equation in a nonuniform triangle mesh. *J. Comp. Physics*, 2:149–172, (1967).

of lines drawn through the intersection points, as in Figure 3.22. The Laplace-Poisson equation (being an archetypical example of an elliptic partial differential equation) produces a smooth set of equipotential lines, provided the boundary conditions and force are smooth. Therefore, generating a high-quality mesh (or, improving the quality of an existing mesh) is tantamount to solving the Laplace-Poisson equation for the natural coordinates ξ and η in the physical domain and defining element edges at equipotential lines of ξ and η. The same logic applies for quadrilateral meshes mapped from square elements in the natural domain, see Figure 3.23. Equipotential relaxation has been shown to produce excellent meshes for

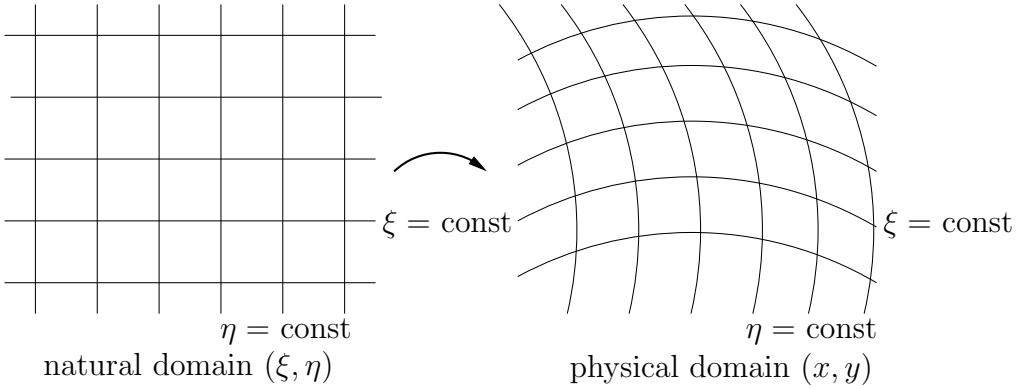

Figure 3.23. *Smooth map between squares in the natural space* (ξ, η) *and general quadrilaterals in the physical space* (x, y)

relatively complex two-dimensional domains.[10]

To derive the equations used for equipotential relaxation, start by considering the general two-dimensional mapping from the natural to the physical domain in the form

$$x = \overline{x}(\xi, \eta) \quad , \quad y = \overline{y}(\xi, \eta) \; . \tag{3.161}$$

Since the mapping is assumed to be invertible, one may also write

$$\xi = \overline{\xi}(x, y) \quad , \quad \eta = \overline{\eta}(x, y) \tag{3.162}$$

where the individual functions $\overline{x}$, $\overline{y}$, $\overline{\xi}$, $\overline{\eta}$ are to be determined, see Figure 3.24. The two Laplace-Poisson problems are now defined by

$$\nabla^2 \xi = 0 \quad , \quad \nabla^2 \eta = 0 \; , \tag{3.163}$$

[10] J.F. Thompson, F.C. Thames, and C.W. Mastin. Automatic numerical generation of body-fitted curvilinear coordinate system for fields containing any number of arbitrary two-dimensional bodies, *J. Comput. Phys.*, 15:299-319 (1974).

where $\nabla^2 = \frac{\partial^2}{\partial x^2} + \frac{\partial^2}{\partial y^2}$. At this stage, it is crucial to observe that the boundary conditions for the equations in (3.163) are given in the physical space (put differently, it is the domain in the physical space that is known and that needs meshing). Therefore, since boundary conditions are enforced on the dependent variable of a differential equation, it is necessary that (3.163) be expressed inversely, that is, to interchange the dependent and independent variables. This is possible since $\overline{x}$, $\overline{y}$ are invertible.

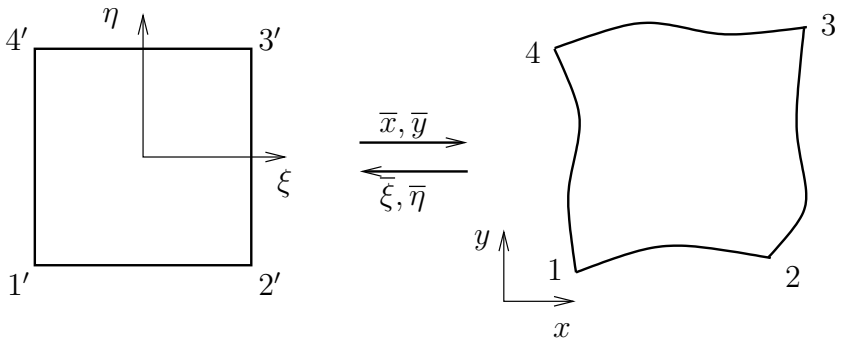

Figure 3.24. *Smooth map from a square in the natural space* (ξ, η) *and a general quadrilateral domain in the physical space* (x, y)

To this end, use the chain rule to write for any differentiable function $f = f(x, y)$,

$$\begin{aligned} \frac{\partial f}{\partial \xi} &= \frac{\partial f}{\partial x}\frac{\partial \overline{x}}{\partial \xi} + \frac{\partial f}{\partial y}\frac{\partial \overline{y}}{\partial \xi} \\ \frac{\partial f}{\partial \eta} &= \frac{\partial f}{\partial x}\frac{\partial \overline{x}}{\partial \eta} + \frac{\partial f}{\partial y}\frac{\partial \overline{y}}{\partial \eta} \end{aligned} \tag{3.164}$$

or, in matrix form,

$$\begin{bmatrix} f_{,\xi} \\ f_{,\eta} \end{bmatrix} = \begin{bmatrix} \overline{x}_{,\xi} & \overline{y}_{,\xi} \\ \overline{x}_{,\eta} & \overline{y}_{,\eta} \end{bmatrix} \begin{bmatrix} f_{,x} \\ f_{,y} \end{bmatrix} . \tag{3.165}$$

Therefore,

$$\begin{bmatrix} f_{,x} \\ f_{,y} \end{bmatrix} = \frac{1}{j} \begin{bmatrix} \overline{y}_{,\eta} & -\overline{y}_{,\xi} \\ -\overline{x}_{,\eta} & \overline{x}_{,\xi} \end{bmatrix} \begin{bmatrix} f_{,\xi} \\ f_{,\eta} \end{bmatrix} , \tag{3.166}$$

where $j = \overline{x}_{,\xi}\overline{y}_{,\eta} - \overline{x}_{,\eta}\overline{y}_{,\xi}$ and $j \neq 0$ owing to the invertibility of $\overline{x}, \overline{y}$. Setting $f = \overline{\xi}$ and $f = \overline{\eta}$, it follows from the above equation that

$$\overline{\xi}_{,x} = \frac{1}{j}\overline{y}_{,\eta} \quad , \quad \overline{\xi}_{,y} = -\frac{1}{j}\overline{x}_{,\eta} \tag{3.167}$$

and

$$\overline{\eta}_{,x} = \frac{1}{j}\overline{y}_{,\xi} \quad , \quad \overline{\eta}_{,y} = -\frac{1}{j}\overline{x}_{,\xi} . \tag{3.168}$$

Repeating this process to calculate expressions for $\overline{\xi}_{,xx}$, $\overline{\xi}_{,yy}$, $\overline{\eta}_{,xx}$, and $\overline{\eta}_{,yy}$, and substituting these in (3.163) results in the two coupled non-linear partial differential equations

$$\alpha x_{,\xi\xi} - 2\beta x_{,\xi\eta} + \gamma x_{,\eta\eta} \;=\; 0 \quad , \quad \alpha y_{,\xi\xi} - 2\beta y_{,\xi\eta} + \gamma y_{,\eta\eta} \;=\; 0 \;, \tag{3.169}$$

where

$$\alpha \;=\; x_{,\eta}^2 + y_{,\eta}^2 \quad , \quad \beta \;=\; x_{,\xi} x_{,\eta} + y_{,\xi} y_{,\eta} \quad , \quad \gamma \;=\; x_{,\xi}^2 + y_{,\xi}^2 \tag{3.170}$$

and the overbars have been dropped for brevity. With reference to Figure 3.24, the boundary conditions take the form

$$\begin{aligned}
x \;&=\; \overline{x}(\xi_1,\eta) \quad \text{on} \quad 1'-4' \quad , \quad y \;=\; \overline{y}(\xi_1,\eta) \quad \text{on} \quad 1'-4' \;, \\
x \;&=\; \overline{x}(\xi_2,\eta) \quad \text{on} \quad 2'-3' \quad , \quad y \;=\; \overline{y}(\xi_2,\eta) \quad \text{on} \quad 2'-3' \;, \\
x \;&=\; \overline{x}(\xi,\eta_1) \quad \text{on} \quad 1'-2' \quad , \quad y \;=\; \overline{y}(\xi,\eta_1) \quad \text{on} \quad 1'-2' \;, \\
x \;&=\; \overline{x}(\xi,\eta_2) \quad \text{on} \quad 3'-4' \quad , \quad y \;=\; \overline{y}(\xi,\eta_2) \quad \text{on} \quad 3'-4' \;,
\end{aligned} \tag{3.171}$$

where $\overline{x}$, $\overline{y}$ are assumed to be known on the boundary of the physical domain. The solutions of the equations (3.169) provide directly the placements of points (x, y) at the intersection of equipotential curves ξ = constant and η = constant.

Note that the differential equations (3.169) are more complex than the original Laplacians in (3.163). However, the domain and boundary conditions of (3.169) are considerably simpler than those of the original Laplacians.

In practice, equations (3.169) are solved approximately by a finite difference method using an iterative technique. For example, consider the case of 3-node triangles with equally-spaced equipotential lines of unit spacing in the natural domain, as in Figure 3.25. Here, it is easy to

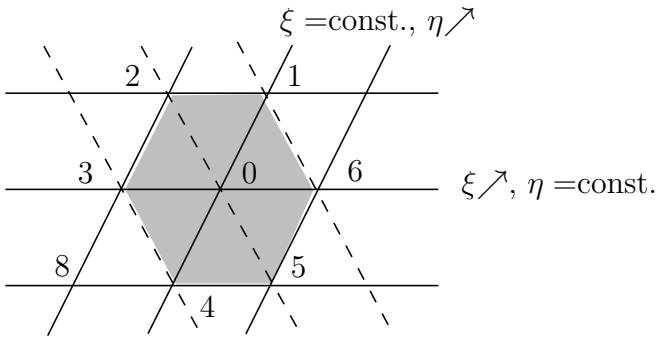

Figure 3.25. *Finite difference stencil for linear triangles with unit spacing in the natural domain*

derive the placement (x_0, y_0) of the center node in terms of the placement of the neighboring

nodes according to

$$\begin{aligned} x_{,\xi}\big|_0 &\doteq \frac{1}{6}\left[(x_1+2x_6+x_5)-(x_2+2x_3+x_4)\right] \ , \\ x_{,\eta}\big|_0 &\doteq \frac{1}{6}\left[(x_2+2x_1+x_6)-(x_3+2x_4+x_5)\right] \ , \\ x_{,\xi\xi}\big|_0 &\doteq x_6-2x_0+x_3 \ , \\ x_{,\eta\eta}\big|_0 &\doteq x_1-2x_0+x_4 \ , \\ x_{,\xi\eta}\big|_0 &\doteq \frac{1}{2}\left[(x_1+x_6+x_3+x_4)-(x_2+x_5+2x_0)\right] \ . \end{aligned} \tag{3.172}$$

with corresponding equations for $y_{,\xi}$, $y_{,\eta}$, $y_{,\xi\xi}$, $y_{,\eta\eta}$, and $y_{,\xi\eta}$. To deduce, say, $(3.172)_1$, use the divergence theorem to write for the shaded region $\Omega_{\bigcirc}$ of Figure 3.25

$$\int_{\Omega_\bigcirc} x_{,\xi}\, dv_\square \ = \ \int_{\partial\Omega_\bigcirc} x n_\xi \, da_\square \ . \tag{3.173}$$

Recalling that all triangles are equilateral with unit side (hence, the area of each triangle is equal to $1/\sqrt{3}$), the above equation implies that, by finite difference approximation,

$$6\frac{1}{\sqrt{3}}x_{,\xi}\Big|_0 \ \doteq \ \frac{x_5+x_6}{2}\frac{2}{\sqrt{3}}+\frac{x_6+x_1}{2}\frac{2}{\sqrt{3}}+0-\frac{x_2+x_3}{2}\frac{2}{\sqrt{3}}-\frac{x_3+x_4}{2}\frac{2}{\sqrt{3}}+0 \ , \tag{3.174}$$

which reduces to $(3.172)_1$. An even simpler formula for $x_{,\xi}\big|_0$ may be obtained by considering the divergence theorem only along the ξ-axis, in which case

$$x_{,\xi}\big|_0 \ \doteq \ \frac{1}{2}(x_6-x_3) \ . \tag{3.175}$$

Similar derivations apply to the remaining formulae in (3.172).

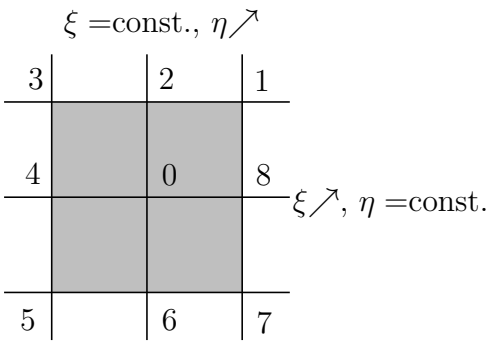

Figure 3.26. *Finite difference stencil for bilinear quadrilaterals with unit spacing in the natural domain*

For the case of bilinear quadrilateral elements, as in Figure 3.26, use of the divergence theorem for the shared region $\Omega_B ox$ yields

$$\int_{\Omega_\square} x_{,\xi}\, dv_\square \;=\; \int_{\partial\Omega} x n_\xi\, da_\square \;, \tag{3.176}$$

or

$$4\; x_{,\xi}\big|_0 \;\doteq\; \frac{x_7+x_8}{2} + \frac{x_8+x_1}{2} + 0 + 0 - \frac{x_3+x_4}{2} - \frac{x_4+x_5}{2} - 0 - 0 \;, \tag{3.177}$$

hence,

$$x_{,\xi}\big|_0 \;\doteq\; \frac{1}{8}\left[(x_7+2x_8+x_1) - (x_3+2x_4+x_5)\right] \;, \tag{3.178}$$

with analogously derived formulae for the remaining derivatives. Again, an even simpler approximation results from one-dimensional finite differencing, so that

$$\begin{aligned}
x_{,\xi}\big|_0 &\doteq \frac{1}{2}(x_8 - x_4) \\
x_{,\eta}\big|_0 &\doteq \frac{1}{2}(x_2 - x_6) \;, \\
x_{,\xi\xi}\big|_0 &\doteq x_8 - 2x_0 + x_4 \;, \\
x_{,\eta\eta}\big|_0 &\doteq x_2 - 2x_0 + x_6 \;, \\
x_{,\xi\eta}\big|_0 &\doteq \frac{1}{4}(x_1 + x_5 - x_7 - x_3) \;,
\end{aligned} \tag{3.179}$$

with corresponding formulae for the derivatives of y.

Upon substituting either (3.172) or (3.179) into the equations in (3.169), one obtains a non-linear algebraic system of two equations for (x_0, y_0). In practical computations, Poisson smoothing is performed using a Gauss-Seidel-like iterative procedure, where the placement of the nodes is updated successively from one node to the next until all nodes are exhausted. Several rounds of Poisson smoothing are typically performed until convergence of the node placements in an appropriate measure.

A variational interpretation of Poisson smoothing is possible and provides useful insights.[11] Indeed, it can be easily shown that the solution of (3.163) is attained by the minimization of the functional

$$I_s \;=\; \int_\Omega \left(|\nabla\xi|^2 + |\nabla n|^2\right)\, dv \;. \tag{3.180}$$

[11] J.U. Brackbill and J.S. Saltzman. Adaptive zoning for singular problems in two dimensions. *J. Comp. Physics*, 46:342–368, (1982).

In this sense, the functional I_s measures the variation in mesh spacing along equipotential curves. Within the variational setting, it is now possible to introduce additional functionals I_o and I_v, as

$$I_o \;=\; \int_\Omega (\nabla\xi\cdot\nabla\eta)^2\; dv \qquad , \qquad I_v \;=\; \int_\Omega w j dV \;, \tag{3.181}$$

where w is a given positive function. These measure orthogonality and (weighted) volume variation, respectively. The minimization of a combined functional of the form $I = I_s + c_1 I_o + c_2 I_v$, where $c_1, c_2 \geq 0$, may be used to simultaneously control mesh quality in all three measures. In addition, mesh grading (*e.g.*, when one needs to refine the mesh in a specified area) may be introduced by solving

$$\nabla^2\xi \;=\; f_1 \qquad , \qquad \nabla^2\eta \;=\; f_2 \;, \tag{3.182}$$

where the sources f_1, f_2 are appropriately chosen to effect mesh refinemenet, as needed.

3.7 Eulerian Methods

In computational mechanics, Eulerian finite element methods are used almost exclusively in applications of fluid dynamics. The weak forms of mass and linear momentum balance can be readily derived from their ALE counterparts (3.135) and (3.142) by setting the mesh velocity $\mathbf{v}_M$ to zero and reinterpreting all mesh time derivatives as partial derivatives with respect to time at a fixed point in space. This leads to the statements

$$\int_{\mathcal{R}} \sigma \left(\frac{\partial\rho}{\partial t} + \frac{\partial\tilde{\rho}}{\partial\mathbf{x}}\cdot\mathbf{v} + \rho\,\mathrm{div}\,\mathbf{v} \right) dv \;=\; 0 \;, \tag{3.183}$$

and

$$\int_{\mathcal{R}} \boldsymbol{\xi}\cdot\rho\left(\frac{\partial\tilde{\mathbf{v}}}{\partial t} + \frac{\partial\tilde{\mathbf{v}}}{\partial\mathbf{x}}\mathbf{v}\right) dv + \int_{\mathcal{R}} \frac{\partial\tilde{\boldsymbol{\xi}}}{\partial\mathbf{x}}\cdot\mathbf{T}\, dv \;=\; \int_{\mathcal{R}} \boldsymbol{\xi}\cdot\rho\mathbf{b}\, dv + \int_{\Gamma_q} \boldsymbol{\xi}\cdot\bar{\mathbf{t}}\, da \;, \tag{3.184}$$

respectively, with $\rho = \tilde{\rho}(\mathbf{x},t)$ and $\mathbf{v} = \tilde{\mathbf{v}}(\mathbf{x},t)$, and with admissible spaces and weights defined accordingly.

The interpolation of velocity and density fields follows (3.143) and (3.144), where $N_i^e = N_i^e(\mathbf{x})$ are the element interpolation functions.

A specific application of Eulerian finite elements for incompressible Newtonian fluids is presented in Section 5.1.

Chapter 4

Solution of Non-linear Field Equations

4.1 Generalities

Recall the semi-discrete form of linear momentum balance (3.61) obtained from a Lagrangian finite element method or a corresponding form resulting from ALE or Eulerian methods. With the use of an implicit time integrator, the above system of non-linear ordinary differential equations in time gives rise to a system of non-linear algebraic equations for $\hat{\mathbf{u}}_{n+1}$ (typically, in solids) or $\hat{v}_{n+1}$ (typically, in fluids). In ALE or Eulerian methods, an additional system of equations is obtained by imposing conservation of mass and $\hat{\boldsymbol{\rho}}_{n+1}$ is added to the list of unknowns to be determined.

By way of background, consider a system of non-linear algebraic equations expressed in column vector form as

$$[\mathbf{f}(\mathbf{x})] \;=\; \begin{bmatrix} f_1(\mathbf{x}) \\ f_2(\mathbf{x}) \\ \vdots \\ f_N(\mathbf{x}) \end{bmatrix} \;=\; [\mathbf{0}] \;, \tag{4.1}$$

where $\mathbf{x}$ is a vector in $\mathbb{R}^N$ (not a position vector!) and $\mathbf{f} : \Omega \subset \mathbb{R}^N \to \mathbb{R}^N$ is a non-linear mapping, in the sense that given any real α, β and any points $\mathbf{x}_1$, $\mathbf{x}_2$ in Ω, then

$$\mathbf{f}(\alpha\mathbf{x}_1 + \beta\mathbf{x}_2) \;\neq\; \alpha\mathbf{f}(\mathbf{x}_1) + \beta\mathbf{g}(\mathbf{x}_2) \;. \tag{4.2}$$

In the interest of simplicity, no brackets are included henceforth to denote general vector equations, therefore (4.1) would be written simply as

$$\mathbf{f}(\mathbf{x}) \;=\; \mathbf{0} \;. \tag{4.3}$$

Next, consider a continuous mapping $\mathbf{g} : \Omega \subset \mathbb{R}^N \to \mathbb{R}^N$, such that $\mathbf{x} \to \mathbf{g}(\mathbf{x})$. A point $\mathbf{x}^* \in \Omega$ is called a *fixed point* of $\mathbf{g}$ if

$$\mathbf{x}^* \;=\; \mathbf{g}(\mathbf{x}^*) \;. \tag{4.4}$$

The solution of the system of non-linear algebraic equations in (4.3) can be trivially reduced to a problem of finding the fixed points of a function, since (4.3) is equivalent to

$$\mathbf{x} \;=\; \mathbf{x} - c\mathbf{f}(\mathbf{x}) \;=\; \mathbf{g}(\mathbf{x}) \;, \tag{4.5}$$

for any constant $c \neq 0$. Here, recall that the function $\mathbf{g}$ is continuous at $\mathbf{x}_0 \in \Omega$ if, given any $\varepsilon > 0$, there exists a $\delta = \delta(\varepsilon) > 0$ such that

$$\|\mathbf{g}(\mathbf{x}) - \mathbf{g}(\mathbf{x}_0)\| \;< \varepsilon \;, \tag{4.6}$$

for all $\mathbf{x} \in B(\mathbf{x}_0, \delta) = \{\mathbf{x} \in \Omega \mid \|\mathbf{x} - \mathbf{x}_0\| < \delta\}$, where, geometrically, $B(\mathbf{x}_0, \delta)$ is an N-dimensional ball of radius δ centered at $\mathbf{x}_0$, as in Figure 4.3.

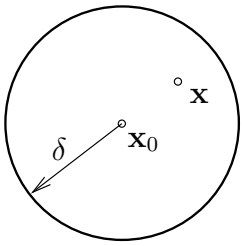

Figure 4.1. *Ball of radius δ centered at $\mathbf{x}_0$*

Let $\mathbf{g}$ be differentiable and its domain Ω be a *convex* subset of $\mathbb{R}^N$, which means that for any $\mathbf{x}$, $\mathbf{y}$ in Ω, the point $(1-\omega)\mathbf{x} + \omega\mathbf{y}$ is also in Ω if $0 < \omega < 1$, as in Figure 4.2. One may

Figure 4.2. *Convex and non-convex sets*

now invoke the *mean-value theorem* in $\mathbb{R}^N$ to write for any points $\mathbf{x}$, $\mathbf{y}$ in Ω,

$$\|\mathbf{g}(\mathbf{x}) - \mathbf{g}(\mathbf{y})\| \;\leq \sup_{\mathbf{z}\in[\mathbf{x},\mathbf{y}]} \|\mathbf{J}(\mathbf{z})\|\|\mathbf{x} - \mathbf{y}\| \;, \tag{4.7}$$

where $\mathbf{z}$ is on the line segment connecting $\mathbf{x}$ and $\mathbf{y}$, that is, $\mathbf{z} = \mathbf{x} + \omega(\mathbf{y} - \mathbf{x}), 0 \leq \omega \leq 1$, and

$$J_{ij}(\mathbf{x}) \;=\; \frac{\partial g_i(\mathbf{x})}{\partial x_j} \tag{4.8}$$

is the Jacobian matrix of $\mathbf{g}$.

Note that any vector norm can be used in the mean-value theorem, such as, for example, the classical Euclidean 2-norm, defined as

$$\|\mathbf{x}\|_2 \;=\; \left(x_1^2 + x_2^2 + \cdots + x_N^2\right)^{\frac{1}{2}} \;. \tag{4.9}$$

Also, recall that all norms in $\mathbb{R}^N$ are equivalent, in the sense that, given any two such norms $\|\cdot\|_a$, $\|\cdot\|_b$, there exist positive scalar c_1 and c_2, such that for any $\mathbf{x} \in \Omega$,

$$c_1\|\mathbf{x}\|_a \;\leq\; \|\mathbf{x}\|_b \;\leq\; c_2\|\mathbf{x}\|_a \;. \tag{4.10}$$

Lastly, the *natural* matrix norm associated with a given vector norm is defined for any given matrix $\mathbf{A}$ (viewed as a linear mapping of a vector $\mathbf{x} \in \mathbb{R}^N$ to another vector $\mathbf{A}\mathbf{x} \in \mathbb{R}^N$) as

$$\|\mathbf{A}\| \;=\; \sup_{\|\mathbf{x}\|\neq 0} \frac{\|\mathbf{A}\mathbf{x}\|}{\|\mathbf{x}\|} \;=\; \sup_{\|\mathbf{x}\|=1} \|\mathbf{A}\mathbf{x}\| \;. \tag{4.11}$$

It is noteworthy that the classical equality form of the mean-value theorem in $\mathbb{R}$, that is,

$$|g(x) - g(y)| \;=\; |g'(z)||x - y| \;, \tag{4.12}$$

for at least one point $z \in [\mathbf{x}, \mathbf{y}]$, does not generalize to $\mathbb{R}^N$.

Returning to (4.7), it is observed that if there is a positive constant λ, such that $\|\mathbf{J}(\mathbf{x})\| \leq \lambda < 1$ for all $\mathbf{x} \in \Omega$, then clearly

$$\|\mathbf{g}(\mathbf{x}) - \mathbf{g}(\mathbf{y})\| \;\leq\; \lambda\|\mathbf{x} - \mathbf{y}\| \;<<\; \|\mathbf{x} - \mathbf{y}\| \;. \tag{4.13}$$

Under the above condition, the operator $\mathbf{g}$ is termed *contractive* (or a *contraction*), in the sense that its application to $\mathbf{x} - \mathbf{y}$ strictly reduces the distance between the two points measured by the vector norm. The following theorem provides a useful connection between contractions and the existence of a solution to (4.3).

Theorem 4.1. (Contraction mapping) *Let* $\mathbf{g}$ *map a closed* $\Omega \subset \mathbb{R}^N$ *onto itself, and be contractive on* Ω *with constant* λ*. It follows that:*

(a) there exists a unique fixed point $\mathbf{x}^*$ *in* Ω*, and*

(b) the fixed point $\mathbf{x}^*$ *can be determined by a* fixed-point iteration*, that is from*

$$\mathbf{x}^{(k+1)} \;=\; \mathbf{g}(\mathbf{x}^{(k)}) \qquad , \qquad k \;=\; 0, 1, 2, \cdots \;, \tag{4.14}$$

starting from any point $\mathbf{x}^{(0)}$ *in* Ω*.*

Proof. Start with part (b) and note that, in view of $(4.13)_1$,

$$\begin{aligned} \|\mathbf{x}^{(k+1)} - \mathbf{x}^{(k)}\| \;&=\; \|\mathbf{g}(\mathbf{x}^{(k)}) - \mathbf{g}(\mathbf{x}^{(k-1)})\| \;\leq\; \lambda \|\mathbf{x}^{(k)} - \mathbf{x}^{(k-1)}\| \\ &\cdots \\ &\leq\; \lambda^k \|\mathbf{x}^{(1)} - \mathbf{x}^{(0)}\| \;=\; \lambda^k \|\mathbf{g}(\mathbf{x}^{(0)}) - \mathbf{x}^{(0)}\| \;. \end{aligned} \tag{4.15}$$

Then, for any positive integers m, n, with $m > n$, (4.15) implies that

$$\begin{aligned} \|\mathbf{x}^{(m)} - \mathbf{x}^{(n)}\| \;&=\; \|\mathbf{x}^{(m)} - \mathbf{x}^{(m-1)} + \mathbf{x}^{(m-1)} - \cdots - \mathbf{x}^{(n+1)} + \mathbf{x}^{(n+1)} - \mathbf{x}^{(n)}\| \\ &\leq\; \|\mathbf{x}^{(m)} - \mathbf{x}^{(m-1)}\| + \|\mathbf{x}^{(m-1)} - \mathbf{x}^{(m-2)}\| + \cdots + \|\mathbf{x}^{(n+1)} - \mathbf{x}^{(n)}\| \\ &\leq\; (\lambda^{m-1} + \lambda^{m-2} + \cdots + \lambda^n) \|\mathbf{x}^{(1)} - \mathbf{x}^{(0)}\| \\ &=\; \lambda^n (\lambda^{m-n-1} + \lambda^{m-n-1} + \cdots + 1) \|\mathbf{x}^{(1)} - \mathbf{x}^{(0)}\| \\ &=\; \lambda^n \frac{1 - \lambda^{m-n}}{1 - \lambda} \|\mathbf{x}^{(1)} - \mathbf{x}^{(0)}\| \;\leq\; \frac{\lambda^n}{1 - \lambda} \|\mathbf{x}^{(1)} - \mathbf{x}^{(0)}\| \;. \end{aligned} \tag{4.16}$$

Hence,

$$\lim_{m,n \to \infty} \|\mathbf{x}^{(m)} - \mathbf{x}^{(n)}\| \;\leq\; \lim_{n \to \infty} \frac{\lambda^n}{1 - \lambda} \|\mathbf{x}^{(1)} - \mathbf{x}^{(0)}\| \;=\; 0 \;. \tag{4.17}$$

Thus, $\mathbf{x}^{(n)}$ is a Cauchy sequence and since $\mathbb{R}^n$ is complete and Ω is closed, it follows that $\lim_{n \to \infty} \mathbf{x}^{(n)} = \mathbf{x}^* \in \Omega$.

Returning to part (a), write for the point $\mathbf{x}^*$ obtained above

$$\begin{aligned} \|\mathbf{x}^* - \mathbf{g}(\mathbf{x}^*)\| \;&=\; \|\mathbf{x}^* - \mathbf{g}(\mathbf{x}^{(n)}) + \mathbf{g}(\mathbf{x}^{(n)}) - \mathbf{g}(\mathbf{x}^*)\| \\ &\leq\; \|\mathbf{x}^* - \mathbf{g}(\mathbf{x}^{(n)})\| + \|\mathbf{g}(\mathbf{x}^{(n)}) - \mathbf{g}(\mathbf{x}^*)\| \\ &\leq\; \|\mathbf{x}^* - \mathbf{x}^{(n+1)}\| + \lambda \|\mathbf{x}^{(n)} - \mathbf{x}^*\| \;. \end{aligned} \tag{4.18}$$

Taking the limit as n goes to infinity of both sides of (4.18),

$$\lim_{n \to \infty} \|\mathbf{x}^* - \mathbf{g}(\mathbf{x}^*)\| \;\leq\; \lim_{n \to \infty} \|\mathbf{x}^* - \mathbf{x}^{(n+1)}\| + \lambda \lim_{n \to \infty} \|\mathbf{x}^{(n)} - \mathbf{x}^*\| \;=\; 0 \;, \tag{4.19}$$

which implies that $\mathbf{x}^*$ is a fixed point.

To show that $\mathbf{x}^*$ is unique, assume, by contradiction, that there exists a second fixed point $\mathbf{y}^* \in \Omega$, such that $\mathbf{y}^* \neq \mathbf{x}^*$. Then,

$$\|\mathbf{x}^* - \mathbf{y}^*\| \;=\; \|\mathbf{g}(\mathbf{x}^*) - \mathbf{g}(\mathbf{y}^*)\| \;\leq\; \lambda\|\mathbf{x}^* - \mathbf{y}^*\| \;<\; \|\mathbf{x}^* - \mathbf{y}^*\| \tag{4.20}$$

which is a contradiction, therefore $\mathbf{x}^* = \mathbf{y}^*$. ■

If there exists no guarantee that g maps the closed set Ω onto itself, the following theorem is useful.

Theorem 4.2. *Let $\mathbf{g} : \Omega \to \mathbb{R}^N$ be contractive on Ω, and assume that $\mathbf{x}^{(0)} \in \Omega$ is such that*

$$\mathcal{S} \;=\; \left\{\mathbf{x} \quad | \quad \|\mathbf{x} - \mathbf{g}(\mathbf{x}^{(0)})\| \;\leq\; \frac{\lambda}{1-\lambda}\|\mathbf{g}(\mathbf{x}^{(0)}) - \mathbf{x}^{(0)}\|\right\} \subset \Omega \;, \tag{4.21}$$

where λ is the contraction constant. Then, the fixed-point iteration $\mathbf{x}^{(k+1)} = \mathbf{g}(\mathbf{x}^{(k)})$ converges to the unique fixed point $\mathbf{x}^* \in \mathcal{S}$.

Proof. For any $\mathbf{x} \in \mathcal{S}$,

$$\begin{aligned}
\|\mathbf{g}(\mathbf{x}) - \mathbf{g}(\mathbf{x}^{(0)})\| \;&\leq\; \lambda\|\mathbf{x} - \mathbf{x}^{(0)}\| \;=\; \lambda\|\mathbf{x} - \mathbf{g}(\mathbf{x}^{(0)}) + \mathbf{g}(\mathbf{x}^{(0)}) - \mathbf{x}^{(0)}\| \\
&\leq\; \lambda\left[\|\mathbf{x} - \mathbf{g}(\mathbf{x}^{(0)})\| + \|\mathbf{g}(\mathbf{x}^{(0)}) - \mathbf{x}^{(0)}\|\right] \\
&\leq\; \left[\frac{\lambda^2}{1-\lambda} + \lambda\right]\|\mathbf{g}(\mathbf{x}^{(0)}) - \mathbf{x}^{(0)}\| \;=\; \frac{\lambda}{1-\lambda}\|\mathbf{g}(\mathbf{x}^{(0)}) - \mathbf{x}^{(0)}\| \;,
\end{aligned} \tag{4.22}$$

therefore $\mathbf{g}(\mathbf{x}) \in \mathcal{S}$, thus $\mathbf{g}$ maps the closed set $\mathcal{S}$ onto itself. Thus, the contraction mapping

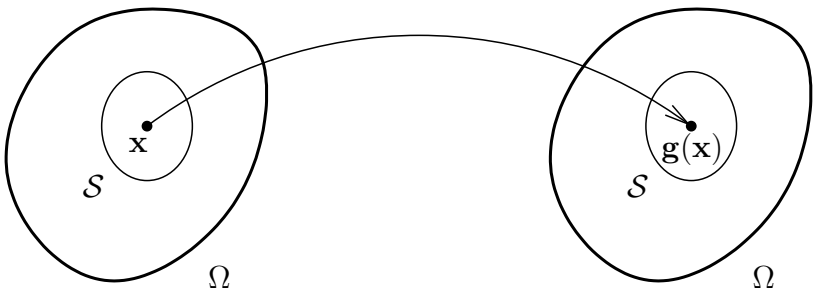

Figure 4.3. *Contraction mapping in $\mathcal{S}$*

theorem is applicable and yields the desired result. ■

The preceding analysis can be carried out in the broader framework of Banach spaces (that is, complete normed linear spaces). However, this is not necessary here since the subsequent development pertains strictly to finite-dimensional spaces (which are, by necessity, complete).

4.2 The Newton-Raphson Method and its Variants

The Newton-Raphson method is one of the most widely used iterative methods for solving non-linear algebraic equations. Its origins may be traced at least as far back as the first century AD work of Heron of Alexandria, who was clearly aware of the iterative formula $x^{(k+1)} = \frac{1}{2}\left(x^{(n)} + \frac{a}{x^{(k)}}\right)$ for estimating the square root of a positive real a starting from any positive guess $x^{(0)}$. It is now widely accepted that the classical Newton-Raphson formula is due to Raphson, although Newton had earlier employed a related, albeit less general, formula.[1]

Recalling (2.13), the idea of the Newton-Raphson method is to approximate $\mathbf{f}(\mathbf{x})$ with its linear part about a point $\mathbf{x}_0 \in \mathbb{R}^N$, that is,

$$\mathbf{f}(\mathbf{x}) \;=\; \underbrace{\mathbf{f}(\mathbf{x}_0) + \mathbf{J}(\mathbf{x}_0)(\mathbf{x}-\mathbf{x}_0)}_{\mathcal{L}[\mathbf{f};\mathbf{x}-\mathbf{x}_0]_{\mathbf{x}_0}} + \underbrace{O\left(\|\mathbf{x}-\mathbf{x}_0\|^2\right)}_{\text{ignore}} \;=\; \mathbf{0}\;. \tag{4.23}$$

In the above equation, $\mathbf{J}(\mathbf{x}_0)$ is the (Fréchet or Gâteaux) derivative of $\mathbf{f}$ at $\mathbf{x}$, with components

$$J_{ij}(\mathbf{x}_0) \;=\; \frac{\partial f_i(\mathbf{x}_0)}{\partial x_j}\;, \tag{4.24}$$

and, similarly, $\mathbf{J}(\mathbf{x}_0)(\mathbf{x}-\mathbf{x}_0)$ is the (Fréchet or Gâteaux) differential at $\mathbf{x}_0$ in the direction $\mathbf{x}-\mathbf{x}_0$. Then, one may use the iterative formula

$$\mathbf{x}^{(k+1)} \;=\; \mathbf{x}^{(k)} - \left[\mathbf{J}(\mathbf{x}^{(k)})\right]^{-1}\mathbf{f}(\mathbf{x}^{(k)}) \tag{4.25}$$

to determine, if possible, the solution $\mathbf{x}^* = \lim_{k\to\infty}\mathbf{x}^{(k)}$, starting with $\mathbf{x}^{(0)}$ as the initial guess, and assuming that $\det\left[\mathbf{J}(\mathbf{x}^{(k)})\right] \neq 0$ for all iterates k. Equation (4.25) is the classical Newton-Raphson formula, see Figure 4.4 for a geometric interpretation.

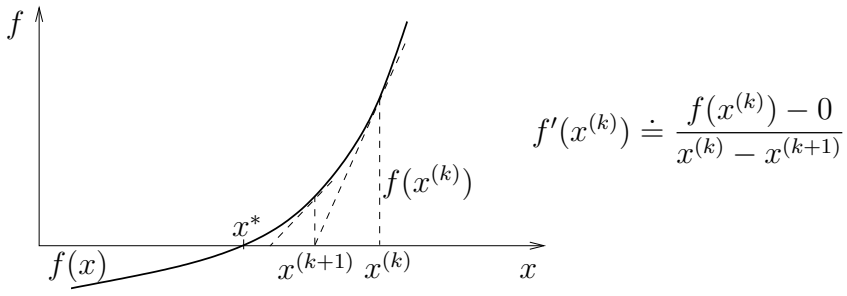

Figure 4.4. *One-dimensional geometric interpretation of the Newton-Raphson method*

[1] For a detailed historical account, see F. Cajori, Historical Note on the Newton-Raphson Method of Approximation, *Amer. Math. Monthly*, 18:29–32, (1911).

The three major drawbacks of the Newton-Raphson method are that (a) the derivative $\mathbf{J}(\mathbf{x})$ must be computed explicitly, which is occasionally difficult to do analytically (although either *automatic* or *symbolic differentiation* software may be used to free the programmer from this task), (b) the condition $\det[\mathbf{J}(\mathbf{x}^{(k)})] \neq 0$ for all $k = 0, 1, 2, \cdots$ is essential and its violation (or near-violation) results in failure of the method, see Figure 4.5, and (c)

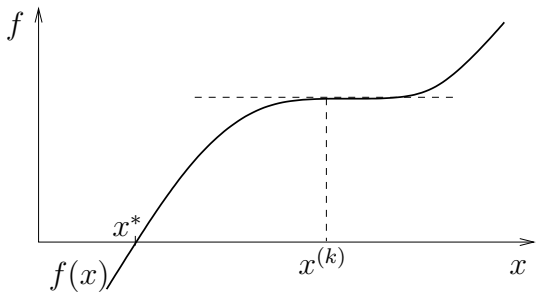

Figure 4.5. *Failure of the Newton-Raphson method due to singular* $J(x^{(k)})$

convergence is not guaranteed unless the initial guess $\mathbf{x}^{(0)}$ is sufficiently close to the solution (a point that will be expounded upon later in this section), see Figure 4.6.

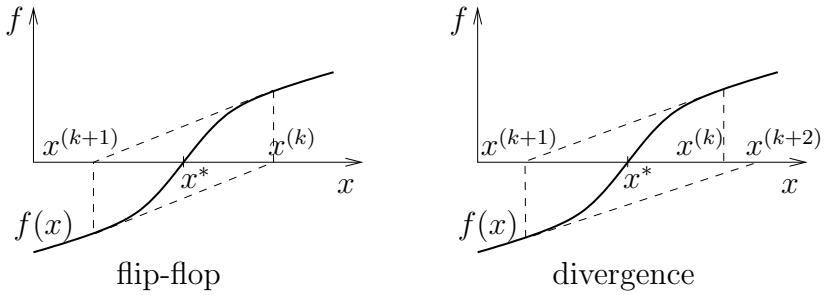

Figure 4.6. *Failure of the Newton-Raphson method due to the large distance of* $x^{(k)}$ *from the solution* x^*

The Newton-Raphson method can be interpreted as a fixed-point iteration (4.7), where

$$\mathbf{g}(\mathbf{x}) \;=\; \mathbf{x} - [\mathbf{J}(\mathbf{x})]^{-1}\,\mathbf{f}(\mathbf{x})\;. \tag{4.26}$$

As an alternative to the Newton-Raphson method, one may define the so-called *modified Newton method*, where

$$\mathbf{g}(\mathbf{x}) \;=\; \mathbf{x} - \left[\mathbf{J}(\mathbf{x}^{(0)})\right]^{-1}\mathbf{f}(\mathbf{x})\;, \tag{4.27}$$

so that now

$$\mathbf{x}^{(k+1)} \;=\; \mathbf{x}^{(k)} - \left[\mathbf{J}(\mathbf{x}^{(0)})\right]^{-1}\mathbf{f}(\mathbf{x}^{(k)}) \quad , \quad k \;=\; 0, 1, 2, \cdots \tag{4.28}$$

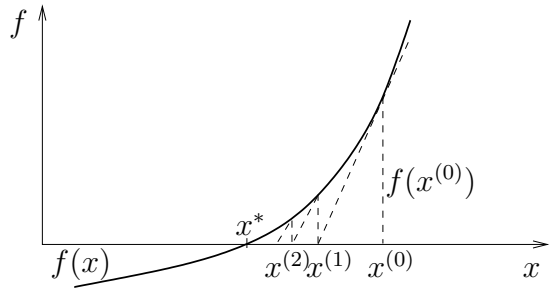

Figure 4.7. *One-dimensional geometric interpretation of the modified Newton-Raphson method*

and $\mathbf{J}(\mathbf{x}^{(0)})$ needs to be factorized only once, see Figure 4.7.

The *generalized Newton method*, where

$$\mathbf{g}(\mathbf{x}) \;=\; \mathbf{x} - [\mathbf{A}(\mathbf{x})]^{-1}\,\mathbf{f}(\mathbf{x})\;, \tag{4.29}$$

where $\mathbf{A}(\mathbf{x}) \;:\; \Omega \mapsto \mathbb{R}^N$ is an invertible matrix which is typically an approximation to $\mathbf{J}(\mathbf{x})$. The generalized Newton method encompasses a wide class of iterative methods for the solution of (4.3), including the Newton-Raphson, the modified Newton method, as well as all approximations to Newton-Raphson resulting from numerical differentiation of $\mathbf{f}$.

The preceding contraction mapping theorem may be used to study the convergence of the Newton-Raphson method. Indeed, in light of (4.26), if the resulting $\mathbf{g}(\mathbf{x})$ maps some closed region Ω to itself and is contractive, then the Newton-Raphson method convergences to the unique solution $\mathbf{x}^* \in \Omega$ starting from any point $\mathbf{x}^{(0)} \in \Omega$. A sharper, and, therefore, more interesting result, is as follows:[2]

Theorem 4.3. *Let a non-linear operator $\mathbf{f} : \Omega \subset \mathbb{R}^N \to \mathbb{R}^N$ be continuously differentiable, and assume that there exists a point $\mathbf{x}^* \in \Omega$, such that $\mathbf{f}(\mathbf{x}^*) = \mathbf{0}$ and $\det \mathbf{J}(\mathbf{x}^*) \neq 0$. Then, there is a $\rho > 0$ such that for all initial guesses $\mathbf{x}^{(0)} \in \mathcal{B}(\mathbf{x}^*; \rho)$, the Newton-Raphson iteration (4.25) is well-defined and converges to $\mathbf{x}^*$.*

Proof. Since $\det \mathbf{J}(\mathbf{x}^*) \neq 0$, one may find an $M > 0$, such that

$$\| \, [\mathbf{J}(\mathbf{x}^*)]^{-1} \, \| \;<\; M \;. \tag{4.30}$$

In addition, since $\mathbf{J}(\mathbf{x})$ is continuous, then, by the inverse function theorem, so is $[\mathbf{J}(\mathbf{x}^*)]^{-1}$ in a neighborhood of $\mathbf{x}^*$. Then, there is a $\delta > 0$, such that

$$\| \, [\mathbf{J}(\mathbf{x})]^{-1} - [\mathbf{J}(\mathbf{x}^*)]^{-1} \, \| \;\leq\; \underbrace{M - \| \, [\mathbf{J}(\mathbf{x}^*)]^{-1} \, \|}_{>0} \;, \tag{4.31}$$

[2] See, *e.g.*, Section 8.1.10 in J.M. Ortega, Numerical Analysis: a Second Course, SIAM, Philadelphia, 1990.

for all $\mathbf{x} \in \mathcal{B}(\mathbf{x}^*;\delta)$. This, in turn, implies that

$$\| \left[\mathbf{J}(\mathbf{x})\right]^{-1} \| \;\leq\; \| \left[\mathbf{J}(\mathbf{x}^*)\right]^{-1} \| + M - \| \left[\mathbf{J}(\mathbf{x}^*)\right]^{-1} \| \;=\; M \;, \tag{4.32}$$

that is, $[\mathbf{J}(\mathbf{x})]^{-1}$ is bounded in the ball $\mathcal{B}(\mathbf{x}^*;\delta) = \{\mathbf{x} \in \Omega \mid \|\mathbf{x}-\mathbf{x}^*\| \leq \delta\}$ of radius δ centered at $\mathbf{x}^*$. Then, for any $\mathbf{x}^{(k)} \in \mathcal{B}(\mathbf{x}^*;\delta)$ it is concluded that

$$\begin{aligned} \mathbf{x}^{(k+1)} - \mathbf{x}^* \;&=\; \mathbf{x}^{(k)} - \left[\mathbf{J}(\mathbf{x}^{(k)})\right]^{-1} \mathbf{f}(\mathbf{x}^{(k)}) - \mathbf{x}^* \\ &=\; \left[\mathbf{J}(\mathbf{x}^{(k)})\right]^{-1} \left\{\mathbf{J}(\mathbf{x}^{(k)})[\mathbf{x}^{(k)} - \mathbf{x}^*] - \mathbf{f}(\mathbf{x}^{(k)})\right\} \;. \end{aligned} \tag{4.33}$$

Since $\mathbf{J}(\mathbf{x})$ is continuous in $\mathcal{B}(\mathbf{x}^*;\delta)$, one may invoke the fundamental theorem of calculus[3] to conclude that

$$\begin{aligned} \mathbf{f}(\mathbf{x}^{(k)}) \;&= \mathbf{f}(\mathbf{x}^*) + \left[\int_0^1 \mathbf{J}\left(\mathbf{x}^* + \omega(\mathbf{x}^{(k)} - \mathbf{x}^*)\right) d\omega\right] (\mathbf{x}^{(k)} - \mathbf{x}^*) \\ &=\; \left[\int_0^1 \mathbf{J}\left(\mathbf{x}^* + \omega(\mathbf{x}^{(k)} - \mathbf{x}^*)\right) d\omega\right] (\mathbf{x}^{(k)} - \mathbf{x}^*) \;. \end{aligned} \tag{4.34}$$

Substituting the above equation in (4.33) yields

$$\mathbf{x}^{(k+1)} - \mathbf{x}^* \;=\; \left[\mathbf{J}(\mathbf{x}^{(k)})\right]^{-1} \int_0^1 \left[\mathbf{J}(\mathbf{x}^{(k)}) - \mathbf{J}\left(\mathbf{x}^* + \omega(\mathbf{x}^{(k)} - \mathbf{x}^*)\right)\right] d\omega (\mathbf{x}^{(k)} - \mathbf{x}^*) \;. \tag{4.35}$$

Taking norms of both sides of (4.35) and using standard norm properties, it follows that

$$\|\mathbf{x}^{(k+1)} - \mathbf{x}^*\| \;\leq\; \| \left[\mathbf{J}(\mathbf{x}^{(k)})\right]^{-1} \| \left[\int_0^1 \|\mathbf{J}(\mathbf{x}^{(k)}) - \mathbf{J}\left(\mathbf{x}^* + \omega(\mathbf{x}^{(k)} - \mathbf{x}^*)\right)\| d\omega\right] \|\mathbf{x}^{(k)} - \mathbf{x}^*\| \;. \tag{4.36}$$

Now, since $\mathbf{J}(\mathbf{x})$ is continuous in $\mathcal{B}(\mathbf{x}^*;\delta)$, there exists a ρ, $0 < \rho \leq \delta$, such that, for any $\mathbf{x}^{(k)} \in \mathcal{B}(\mathbf{x}^*;\rho)$ and all ω, $0 \leq \omega \leq 1$,

$$\|\mathbf{J}(\mathbf{x}^{(k)}) - \mathbf{J}\left(\mathbf{x}^* + \omega(\mathbf{x}^{(k)} - \mathbf{x}^*)\right)\| \;\leq\; \frac{1}{2M} \;, \tag{4.37}$$

as in Figure 4.8. Indeed, taking advantage of the aforementioned continuity of $\mathbf{J}(\mathbf{x})$, one may always find a ρ, $0 < \rho \leq \delta$, such that

$$\begin{aligned} \|\mathbf{J}(\mathbf{x}^{(k)}) - \mathbf{J}\left(\mathbf{x}^* + \omega(\mathbf{x}^{(k)} - \mathbf{x}^*)\right)\| \;&= \|\mathbf{J}(\mathbf{x}^{(k)}) - \mathbf{J}(\mathbf{x}^*) + \mathbf{J}(\mathbf{x}^*) - \mathbf{J}\left(\mathbf{x}^* + \omega(\mathbf{x}^{(k)} - \mathbf{x}^*)\right)\| \\ &\leq\; \|\mathbf{J}(\mathbf{x}^{(k)}) - \mathbf{J}(\mathbf{x}^*)\| + \|\mathbf{J}(\mathbf{x}^*) - \mathbf{J}\left(\mathbf{x}^* + \omega(\mathbf{x}^{(k)} - \mathbf{x}^*)\right)\| \\ &\leq\; \frac{1}{4M} + \frac{1}{4M} \;=\; \frac{1}{2M} \;. \end{aligned} \tag{4.38}$$

[3] The one-dimensional version of the fundamental theorem of calculus, $f(b) = f(a) + \int_b^a \frac{df}{dx} dx$ readily generalizes in $\mathbb{R}^N$ to $\mathbf{f}(\mathbf{b}) = \mathbf{f}(\mathbf{a}) + \int_0^1 \frac{d\mathbf{f}(\mathbf{a}+\omega(\mathbf{b}-\mathbf{a}))}{d(\mathbf{a}+\omega(\mathbf{b}-\mathbf{a}))} \frac{d(\mathbf{a}+\omega(\mathbf{b}-\mathbf{a}))}{d\omega} = \mathbf{f}(\mathbf{a}) + \left[\int_0^1 \mathbf{J}\left(\mathbf{a}+\omega(\mathbf{b}-\mathbf{a})\right) d\omega\right] (\mathbf{b}-\mathbf{a})$.

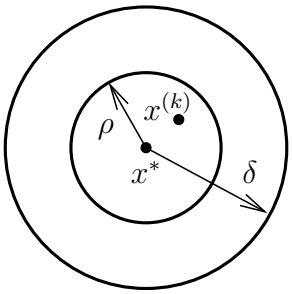

Figure 4.8. *Balls $\mathcal{B}(\mathbf{x}^*;\rho)$ and $\mathcal{B}(\mathbf{x}^*;\delta)$ around the solution $\mathbf{x}^*$*

Taking advantage of (4.30) and (4.37), it follows from (4.36) that

$$\|\mathbf{x}^{(k+1)} - \mathbf{x}^*\| \;\leq\; M\frac{1}{2M}\|\mathbf{x}^{(k)} - \mathbf{x}^*\| \;=\; \frac{1}{2}\|\mathbf{x}^{(k)} - \mathbf{x}^*\| \;. \tag{4.39}$$

Note that clearly $\mathbf{x}^{(k+1)} \in \mathcal{B}(\mathbf{x}^*;\rho)$ and a standard argument of induction leads to

$$\lim_{k\to\infty} \|\mathbf{x}^{(k+1)} - \mathbf{x}^*\| \;=\; 0 \;, \tag{4.40}$$

therefore $\lim_{k\to\infty} \mathbf{x}^{(k+1)} = \mathbf{x}^*$. ■

An additional condition may be included with the original assumptions of the preceding theorem, whereby it is assumed that there exists a constant $\lambda > 0$ such that

$$\|\mathbf{J}(\mathbf{x}) - \mathbf{J}(\mathbf{y})\| \;\leq\; \lambda\|\mathbf{x} - \mathbf{y}\| \;, \tag{4.41}$$

for all $\mathbf{x}, \mathbf{y} \in \mathcal{B}(\mathbf{x}^*;\rho)$. Under this condition, $\mathbf{J}$ is called *Lipschitz continuous* in $\mathcal{B}(\mathbf{x}^*;\rho)$ with *Lipschitz constant* λ. Under the additional assumption of Lipschitz continuity for $\mathbf{J}$, one may start again (4.36) and use (4.30) to conclude that

$$\begin{aligned}
\|\mathbf{x}^{(k+1)} - \mathbf{x}^*\| \;&\leq\; \|\left[\mathbf{J}(\mathbf{x}^{(k)})\right]^{-1}\| \left\{\int_0^1 \|\mathbf{J}(\mathbf{x}^{(k)}) - \mathbf{J}\left(\mathbf{x}^* + \omega(\mathbf{x}^{(k)} - \mathbf{x}^*)\right)\| d\omega\right\} \|\mathbf{x}^{(k)} - \mathbf{x}^*\| \\
&\leq\; M\left\{\int_0^1 \lambda(1-\omega)\|\mathbf{x}^{(k)} - \mathbf{x}^*\| d\omega\right\} \|\mathbf{x}^{(k)} - \mathbf{x}^*\| \\
&=\; M\lambda\left[\omega - \frac{\omega^2}{2}\right]_0^1 \|\mathbf{x}^{(k)} - \mathbf{x}^*\|^2 \;=\; \frac{1}{2}\lambda M\|\mathbf{x}^{(k)} - \mathbf{x}^*\|^2 \;.
\end{aligned} \tag{4.42}$$

This implies that the Newton-Raphson method converges quadratically in the sense that

$$\frac{\|\mathbf{x}^{(k+1)} - \mathbf{x}^*\|}{\|\mathbf{x}^{(k)} - \mathbf{x}^*\|^2} \;\leq\; \frac{1}{2}\lambda M \;=\; \text{constant} \;. \tag{4.43}$$

The scalar $\rho > 0$ is referred to as the *radius of attraction* for the Newton-Raphson method. Clearly, convergence to $\mathbf{x}^*$ is not guaranteed when starting from $\mathbf{x}^{(0)} \notin \mathcal{B}(\mathbf{x}^*; \rho)$. This, in effect, limits the step-size when using the Newton-Raphson method. The radius of attraction depends on the spatial variation of $\mathbf{J}$ around the solution $\mathbf{x}^*$, as depicted in Figure 4.9. Note that, contrary to statements in some texts, quadratic convergence does

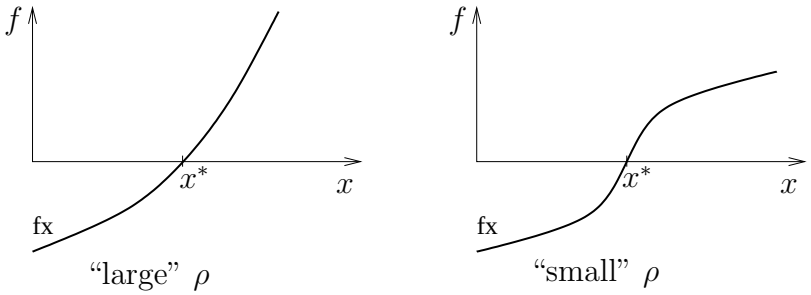

Figure 4.9. *Functions with different radii of attractions for the Newton-Raphson method*

not require differentiability of $\mathbf{J}(\mathbf{x}), \mathbf{x} \in \mathcal{B}(\mathbf{x}^*; \rho)$. Indeed, Lipschitz continuity is a stronger condition than continuity but weaker than differentiability.

The above theorem is local in nature, in the sense that it assumes that the solution $\mathbf{x}^*$ exists, and subsequently asserts that there exists a neighborhood $\mathcal{B}(\mathbf{x}^*; \rho)$ around $\mathbf{x}^*$, such that starting with any point $\mathbf{x}^{(0)}$ in it, the Newton-Raphson sequence will converge to $\mathbf{x}^*$. This theorem does not allow for any computable error estimate for the quantity $\|\mathbf{x}^{(k)} - \mathbf{x}^*\|$. A semi-local result (that is, one for in which the existence of a solution $\mathbf{x}^*$ is not assumed at the outset) is the celebrated *Newton-Kantorovich theorem*:[4]

Theorem 4.4. *Let a non-linear operator* $\mathbf{f} : \mathbb{R}^N \to \mathbb{R}^N$ *be differentiable in a convex set* $\Omega \subset \mathbb{R}^N$ *and its derivative* $\mathbf{J}$ *be Lipschitz continuous with constant* λ *in* Ω*. Suppose that there is a point* $\mathbf{x}^{(0)} \in \Omega$*, such that*

$$\| \left[\mathbf{J}(\mathbf{x}^{(0)})\right]^{-1} \| \leq M \quad , \quad \| \left[\mathbf{J}(\mathbf{x}^{(0)})\right]^{-1} \mathbf{f}(\mathbf{x}^{(0)}) \| \leq \eta \tag{4.44}$$

and

$$\alpha = \lambda \eta M \leq \frac{1}{2} \, . \tag{4.45}$$

Also, assume that $\mathcal{B}(\mathbf{x}^{(0)}; \rho_*) \subset \Omega$ *where*

$$\rho_* = \frac{1}{\lambda M} \left[1 - (1 - 2\alpha)^{\frac{1}{2}}\right] \, , \tag{4.46}$$

[4] See p. 421 in J.M. Ortega and W. Rheinboldt, Iterative Solution of Nonlinear Equations in Several Variables, Academic Press, New York, 1970.

see Figure 4.10.

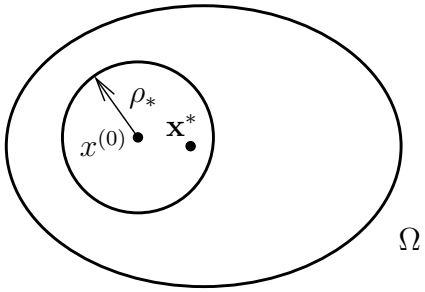

Figure 4.10. *Convergence under the Newton-Kantorovich conditions*

Then, the Newton-Raphson iteration is well-defined and converges to the unique solution $\mathbf{x}^*$ *of* $\mathbf{f}(\mathbf{x}) = \mathbf{0}$ *in* $\mathcal{B}(\mathbf{x}^{(0)}; \rho_*)$*. In addition, an error estimate is obtained in the form*

$$\|\mathbf{x}^* - \mathbf{x}^{(k)}\| \;\leq\; \frac{(2\alpha)^{2^k}}{2^k \lambda M} \;. \tag{4.47}$$

Even sharper error estimates can be obtained for $\|\mathbf{x}^* - \mathbf{x}^{(k)}\|$ by further assuming that the second derivative of $\mathbf{f}$ exists everywhere and is bounded.[5]

4.3 The Newton-Raphson Method in Non-linear Finite Elements

The Newton-Raphson method enjoys wide use in non-linear computational mechanics. To demonstrate its application, consider first the system of ordinary differential equations (3.61) emanating from the spatial discretization of a Lagrangian finite element method and the corresponding algebraic system (3.72) resulting from the application of discrete time integrator. The latter may be put in the form

$$\mathbf{f}(\hat{\mathbf{u}}_{n+1}) \;=\; \frac{1}{\beta \Delta t_n^2}\mathbf{M}\hat{\mathbf{u}}_{n+1} + \mathbf{R}(\hat{\mathbf{u}}_{n+1}) - \mathbf{M}\left\{(\hat{\mathbf{u}}_n + \hat{\mathbf{v}}_n \Delta t_n)\frac{1}{\beta \Delta t_n^2} + \frac{1-2\beta}{2\beta}\hat{\mathbf{a}}_n\right\} - \mathbf{F}_{n+1} \;=\; \mathbf{0} \tag{4.48}$$

To find $\hat{\mathbf{u}}_{n+1}$ using the Newton-Raphson method, start with the initial guess $\hat{\mathbf{u}}_{n+1}^{(0)} = \hat{\mathbf{u}}_n$, that is, the displacement field of the converged solution at $t = t_n$, and, recalling (4.23), write

$$\mathbf{0} \;=\; \mathbf{f}(\hat{\mathbf{u}}_{n+1}^{(k+1)}) \;\doteq\; \mathbf{f}(\hat{\mathbf{u}}_{n+1}^{(k)}) + D\mathbf{f}(\hat{\mathbf{u}}_{n+1}^{(k)})\left(\hat{\mathbf{u}}_{n+1}^{(k+1)} - \hat{\mathbf{u}}_{n+1}^{(k)}\right) \;, \tag{4.49}$$

[5] See p. 708 in L.V. Kantorovich and G.P.Akilov, Functional Analysis, Pergamon Press, New York, 1982.

where $\Delta\hat{\mathbf{u}}_{n+1}^{(k)} = \hat{\mathbf{u}}_{n+1}^{(k+1)} - \hat{\mathbf{u}}_{n+1}^{(k)}$ is the (yet unknown) increment of the displacement vector from iteration (k) to iteration $(k+1)$. Then,

$$\hat{\mathbf{u}}_{n+1}^{(k+1)} \;=\; \hat{\mathbf{u}}_{n+1}^{(k)} - \Big[D\mathbf{f}(\hat{\mathbf{u}}_{n+1}^{(k)})\Big]^{-1}\,\mathbf{f}(\hat{\mathbf{u}}_{n+1}^{(k)}) \quad , \quad k \;=\; 0,1,2,\ldots\,. \tag{4.50}$$

Clearly, the term $D\mathbf{f}(\hat{\mathbf{u}}_{n+1}^{(k)})\left(\hat{\mathbf{u}}_{n+1}^{(k+1)} - \hat{\mathbf{u}}_{n+1}^{(k)}\right)$ is the differential (Fréchet or Gâteaux) of the vector $\mathbf{f}$ at $\hat{\mathbf{u}}_{n+1}^{(k)}$ in the direction $\Delta\hat{\mathbf{u}}_{n+1}^{(k)}$. In order for the Newton-Raphson method to be employed, the derivative $D\mathbf{f}(\hat{\mathbf{u}}_{n+1}^{(k)})$ must be determined explicitly. This can be done at the level of the full post-assembly algebraic system, or more conveniently, at the element level using the original weak forms of the balance laws. To explore the latter option, recall the discrete linear momentum balance equations (3.59) derived from (3.42), as restricted to the element e with domain Ω_0^e, that is,

$$\begin{aligned}&\int_{\Omega_0^e} \boldsymbol{\xi}_{n+1}\cdot\rho_0\mathbf{a}_{n+1}\,dV + \int_{\Omega_0^e}\frac{\partial\boldsymbol{\xi}_{n+1}}{\partial\mathbf{X}}\cdot\mathbf{P}_{n+1}\,dV \\ &\qquad=\; \int_{\Omega_0^e}\boldsymbol{\xi}_{n+1}\cdot\rho_0\mathbf{b}_{n+1}\,dV + \int_{\partial\Omega_0^e\cap\Gamma_{q_0}}\boldsymbol{\xi}_{n+1}\cdot\bar{\mathbf{p}}_{n+1}\,dA + \int_{\partial\Omega_0^e\setminus\Gamma_{q_0}}\boldsymbol{\xi}_{n+1}\cdot\mathbf{p}_{n+1}\,dA\;.\end{aligned} \tag{4.51}$$

Next, proceed with obtaining the differential in the direction $\Delta\mathbf{u}_{n+1}$ of each of the terms in the above weak form, except for the last one which will not appear in the global balance statements. For the acceleration term, one may write

$$\begin{aligned}D\left[\int_{\Omega_0^e}\boldsymbol{\xi}_{n+1}\cdot\rho_0\mathbf{a}_{n+1}\,dV\right](\mathbf{u}_{n+1},\Delta\mathbf{u}_{n+1}) \;&=\; \left[\frac{d}{d\omega}\int_{\Omega_0^e}\boldsymbol{\xi}_{n+1}\cdot\rho_0\overset{\cdot\cdot}{(\mathbf{u}_{n+1}+\omega\Delta\mathbf{u}_{n+1})}\,dV\right]_{\omega=0}\\ &=\; \int_{\Omega_0^e}\boldsymbol{\xi}_{n+1}\cdot\rho_0\Delta\ddot{\mathbf{u}}_{n+1}\,dV\;.\end{aligned} \tag{4.52}$$

Assuming that the body forces are known and independent of $\mathbf{u}$, and also that the prescribed tractions are deformation-independent (that is, they are *dead loads*), then clearly

$$D\left[\int_{\Omega_0^e}\boldsymbol{\xi}_{n+1}\cdot\rho_0\mathbf{b}_{n+1}\,dV + \int_{\partial\Omega_0^e\cap\Gamma_{q_0}}\boldsymbol{\xi}_{n+1}\cdot\bar{\mathbf{p}}_{n+1}\,dA\right](\mathbf{u}_{n+1},\Delta\mathbf{u}_{n+1}) \;=\; 0\;. \tag{4.53}$$

An additional important assumption made above is that Γ_{q_0} is itself independent of $\mathbf{u}$, that is, the characterization of traction boundaries does not depend on the solution.

Alternatively, it is possible to have deformation-dependent tractions. For example, a *follower load* of the form ($\bar{\mathbf{t}}_{n+1} = -\bar{p}\mathbf{n}_{n+1}$) may be imposed on Γ_{q_0}, so that, upon recalling (1.12) and (1.75),

$$\bar{\mathbf{p}}_{n+1} \;=\; -\bar{p}J_{n+1}\mathbf{F}_{n+1}^{-T}\mathbf{N}\;. \tag{4.54}$$

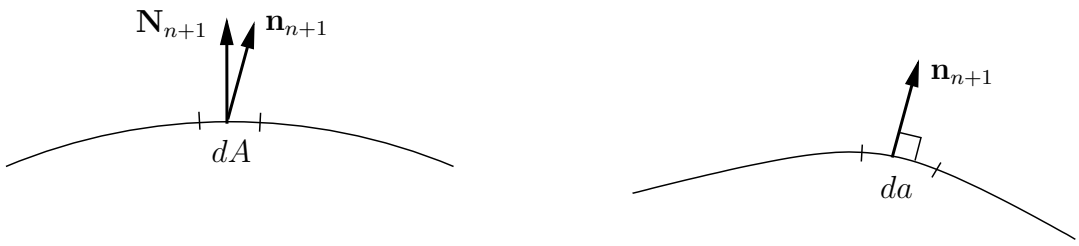

Figure 4.11. *Pressure-type follower traction*

where $\bar{p}$ is a constant pressure, as in Figure 4.11. These traction loads are clearly subject to non-trivial linearization.

Similarly, it is possible to model body forces which are derived from a potential, such as gravitational forces which are changing with position, as in Figure 4.12. These also lead to

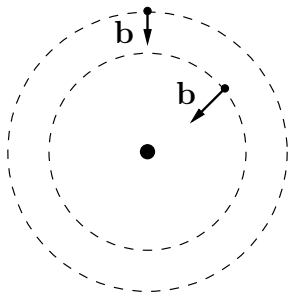

Figure 4.12. *Body force in a gravitational field*

a non-trivial linearization.

Generally, the principal concern in formulating the Newton-Raphson iteration in finite element methods is to obtain the differential of the stress-divergence term. For the case of solids, write

$$\begin{aligned} D\left[\int_{\Omega_0^e} \frac{\partial \boldsymbol{\xi}_{n+1}}{\partial \mathbf{X}} \cdot \mathbf{P}_{n+1}\, dV\right](\mathbf{u}_{n+1}, \Delta\mathbf{u}_{n+1}) &= \left[\frac{d}{d\omega}\int_{\Omega_0^e} \frac{\partial \boldsymbol{\xi}_{n+1}}{\partial \mathbf{X}} \cdot \mathbf{P}\left(\mathbf{u}_{n+1} + \omega\Delta\mathbf{u}_{n+1}\right) dV\right]_{\omega=0} \\ &= \int_{\Omega_0^e} \frac{\partial \boldsymbol{\xi}_{n+1}}{\partial \mathbf{X}} \cdot \left[\frac{d}{d\omega}\mathbf{P}\left(\mathbf{u}_{n+1} + \omega\Delta\mathbf{u}_{n+1}\right)\right]_{\omega=0} dV \\ &= \int_{\Omega_0^e} \frac{\partial \boldsymbol{\xi}_{n+1}}{\partial \mathbf{X}} \cdot D\mathbf{P}\left(\mathbf{u}_{n+1}, \Delta\mathbf{u}_{n+1}\right) dV\ . \end{aligned} \tag{4.55}$$

If the stress depends only on the deformation gradient (as in the case of elastic materials discussed in Chapter 5), then

$$D\mathbf{P}\left(\mathbf{u}_{n+1}, \Delta\mathbf{u}_{n+1}\right) = D\mathbf{P}\left(\mathbf{F}_{n+1}, \Delta\mathbf{F}_{n+1}\right) = \frac{\partial \mathbf{P}_{n+1}}{\partial \mathbf{F}_{n+1}}\Delta\mathbf{F}_{n+1}\ , \tag{4.56}$$

where

$$\Delta\mathbf{F}_{n+1} \;=\; \frac{\partial\Delta\mathbf{u}_{n+1}}{\partial\mathbf{X}} \;. \tag{4.57}$$

Thus

$$D\left[\int_{\Omega_0^e}\frac{\partial\boldsymbol{\xi}_{n+1}}{\partial\mathbf{X}}\cdot\mathbf{P}_{n+1}\,dV\right](\mathbf{u}_{n+1},\Delta\mathbf{u}_{n+1}) \;=\; \int_{\Omega_0^e}\frac{\partial\boldsymbol{\xi}_{n+1}}{\partial\mathbf{X}}\cdot\frac{\partial\mathbf{P}_{n+1}}{\partial\mathbf{F}_{n+1}}\frac{\partial\Delta\mathbf{u}_{n+1}}{\partial\mathbf{X}}\,dV \;. \tag{4.58}$$

For materials which exhibit rate-dependence, *e.g.*, when $\mathbf{P} = \mathbf{P}(\mathbf{F},\dot{\mathbf{F}})$, the differential $D\mathbf{P}\,(\mathbf{u}_{n+1},\Delta\mathbf{u}_{n+1})$ does not capture the rate-dependence and needs to be augmented to

$$D\mathbf{P}(\mathbf{u}_{n+1};\mathbf{v}_{n+1},\Delta\mathbf{u}_{n+1};\Delta\mathbf{v}_{n+1}) \;. \tag{4.59}$$

Upon time discretization, this augmented differential is not necessary because the rate quantities can be expressed in terms of the primary variable $\mathbf{u}$ through the use of a discrete time integrator.

Example 4.3.1: By way of example, consider the simple one-dimensional *Kelvin-Voigt solid* (spring-dashpot in parallel), as in Figure 4.13. Here,

$$\sigma \;=\; E\varepsilon + \eta\dot{\varepsilon} \;, \tag{4.60}$$

where ε is the infinitesimal strain, σ is the uniaxial stress, E is the Young's modulus, and η is the viscosity coefficient. Clearly, at $t = t_{n+1}$,

$$\sigma_{n+1} \;=\; E\varepsilon_{n+1} + \eta\dot{\varepsilon}_{n+1} \;, \tag{4.61}$$

therefore

$$D\sigma(\varepsilon_{n+1};\dot{\varepsilon}_{n+1},\Delta\varepsilon_{n+1};\Delta\dot{\varepsilon}_{n+1}) \;=\; E\Delta\varepsilon_{n+1} + \eta\Delta\dot{\varepsilon}_{n+1} \;. \tag{4.62}$$

Upon integrating in time using the backward Euler method, it follows that

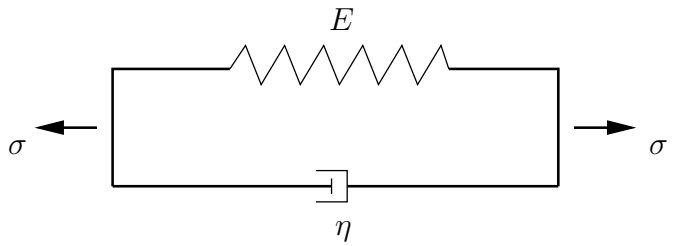

Figure 4.13. The Kelvin-Voigt solid

$$\varepsilon_{n+1} \;\doteq\; \varepsilon_n + \Delta t_n\dot{\varepsilon}_{n+1} \;, \tag{4.63}$$

therefore (4.61) becomes

$$\sigma_{n+1} \doteq E\varepsilon_{n+1} + \eta\frac{\varepsilon_{n+1}-\varepsilon_n}{\Delta t_n} \ . \tag{4.64}$$

This, in turn, implies that the differential of the stress is

$$D\sigma(\varepsilon_{n+1},\Delta\varepsilon_{n+1}) = \left(E+\frac{\eta}{\Delta t_n}\right)\Delta\varepsilon_{n+1} \ , \tag{4.65}$$

hence the algorithmic tangent modulus equals $E+\frac{\eta}{\Delta t_n}$.

It is important to recognize that in determining the differential of $\mathbf{P}$ in an algorithmic framework, one needs to first account for all approximations to rate-type quantities on which $\mathbf{P}$ depends. In solid mechanics problems, this leads to a functional expression of the form

$$\mathbf{P}_{n+1} = \widetilde{\mathbf{P}}(\mathbf{F}_{n+1},\cdots|_n,\cdots) \ , \tag{4.66}$$

where the notation $\cdots|_n$ is used to denote generic functional dependency on quantities at $t=t_n$. Sssuming sufficient smoothness of $\mathbf{P}$, this leads to an *algorithmically consistent differentiation* of $\mathbf{P}$ as

$$D\widetilde{\mathbf{P}}(\mathbf{F}_{n+1},\Delta\mathbf{F}_{n+1}) = \left(\frac{\partial\widetilde{\mathbf{P}}}{\partial\mathbf{F}}\right)_{n+1}\Delta\mathbf{F}_{n+1} \ . \tag{4.67}$$

The quantity $\left(\dfrac{\partial\widetilde{\mathbf{P}}}{\partial\mathbf{F}}\right)_{n+1}$ is referred to as the *algorithmic tangent modulus* at $t=t_{n+1}$.

Using the above results, one may obtain the linear part of the weak form (4.51) at $\mathbf{u}_{n+1}^{(k)}$ in the direction $\Delta^{(k)}\mathbf{u}_{n+1}$, as

$$\begin{aligned}\int_{\Omega_0^e}\boldsymbol{\xi}_{n+1}\cdot\rho_0\mathbf{a}_{n+1}^{(k)}\,dV + \int_{\Omega_0^e}\frac{\partial\boldsymbol{\xi}_{n+1}}{\partial\mathbf{X}}\cdot\mathbf{P}_{n+1}^{(k)}\,dV - \int_{\Omega_0^e}\boldsymbol{\xi}_{n+1}\cdot\rho_0\mathbf{b}\,dV \\ - \int_{\partial\Omega_0^e\cap\Gamma_{q0}}\boldsymbol{\xi}_{n+1}\cdot\bar{\mathbf{p}}_{n+1}\,dA - \int_{\partial\Omega_0^e\setminus\Gamma_{q0}}\boldsymbol{\xi}_{n+1}\cdot\mathbf{p}_{n+1}^{(k)}\,dA \\ + \int_{\Omega_0^e}\boldsymbol{\xi}_{n+1}\cdot\rho_0\Delta\ddot{\mathbf{u}}_{n+1}^{(k)}\,dV + \int_{\Omega_0^e}\frac{\partial\boldsymbol{\xi}_{n+1}}{\partial\mathbf{X}}\cdot\left(\frac{\partial\widetilde{\mathbf{P}}}{\partial\mathbf{F}}\right)_{n+1}^{(k)}\frac{\partial\Delta\mathbf{u}_{n+1}^{(k)}}{\partial\mathbf{X}}\,dV = 0 \ ,\end{aligned} \tag{4.68}$$

where use is made of (4.52), (4.53), and (4.67). Recalling the implicit Newmark formula (3.71), one may write for element e

$$\mathbf{a}_{n+1}^{(k)} = \frac{1}{\beta\Delta t_n^2}\left(\mathbf{u}_{n+1}^{(k)}-\mathbf{u}_n-\mathbf{v}_n\Delta t_n\right)-\frac{1-2\beta}{2\beta}\mathbf{a}_n \ , \tag{4.69}$$

therefore

$$\Delta\ddot{\mathbf{u}}^{(k)}_{n+1} \;=\; \frac{1}{\beta\Delta t_n^2}\Delta\mathbf{u}^{(k)}_{n+1}\;. \tag{4.70}$$

Substituting (4.70) into (4.69) and introducing the standard element interpolations (3.43) results in

$$\begin{aligned}&[\hat{\boldsymbol{\xi}}^e_{n+1}]^T\left\{[\mathbf{M}^e][\hat{\mathbf{a}}^{e\,(k)}_{n+1}]+[\mathbf{R}^e(\hat{\mathbf{u}}^{e\,(k)}_{n+1})]-[\mathbf{F}^e_{n+1}]-[\mathbf{F}^{e\,\mathrm{int}\,(k)}_{n+1}]\right\}\\&+[\hat{\boldsymbol{\xi}}^e_{n+1}]^T\left\{\int_{\Omega^e_0}[\mathbf{N}^e]^T\frac{\rho_0}{\beta\Delta t_n^2}[\mathbf{N}^e]\,dV+\int_{\Omega^e_0}[\mathbf{B}^e]^T\left[\frac{\partial\widetilde{\mathbf{P}}}{\partial\mathbf{F}}\right]^{(k)}_{n+1}[\mathbf{B}^e]\,dV\right\}[\Delta\hat{\mathbf{u}}^{e\,(k)}_{n+1}]\;=\;0\;,\end{aligned}\tag{4.71}$$

where $\left[\frac{\partial\widetilde{\mathbf{P}}}{\partial\mathbf{F}}\right]^{(k)}_{n+1}$ is a 9×9 matrix containing the components $\dfrac{\partial\widetilde{P}_{iA}}{\partial F_{jB}}$, consistently with the convention adopted in (3.46). The quantity inside the large brackets in (4.71) is the element tangent stiffness matrix $\mathbf{K}^{e\,(k)}_{n+1}$, that is,

$$\mathbf{K}^{e\,(k)}_{n+1} \;=\; \underbrace{\int_{\Omega^e_0}[\mathbf{N}^e]^T\frac{\rho_0}{\beta\Delta t_n^2}[\mathbf{N}^e]\,dV}_{\text{inertial stiffness}}+\underbrace{\int_{\Omega^e_0}[\mathbf{B}^e]^T\left[\frac{\partial\widetilde{\mathbf{P}}}{\partial\mathbf{F}}\right]^{(k)}_{n+1}[\mathbf{B}^e]\,dV}_{\text{material stiffness}}\;. \tag{4.72}$$

Likewise, the quantity inside the small brackets in (4.71) is the residual vector, which quantifies the imbalance of linear momentum at the (k)-th iteration of the Newton-Raphson method. Upon assemblying (4.71), the global Newton-Raphson equations take the form

$$\left(\mathbf{M}\hat{\mathbf{a}}^{(k)}_{n+1}+\mathbf{R}(\hat{\mathbf{u}}^{(k)}_{n+1})-\mathbf{F}_{n+1}\right)+\mathbf{K}^{(k)}_{n+1}\Delta\hat{\mathbf{u}}^{(k)}_{n+1}\;=\;\mathbf{0}\quad,\quad k=0,1,\cdots\;, \tag{4.73}$$

where $\mathbf{K}^{(k)}_{n+1}=\mathop{\mathbf{A}}_{e}\mathbf{K}^{e\,(k)}_{n+1}$ is the *global tangent stiffness matrix*.

A similar analysis may be carried out starting from the Eulerian form of linear momentum balance (3.41) restricted to an element e with domain Ω^e, such that

$$\begin{aligned}&\int_{\Omega^e}\boldsymbol{\xi}_{n+1}\cdot\rho_{n+1}\mathbf{a}_{n+1}\,dv+\int_{\Omega^e}\frac{\partial\boldsymbol{\xi}_{n+1}}{\partial\mathbf{x}_{n+1}}\cdot\mathbf{T}_{n+1}\,dv\;=\\&\qquad\int_{\Omega^e}\boldsymbol{\xi}_{n+1}\cdot\rho_{n+1}\mathbf{b}_{n+1}\,dv+\int_{\partial\Omega^e\cap\Gamma_q}\boldsymbol{\xi}_{n+1}\cdot\bar{\mathbf{t}}_{n+1}\,da+\int_{\partial\Omega^e\setminus\Gamma_q}\boldsymbol{\xi}_{n+1}\cdot\mathbf{t}_{n+1}\,da\;.\end{aligned}\tag{4.74}$$

By appealing to mass conservation, it is immediately seen that

$$\begin{aligned}D\left[\int_{\Omega^e}\boldsymbol{\xi}_{n+1}\cdot\rho_{n+1}\mathbf{a}_{n+1}\,dv\right](\mathbf{u}_{n+1},\Delta\mathbf{u}_{n+1}) \;&=\; \int_{\Omega^e}\boldsymbol{\xi}_{n+1}\cdot\rho_{n+1}D\mathbf{a}_{n+1}(\mathbf{u}_{n+1},\Delta\mathbf{u}_{n+1})\,dv\\&=\;\int_{\Omega^e}\boldsymbol{\xi}_{n+1}\cdot\rho_{n+1}\Delta\ddot{\mathbf{u}}_{n+1}\,dv\;.\end{aligned}\tag{4.75}$$

A similar procedure can be employed for the term involving the body forces.

Neglecting non-linearities due to body force or surface traction, proceed next with the differentiation of the stress-divergence term in (4.74). First, note that, upon using (1.85) and the chain rule, one may conclude for a solid mechanics problem that

$$\frac{\partial \boldsymbol{\xi}}{\partial \mathbf{x}} \cdot \mathbf{T} \;=\; \left(\frac{\partial \boldsymbol{\xi}}{\partial \mathbf{X}} \mathbf{F}^{-1}\right) \cdot \left(\frac{1}{J} \mathbf{F}\mathbf{S}\mathbf{F}^{T}\right) \;=\; \frac{1}{J} \frac{\partial \boldsymbol{\xi}}{\partial \mathbf{X}} \cdot (\mathbf{F}\mathbf{S}) \;. \tag{4.76}$$

Taking into account the preceding relation, as well as (2.36), the differentiation of the stress-divergence term may be obtained as

$$\begin{aligned} & D\left[\int_{\Omega^e} \frac{\partial \boldsymbol{\xi}_{n+1}}{\partial \mathbf{x}_{n+1}} \cdot \mathbf{T}_{n+1}\, dv\right](\mathbf{u}_{n+1}, \Delta\mathbf{u}_{n+1}) \qquad (4.77) \\ &= D\left[\int_{\Omega_0^e} \frac{1}{J_{n+1}} \frac{\partial \boldsymbol{\xi}_{n+1}}{\partial \mathbf{X}} \cdot (\mathbf{F}_{n+1}\mathbf{S}_{n+1})\, J_{n+1}\, dV\right](\mathbf{u}_{n+1}, \Delta\mathbf{u}_{n+1}) \\ &= D\left[\int_{\Omega_0^e} \frac{\partial \boldsymbol{\xi}_{n+1}}{\partial \mathbf{X}} \cdot (\mathbf{F}_{n+1}\mathbf{S}_{n+1})\, dV\right](\mathbf{u}_{n+1}, \Delta\mathbf{u}_{n+1}) \\ &= \int_{\Omega_0^e} \frac{\partial \boldsymbol{\xi}_{n+1}}{\partial \mathbf{X}} \cdot \left[D\mathbf{F}\,(\mathbf{u}_{n+1}, \Delta\mathbf{u}_{n+1})\,\mathbf{S}_{n+1}\right] dV + \int_{\Omega_0^e} \frac{\partial \boldsymbol{\xi}_{n+1}}{\partial \mathbf{X}} \cdot \left[\mathbf{F}_{n+1} D\mathbf{S}\,(\mathbf{u}_{n+1}, \Delta\mathbf{u}_{n+1})\right] dV \\ &= \int_{\Omega_0^e} \frac{\partial \boldsymbol{\xi}_{n+1}}{\partial \mathbf{X}} \cdot \left(\frac{\partial \Delta\mathbf{u}_{n+1}}{\partial \mathbf{X}} \mathbf{S}_{n+1}\right) dV + \int_{\Omega_0^e} \frac{\partial \boldsymbol{\xi}_{n+1}}{\partial \mathbf{X}} \cdot \left[\mathbf{F}_{n+1} D\mathbf{S}\,(\mathbf{u}_{n+1}, \Delta\mathbf{u}_{n+1})\right] dV \;. \qquad (4.78) \end{aligned}$$

Assuming, in analogy to earlier discussion on $\mathbf{P}$, that

$$\mathbf{S}_{n+1} \;=\; \widetilde{\mathbf{S}}(\mathbf{E}_{n+1}, \cdots|_n, \cdots) \;, \tag{4.79}$$

one may write

$$D\widetilde{\mathbf{S}}\,(\mathbf{E}_{n+1}, \Delta\mathbf{E}_{n+1}) \;=\; \left(\frac{\partial \widetilde{\mathbf{S}}}{\partial \mathbf{E}}\right)_{n+1} \Delta\mathbf{E}_{n+1} \;. \tag{4.80}$$

It is now possible to push-forward to the current configuration the first term on the right-hand side of (4.77) to find that

$$\begin{aligned} \int_{\Omega_0^e} \frac{\partial \boldsymbol{\xi}_{n+1}}{\partial \mathbf{X}} \cdot \left(\frac{\partial \Delta\mathbf{u}_{n+1}}{\partial \mathbf{X}} \mathbf{S}_{n+1}\right) dV \;&=\; \int_{\Omega_0^e} \left(\frac{\partial \boldsymbol{\xi}_{n+1}}{\partial \mathbf{x}_{n+1}} \mathbf{F}_{n+1}\right) \cdot \left[\frac{\partial \Delta\mathbf{u}_{n+1}}{\partial \mathbf{x}_{n+1}} \mathbf{F}_{n+1} \left(J_{n+1} \mathbf{F}_{n+1}^{-1} \mathbf{T}_{n+1} \mathbf{F}_{n+1}^{-T}\right)\right] dV \\ &=\; \int_{\Omega^e} \frac{\partial \boldsymbol{\xi}_{n+1}}{\partial \mathbf{x}_{n+1}} \cdot \left(\frac{\partial \Delta\mathbf{u}_{n+1}}{\partial \mathbf{x}_{n+1}} \mathbf{T}_{n+1}\right) dv \;, \qquad (4.81) \end{aligned}$$

where use is again made of (1.85) and the chain rule. This term gives rise to the *geometric stiffness*, namely the part of the tangent stiffness matrix which is due to the change of the geometry in the current configuration for *fixed* stress $\mathbf{T}_{n+1}$.

Repeat the above procedure for the second term in the differentiation to conclude that

$$\begin{aligned}
&\int_{\Omega_0^e} \frac{\partial \boldsymbol{\xi}_{n+1}}{\partial \mathbf{X}} \cdot \left[\mathbf{F}_{n+1} D\mathbf{S}\left(\mathbf{u}_{n+1}, \Delta\mathbf{u}_{n+1}\right)\right] dV \\
&= \int_{\Omega_0^e} \frac{\partial \boldsymbol{\xi}_{n+1}}{\partial \mathbf{X}} \cdot \left\{ \mathbf{F}_{n+1} \left[\left(\frac{\partial \widetilde{\mathbf{S}}}{\partial \mathbf{E}} \right)_{n+1} \frac{1}{2} \left(\Delta\mathbf{F}_{n+1}^T \mathbf{F}_{n+1} + \mathbf{F}_{n+1}^T \Delta\mathbf{F}_{n+1} \right) \right] \right\} dV \\
&= \int_{\Omega_0^e} \left(\mathbf{F}_{n+1}^T \frac{\partial \boldsymbol{\xi}_{n+1}}{\partial \mathbf{X}} \right) \cdot \left\{ \left[\left(\frac{\partial \widetilde{\mathbf{S}}}{\partial \mathbf{E}} \right)_{n+1} \frac{1}{2} \left[\left(\frac{\partial \Delta\mathbf{u}_{n+1}}{\partial \mathbf{X}} \right)^T \mathbf{F}_{n+1} + \mathbf{F}_{n+1}^T \left(\frac{\partial \Delta\mathbf{u}_{n+1}}{\partial \mathbf{X}} \right) \right] \right] \right\} dV \ ,
\end{aligned} \tag{4.82}$$

where use is made of (2.36), (2.41), and the chain rule. Pushing the right-hand side of (4.82) forward to the current configuration leads to

$$\begin{aligned}
&\int_{\Omega_0^e} \frac{\partial \boldsymbol{\xi}_{n+1}}{\partial \mathbf{X}} \cdot \left[\mathbf{F}_{n+1} D\mathbf{S}\left(\mathbf{u}_{n+1}, \Delta\mathbf{u}_{n+1}\right)\right] dV \\
&\qquad = \int_{\Omega^e} \frac{1}{J_{n+1}} \left(\mathbf{F}_{n+1}^T \frac{\partial \boldsymbol{\xi}_{n+1}}{\partial \mathbf{x}_{n+1}} \mathbf{F}_{n+1} \right) \cdot \left[\left(\frac{\partial \widetilde{\mathbf{S}}}{\partial \mathbf{E}} \right)_{n+1} \mathbf{F}_{n+1}^T \left(\frac{\partial \Delta\mathbf{u}_{n+1}}{\partial \mathbf{x}_{n+1}} \right) \mathbf{F}_{n+1} \right] dv \ ,
\end{aligned} \tag{4.83}$$

with the aid of (1.10), the chain rule, and exploiting the symmetry of the fourth-order tensor $\dfrac{\partial \widetilde{\mathbf{S}}}{\partial \mathbf{E}}$ in its third and fourth legs. This term gives rise to the *material stiffness*, namely the part of the tangent stiffness matrix which is due to the non-linearity of the constitutive law for stress at the *fixed* geometry of the body in the current configuration. In component form, one may express the integral in (4.83) as $\frac{1}{J}(F_{iA}\xi_{i,j}F_{jB})\left(\frac{\widetilde{S}_{AB}}{E_{CD}}F_{kC}\Delta u_{k,l}F_{lD}\right)$, where the subscript "$n+1$" is omitted for brevity.

Now obtain again the linear part of the weak form of linear momentum balance (4.74) at $\mathbf{u}_{n+1}^{(k)}$ in the direction $\Delta\mathbf{u}_{n+1}^{(k)}$ as

$$\begin{aligned}
&\int_{\Omega^e} \boldsymbol{\xi}_{n+1} \cdot \rho_{n+1}^{(k)} \mathbf{a}_{n+1}^{(k)} \, dv + \int_{\Omega^e} \frac{\partial \boldsymbol{\xi}_{n+1}}{\partial \mathbf{x}_{n+1}^{(k)}} \cdot \mathbf{T}_{n+1}^{(k)} \, dv - \int_{\Omega^e} \boldsymbol{\xi}_{n+1} \cdot \rho_{n+1}^{(k)} \mathbf{b}_{n+1} \, dv \\
&\qquad - \int_{\partial\Omega^e \cap \Gamma_q} \boldsymbol{\xi}_{n+1} \cdot \bar{\mathbf{t}}_{n+1} \, da - \int_{\partial\Omega^e \setminus \Gamma_q} \boldsymbol{\xi}_{n+1} \cdot \mathbf{t}_{n+1} \, da \\
&\qquad + \int_{\Omega^e} \boldsymbol{\xi}_{n+1} \cdot \rho_{n+1}^{(k)} \Delta\ddot{\mathbf{u}}_{n+1}^{(k)} \, dv + \int_{\Omega^e} \frac{\partial \boldsymbol{\xi}_{n+1}}{\partial \mathbf{x}_{n+1}^{(k)}} \cdot \left(\frac{\partial \Delta\mathbf{u}_{n+1}^{(k)}}{\partial \mathbf{x}_{n+1}^{(k)}} \mathbf{T}_{n+1}^{(k)} \right) dv \\
&+ \int_{\Omega^e} \frac{1}{J_{n+1}^{(k)}} \left(\mathbf{F}_{n+1}^{(k)\,T} \frac{\partial \boldsymbol{\xi}_{n+1}}{\partial \mathbf{x}_{n+1}^{(k)}} \mathbf{F}_{n+1}^{(k)} \right) \cdot \left[\left(\frac{\partial \widetilde{\mathbf{S}}}{\partial \mathbf{E}} \right)_{n+1}^{(k)} \mathbf{F}_{n+1}^{(k)\,T} \left(\frac{\partial \Delta\mathbf{u}_{n+1}^{(k)}}{\partial \mathbf{x}_{n+1}^{(k)}} \right) \mathbf{F}_{n+1}^{(k)} \right] dv \ = \ 0 \ ,
\end{aligned} \tag{4.84}$$

where use is made of (4.81) and (4.83). Admitting the standard element interpolations and recalling the implicit Newmark formula (3.71), as done earlier in this section for the referential description, it follows that

$$
\begin{aligned}
&[\hat{\boldsymbol{\xi}}^e_{n+1}]^T \left\{ [\mathbf{M}^e][\hat{\mathbf{a}}^{e\,(k)}_{n+1}] + [\mathbf{R}^e(\hat{\mathbf{u}}^{e\,(k)}_{n+1})] - [\mathbf{F}^{e\,(k)}_{n+1}] - [\mathbf{F}^{e\,\mathrm{int}\,(k)}_{n+1}] \right\} \\
&\qquad + [\hat{\boldsymbol{\xi}}^e_{n+1}]^T \left\{ \underbrace{\int_{\Omega^e} [\mathbf{N}^e]^T \frac{\rho^{(k)}_{n+1}}{\beta \Delta t_n^2} [\mathbf{N}^e] dv}_{\text{inertial stiffness}} + \underbrace{\int_{\Omega^e} [\mathbf{B}^{e\,(k)}_{n+1}]^T [\mathbf{A}^{e\,(k)}_{n+1}][\mathbf{B}^{e\,(k)}_{n+1}] dv}_{\text{geometric stiffness}} \right. \\
&\qquad\qquad \left. + \underbrace{\int_{\Omega^e} [\mathbf{B}^{e\,(k)}_{n+1}]^T [\mathbf{c}^{(k)}_{n+1}][\mathbf{B}^{e\,(k)}_{n+1}] dv}_{\text{material stiffness}} \right\} [\Delta \hat{\mathbf{u}}^{e\,(k)}_{n+1}] \;=\; 0 \,, \qquad (4.85)
\end{aligned}
$$

where $[\mathbf{A}^{e\,(k)}_{n+1}]$ is a 9×9 array, such that

$$
\frac{\partial \boldsymbol{\xi}^{(k)}_{n+1}}{\partial \mathbf{x}^{(k)}_{n+1}} \cdot \frac{\partial \Delta \mathbf{u}^{(k)}_{n+1}}{\partial \mathbf{x}^{(k)}_{n+1}} \mathbf{T}^{(k)}_{n+1} \;=\; [\hat{\boldsymbol{\xi}}^e_{n+1}]^T [\mathbf{B}^{e\,(k)}_{n+1}]^T [\mathbf{A}^{e\,(k)}_{n+1}][\mathbf{B}^{e\,(k)}_{n+1}][\Delta \hat{\mathbf{u}}^{e\,(k)}_{n+1}] \qquad (4.86)
$$

in Ω^e, while, in light of (4.83), $[\mathbf{c}^{(k)}_{n+1}]$ is a 9×9 array whose components in full tensorial form are

$$
c^{(k)}_{ijkl} \;=\; \frac{1}{J^{(k)}} F^{(k)}_{iA} F^{(k)}_{jB} \frac{\partial \widetilde{S}^{(k)}_{AB}}{\partial E_{CD}} F^{(k)}_{kC} F^{(k)}_{lD} \,, \qquad (4.87)
$$

where the subscript "$n+1$" is omitted. The symmetry of $\mathbf{T}$ is sufficient to deduce that $\dfrac{\partial \boldsymbol{\xi}}{\partial \mathbf{x}} \cdot \dfrac{\partial \Delta \mathbf{u}}{\partial \mathbf{x}} \mathbf{T} = \dfrac{\partial \Delta \mathbf{u}}{\partial \mathbf{x}} \cdot \dfrac{\partial \boldsymbol{\xi}}{\partial \mathbf{x}} \mathbf{T}$, which implies that the matrix $[\mathbf{A}^{e\,(k)}_{n+1}]$ is necessarily symmetric provided the element interpolation functions for $\mathbf{u}$ and $\boldsymbol{\xi}$ are identical. Indeed, it is easy to show using the ordering convention in (3.46) that

$$
[\mathbf{A}^e] \;=\; \begin{bmatrix}
T_{11} & 0 & 0 & T_{21} & 0 & 0 & T_{31} & 0 & 0 \\
0 & T_{22} & 0 & 0 & T_{32} & 0 & 0 & T_{12} & 0 \\
0 & 0 & T_{33} & 0 & 0 & T_{13} & 0 & 0 & T_{23} \\
T_{12} & 0 & 0 & T_{22} & 0 & 0 & T_{32} & 0 & 0 \\
0 & T_{23} & 0 & 0 & T_{33} & 0 & 0 & T_{13} & 0 \\
0 & 0 & T_{31} & 0 & 0 & T_{11} & 0 & 0 & T_{21} \\
T_{13} & 0 & 0 & T_{23} & 0 & 0 & T_{33} & 0 & 0 \\
0 & T_{21} & 0 & 0 & T_{31} & 0 & 0 & T_{11} & 0 \\
0 & 0 & T_{32} & 0 & 0 & T_{12} & 0 & 0 & T_{22}
\end{bmatrix} . \qquad (4.88)
$$

This, in turn, implies that the geometric stiffness is always symmetric. The material stiffness is symmetric only when the matrix $[\mathbf{c}]$ is symmetric, which, according to (4.87) is contingent on the symmetry of $\dfrac{\partial \widetilde{S}^{(k)}_{AB}}{\partial E_{CD}}$ in both the first two and the last two pairs of legs. Further dimensional reduction to the arrays used to represent the geometric and material stiffness may be introduced by exploiting the fact that $\dfrac{\partial \boldsymbol{\xi}}{\partial \mathbf{x}} \cdot \mathbf{T} = \left(\dfrac{\partial \boldsymbol{\xi}}{\partial \mathbf{x}}\right)^s \cdot \mathbf{T}$, owing to the symmetry of $\mathbf{T}$.

Upon assembly of the element-wise equations stemming from (4.85) one readily recovers a global system analogous to the one in (4.73).

Equation (4.74) is the starting point for the Newton-Raphson method in fluids. In contrast with solids, the inertial term is more complex, since

$$
\begin{aligned}
D\left[\int_{\Omega^e} \boldsymbol{\xi}_{n+1} \cdot \rho_{n+1}\mathbf{a}_{n+1}\, dv\right](\mathbf{v}_{n+1}, \Delta\mathbf{v}_{n+1}) & \\
&= \int_{\Omega^e} \boldsymbol{\xi}_{n+1} \cdot \rho_{n+1} D\mathbf{a}_{n+1}(\mathbf{v}_{n+1}, \Delta\mathbf{v}_{n+1})\, dv \\
&= \int_{\Omega^e} \boldsymbol{\xi}_{n+1} \cdot \rho_{n+1} \Delta\dot{\mathbf{v}}_{n+1}\, dv \\
&= \int_{\Omega^e} \boldsymbol{\xi}_{n+1} \cdot \rho_{n+1} \left(\frac{\partial \Delta\mathbf{v}_{n+1}}{\partial t} + \frac{\partial \Delta\mathbf{v}_{n+1}}{\partial \mathbf{x}_{n+1}}\mathbf{v}_{n+1} + \frac{\partial \mathbf{v}_{n+1}}{\partial \mathbf{x}_{n+1}}\Delta\mathbf{v}_{n+1}\right) dv\ .
\end{aligned}
\tag{4.89}
$$

On the other hand, the term emanating from stress-divergence is much simplified compared to solids and is given by

$$
D\left[\int_{\Omega^e} \frac{\partial \boldsymbol{\xi}_{n+1}}{\partial \mathbf{x}_{n+1}} \cdot \mathbf{T}_{n+1}\, dv\right](\mathbf{v}_{n+1}, \Delta\mathbf{v}_{n+1}) \;=\; \int_{\Omega^e} \frac{\partial \boldsymbol{\xi}_{n+1}}{\partial \mathbf{x}_{n+1}} \cdot D\mathbf{T}(\mathbf{v}_{n+1}, \Delta\mathbf{v}_{n+1})\, dv\ . \tag{4.90}
$$

This is because the Eulerian nature of the analysis implies that spatial derivatives are not subject to linearization due to changes in the velocity unless the argument of the derivative depends itself on the velocity. Of course, the weak form of linear momentum balance must be supplemented by an equation that enforces mass balance in a weak form.

Revisit the Newton-Raphson method in the form of (4.73) and write it succinctly as

$$
\mathbf{f}(\hat{\mathbf{u}}^{(k)}_{n+1}) + \mathbf{K}(\hat{\mathbf{u}}^{(k)}_{n+1})\Delta\hat{\mathbf{u}}^{(k)}_{n+1} \;=\; \mathbf{0} \qquad , \qquad k \;=\; 0, 1, 2, \cdots\ , \tag{4.91}
$$

with initial guess $\hat{\mathbf{u}}^{(0)}_{n+1} = \hat{\mathbf{u}}_n$. The algorithmic steps for the Newton-Raphson method are outlined in Algorithm 1 below.

Algorithm 1: *Newton-Raphson method*

Data: Δt_n, state at time t_n, $maxit$, tol
Set $k = 0$, $\hat{\mathbf{u}}_{n+1}^{(0)} = \hat{\mathbf{u}}_n$;
while $k \leq maxit$
  Form residual $\mathbf{f}(\mathbf{u}_{n+1}^{(k)})$;
  if $\|\mathbf{f}(\hat{\mathbf{u}}_{n+1}^{(k)})\| < tol$ **then**
    return $\hat{\mathbf{u}}_{n+1}^{(k)}$ and rest of state at time t_{n+1}
  else
    Form and factorize tangent stiffness $\mathbf{K}(\hat{\mathbf{u}}_{n+1}^{(k)})$;
    Solve (4.91) for $\Delta\hat{\mathbf{u}}_{n+1}^{(k)}$ and set $\hat{\mathbf{u}}_{n+1}^{(k+1)} = \hat{\mathbf{u}}_{n+1}^{(k)} + \Delta\hat{\mathbf{u}}_{n+1}^{(k)}$;
    Set $k \leftarrow k + 1$;
  end
end

The Newton-Raphson iterations are terminated based on a pre-selected stopping criterion. Such possible criteria include

(a) The *residual norm* criterion, $\|\mathbf{f}(\hat{\mathbf{u}}_{n+1}^{(k)})\| < tol$, which is shown in Algorithm 1,

(b) The *"absolute" error* criterion, $\|\Delta\hat{\mathbf{u}}_{n+1}^{(k)}\| < tol$,

(c) The *"relative" error* criterion, $\frac{\|\Delta\hat{\mathbf{u}}_{n+1}^{(k)}\|}{\|\hat{\mathbf{u}}_{n+1}^{(k)}\|} < tol$,

(d) The *"energy" norm* criterion $E_{n+1}^{(k)} = \Delta\hat{\mathbf{u}}_{n+1}^{(k)T}\mathbf{f}(\hat{\mathbf{u}}_{n+1}^{(k)}) < tol$. In essence, $E^{(k)}$ is the work done by the unbalanced forces $\mathbf{f}\left(\hat{\mathbf{u}}_{n+1}^{(k)}\right) \neq \mathbf{0}$ going over the displacement increment $\Delta\hat{\mathbf{u}}_{n+1}^{(k)}$.

The tolerance *tol* is typically set to be a multiple of the machine epsilon *eps*, say $10^m * eps$ for some positive integer m.

The modified Newton method of (4.28) leads to

$$\mathbf{f}(\hat{\mathbf{u}}_{n+1}^{(k)}) + \mathbf{K}(\hat{\mathbf{u}}_{n+1}^{(0)})\Delta\hat{\mathbf{u}}_{n+1}^{(k)} = \mathbf{0} \quad , \quad k = 0, 1, 2, \cdots , \tag{4.92}$$

with initial guess $\hat{\mathbf{u}}_{n+1}^{(0)} = \hat{\mathbf{u}}_n$. This is implemented very similarly to the original Newton-Raphson method, as shown in Algorithm 2.

Algorithm 2: *Modified Newton method*

Data: Δt_n, state at time t_n, *maxit*, *tol*

Set $k = 0$, $\hat{\mathbf{u}}_{n+1}^{(0)} = \hat{\mathbf{u}}_n$;

Form and factorize tangent stiffness $\mathbf{K}(\hat{\mathbf{u}}_{n+1}^{(0)})$;

while $k \leq maxit$

  Form residual $\mathbf{f}(\mathbf{u}_{n+1}^{(k)})$;

  if $\|\mathbf{f}(\hat{\mathbf{u}}_{n+1}^{(k)})\| < tol$ **then**

    return $\hat{\mathbf{u}}_{n+1}^{(k)}$ and rest of state at time t_{n+1}

  else

    Solve (4.92) for $\Delta\hat{\mathbf{u}}_{n+1}^{(k)}$ and set $\hat{\mathbf{u}}_{n+1}^{(k+1)} = \hat{\mathbf{u}}_{n+1}^{(k)} + \Delta\hat{\mathbf{u}}_{n+1}^{(k)}$;

    Set $k \leftarrow k + 1$;

  end

end

In highly non-linear problems, it may be necessary to perform a *line-search* to either accelerate convergence or to prevent divergence of the Newton-Raphson or modified Newton iteration. Here, one obtains the increment $\Delta\hat{\mathbf{u}}_{n+1}^{(k)}$ by solving (4.91) or (4.92), as usual. However, the displacement vector update is defined as

$$\hat{\mathbf{u}}_{n+1}^{(k+1)} \;=\; \hat{\mathbf{u}}_{n+1}^{(k)} + \eta_k \Delta\hat{\mathbf{u}}_{n+1}^{(k)} \;, \tag{4.93}$$

where $0 < \eta_k \leq 1$ is a scalar parameter. The value of η_k is determined so that the scalar function

$$g(\eta) \;=\; \Delta\hat{\mathbf{u}}_{n+1}^{(k)\,T} \mathbf{f}(\hat{\mathbf{u}}_{n+1}^{(k)} + \eta \Delta\hat{\mathbf{u}}_{n+1}^{(k)}) \tag{4.94}$$

satisfies $g(\eta_k) = 0$, that is, given $\hat{\mathbf{u}}_{n+1}^{(k)}$ and $\Delta\hat{\mathbf{u}}_{n+1}^{(k)}$, the residual $\mathbf{f}(\hat{\mathbf{u}}_{n+1}^{(k+1)})$ is orthogonal to $\Delta\hat{\mathbf{u}}_{n+1}^{(k)}$, as in Figure 4.14.

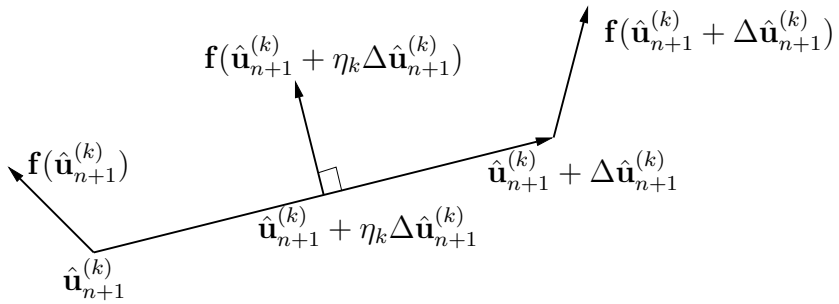

Figure 4.14. Schematic of line search

The existence of such an η_k is not guaranteed for any given $\mathbf{f}$, $\hat{\mathbf{u}}_{n+1}^{(k)}$, and $\Delta\hat{\mathbf{u}}_{n+1}^{(k)}$. In practice, one typically seeks to find a η_k, such that

$$\left|\Delta\hat{\mathbf{u}}_{n+1}^{(k)T}\mathbf{f}(\hat{\mathbf{u}}_{n+1}^{(k)}+\eta\Delta\hat{\mathbf{u}}_{n+1}^{(k)})\right| \;\leq\; s\left|\Delta\hat{\mathbf{u}}_{n+1}^{(k)T}\mathbf{f}(\hat{\mathbf{u}}_{n+1}^{(k)})\right| \;, \tag{4.95}$$

where s is a user-specified positive parameter less than unity (*e.g.*, $s = 0.8$). Clearly, line search involves (relatively inexpensive) residual evaluations for different values of η, until the above condition is met. A coarse one-dimensional exhaustive search is effective in searching for an η_k that satisfies (4.95), as shown in Algorithm 3 below.

Algorithm 3: *Line search with Newton-Raphson method*

Data: $\hat{\mathbf{u}}_{n+1}^{(k)}$, s, m
Form $\mathbf{K}(\hat{\mathbf{u}}_{n+1}^{(k)})$ and $\mathbf{f}(\hat{\mathbf{u}}_{n+1}^{(k)})$ and solve (4.91) for $\Delta\hat{\mathbf{u}}_{n+1}^{(k)}$;
Form $\mathbf{f}(\hat{\mathbf{u}}_{n+1}^{(k)}+\Delta\hat{\mathbf{u}}_{n+1}^{(k)})$;
if $\left|\Delta\hat{\mathbf{u}}_{n+1}^{(k)T}\mathbf{f}(\hat{\mathbf{u}}_{n+1}^{(k)}+\Delta\hat{\mathbf{u}}_{n+1}^{(k)})\right| \leq s\left|\Delta\hat{\mathbf{u}}_{n+1}^{(k)T}\mathbf{f}(\hat{\mathbf{u}}_{n+1}^{(k)})\right|$ **then**
  return $\hat{\mathbf{u}}_{n+1}^{(k+1)} = \hat{\mathbf{u}}_{n+1}^{(k)}+\Delta\hat{\mathbf{u}}_{n+1}^{(k)}$;
else
  Set $i = 0$;
  while $i \leq m$
    Set $\eta_k = (m-i+1)/m$;
    Form $\mathbf{f}(\hat{\mathbf{u}}_{n+1}^{(k)}+\eta_k\Delta\hat{\mathbf{u}}_{n+1}^{(k)})$;
    if $\left|\Delta\hat{\mathbf{u}}_{n+1}^{(k)T}\mathbf{f}(\hat{\mathbf{u}}_{n+1}^{(k)}+\eta_k\Delta\hat{\mathbf{u}}_{n+1}^{(k)})\right| \leq s\left|\Delta\hat{\mathbf{u}}_{n+1}^{(k)T}\mathbf{f}(\hat{\mathbf{u}}_{n+1}^{(k)})\right|$ **then**
      return $\hat{\mathbf{u}}_{n+1}^{(k+1)} = \hat{\mathbf{u}}_{n+1}^{(k)}+\eta_k\Delta\hat{\mathbf{u}}_{n+1}^{(k)}$;
    else
      Set $i \leftarrow i+1$;
    end
  end
end

Quasi-Newton methods are iterative schemes with convergence properties generally somewhere between those of the Newton-Raphson and the modified Newton method. The general idea is to obtain an approximation $\overline{\mathbf{K}}_{n+1}^{(k)}$ to the tangent stiffness matrix $\mathbf{K}(\hat{\mathbf{u}}_{n+1}^{(k)})$, which satisfies the condition

$$\overline{\mathbf{K}}_{n+1}^{(k)}(\hat{\mathbf{u}}_{n+1}^{(k)}-\hat{\mathbf{u}}_{n+1}^{(k-1)}) \;=\; \mathbf{f}(\hat{\mathbf{u}}_{n+1}^{(k)})-\mathbf{f}(\hat{\mathbf{u}}_{n+1}^{(k-1)}) \;, \tag{4.96}$$

which is referred to as the *quasi-Newton* or *secant property*. Subsequently, one uses the approximate stiffness to efficiently solve

$$\overline{\mathbf{K}}_{n+1}^{(k)} \Delta\hat{\mathbf{u}}_{n+1}^{(k)} \;=\; -\mathbf{f}(\hat{\mathbf{u}}_{n+1}^{(k)}) \tag{4.97}$$

for $\Delta\hat{\mathbf{u}}_{n+1}^{(k)}$ and update the displacement vector as

$$\hat{\mathbf{u}}_{n+1}^{(k+1)} \;=\; \hat{\mathbf{u}}_{n+1}^{(k)} + \Delta\hat{\mathbf{u}}_{n+1}^{(k)} \;. \tag{4.98}$$

Note that the quasi-Newton property (4.96) shows that the approximate stiffness $\overline{\mathbf{K}}_{n+1}^{(k)}$ is obtained by backward interpolation from the state at the k-th to the $(k-1)$-st iterate, see also Figure 4.15.

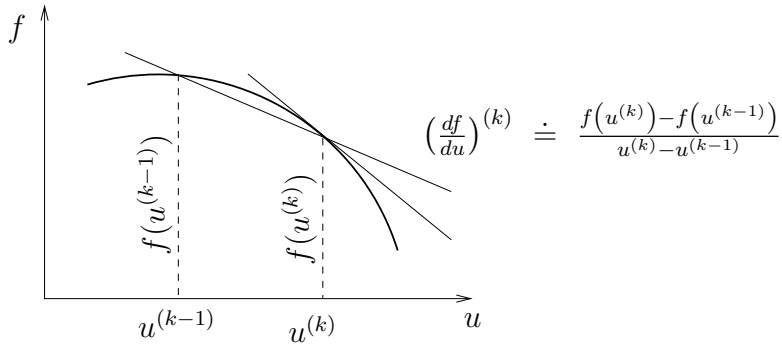

Figure 4.15. Schematic of quasi-Newton method in one-dimension

There exist many different ways (each corresponding to a different quasi-Newton method) for constructing $\overline{\mathbf{K}}_{n+1}^{(k)}$. Ideally, one expects of a quasi-Newton method that:

(a) The incremental displacement $\Delta\hat{\mathbf{u}}_{n+1}^{(k)}$ can be obtained efficiently, that is, without having to factorize $\overline{\mathbf{K}}_{n+1}^{(k)}$. This is possible if $\overline{\mathbf{K}}_{n+1}^{(k)}$ is obtained from $\overline{\mathbf{K}}_{n+1}^{(k-1)}$ as a low-rank update. In such a case, one may use the *Sherman-Morrison-Woodbury formula*, according to which, given an invertible $n \times n$ matrix $\overline{\mathbf{K}}$ and two $n \times m$ matrices $\mathbf{G}$ and $\mathbf{H}$ with $m < n$, then

$$\left(\overline{\mathbf{K}} + \mathbf{G}\mathbf{H}^T\right)^{-1} \;=\; \overline{\mathbf{K}}^{-1} - \overline{\mathbf{K}}^{-1}\mathbf{G}\left(\mathbf{I}_m + \mathbf{H}^T\overline{\mathbf{K}}^{-1}\mathbf{G}\right)^{-1}\mathbf{H}^T\overline{\mathbf{K}}^{-1} \;, \tag{4.99}$$

where $\mathbf{I}_m$ stands for the $m \times m$ identity matrix. Thus, the cost of finding $\Delta\hat{\mathbf{u}}_{n+1}^{(k)}$ is very small when, say, $m = 1$ or 2.

(b) The stiffness matrix update preserves properties such as symmetry and positive-definiteness, if these are present in the initial stiffness $\overline{\mathbf{K}}_{n+1}^{(0)}$.

Proceeding constructively, assume that $\overline{\mathbf{K}}^{(0)}_{n+1}$ is symmetric and one wants to develop a rank-one quasi-Newton method that preserves symmetry. Then, by necessity,

$$\overline{\mathbf{K}}^{(k)} \;=\; \overline{\mathbf{K}}^{(k-1)} + \mathbf{z}\mathbf{z}^T \;, \tag{4.100}$$

where $\mathbf{z}$ is a vector to be determined and the subscript $n+1$ is ignored henceforth for the sake of brevity. Since the quasi-Newton property (4.96) needs to be enforced, it follows that

$$\overline{\mathbf{K}}^{(k-1)}\Delta\hat{\mathbf{u}}^{(k-1)} + \mathbf{z}\mathbf{z}^T\Delta\hat{\mathbf{u}}^{(k-1)} \;=\; \mathbf{f}(\hat{\mathbf{u}}^{(k)}) - \mathbf{f}(\hat{\mathbf{u}}^{(k-1)}) \;, \tag{4.101}$$

which implies that

$$\mathbf{z} \;=\; \frac{1}{\mathbf{z}^T\Delta\hat{\mathbf{u}}^{(k-1)}}\left[\mathbf{f}(\hat{\mathbf{u}}^{(k)}) - \mathbf{f}(\hat{\mathbf{u}}^{(k-1)}) - \overline{\mathbf{K}}^{(k-1)}\Delta\hat{\mathbf{u}}^{(k-1)}\right] \tag{4.102}$$

and also

$$\Delta\hat{\mathbf{u}}^{(k-1)\,T}\overline{\mathbf{K}}^{(k-1)}\Delta\hat{\mathbf{u}}^{(k-1)} + \left(\mathbf{z}^T\Delta\hat{\mathbf{u}}^{(k-1)}\right)^2 \;=\; \left[\mathbf{f}^T(\hat{\mathbf{u}}^{(k)}) - \mathbf{f}^T(\hat{\mathbf{u}}^{(k-1)})\right]\Delta\hat{\mathbf{u}}^{(k-1)} \;. \tag{4.103}$$

The last two equations lead to

$$\begin{aligned}\overline{\mathbf{K}}^{(k)} \;=\; \overline{\mathbf{K}}^{(k-1)} &+ \frac{1}{\left[\mathbf{f}(\hat{\mathbf{u}}^{(k)}) - \mathbf{f}(\hat{\mathbf{u}}^{(k-1)})\right]^T\Delta\hat{\mathbf{u}}^{(k-1)} - \Delta\hat{\mathbf{u}}^{(k-1)\,T}\overline{\mathbf{K}}^{(k-1)}\Delta\hat{\mathbf{u}}^{(k-1)}} \\ &\left[\mathbf{f}(\hat{\mathbf{u}}^{(k)}) - \mathbf{f}(\hat{\mathbf{u}}^{(k-1)}) - \overline{\mathbf{K}}^{(k-1)}\Delta\hat{\mathbf{u}}^{(k-1)}\right]\left[\mathbf{f}(\hat{\mathbf{u}}^{(k)}) - \mathbf{f}(\hat{\mathbf{u}}^{(k-1)}) - \overline{\mathbf{K}}^{(k-1)}\Delta\hat{\mathbf{u}}^{(k-1)}\right]^T \;.\end{aligned} \tag{4.104}$$

Regrettably, this quasi-Newton method does not necessarily preserve definiteness and, in fact, can become unbounded due to the term in the denominator of the right-hand side.

Unlike the preceding symmetric case, where satisfaction of the quasi-Newton property uniquely determines the rank-one update, more assumptions are needed in the unsymmetric rank-one case

$$\overline{\mathbf{K}}^{(k)} \;=\; \overline{\mathbf{K}}^{(k-1)} + \mathbf{z}_1\mathbf{z}_2^T \;, \tag{4.105}$$

where $\mathbf{z}_1$ and $\mathbf{z}_2$ are vectors, and $\mathbf{z}_1 \neq \mathbf{z}_2$.

Broyden[6] further assumed that,

$$\overline{\mathbf{K}}^{(k)}\mathbf{q}^{(k-1)} \;=\; \overline{\mathbf{K}}^{(k-1)}\mathbf{q}^{(k-1)} \qquad ; \qquad \mathbf{q}^{(k-1)\,T}\Delta\hat{\mathbf{u}}^{(k-1)} \;=\; 0 \;, \tag{4.106}$$

[6] C.G. Broyden, A class of methods for solving nonlinear simultaneous equations, *Mathematics of Computation*, 19:577-593, (1965).

which asserts that the change in $\mathbf{f}$ predicted by $\overline{\mathbf{K}}^{(k)}$ along a direction orthogonal to $\Delta\hat{\mathbf{u}}^{(k-1)}$ is the same with the change predicted by $\overline{\mathbf{K}}^{(k-1)}$ (stated differently, $\overline{\mathbf{K}}^{(k)}$ and $\overline{\mathbf{K}}^{(k-1)}$ are identical in the direction normal to $\Delta\hat{\mathbf{u}}^{(k-1)}$). It follows from (4.105) that

$$\overline{\mathbf{K}}^{(k)}\mathbf{q}^{(k-1)} \;=\; \overline{\mathbf{K}}^{(k-1)}\mathbf{q}^{(k-1)} + \mathbf{z}_1\mathbf{z}_2^T\mathbf{q}^{(k-1)} \;, \tag{4.107}$$

so that, in view of (4.106),

$$\mathbf{z}_2 \;=\; \Delta\hat{\mathbf{u}}^{(k-1)} \;, \tag{4.108}$$

to within a scalar multiplier. Furthermore, the quasi-Newton property (4.96) necessitates that

$$\left[\overline{\mathbf{K}}^{(k-1)} + \mathbf{z}_1\Delta\hat{\mathbf{u}}^{(k-1)\,T}\right]\Delta\hat{\mathbf{u}}^{(k-1)} \;=\; \mathbf{f}(\hat{\mathbf{u}}^{(k)}) - \mathbf{f}(\hat{\mathbf{u}}^{(k-1)}) \;, \tag{4.109}$$

which, in turn, implies that

$$\mathbf{z}_1 \;=\; \frac{1}{\Delta\hat{\mathbf{u}}^{(k-1)\,T}\Delta\hat{\mathbf{u}}^{(k-1)}}\left[\mathbf{f}(\hat{\mathbf{u}}^{(k)}) - \mathbf{f}(\hat{\mathbf{u}}^{(k-1)}) - \overline{\mathbf{K}}^{(k-1)}\Delta\hat{\mathbf{u}}^{(k-1)}\right] \;. \tag{4.110}$$

A quasi-Newton method may be implemented as shown in Algorithm 4.

Algorithm 4: *Quasi-Newton method*

Data: Δt_n, state at time t_n, *maxit*, *tol*
Set $\hat{\mathbf{u}}_{n+1}^{(0)} = \hat{\mathbf{u}}_n$;
Form $\mathbf{K}(\hat{\mathbf{u}}_{n+1}^{(0)})$ and $\mathbf{f}(\hat{\mathbf{u}}_{n+1}^{(0)})$ and solve (4.91) for $\Delta\hat{\mathbf{u}}_{n+1}^{(0)}$;
Set $\hat{\mathbf{u}}_{n+1}^{(1)} = \hat{\mathbf{u}}_{n+1}^{(0)} + \Delta\hat{\mathbf{u}}_{n+1}^{(0)}$;
while $k \le maxit$
  Form residual $\mathbf{f}(\mathbf{u}_{n+1}^{(k)})$;
  if $\|\mathbf{f}(\hat{\mathbf{u}}_{n+1}^{(k)})\| < tol$ **then**
    return $\hat{\mathbf{u}}_{n+1}^{(k)}$ and rest of state at time t_{n+1}
  else
    Form and factorize $\overline{\mathbf{K}}_{n+1}^{(k)}$;
    Solve (4.97) for $\Delta\hat{\mathbf{u}}_{n+1}^{(k)}$ and set $\hat{\mathbf{u}}_{n+1}^{(k+1)} = \hat{\mathbf{u}}_{n+1}^{(k)} + \Delta\hat{\mathbf{u}}_{n+1}^{(k)}$;
    Set $k \leftarrow k+1$;
  end
end

The *BFGS method* (named after Broyden-Fletcher-Goldfard-Shanno) is a quasi-Newton method intended for problems that lead to symmetric tangent stiffness matrix. The method makes use of two rank-one updates, such that

$$\overline{\mathbf{K}}^{(k)} \;=\; \overline{\mathbf{K}}^{(k-1)} + \mathbf{z}_1\mathbf{z}_1^T + \mathbf{z}_2\mathbf{z}_2^T \;, \tag{4.111}$$

where $\mathbf{z}_1$ and $\mathbf{z}_2$ are vectors with $\mathbf{z}_1 \neq \mathbf{z}_2$. The BFGS method is employed as follows:

(i) Assuming $\overline{\mathbf{K}}^{(k-1)}$ (symmetric) and $\hat{\mathbf{u}}^{(k-1)}$ assumed known, determine the increment $\Delta\hat{\mathbf{u}}^{(k-1)}$ from the standard quasi-Newton formula (4.97) as

$$\overline{\mathbf{K}}^{(k-1)}\Delta\hat{\mathbf{u}}^{(k-1)} + \mathbf{f}(\hat{\mathbf{u}}^{(k-1)}) \;=\; \mathbf{0}\;. \tag{4.112}$$

(ii) Perform a line search along $\hat{\mathbf{u}}^{(k-1)}$, that is determine η_{k-1}, $0 < \eta_{k-1} \leq 1$, such that

$$\hat{\mathbf{u}}^{(k)} \;=\; \hat{\mathbf{u}}^{(k-1)} + \eta_{k-1}\Delta\hat{\mathbf{u}}^{(k-1)}\;. \tag{4.113}$$

(iii) Update the stiffness matrix consistently with a quasi-Newton property (4.96), where, in particular,

$$\begin{aligned}\overline{\mathbf{K}}^{(k)} \;=\; \overline{\mathbf{K}}^{(k-1)} &+ \frac{\left[\mathbf{f}(\hat{\mathbf{u}}^{(k)}) - \mathbf{f}(\hat{\mathbf{u}}^{(k-1)})\right]\left[\mathbf{f}(\hat{\mathbf{u}}^{(k)}) - \mathbf{f}(\hat{\mathbf{u}}^{(k-1)})\right]^T}{\eta_{k-1}\left[\mathbf{f}(\hat{\mathbf{u}}^{(k)}) - \mathbf{f}(\hat{\mathbf{u}}^{(k-1)})\right]^T\Delta\hat{\mathbf{u}}^{(k-1)}} \\ &- \frac{\left[\overline{\mathbf{K}}^{(k-1)}\Delta\hat{\mathbf{u}}^{(k-1)}\right]\left[\overline{\mathbf{K}}^{(k-1)}\Delta\hat{\mathbf{u}}^{(k-1)}\right]^T}{\Delta\hat{\mathbf{u}}^{(k-1)\,T}\overline{\mathbf{K}}^{(k-1)}\Delta\hat{\mathbf{u}}^{(k-1)}}\;.\end{aligned} \tag{4.114}$$

The update formula (4.114) is derived from (4.111) by imposing the quasi-Newton property (4.96) and also setting $\mathbf{z}_1$ to be proportional to the change in the force imbalance $\mathbf{f}(\hat{\mathbf{u}}^{(k)}) - \mathbf{f}(\hat{\mathbf{u}}^{(k-1)})$. It can be easily shown that if $\overline{\mathbf{K}}^{(k-1)}$ is positive-definite, then $\overline{\mathbf{K}}^{(k)}$ may or may not be positive-definite but is at least positive semi-definite.

The inverse of the stiffness matrix in (4.114) may be obtained in closed form by two successive applications of the formula in (4.99). Special case is typically needed to ensure that the terms in (4.114) are computed in a manner than minimizes errors associated with algebraic operations involving small numbers.

The BFGS method is implemented as shown in Algorithm 5.

Algorithm 5: *BFGS method*

Data: Δt_n, state at time t_n, $maxit$, tol, s

Set $\hat{\mathbf{u}}_{n+1}^{(0)} = \hat{\mathbf{u}}_n$;

Form $\mathbf{K}(\hat{\mathbf{u}}_{n+1}^{(0)})$ and $\mathbf{f}(\hat{\mathbf{u}}_{n+1}^{(0)})$ and solve (4.91) for $\Delta\hat{\mathbf{u}}_{n+1}^{(0)}$;

Perform line search according to Algorithm 3 for given s and set $\hat{\mathbf{u}}_{n+1}^{(1)} = \hat{\mathbf{u}}_{n+1}^{(0)} + \eta_0 \Delta\hat{\mathbf{u}}_{n+1}^{(0)}$;

while $k \leq maxit$

  Form residual $\mathbf{f}(\mathbf{u}_{n+1}^{(k)})$;

  if $\|\mathbf{f}(\hat{\mathbf{u}}_{n+1}^{(k)})\| < tol$ **then**

    return $\hat{\mathbf{u}}_{n+1}^{(k)}$ and rest of state at time t_{n+1}

  else

    Form $\overline{\mathbf{K}}_{n+1}^{(k)}$ as in (4.114) and factorize;

    Solve (4.97) for $\Delta\hat{\mathbf{u}}_{n+1}^{(k)}$;

    Perform line search and set $\hat{\mathbf{u}}_{n+1}^{(k+1)} = \hat{\mathbf{u}}_{n+1}^{(k)} + \eta_k \Delta\hat{\mathbf{u}}_{n+1}^{(k)}$;

    Set $k \leftarrow k + 1$;

  end

end

4.4 Continuation Methods

Recall the discrete equations of motion for solids, in the form of equation (3.72), and consider a special case, in which inertial effects may be neglected (rendering the problem quasi-static) and the external loading is *proportional* with proportionality factor $\lambda = \lambda(s)$. Here, s may be thought of an "implicit" measure of time and λ is taken to be a smooth function of s. Under these conditions, the N-dimensional discrete equilibrium equations (3.72) reduce to

$$\mathbf{f}(\hat{\mathbf{u}}_{n+1}) \;=\; \mathbf{R}(\hat{\mathbf{u}}_{n+1}) - \mathbf{F}_{n+1} \;=\; \bar{\mathbf{f}}(\hat{\mathbf{u}}_{n+1}) - \lambda_{n+1}\mathbf{c}\ ,$$

where $\mathbf{c}$ is a constant force vector in $\mathbb{R}^N$ and λ_{n+1} effects an alternative parametrization of loading. Therefore, one may express the equilibrium equation at any load level as

$$\mathbf{f}\,(\mathbf{u},\lambda) \;=\; \bar{\mathbf{f}}\,(\mathbf{u}) - \lambda\mathbf{c} \;=\; \mathbf{0}\ . \tag{4.115}$$

Now identify two distinct types of *stability points* $(\mathbf{u},\lambda) \in \mathbb{R}^N \times \mathbb{R}$, that is *limit points* (also referred to as *turning points*) and *bifurcation points*. A one-dimensional representation of

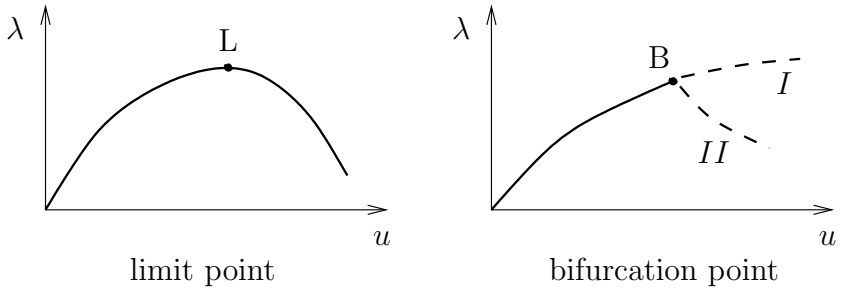

Figure 4.16. Limit and bifurcation points in (u, λ)-space

these points is included in Figure 4.16. The distinction between limit and bifurcation points was originally suggested by Poincaré[7].

Some typical examples of stability problems from solid mechanics are shown below.

Example 4.4.1: Snapping of a deep arch

This problem involves an arch made of an elastic material. The arch is loaded by a downward-pointing force at its midpoint. As the load increases, the arch resists the load in compression until it snaps through, as shown in Figure 4.17. Subsequently, the arch resists the load in tension. This is an example of a structure whose response exhibits two limit loads (one in the pre- and the other in the post-snap-through phase).

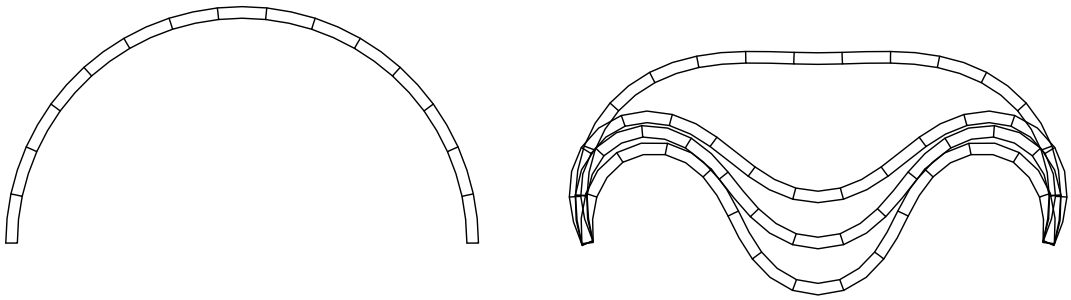

Figure 4.17. *Snapping of a deep arch*

Example 4.4.2: Buckling of a cantilever column

This is the classical buckling problem of a column made of an elastic material and loaded by a compressive force. It is well-known that upon reaching a critical value, the force induces buckling of the column, in which case multiple equilibrium states become possible. This is an example of a bifurcation of the original equilibrium state into a set of possible such states.

[7] H. Poincaré, Sur l' équilibre d' une mass fluide animée d' un mouvement de rotation, *Acta Mathematica*, 7:259–380, (1885).

An *equilibrium path* (or *solution path*) is defined as a set of functions $\mathbf{u}(s), \lambda(s)$, such that

$$\mathbf{f}\left(\mathbf{u}, \lambda\right) \;=\; \mathbf{0}\;. \tag{4.116}$$

Let $\mathbf{f} : \mathbb{R}^N \times \mathbb{R} \to \mathbb{R}^N$ be continuously differentiable, and also such that for a given s associated with a solution $(\mathbf{u}(s), \lambda(s))$

$$\det\left[\frac{\partial \mathbf{f}}{\partial \mathbf{u}}\big(\mathbf{u}(s), \lambda(s)\big)\right] \;\neq\; 0\;. \tag{4.117}$$

Then, by the implicit function theorem, one may conclude that there exists an open neighborhood $\mathcal{U} \subset \mathbb{R}^N$ around $\mathbf{u}(s)$, an open neighborhood $\mathcal{V} \subset \mathbb{R}$ around $\lambda(s)$, and a unique continuously differentiable function $\check{\mathbf{u}} :\; \mathcal{V} \;\to\; \mathcal{U}$, such that

$$\mathbf{f}\left(\check{\mathbf{u}}(\lambda), \lambda\right) \;=\; \mathbf{0}\;, \tag{4.118}$$

see Figure 4.18.

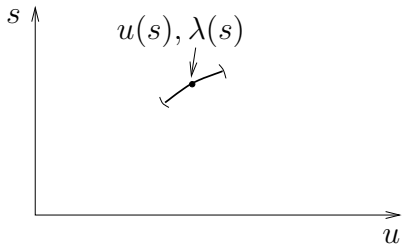

Figure 4.18. Solution in neighborhood of point $(u(s), \lambda(s))$

Upon differentiating the original equation with respect to s, it follows that

$$\frac{\partial \mathbf{f}}{\partial \mathbf{u}}\frac{d\mathbf{u}}{ds} + \frac{\partial \mathbf{f}}{\partial \lambda}\frac{d\lambda}{ds} \;=\; \mathbf{0}\;. \tag{4.119}$$

A solution point $(\bar{\mathbf{u}}, \bar{\lambda})$ is termed a *stability point* if:

(a)

$$\det\left[\frac{\partial \mathbf{f}}{\partial \mathbf{u}}\left(\bar{\mathbf{u}}, \bar{\lambda}\right)\right] \;=\; 0\;, \tag{4.120}$$

(b)

$$\ker\left[\frac{\partial \mathbf{f}}{\partial \mathbf{u}}\left(\bar{\mathbf{u}}, \bar{\lambda}\right)\right] \;=\; \sum_{i=1}^{n} \alpha_i \bar{\boldsymbol{\phi}}_i \qquad , \qquad n < N \tag{4.121}$$

where $n < N$, $\alpha_i \in \mathbb{R}$ and $\bar{\boldsymbol{\phi}}_i \in \mathbb{R}^N$, $i = 1, 2, \ldots, n$, that is,

$$\left[\frac{\partial \mathbf{f}}{\partial \mathbf{u}}\left(\bar{\mathbf{u}}, \bar{\lambda}\right)\right] \bar{\boldsymbol{\phi}}_i \;=\; \mathbf{0} \quad , \quad i \;=\; 1, \cdots, n\;, \tag{4.122}$$

(c)

$$\text{range}\left[\frac{\partial \mathbf{f}}{\partial \mathbf{u}}\left(\bar{\mathbf{u}},\bar{\lambda}\right)\right] \;=\; \left\{\mathbf{y}\in\mathbb{R}^N \;\;\middle|\;\; \bar{\boldsymbol{\phi}}_i^T\mathbf{y} \;=\; 0 \quad,\quad i \;=\; 1,\cdots,n\right\}\,. \tag{4.123}$$

Note that in the context of a finite element analysis, $\dfrac{\partial \mathbf{f}}{\partial \mathbf{u}}(\mathbf{u},\lambda) = \mathbf{K}(\mathbf{u},\lambda)$. Also, condition (a) is implied by condition (b), if it is stated explicitly that $\bar{\boldsymbol{\phi}}_i \neq \mathbf{0}$, that is, if there exists a non-trivial null eigenvector of $\dfrac{\partial \mathbf{f}}{\partial \mathbf{u}}(\bar{\mathbf{u}},\bar{\lambda})$. In addition, condition (c) is implied by condition (b) when $\dfrac{\partial \mathbf{f}}{\partial \mathbf{u}}$ is symmetric. Indeed, in this case note that, for any $\mathbf{x}\in\mathbb{R}^N$,

$$\begin{aligned}\left[\frac{\partial \mathbf{f}}{\partial \mathbf{u}}\left(\bar{\mathbf{u}},\bar{\lambda}\right)\right]\mathbf{x} \;=\; \mathbf{y} \Rightarrow \bar{\boldsymbol{\phi}}_i^T\left[\frac{\partial \mathbf{f}}{\partial \mathbf{u}}\left(\bar{\mathbf{u}},\bar{\lambda}\right)\right]\mathbf{x} \;&=\; \mathbf{x}^T\left[\frac{\partial \mathbf{f}}{\partial \mathbf{u}}\left(\bar{\mathbf{u}},\bar{\lambda}\right)\right]^T\bar{\boldsymbol{\phi}}_i \\ &=\; \mathbf{x}^T\left[\frac{\partial \mathbf{f}}{\partial \mathbf{u}}\left(\bar{\mathbf{u}},\bar{\lambda}\right)\right]\bar{\boldsymbol{\phi}}_i \;=\; \bar{\boldsymbol{\phi}}_i^T\mathbf{y} \;=\; \mathbf{0}\,,\end{aligned} \tag{4.124}$$

where use is made of (4.121) and (4.123).

Now consider (4.119) at $(\bar{\mathbf{u}},\bar{\lambda}) = (\mathbf{u}(\bar{s}),\lambda(\bar{s}))$, in the form

$$\frac{\partial \mathbf{f}}{\partial \mathbf{u}}\left(\bar{\mathbf{u}},\bar{\lambda}\right)\left[\frac{d\mathbf{u}}{ds}\right]_{s=\bar{s}} + \frac{\partial \mathbf{f}}{\partial \lambda}\left(\bar{\mathbf{u}},\bar{\lambda}\right)\left[\frac{d\lambda}{ds}\right]_{s=\bar{s}} \;=\; \mathbf{0} \tag{4.125}$$

and dot this equation with a non-trivial null eigenvector $\bar{\boldsymbol{\phi}}$ of $\dfrac{\partial \mathbf{f}}{\partial \mathbf{u}}(\bar{\mathbf{u}},\bar{\lambda})$ to conclude that

$$\bar{\boldsymbol{\phi}}^T\frac{\partial \mathbf{f}}{\partial \mathbf{u}}\left(\bar{\mathbf{u}},\bar{\lambda}\right)\left[\frac{d\mathbf{u}}{ds}\right]_{s=\bar{s}} + \bar{\boldsymbol{\phi}}^T\frac{\partial \mathbf{f}}{\partial \lambda}\left(\bar{\mathbf{u}},\bar{\lambda}\right)\left[\frac{d\lambda}{ds}\right]_{s=\bar{s}} \;=\; 0\,. \tag{4.126}$$

However, owing to condition (c), the first term on the right-hand side of (4.126) vanishes, therefore

$$\bar{\boldsymbol{\phi}}^T\frac{\partial \mathbf{f}}{\partial \lambda}\left(\bar{\mathbf{u}},\bar{\lambda}\right)\left[\frac{d\lambda}{ds}\right]_{s=\bar{s}} \;=\; 0\,. \tag{4.127}$$

One may now distinguish between two cases in connection with (4.127):

(i) $\bar{\boldsymbol{\phi}}^T\dfrac{\partial \mathbf{f}}{\partial \lambda}\left(\bar{\mathbf{u}},\bar{\lambda}\right) = 0$ (or, equivalently, $\bar{\boldsymbol{\phi}}^T\mathbf{c} = 0$)
In this case, $(\bar{\mathbf{u}},\bar{\lambda})$ is a *bifurcation point*. Note that here it is typically true that $\left[\dfrac{d\lambda}{ds}\right]_{s=\bar{s}} \neq 0$.

(ii) $\bar{\boldsymbol{\phi}}^T\dfrac{\partial \mathbf{f}}{\partial \lambda}\left(\bar{\mathbf{u}},\bar{\lambda}\right) \neq 0$ (or, equivalently, $\bar{\boldsymbol{\phi}}^T\mathbf{c} \neq 0$)
In this case, $\left(\bar{\mathbf{u}},\bar{\lambda}\right)$ is a *limit point*. Note that for (4.127) to hold it is now necessary that $\left[\dfrac{d\lambda}{ds}\right]_{s=\bar{s}} = 0$.

In extraordinary circumstances, it is possible that $\bar{\boldsymbol{\phi}}^T \mathbf{c} = 0$ and $\left[\dfrac{d\lambda}{ds}\right]_{s=\bar{s}} = 0$. Such a stability point is simultaneously a bifurcation and limit point.

In the computational investigation of stability, the key tasks are:

(a) To detect stability points and classify them as limit or bifurcation points,

(b) To develop methods which allow the analyst to follow specific non-linear solution paths past stability points. These are referred to as *continuation methods*.

(c) To develop methods which effect switching from one solution path to another in bifurcation problems. These are referred to as *branch-switching methods*.

Here, attention is focused on continuation methods. The classical approach is to define an extended system of the form

$$\begin{aligned} \bar{\mathbf{f}}(\mathbf{u}) - \lambda \mathbf{c} &= \mathbf{0} \ , \\ g(\mathbf{u}, \lambda) &= 0 \ , \end{aligned} \tag{4.128}$$

where $g : \mathbb{R}^N \times \mathbb{R} \to \mathbb{R}$ is a given continuously differentiable function. The second of the above equations is a global constraint equation which completely characterizes the continuation method.

The extended system may be solved using the classical Newton-Raphson method. Here, a typical iteration is

$$\begin{aligned} \left[\bar{\mathbf{f}}\left(\mathbf{u}^{(k)}\right) - \lambda^{(k)}\mathbf{c}\right] + \mathbf{K}\left(\mathbf{u}^{(k)}\right)\Delta\mathbf{u}^{(k)} - \Delta\lambda^{(k)}\mathbf{c} &= \mathbf{0} \\ g\left(\mathbf{u}^{(k)}, \lambda^{(k)}\right) + \left[\frac{\partial g}{\partial \mathbf{u}}\left(\mathbf{u}^{(k)}, \lambda^{(k)}\right)\right]^T \Delta\mathbf{u}^{(k)} + \left[\frac{\partial g}{\partial \lambda}\left(\mathbf{u}^{(k)}, \lambda^{(k)}\right)\right]\Delta\lambda^{(k)} &= 0 \end{aligned} \tag{4.129}$$

or, put in matrix form,

$$\begin{bmatrix} \mathbf{K}\left(\mathbf{u}^{(k)}\right) & -\mathbf{c} \\ \left[\dfrac{\partial g}{\partial \mathbf{u}}\left(\mathbf{u}^{(k)}, \lambda^{(k)}\right)\right]^T & \dfrac{\partial g}{\partial \lambda}\left(\mathbf{u}^{(k)}, \lambda^{(k)}\right) \end{bmatrix} \begin{bmatrix} \Delta\mathbf{u}^{(k)} \\ \Delta\lambda^{(k)} \end{bmatrix} = - \begin{bmatrix} \bar{\mathbf{f}}\left(\mathbf{u}^{(k)}\right) - \lambda^{(k)}\mathbf{c} \\ g\left(\mathbf{u}^{(k)}, \lambda^{(k)}\right) \end{bmatrix} , \tag{4.130}$$

from where one derives the update relations

$$\mathbf{u}^{(k+1)} = \mathbf{u}^{(k)} + \Delta\mathbf{u}^{(k)} \quad , \quad \lambda^{(k+1)} = \lambda^{(k)} + \Delta\lambda^{(k)} \ . \tag{4.131}$$

A crucial observation here is that the tangent stiffness of the extended system of non-linear equations (4.128) may be non-singular, even when $\mathbf{K}\left(\mathbf{u}^{(k)}\right)$ is singular. At the same time,

this tangent stiffness matrix of the extended system is neither symmetric (even when $\mathbf{K}\left(\mathbf{u}^{(k)}\right)$ is) nor banded.

If both $\mathbf{K}\left(\mathbf{u}^{(k)}\right)$ and the stiffness matric of the extended system are non-singular, then one may solve $(4.130)_1$ for $\Delta\mathbf{u}^{(k)}$ according to

$$\Delta\mathbf{u}^{(k)} \;=\; -\mathbf{K}^{-1}\left(\mathbf{u}^{(k)}\right)\left[\bar{\mathbf{f}}\left(\mathbf{u}^{(k)}\right) - \left(\lambda^{(k)} + \Delta\lambda^{(k)}\right)\mathbf{c}\right] \tag{4.132}$$

and then substitute the above to $(4.130)_2$ to find that

$$-\frac{\partial\mathbf{g}}{\partial\mathbf{u}}\left(\mathbf{u}^{(k)},\lambda^{(k)}\right)\mathbf{K}^{-1}\left(\mathbf{u}^{(k)}\right)\left[\bar{\mathbf{f}}\left(\mathbf{u}^{(k)}\right) - \left(\lambda^{(k)} + \Delta\lambda^{(k)}\right)\mathbf{c}\right] + \frac{\partial\mathbf{g}}{\partial\lambda}\left(\mathbf{u}^{(k)},\lambda^{(k)}\right)\Delta\lambda^{(k)} \;=\; -\mathbf{g}\left(\mathbf{u}^{(k)},\lambda^{(k)}\right)\;. \tag{4.133}$$

Solving (4.133) for $\Delta\lambda^{(k)}$ leads to

$$\Delta\lambda^{(k)} \;=\; -\left[\frac{\partial\mathbf{g}}{\partial\lambda}\left(\mathbf{u}^{(k)},\lambda^{(k)}\right) + \frac{\partial\mathbf{g}}{\partial\mathbf{u}}\left(\mathbf{u}^{(k)},\lambda^{(k)}\right)\mathbf{K}^{-1}\left(\mathbf{u}^{(k)}\right)\mathbf{c}\right]^{-1} \left\{\mathbf{g}\left(\mathbf{u}^{(k)},\lambda^{(k)}\right) - \frac{\partial\mathbf{g}}{\partial\mathbf{u}}\left(\mathbf{u}^{(k)},\lambda^{(k)}\right)\mathbf{K}^{-1}\left[\bar{\mathbf{f}}\left(\mathbf{u}^{(k)}\right) - \lambda^{(k)}\mathbf{c}\right]\right\}\;, \tag{4.134}$$

with $\Delta\mathbf{u}^{(k)}$ subsequently computed by substituting $\Delta\lambda^{(k)}$ from (4.134) in (4.132). This solution procedure is referred to a *bordering algorithm* and the quantity inside the square bracket in (4.134) is known as the *Schur complement* of $\mathbf{K}\left(\mathbf{u}^{(k)}\right)$ in the extended tangent stiffness matrix in (4.130).

It can be shown[8] that the necessary and sufficient conditions for the tangent stiffness matrix of the extended system to be non-singular when $\mathbf{K}\left(\mathbf{u}^{(k)}\right)$ is singular with $\ker\left[\mathbf{K}\left(\mathbf{u}^{(k)}\right)\right] = \boldsymbol{\phi} \neq \mathbf{0}$, that is, when there is a single non-trivial null eigenvector, are

$$\mathbf{c} \;\notin\; \text{range}\left[\mathbf{K}\left(\mathbf{u}^{(k)}\right)\right] \qquad , \qquad \frac{\partial\mathbf{g}}{\partial\mathbf{u}}\left(\mathbf{u}^{(k)},\lambda^{(k)}\right) \;\notin\; \text{range}\left[\mathbf{K}^T\left(\mathbf{u}^{(k)}\right)\right]\;. \tag{4.135}$$

Indeed, in this case

$$\mathbf{K}\left(\mathbf{u}^{(k)}\right)\mathbf{x} \;\neq\; \mathbf{c}\;, \tag{4.136}$$

for any $\mathbf{x} \in \mathbb{R}^N$, therefore if $\boldsymbol{\psi}$ is the null eigenvector of $\mathbf{K}^T$, that is,

$$\mathbf{K}^T\left(\mathbf{u}^{(k)}\right)\boldsymbol{\psi} \;=\; \mathbf{0}\;, \tag{4.137}$$

[8] See Section 4.1.1 in H.B. Keller, Numerical Methods in Bifurcation Problems, Springer-Verlag, Berlin, 1987, and also D.W. Decker and H.B Keller, Multiple limit point bifurcation, *J. Math. Anal. Appl.*, 75:417–430, (1980).

it follows, in view of the arbitrariness of $\mathbf{x}$, that

$$0 \;=\; \boldsymbol{\psi}^T \mathbf{K}\left(\mathbf{u}^{(k)}\right)\mathbf{x} \;\neq\; \boldsymbol{\psi}^T\mathbf{c} \tag{4.138}$$

or

$$\boldsymbol{\psi}^T\mathbf{c} \;\neq\; 0\;, \tag{4.139}$$

as in Figure 4.19.

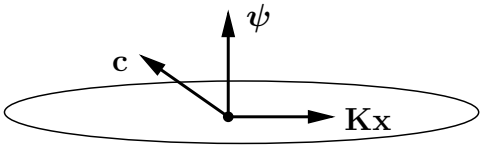

Figure 4.19. Relation between the loading vector $\mathbf{c}$ and the null eigenvector $\boldsymbol{\psi}$ of $\mathbf{K}^T$

Note here that if $\mathbf{K}$ is symmetric (hence, the null eigenvectors $\boldsymbol{\phi}$ of $\mathbf{K}$ and $\boldsymbol{\psi}$ of $\mathbf{K}^T$ coincide), then it follows from the above and the defining property of bifurcations that at a bifurcation point $\left(\bar{\mathbf{u}}, \bar{\lambda}\right)$, there is a $\boldsymbol{\phi} \neq 0$, such that

$$\mathbf{K}\left(\bar{\mathbf{u}}, \bar{\lambda}\right)\bar{\boldsymbol{\phi}} \;=\; \mathbf{0} \quad , \quad \boldsymbol{\phi}^T\mathbf{c} \;\neq\; 0\;. \tag{4.140}$$

Therefore, if $\mathbf{K}$ is symmetric, then the extended system is singular at *any* bifurcation point.

Returning to the original condition $(4.135)_2$, note that

$$\mathbf{K}^T\left(\mathbf{u}^{(k)}\right)\mathbf{y} \;\neq\; \frac{\partial \mathbf{g}}{\partial \mathbf{u}}\left(\mathbf{u}^{(k)}, \lambda^{(k)}\right)\;, \tag{4.141}$$

for any $\mathbf{y} \in \mathbb{R}^N$. Therefore, given the null eigenvector $\boldsymbol{\phi}$ of $\mathbf{K}\left(\mathbf{u}^{(k)}\right)$, it follows as earlier from the arbitrariness of $\mathbf{y}$ that

$$0 \;=\; \boldsymbol{\phi}^T\mathbf{K}^T\left(\mathbf{u}^{(k)}\right)\mathbf{y} \;\neq\; \boldsymbol{\phi}^T\frac{\partial \mathbf{g}}{\partial \mathbf{u}}\left(\mathbf{u}^{(k)}, \lambda^{(k)}\right) \tag{4.142}$$

or

$$\boldsymbol{\phi}^T\frac{\partial \mathbf{g}}{\partial \mathbf{u}}\left(\mathbf{u}^{(k)}, \lambda^{(k)}\right) \;\neq\; 0\;. \tag{4.143}$$

Now, return to the extended system (4.130) and pre-multiply the first set of equations with $\boldsymbol{\psi}^T$ to get

$$\boldsymbol{\psi}^T\mathbf{K}\left(\mathbf{u}^{(k)}\right)\Delta\mathbf{u}^{(k)} - \boldsymbol{\psi}^T\mathbf{c}\Delta\lambda^{(k)} \;=\; -\boldsymbol{\psi}^T\left[\bar{\mathbf{f}}\left(\mathbf{u}^{(k)}\right) - \lambda^{(k)}\mathbf{c}\right]\;, \tag{4.144}$$

so that, in light of (4.137) and (4.139), one may deduce that

$$\Delta\lambda^{(k)} \;=\; \frac{\boldsymbol{\psi}^T\left[\bar{\mathbf{f}}\left(\mathbf{u}^{(k)}\right)-\lambda^{(k)}\mathbf{c}\right]}{\boldsymbol{\psi}^T\mathbf{c}}\;. \tag{4.145}$$

This implies that $(4.130)_2$ takes the form

$$\mathbf{K}\left(\mathbf{u}^{(k)}\right)\Delta\mathbf{u}^{(k)} \;=\; -\left[\bar{\mathbf{f}}\left(\mathbf{u}^{(k)}\right)-\lambda^{(k)}\mathbf{c}\right]+\frac{\boldsymbol{\psi}^T\left[\bar{\mathbf{f}}\left(\mathbf{u}^{(k)}\right)-\lambda^{(k)}\mathbf{c}\right]}{\boldsymbol{\psi}^T\mathbf{c}}\,\mathbf{c}\;. \tag{4.146}$$

Since $\mathbf{K}\left(\mathbf{u}^{(k)}\right)$ is singular, one may stipulate that the (unique) solution $\Delta\mathbf{u}^{(k)}$ of the above system is of the form

$$\Delta\mathbf{u}^{(k)} \;=\; \Delta\mathbf{u}_p^{(k)}+z^{(k)}\boldsymbol{\phi}\;, \tag{4.147}$$

where $\Delta\mathbf{u}_p^{(k)}$ is a particular solution obtained by fixing one of the degrees of freedom and solving for the rest, and $z^{(k)}$ is a scalar to be determined. Substituting (4.147) to $(4.130)_2$, one gets

$$\left[\frac{\partial\mathbf{g}}{\partial\mathbf{u}}\left(\mathbf{u}^{(k)},\lambda^{(k)}\right)\right]^T\left(\Delta\mathbf{u}_p^{(k)}+\mathbf{z}^{(k)}\boldsymbol{\phi}\right)+\frac{\partial\mathbf{g}}{\partial\lambda}\left(\mathbf{u}^{(k)},\lambda^{(k)}\right)\Delta\lambda^{(k)} \;=\; -g\left(\mathbf{u}^{(k)},\lambda^{(k)}\right)\;, \tag{4.148}$$

from where $z^{(k)}$ is determined in light of (4.143). Thus, the exact solution $\left(\Delta\mathbf{u}^{(k)},\Delta\lambda^{(k)}\right)$ is obtained as a function of $\boldsymbol{\phi}$, $\boldsymbol{\psi}$ and $\Delta\mathbf{u}_p^{(k)}$. These arrays can be computed without a substantially higher effort than required for the original bordering algorithm.

Finally, when $\ker\left[\mathbf{K}\left(\mathbf{u}^{(k)},\lambda^{(k)}\right)\right]=\sum_{i=1}^{n}\alpha_i\bar{\phi}_i$, $n>1$, that is, when the tangent stiffness matrix of the original system possesses more than one non-trivial null eigenvectors, then it can be shown that the tangent stiffness matrix of the extended system is always singular.

Next, several choices for the constraint function $g(\mathbf{u},\lambda)$ are reviewed in detail.

4.4.1 Force control

Here, the constraint function takes the form

$$g(\mathbf{u},\lambda) \;=\; \lambda-\tilde{\lambda}\;, \tag{4.149}$$

where $\tilde{\lambda}$ is a specified positive scalar, see Figure 4.20.

In this case, the extended system becomes

$$\begin{bmatrix}\mathbf{K}\left(\mathbf{u}^{(k)}\right) & -\mathbf{c}\\ \mathbf{0}^T & 1\end{bmatrix}\begin{bmatrix}\Delta\mathbf{u}^{(k)}\\ \Delta\lambda^{(i)}\end{bmatrix} \;=\; -\begin{bmatrix}\bar{\mathbf{f}}\left(\mathbf{u}^{(k)}\right)-\lambda^{(k)}\mathbf{c}\\ \lambda^{(k)}-\tilde{\lambda}\end{bmatrix} \tag{4.150}$$

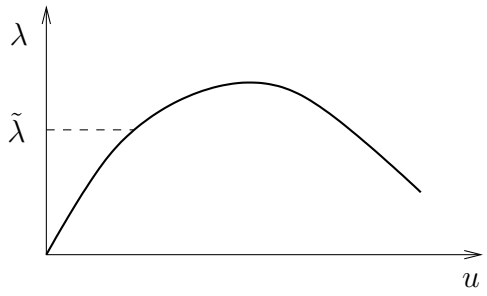

Figure 4.20. Force control in (u, λ)-space

It follows from the above that

$$\mathbf{K}\left(\mathbf{u}^{(k)}\right)\Delta\mathbf{u}^{(k)} \;=\; -\left[\bar{\mathbf{f}}\left(\mathbf{u}^{(k)}\right) - \tilde{\lambda}\mathbf{c}\right] \;. \tag{4.151}$$

Clearly, force control fails when $\mathbf{K}\left(\mathbf{u}^{(i)}\right)$ becomes singular. This is consistent with $(4.135)_2$, whose violation implies that $\mathbf{0}^T \in \text{range}\left[\mathbf{K}^T\left(\mathbf{u}^{(i)}\right)\right]$, see Figure 4.21.

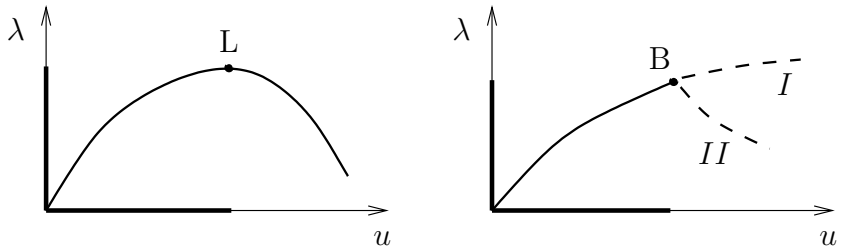

Figure 4.21. Range of validity of force control in (u, λ)-space

Force control is easily implemented by updating $\lambda = \tilde{\lambda}(s)$ at the end of each time step.

4.4.2 Displacement control

Here, the constraint function is defined as

$$g(\mathbf{u}, \lambda) \;=\; \mathbf{e}_l^T\mathbf{u} - \tilde{u}_l \;, \tag{4.152}$$

where $\tilde{u}_l$ is a specified scalar and $\mathbf{e}_l$ is an N-dimensional column vector given by

$$[\mathbf{e}_l] \;=\; [0\ldots 0\ldots \underbrace{1}_{l-\text{th entry}} \ldots 0]^T \;, \tag{4.153}$$

see Figure 4.22. Essentially, the motion of the body is externally constrained by (4.152)

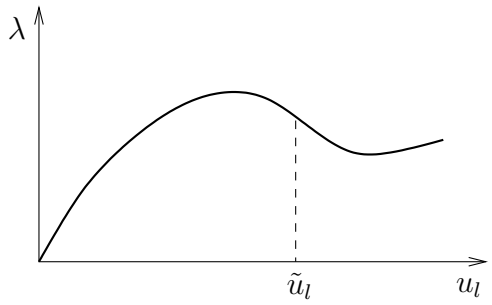

Figure 4.22. Displacement control in (u_l, λ)-space

so that the extended system be non-singular and the equilibrium path is traced for the prescribed displacement u_l.

Under displacement control the extended system (4.130) becomes

$$\begin{bmatrix} \mathbf{K}\left(\mathbf{u}^{(k)}\right) & -\mathbf{c} \\ \mathbf{e}_l^T & 0 \end{bmatrix} \begin{bmatrix} \Delta\mathbf{u}^{(k)} \\ \Delta\lambda^{(k)} \end{bmatrix} = - \begin{bmatrix} \bar{\mathbf{f}}\left(\mathbf{u}^{(k)}\right) - \lambda^{(k)}\mathbf{c} \\ \mathbf{e}_l^T\mathbf{u}^{(k)} - \tilde{u}_l \end{bmatrix} \tag{4.154}$$

It follows from $(4.135)_2$ that displacement control fails if there is a vector $\mathbf{x} \in \mathbb{R}^N$, such that $\mathbf{K}\left(\mathbf{u}^{(k)}\right)\mathbf{x} = \mathbf{e}_l$, in which case displacement control along $\mathbf{e}_l$ is unable to remove the singularity of the extended system, see Figure 4.23.

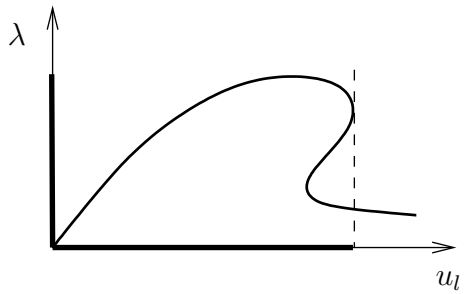

Figure 4.23. Range of validity of displacement control in (u_l, λ)-space

The implementation of displacement control in finite element codes is trivial, since it merely amounts to imposing displacement boundary conditions, as routinely done for Dirichlet boundary conditions.

More generally, one may impose a set of M constraints of the form

$$g_m(\mathbf{u}, \lambda) = \mathbf{e}_m^T(\mathbf{u}) - \tilde{u}_m \quad , \quad m = 1, 2, \ldots, M \ , \tag{4.155}$$

where $M < N$. This would lead to an extended system with $N + M$ equations and M load vectors λ_m along directions $\mathbf{c}_m$.

4.4.3 Arc-length control

The idea of arc-length methods is impose a constraint to the arc-length s of the equilibrium path, defined as

$$s \;=\; \int ds \;=\; \int \sqrt{d\mathbf{u}^T d\mathbf{u} + \tau^2 d\lambda^2}\;, \tag{4.156}$$

where τ is a scaling parameter that effects consistency of units in (4.156), see Figure 4.24.

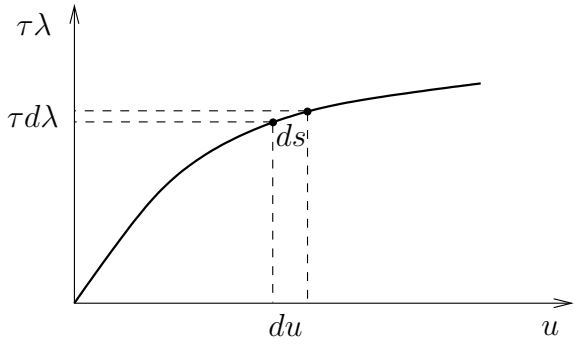

Figure 4.24. Arc-length in $(u, \tau\lambda)$-space

Arc-length methods fix an $s = s_0$ at a given solution point $(\mathbf{u}_n, \tau\lambda_n)$, and seek to determine a new equilibrium point under this constraint. Various arc-length methods are possible by means of different approximations to the actual arc-length of the solution curve (since the latter is not known in advance).

In the *spherical arc-length* method around the solution point $(\mathbf{u}_n, \tau\lambda_n)$, the constraint function takes the form

$$g(\mathbf{u}, \lambda) \;=\; (\mathbf{u} - \mathbf{u}_n)^T(\mathbf{u} - \mathbf{u}_n) + \tau^2(\lambda - \lambda_n)^2 - s_0^2\;, \tag{4.157}$$

see Figure 4.25.

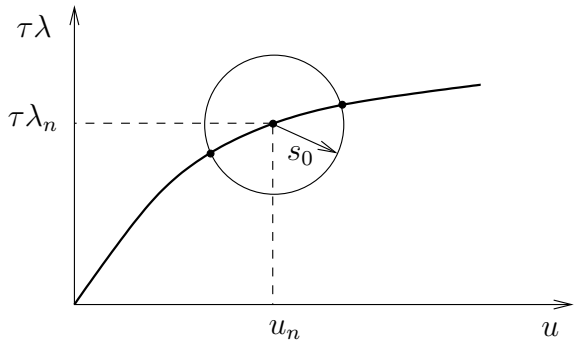

Figure 4.25. Spherical arc-length in $(u, \tau\lambda)$-space

A simplified version of the spherical arc-length method is obtained by linearizing the constraint function along the tangent $[\mathbf{t}_n]$ to the solution path at $(\mathbf{u}_n, \tau\lambda_n)$, where

$$[\mathbf{t}_n] \;=\; \begin{bmatrix} \mathbf{u}_{nt} - \mathbf{u}_n \\ \tau(\lambda_{nt} - \lambda_n) \end{bmatrix}, \tag{4.158}$$

with magnitude s_0, hence,

$$(\mathbf{u}_{nt} - \mathbf{u}_n)^T(\mathbf{u}_{nt} - \mathbf{u}_n) + \tau^2(\lambda_{nt} - \lambda_n)^2 \;=\; s_0^2 \;, \tag{4.159}$$

see Figure 4.26. If follows that the constraint function at $(\mathbf{u}_n, \tau\lambda_n)$ becomes

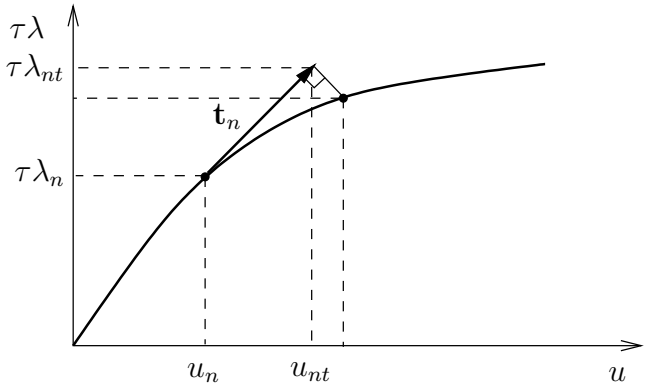

Figure 4.26. Normal-plane arc-length in $(u, \tau\lambda)$-space

$$g(\mathbf{u}, \lambda) \;=\; (\mathbf{u}_{nt} - \mathbf{u}_n)^T(\mathbf{u} - \mathbf{u}_n) + \tau^2(\lambda_{nt} - \lambda_n)(\lambda - \lambda_n) - s_0^2 \;. \tag{4.160}$$

In view of (4.159), one may also write

$$\begin{aligned} g(\mathbf{u}, \lambda) \;&=\; (\mathbf{u}_{nt} - \mathbf{u}_n)^T(\mathbf{u} - \mathbf{u}_n) + \tau^2(\lambda_{nt} - \lambda_n)(\lambda - \lambda_n) \\ &\quad - (\mathbf{u}_{nt} - \mathbf{u}_n)^T(\mathbf{u}_{nt} - \mathbf{u}_n) + \tau^2(\lambda_{nt} - \lambda_n)(\lambda_{nt} - \lambda_n) \\ &=\; (\mathbf{u}_{nt} - \mathbf{u}_n)^T(\mathbf{u} - \mathbf{u}_{nt}) + \tau^2(\lambda_{nt} - \lambda_n)(\lambda - \lambda_{nt}) \;, \end{aligned} \tag{4.161}$$

so that $g(\mathbf{u}, \lambda) = 0$ implies that $[\mathbf{t}_n]$ is orthogonal to $\begin{bmatrix} \mathbf{u} - \mathbf{u}_{nt} \\ \tau(\lambda - \lambda_{nt}) \end{bmatrix}$, see Figure 4.26. Owing to this property, the preceding method is referred to as the *normal-plane arc-length* method. Given (4.160), the extended system now takes the form

$$\begin{bmatrix} \mathbf{K}\left(\mathbf{u}^{(k)}\right) & -\mathbf{c} \\ (\mathbf{u}_{nt} - \mathbf{u}_n)^T & \tau^2(\lambda_{nt} - \lambda_n) \end{bmatrix} \begin{bmatrix} \Delta\mathbf{u}^{(k)} \\ \Delta\lambda^{(k)} \end{bmatrix} \;=\; -\begin{bmatrix} \bar{\mathbf{f}}\left(\mathbf{u}^{(k)}\right) - \lambda^{(k)}\mathbf{c} \\ g(\mathbf{u}^{(k)}, \lambda^{(k)}) \end{bmatrix} \;. \tag{4.162}$$

Its main advantage over its spherical arc-length counterpart is that all extra terms in the extended stiffness matrix are constant.

The implementation of normal-plane arc-length in connection with the Newton-Raphson method is summarized in Algorithm 6 below, following the so-called *Riks-Wempner method*[9]

Algorithm 6: *Riks-Wempner method*

Data: state at time t_n, s_0

Solve $\mathbf{K}(\mathbf{u}_n)\Delta\mathbf{u}_n^* = \Delta\lambda_n^*\mathbf{c}$

for any $\Delta\lambda_n^* > 0$ (ascending part of curve) or $\Delta\lambda_n^* < 0$ (descending part of curve);

Use (4.158) to write $[\mathbf{t}_n^*] = \begin{bmatrix} \Delta\mathbf{u}_n^* \\ \tau\Delta\lambda_n^* \end{bmatrix}$;

Compute $[\mathbf{t}_n] = \alpha^*[\mathbf{t}_n^*]$, where α^* enforces (4.159);

Solve (4.162) using the Newton-Raphson method;

Note that the preceding algorithm requires that $\mathbf{K}(\mathbf{u}_n)$ be non-singular and also that the extended system in (4.159) be non-singular during the Newton-Raphson iterations. As already argued, the latter is possible even when tracing bifurcation points, as long as the continuation method does not "hit" the singularity at one the iterations.

A simple brute-force computational method for detecting and classifying stability points with the aid of arc-length continuation is described in Algorithm 8 below.

[9] E. Riks, The application of Newton's method to the problem of elastic stability. *ASME J. Appl. Mech.*, 39:1060–1065, (1972).

Algorithm 7: *A method for detecting and classifying stability points*

Data: state at time t_n, s_0, tol, $tolk$, $tolp$, $maxit$
Form $\mathbf{K}(\mathbf{u}_n)$;
Perform an LU decomposition on $\mathbf{K}(\mathbf{u}_n)$ and store the signs of the diagonal terms in U;
while $k \leq maxit$
  Use arc-length with $s = s_0$ to advance solution to $(\mathbf{u}_{n+1}, \lambda_{n+1})$;
  Perform an LU decomposition on $\mathbf{K}(\mathbf{u}_{n+1})$ and store the signs of the diagonal terms in U;
  if no change in the signs of the diagonal terms of U from n to $n+1$ **then**
    return $(\mathbf{u}_{n+1}, \lambda_{n+1})$ and advance time (no stability points detected);
  else if change to exactly one diagonal term of U from n to $n+1$ **then**
    Use bisection to bracket stability point until $\bar{\mathbf{u}}$ such that $|\det \mathbf{K}(\bar{\mathbf{u}})| \doteq tolk$
    Use subspace iteration to find the null eigenvector $\bar{\boldsymbol{\phi}}$ of $\mathbf{K}(\bar{\mathbf{u}})$
    if $\left|\bar{\boldsymbol{\phi}}^T \mathbf{c}\right| \geq tolp$ **then**
      $(\bar{\mathbf{u}}, \bar{\lambda})$ is a limit point
    else
      $(\bar{\mathbf{u}}, \bar{\lambda})$ is a bifurcation point
    end
  else
    Set $k \leftarrow k+1$, $s_0 \leftarrow s_0/2$ and repeat
  end
end

Note, in connection to the preceding algorithm, that the LU decomposition of a square matrix such as $\mathbf{K}$ is unique as long as the matrix is non-singular.

There exist alternative procedures for the determination of stability points, which are not discussed here.

4.5 Computational Treatment of Constraints

The motion of a continuum is often subject to constraints. Typical examples of such constraints are noted below.

Example 4.5.1: Incompressibility
Certain rubber-like solid materials are practically incompressible, that is their deformation is always

volume-preserving. In light of (1.10), this implies that their motion is subject to the constraint

$$\det \mathbf{F} \;=\; 1 \;, \tag{4.163}$$

or, equivalently in terms of the principal stretches in (1.30),

$$\lambda_1 \lambda_2 \lambda_3 \;=\; 1 \;. \tag{4.164}$$

Many fluids (especially, liquids) are also practically incompressible. In this case, taking into consideration (1.52), it is readily concluded that an incompressible fluid is subject to the constraint

$$\operatorname{tr} \mathbf{L} \;=\; \operatorname{div} \mathbf{v} \;=\; 0 \;. \tag{4.165}$$

Example 4.5.2: Inextensibility along a given direction

Some solids are reinforced by inextensible rod-like structures along a given direction, say $\mathbf{M}$, in the reference configuration. In this case, no stretching is permitted along $\mathbf{M}$, which leads to the constraint

$$\lambda_M^2 \;=\; \mathbf{M} \cdot \mathbf{C}\mathbf{M} \;=\; 1 \;. \tag{4.166}$$

Example 4.5.3: Impenetrability of matter

According to this fundamental postulate, two material points may not occupy the same position in space at the same time. In the context of a deformable solid coming to contact with a rigid foundation, as in Figure 4.27, the *gap (penetration) function* g, defined as

$$g \;=\; (\mathbf{x}_f - \mathbf{x}) \cdot \mathbf{n} \tag{4.167}$$

must satisfy the constraint condition

$$g \;\geq\; 0 \;. \tag{4.168}$$

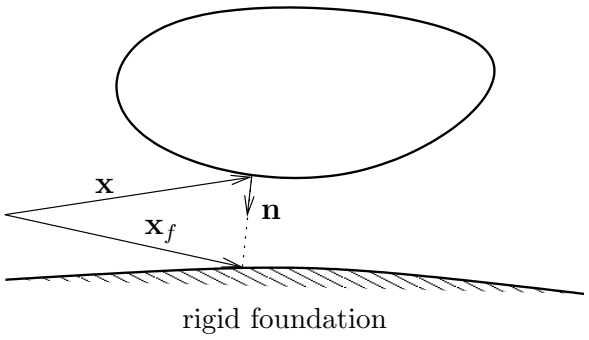

Figure 4.27. *Contact of deformable solid with rigid foundation*

Constraints are classified in various ways. Here, attention is placed on the distinction between:

(a) *equality (bilateral) and inequality (unilateral) constraints*

Equality (resp. inequality) constraints are mathematically expressed by equalities (resp. inequalities). For instance, incompressibility is an equality constraint, while impenetrability is an inequality constraint.

(b) *internal and external constraints*

Internal constraints are expressed in terms of measures of deformation (or rate of deformation), while external constraints cannot. For instance, in view of (4.163), (4.165) and (4.168), incompressibility is an internal constraint, while impenetrability is an external constraint.

(c) *rheonomous and scleronomous constraints*

Rheonomous constraints depend explicitly on time, while scleronomous constraints do not. For instance, all time-dependent (resp. time-independent) Dirichlet boundary conditions may be thought of as rheonomous (resp. scleronomous) constraints.

Consider a bilateral scleronomous constraint written for a solid in the form

$$\mathbf{c}\left(\mathbf{u}(\mathbf{X},t)\right) \;=\; \mathbf{0} \tag{4.169}$$

and assumed to apply on a part $\mathcal{C}_0$ of either the domain $\mathcal{R}_0$ or the external boundary $\partial\mathcal{R}_0$. While the constraint is expressed in (4.169) in terms of the displacement field, it may be thought of as either internal or external.

When the motion of the solid is subject to (4.169), the space of constraint admissible displacements becomes

$$\mathcal{U}_c \;=\; \left\{\mathbf{u} : \mathcal{R}_0 \times \mathbb{R} \to \mathbb{R}^3 \quad | \quad \mathbf{u}\left(\mathbf{X},t\right) \;=\; \bar{\mathbf{u}}\left(\mathbf{X},t\right) \text{ on } \Gamma_u \;,\; \mathbf{c}(\mathbf{u}) \;=\; \mathbf{0} \text{ on } \mathcal{C}_0 \times \mathbb{R}\right\} \;. \tag{4.170}$$

In the context of finite element approximations, one may choose to construct subsets $\mathcal{U}_{ch}$ of $\mathcal{U}_c$, and satisfy (weakly) the balance laws over $\mathcal{U}_{ch}$. Such a so-called *primal method* may be impractical if the constraint condition is difficult to enforce by the choice of admissible displacements.

An alternative, so called *dual method* retains the original space of admissible functions $\mathcal{U}$ and introduces a new Lagrange multiplier field. To this end, recall that the constraint (4.169) is imposed on kinematic variables and rewrite the linear momentum balance equations (3.42)

as

$$\int_{\mathcal{R}_0} \boldsymbol{\xi}\cdot\rho_0\mathbf{a}\,dV+\int_{\mathcal{R}_0}\frac{\partial\boldsymbol{\xi}}{\partial\mathbf{X}}\cdot\mathbf{P}\,dV \;=\; \int_{\mathcal{R}_0}\boldsymbol{\xi}\cdot\rho_0\mathbf{b}\,dV+\int_{\Gamma_{q_0}}\boldsymbol{\xi}\cdot\bar{\mathbf{p}}\,dA-\int_{\mathcal{C}_0}D\mathbf{c}(\mathbf{u},\boldsymbol{\xi})\cdot\boldsymbol{\Lambda}\,dV\;, \tag{4.171}$$

where $\boldsymbol{\Lambda} = \boldsymbol{\Lambda}(\mathbf{X},t)$ is a Lagrange multiplier field on $C_0\times\mathbb{R}$. Note that the term in (4.171) associated with the constraint could be a surface rather than a volume integral. Also note that, since $\mathbf{c}(\mathbf{u})=\mathbf{0}$ for all admissible displacement fields, then

$$D\mathbf{c}(\mathbf{u},\boldsymbol{\xi}) \;=\; \mathbf{0}\;, \tag{4.172}$$

and the Lagrange multiplier field $\boldsymbol{\Lambda}$ which enforces the constraint is workless, in the sense that

$$\int_{\mathcal{C}_0} D\mathbf{c}(\mathbf{u},\boldsymbol{\xi})\cdot\boldsymbol{\Lambda}\,dV \;=\; 0\;. \tag{4.173}$$

The preceding observation does not generally hold for rheonomous constraints.

Example 4.5.4: Incompressibility in dual methods

Taking into account (2.60) and (4.163), the constraint integral term in (4.173) becomes

$$\int_{\mathcal{R}_0} D\mathbf{c}(\mathbf{u},\boldsymbol{\xi})\cdot\boldsymbol{\Lambda}\,dV \;=\; \int_{\mathcal{R}_0} J\frac{\partial\hat{\boldsymbol{\xi}}}{\partial\mathbf{X}}\cdot\mathbf{F}^{-T}\Lambda\,dV\;. \tag{4.174}$$

One may now combine this term with the stress-divergence term in (4.171) to conclude that

$$\int_{\mathcal{R}_0}\frac{\partial\boldsymbol{\xi}}{\partial\mathbf{X}}\cdot\mathbf{P}\,dV+\int_{\mathcal{R}_0}J\frac{\partial\boldsymbol{\xi}}{\partial\mathbf{X}}\cdot\mathbf{F}^{-T}\Lambda\,dV \;=\; \int_{\mathcal{R}_0}\frac{\partial\boldsymbol{\xi}}{\partial\mathbf{X}}\cdot(\mathbf{P}+\Lambda\mathbf{F}^{-T})\,dV \tag{4.175}$$

$$=\int_{\mathcal{R}}\frac{\partial\boldsymbol{\xi}}{\partial\mathbf{x}}\cdot(\mathbf{T}+\Lambda\mathbf{i})\,dv\;, \tag{4.176}$$

where use is made of (1.73) and the chain rule. The preceding relation shows that the scalar Lagrange multiplier field Λ may be interpreted as a pressure. Ideally, the Cauchy stress $\mathbf{T}$ should be decomposed to a pressure-independent part (which remains constitutively specified) and a pressure part, which coincides with the Lagrange multiplier Λ.

A similar analysis applies to incompressibility in fluids, where, according to (4.165),

$$\int_{\mathcal{R}} D\mathbf{c}(\mathbf{v},\boldsymbol{\xi})\cdot\boldsymbol{\Lambda}\,dv \;=\; \int_{\mathcal{R}}\operatorname{tr}\left(\frac{\partial\boldsymbol{\xi}}{\partial\mathbf{x}}\right)\Lambda\,dv \;=\; \int_{\mathcal{R}}\frac{\partial\boldsymbol{\xi}}{\partial\mathbf{x}}\cdot\Lambda\mathbf{i}\,dv\;. \tag{4.177}$$

Example 4.5.5: Tied sliding in dual methods

Consider a special case of the impenetrability constraint in which a given part $\mathcal{C}$ is a deformable body's boundary is in persistent contact with a rigid foundation, but is allowed to slide on it. This is the case of *tied sliding*. Now, the constraint condition (4.168) is imposed as an equality. Hence, in light of (4.167), the constraint integral term in (4.173) becomes

$$\int_{\mathcal{C}_0} D\mathbf{c}(\mathbf{u},\boldsymbol{\xi})\cdot\boldsymbol{\Lambda}\,dA \;=\; \int_{\mathcal{C}_0}\boldsymbol{\xi}\cdot\Lambda\mathbf{n}\,dA\;, \tag{4.178}$$

therefore the scalar Lagrange multiplier field may be interpreted as the magnitude of the normal traction (pressure) necessary to resist penetration or separation of the two bodies.

The extended equations of motion now read

$$\int_{\mathcal{R}_0} \boldsymbol{\xi} \cdot \rho_0 \mathbf{a}\, dV + \int_{\mathcal{R}_0} \frac{\partial \boldsymbol{\xi}}{\partial \mathbf{X}} \cdot \mathbf{P}\, dV - \int_{\mathcal{R}_0} \boldsymbol{\xi} \cdot \rho_0 \mathbf{b}\, dV - \int_{\Gamma_{q0}} \boldsymbol{\xi} \cdot \bar{\mathbf{p}}\, dA + \int_{\mathcal{C}_0} D\mathbf{c}(\mathbf{u}, \boldsymbol{\xi}) \cdot \boldsymbol{\Lambda}\, dV \;=\; 0 \;, \tag{4.179}$$

$$\int_{\mathcal{C}_0} \boldsymbol{\theta} \cdot \mathbf{c}(\mathbf{u}) dV \;=\; 0 \;, \tag{4.180}$$

where $\boldsymbol{\theta} = \boldsymbol{\theta}(\mathbf{X}, t)$ is an arbitrary weight field on $\mathcal{C}_0 \times \mathbb{R}$.

In discrete form, one may write

$$\begin{aligned} \int_{\mathcal{C}_0} D\mathbf{c}(\mathbf{u}, \boldsymbol{\xi}) \cdot \boldsymbol{\Lambda}\, dV \;&\doteq\; \hat{\boldsymbol{\xi}}^T \mathbf{d}(\hat{\mathbf{u}}) \hat{\boldsymbol{\Lambda}} \;, \\ \int_{\mathcal{C}_0} \boldsymbol{\theta} \cdot \mathbf{c}(\mathbf{u})\, dV \;&\doteq\; \hat{\boldsymbol{\theta}}^T \mathbf{g}(\hat{\mathbf{u}}) \;, \end{aligned} \tag{4.181}$$

where $\hat{\mathbf{u}}, \hat{\boldsymbol{\xi}} \in \mathbb{R}^N$ and where $\hat{\boldsymbol{\Lambda}}, \hat{\boldsymbol{\theta}} \in \mathbb{R}^M$ with $N > M$, consequently $\mathbf{d} : \mathbb{R}^N \mapsto \mathbb{R}^N \times \mathbb{R}^M$ and $\mathbf{g} : \mathbb{R}^N \mapsto \mathbb{R}^M$. Taking into account (4.181), one may write

$$\begin{aligned} \int_{\mathcal{C}_0} \boldsymbol{\theta} \cdot D\mathbf{c}(\mathbf{u}, \boldsymbol{\xi})\, dV \;\doteq\; \hat{\boldsymbol{\theta}}^T D\mathbf{g}(\hat{\mathbf{u}}) \hat{\boldsymbol{\xi}} \;&=\; \hat{\boldsymbol{\xi}}^T D^T \mathbf{g}(\hat{\mathbf{u}}) \hat{\boldsymbol{\theta}} \\ &=\; \hat{\boldsymbol{\xi}}^T \mathbf{d}(\hat{\mathbf{u}}) \hat{\boldsymbol{\theta}}^T \;, \end{aligned} \tag{4.182}$$

therefore

$$\mathbf{d}(\hat{\mathbf{u}}) \;=\; D^T \mathbf{g}(\hat{\mathbf{u}}) \;. \tag{4.183}$$

Given (4.179), (4.180), and (4.181), the discrete equations of motion become

$$\begin{aligned} \hat{\boldsymbol{\xi}}^T \left[\mathbf{f}(\hat{\mathbf{u}}) + \mathbf{d}(\hat{\mathbf{u}}) \hat{\boldsymbol{\Lambda}} \right] \;&=\; 0 \;, \\ \hat{\boldsymbol{\theta}}^T \mathbf{g}(\hat{\mathbf{u}}) \;&=\; 0 \;, \end{aligned} \tag{4.184}$$

or, after accounting for the arbitrariness of $\hat{\boldsymbol{\xi}}$ and $\hat{\boldsymbol{\theta}}$,

$$\begin{aligned} \mathbf{f}(\hat{\mathbf{u}}) + \mathbf{d}(\hat{\mathbf{u}}) \hat{\boldsymbol{\Lambda}} \;&=\; \mathbf{0} \;, \\ \mathbf{g}(\hat{\mathbf{u}}) \;&=\; \mathbf{0} \;. \end{aligned} \tag{4.185}$$

Note that in the dual method, the original N equations for the unconstrained problem with $\hat{\mathbf{u}}$ as unknowns are replaced by $N+M$ equations for the constrained problem with $\hat{\mathbf{u}}$ and $\hat{\mathbf{\Lambda}}$ as unknowns.

To use the Newton-Raphson method in (4.185), write

$$\begin{aligned}\mathbf{f}\left(\hat{\mathbf{u}}^{(k)}\right)+\mathbf{K}\left(\hat{\mathbf{u}}^{(k)}\right)\Delta\hat{\mathbf{u}}^{(k)}+\mathbf{d}\left(\hat{\mathbf{u}}^{(k)}\right)\hat{\mathbf{\Lambda}}^{(k)}+D^T\mathbf{d}\left(\hat{\mathbf{u}}^{(k)}\right)\hat{\mathbf{\Lambda}}^{(k)}\Delta\hat{\mathbf{u}}^{(k)}+\mathbf{d}\left(\hat{\mathbf{u}}^{(k)}\right)\Delta\hat{\mathbf{\Lambda}}^{(k)} &= \mathbf{0}\\ \mathbf{g}\left(\hat{\mathbf{u}}^{(k)}\right)+D\mathbf{g}\left(\hat{\mathbf{u}}^{(k)}\right)\Delta\hat{\mathbf{u}}^{(k)} &= \mathbf{0}\end{aligned} \tag{4.186}$$

where, as usual,

$$\begin{aligned}\mathbf{f}\left(\hat{\mathbf{u}}^{(k)}+\Delta\hat{\mathbf{u}}^{(k)}\right) &\doteq \mathbf{f}\left(\hat{\mathbf{u}}^{(k)}\right)+\mathbf{K}\left(\hat{\mathbf{u}}^{(k)}\right)\Delta\hat{\mathbf{u}}^{(k)}\ ,\\ D\left[\int_{C_0}D\mathbf{c}(\mathbf{u},\boldsymbol{\xi})\cdot\mathbf{\Lambda}^{(k)}\,dV\right]\left(\mathbf{u}^{(k)},\Delta\mathbf{u}^{(k)}\right) &\doteq \hat{\boldsymbol{\xi}}^T D^T\mathbf{d}\left(\hat{\mathbf{u}}^{(k)}\right)\hat{\mathbf{\Lambda}}^{(k)}\Delta\hat{\mathbf{u}}^{(k)}\end{aligned} \tag{4.187}$$

and also, upon recalling (4.183),

$$\begin{aligned}D\left[\int_{C_0}\boldsymbol{\theta}\cdot\mathbf{c}(\mathbf{u})dV\right]\left(\mathbf{u}^{(k)},\Delta\mathbf{u}^{(k)}\right) &\doteq \hat{\boldsymbol{\theta}}^T D\mathbf{g}(\hat{\mathbf{u}}^{(k)})\hat{\mathbf{\Lambda}}^{(k)}\Delta\hat{\mathbf{u}}^{(k)}\\ &\doteq \Delta\mathbf{u}^{(k)\ T}\mathbf{d}\left(\hat{\mathbf{u}}^{(k)}\right)\hat{\boldsymbol{\theta}} = \hat{\boldsymbol{\theta}}^T\mathbf{d}^T\left(\hat{\mathbf{u}}^{(k)}\right)\Delta\mathbf{u}^{(k)}\ .\end{aligned} \tag{4.188}$$

The linearized system of equations (4.186) may be put in bordered matrix form as

$$\begin{bmatrix}\mathbf{K}\left(\hat{\mathbf{u}}^{(k)}\right)+D^T\mathbf{d}\left(\hat{\mathbf{u}}^{(k)}\right)\hat{\mathbf{\Lambda}}^{(k)} & \mathbf{d}\left(\hat{\mathbf{u}}^{(k)}\right)\\ \mathbf{d}^T\left(\hat{\mathbf{u}}^{(k)}\right) & \mathbf{0}\end{bmatrix}\begin{bmatrix}\Delta\hat{\mathbf{u}}^{(k)}\\ \Delta\hat{\mathbf{\Lambda}}^{(k)}\end{bmatrix} = -\begin{bmatrix}\mathbf{f}\left(\hat{\mathbf{u}}^{(k)}\right)+\mathbf{d}\left(\hat{\mathbf{u}}^{(k)}\right)\hat{\mathbf{\Lambda}}^{(k)}\\ \mathbf{g}\left(\hat{\mathbf{u}}^{(k)}\right)\end{bmatrix}\ . \tag{4.189}$$

The extended tangent stiffness matrix in (4.189)above is symmetric provided both $\mathbf{K}\left(\hat{\mathbf{u}}^{(k)}\right)$ and $D^T\mathbf{d}\left(\hat{\mathbf{u}}^{(k)}\right)\hat{\mathbf{\Lambda}}^{(k)}$ are symmetric. However, this stiffness matrix is not banded. In fact, given its structure, a special equation solver is required to take care of zero diagonals, as the classical Gauss elimination procedure without pivoting would generally fail.

Dual methods enable the use of the original (unconstrained) space of admissible displacements $\mathcal{U}$ and its finite element subspaces $\mathcal{U}_h$, which is convenient. The price for this convenience is in the need to solve an extended system of equations, including the Lagrange multipliers $\mathbf{\Lambda}\in\mathcal{L}$, where $\mathcal{L}$ is the space of admissible multiplier fields. Also, the choice of discrete admissible fields $\mathcal{U}_h$ and $\mathcal{L}_h$ is subject to substantial restrictions and one needs to exercise caution in order to ensure solvability of (4.189).

In the special case of linear elastic response subject to a constraint which is also linear in $\mathbf{u}$ (or $\mathbf{F}$), the matrix form of the extended system becomes

$$\begin{bmatrix}\mathbf{K} & \mathbf{d}\\ \mathbf{d}^T & \mathbf{0}\end{bmatrix}\begin{bmatrix}\hat{\mathbf{u}}\\ \hat{\mathbf{\Lambda}}\end{bmatrix} = -\begin{bmatrix}\mathbf{f}\left(\mathbf{0}\right)\\ \mathbf{g}\left(\mathbf{0}\right)\end{bmatrix}\ , \tag{4.190}$$

where $\mathbf{K}$ and $\mathbf{d}$ are constant matrices. This would be the case for the problem of incompressible linear elasticity.

A corresponding analysis applies to a constrained problem in fluid dynamics.

The treatment of constraints by Lagrange multipliers in continuum mechanics is often motivated by the formalization of constrained non-linear optimization problems of the general form: find the extremum of a functional $G(\mathbf{u})$, subject to constraint condition $\mathbf{c}(\mathbf{u}) = \mathbf{0}$. In solid mechanics, *under severe restrictions*, there exist variational theorems, according to which the equations of motion are derived as extrema of a functional $G(\mathbf{u})$ to zero. For example, in linear elastostatics, one may define the *total potential energy functional* $G(\mathbf{u})$ of a body occupying the region $\mathcal{R}_0$ as

$$G(\mathbf{u}) \;=\; \frac{1}{2}\int_{\mathcal{R}_0} \boldsymbol{\sigma}(\mathbf{u})\cdot\boldsymbol{\varepsilon}(\mathbf{u})\,dV - \int_{\mathcal{R}_0} \mathbf{u}\cdot\rho_0\mathbf{b}\,dV - \int_{\Gamma_{q_0}} \mathbf{u}\cdot\bar{\mathbf{p}}\,dV\ . \tag{4.191}$$

Here $\boldsymbol{\sigma}$ and $\boldsymbol{\varepsilon}$ are the stress and strain of the infinitesimal theory. It is easy to confirm that the equations of motion are recovered by setting $DG(\mathbf{u},\boldsymbol{\xi}) = 0$, where, under mild assumptions, G attains an infimum (which reduces to a minimum for the discrete case) at the solution $\mathbf{u}^*$, that is $G(\mathbf{u}^*) = \inf_{\mathcal{U}} G(\mathbf{u})$, where $\mathcal{U}$ is the space of admissible displacements. A corresponding variational principle may be also established for the problem of finite elastic deformations, see Section 5.2.

In this restricted context, the Lagrange multiplier method of (4.179) and (4.180) can be interpreted as a constrained extremization method. To this end, define the *Lagrange multiplier functional* G_L as

$$G_L(\mathbf{u},\boldsymbol{\Lambda}) \;=\; G(\mathbf{u}) + \int_{\mathcal{C}_0} \boldsymbol{\Lambda}\cdot\mathbf{c}(\mathbf{u})\,dV\ . \tag{4.192}$$

Then, the preceding extended system is recovered by setting

$$DG_L(\mathbf{u},\boldsymbol{\xi};\boldsymbol{\Lambda},\boldsymbol{\theta}) \;=\; 0\ . \tag{4.193}$$

Indeed, this *saddle-point problem* may be equivalently expressed as

$$DG_L(\mathbf{u},\boldsymbol{\xi};\boldsymbol{\Lambda},\boldsymbol{\theta}) \;=\; \underbrace{DG_L(\mathbf{u},\boldsymbol{\xi})}_{\boldsymbol{\Lambda}\text{ fixed}} + \underbrace{DG_L(\boldsymbol{\Lambda},\boldsymbol{\theta})}_{\mathbf{u}\text{ fixed}} \;=\; 0\ , \tag{4.194}$$

which implies that

$$DG_L(\mathbf{u},\boldsymbol{\xi}) \;=\; 0 \quad , \quad DG_L(\boldsymbol{\Lambda},\boldsymbol{\theta}) \;=\; 0\ . \tag{4.195}$$

It is then immediately clear that $(4.195)_{1,2}$ coincide with (4.179) and (4.180). Various approximations of the above Lagrange multiplier method are possible to bypass the need for the direct solution of the extended system of $N + M$ equations. Three such regularizations discussed here are the classical penalty, the perturbed Lagrangian, and the augmented Lagrangian methods

In the *classical penalty method*[10], one considers the functional G_P defined as

$$G_P(\mathbf{u}, \varepsilon) \;=\; G(\mathbf{u}) + \frac{1}{2}\int_{\mathcal{C}_0} \varepsilon \mathbf{c}(\mathbf{u}) \cdot \mathbf{c}(\mathbf{u})\, dV \;, \tag{4.196}$$

The *perturbed Lagrangian method* is associated with the functional G_{PL} given as

$$G_{PL}(\mathbf{u}, \boldsymbol{\Lambda}; \varepsilon) \;=\; G(\mathbf{u}) + \int_{\mathcal{C}_0} \boldsymbol{\Lambda} \cdot \mathbf{c}(\mathbf{u})\, dV \frac{1}{2\varepsilon}\int_{\mathcal{C}_0} \boldsymbol{\Lambda} \cdot \boldsymbol{\Lambda}\, dV \;, \tag{4.197}$$

where, again, $\varepsilon > 0$ is a penalty parameter. Lastly, the *augmented Lagrangian method* is defined in terms of the functional G_{AL} written as

$$G_{AL}(\mathbf{u}, \boldsymbol{\Lambda}; \varepsilon) \;=\; G(\mathbf{u}) + \int_{\mathcal{C}_0} \boldsymbol{\Lambda} \cdot \mathbf{c}(\mathbf{u})\, dV + \frac{1}{2}\int_{\mathcal{C}_0} \varepsilon \mathbf{c}(\mathbf{u}) \cdot \mathbf{c}(\mathbf{u})\, dV \;. \tag{4.198}$$

In all three functionals, $\varepsilon > 0$ is a penalty parameters.

First, examine the classical penalty method and assume that $G(\mathbf{u})$ attains an infimum at the solution $\mathbf{u}^*$ of the equations of motion, such that $\mathbf{c}(\bar{\mathbf{u}}) = \mathbf{0}$. Then, it can be proved conditional upon sufficient smoothness of the involved functions that if $\mathbf{u}^*_\varepsilon$ is such that

$$DG_P\left(\mathbf{u}^*_\varepsilon, \boldsymbol{\xi}\right) \;=\; 0 \tag{4.199}$$

and $G_P(\mathbf{u}, \varepsilon)$ attains an infimum at $\mathbf{u}^*_\varepsilon$, then

$$\lim_{\varepsilon \to \infty} \mathbf{u}^*_\varepsilon \;=\; \mathbf{u}^* \;. \tag{4.200}$$

While the formal proof of this result is omitted here,[11] a simple intuitive argument can be made by observing that as $\varepsilon \to \infty$ the penalty term would become unbounded unless $\mathbf{c}(\mathbf{u}) = 0$, which is necessary to attain an infimum of G_P.

Upon setting the differential of G_P in the direction $\boldsymbol{\xi}$ to zero, one finds that

$$DG(\mathbf{u}, \boldsymbol{\xi}) + \int_{\mathcal{C}_0} \varepsilon \left[D\mathbf{c}(\mathbf{u}, \boldsymbol{\xi})\right] \cdot \mathbf{c}(\mathbf{u})\, dV \;=\; 0 \;. \tag{4.201}$$

[10] See R. Courant, Variational methods for the solution of problems of equilibrium and vibration, *Bulletin of the American Mathematical Society*, 49:1-23, (1943).

[11] See p. 366 in D.G. Luenberger, **Linear and Nonlinear Programming**, 2nd edition, Addison-Wesley, Reading, (1984).

In discrete form, this translates to

$$\hat{\boldsymbol{\xi}}^T \left[\mathbf{f}\left(\hat{\mathbf{u}}\right) + \varepsilon \mathbf{d}\left(\hat{\mathbf{u}}\right) \mathbf{g}\left(\hat{\mathbf{u}}\right)\right] \;=\; 0 \;, \tag{4.202}$$

where use is made of (4.181). A typical step of the Newton-Raphson method would then be

$$\hat{\boldsymbol{\xi}}^T \Big[\mathbf{f}\left(\hat{\mathbf{u}}^{(k)}\right) + \mathbf{K}\left(\hat{\mathbf{u}}^{(k)}\right) \Delta\hat{\mathbf{u}}^{(k)} + \varepsilon \mathbf{d}\left(\hat{\mathbf{u}}^{(k)}\right) \mathbf{g}\left(\hat{\mathbf{u}}^{(k)}\right) + \varepsilon \left\{D^T \mathbf{d}\left(\hat{\mathbf{u}}^{(k)}\right) \mathbf{g}\left(\hat{\mathbf{u}}^{(k)}\right) + \mathbf{d}\left(\hat{\mathbf{u}}^{(k)}\right) D\mathbf{g}\left(\hat{\mathbf{u}}^{(k)}\right)\right\} \Delta\hat{\mathbf{u}}^{(k)}\Big] \;=\; 0 \tag{4.203}$$

or, upon recalling (4.183), it follows that

$$\left[\mathbf{K}\left(\hat{\mathbf{u}}^{(k)}\right) + \varepsilon \left\{D^T \mathbf{d}\left(\hat{\mathbf{u}}^{(k)}\right) + \mathbf{g}\left(\hat{\mathbf{u}}^{(k)}\right) \mathbf{d}\left(\hat{\mathbf{u}}^{(k)}\right) \mathbf{d}^T\left(\hat{\mathbf{u}}^{(k)}\right)\right\}\right] \Delta\hat{\mathbf{u}}^{(k)} \;=\; -\mathbf{f}\left(\hat{\mathbf{u}}^{(k)}\right) - \varepsilon \mathbf{d}\left(\hat{\mathbf{u}}^{(k)}\right) \mathbf{g}\left(\hat{\mathbf{u}}^{(k)}\right) \;. \tag{4.204}$$

Clearly, the classical penalty method requires the solution of only N algebraic equations and $\mathbf{u}^*_\varepsilon$ satisfies the constraint only approximately, see Figure 4.28. The extended stiffness

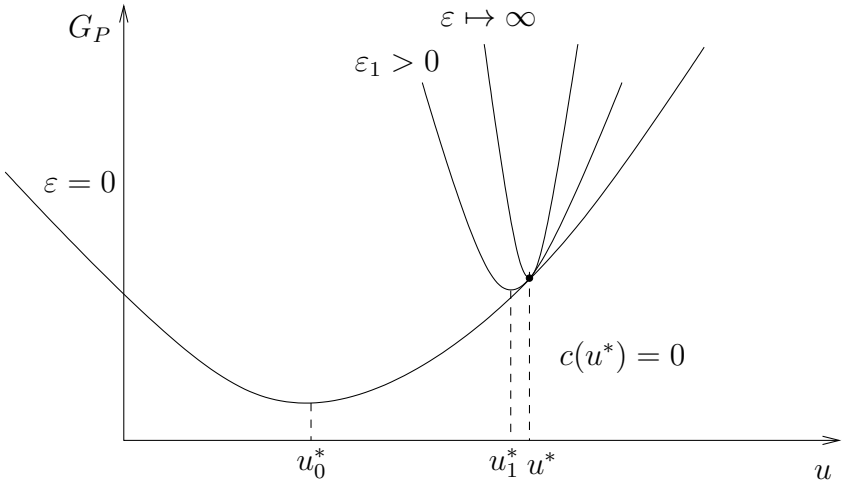

Figure 4.28. *Penalty functional and the enforcement of the constraint* $c = 0$

matrix in (4.204) will be symmetric if $\mathbf{K}$ itself is symmetric. This is immediately concluded from the identity

$$D\left\{D\left[\int \frac{1}{2}\varepsilon \mathbf{c}(\mathbf{u}) \cdot \mathbf{c}(\mathbf{u}) dV\right](\mathbf{u}, \boldsymbol{\xi})\right\}(\mathbf{u}, \Delta\mathbf{u}) \;=\; D\left\{D\left[\int \frac{1}{2}\varepsilon \mathbf{c}(\mathbf{u}) \cdot \mathbf{c}(\mathbf{u}) dV\right](\mathbf{u}, \Delta\mathbf{u})\right\}(\mathbf{u}, \boldsymbol{\xi}) \;, \tag{4.205}$$

as the order of differentiation in the directions $\boldsymbol{\xi}$ and $\Delta\mathbf{u}$ does not matter, conditional upon sufficient smoothness of the integral in $\mathbf{u}$. At the same time, the form of the extended stiffness matrix in (4.204) reveals that ill-conditioning is bound to occur for large values of ε.

Next, consider the perturbed Lagrangian method. Here, extremization of the functional in (4.197) leads to the set of equations

$$DG(\mathbf{u},\boldsymbol{\xi}) + \int_{\mathcal{C}_0} [D\mathbf{c}(\mathbf{u},\boldsymbol{\xi})] \cdot \boldsymbol{\Lambda}\, dV \;=\; 0 \tag{4.206}$$

and

$$\int_{\mathcal{C}_0} \left[\mathbf{c}(\mathbf{u}) - \frac{1}{\varepsilon}\boldsymbol{\Lambda}\right] \cdot \boldsymbol{\theta}\, dV \;=\; 0\ . \tag{4.207}$$

The second of the above equations is strongly satisfied when

$$\boldsymbol{\Lambda} \;=\; \varepsilon \mathbf{c}(\mathbf{u}) \tag{4.208}$$

in $\mathcal{R}_0$, in which case the first equation becomes reduces to the equation (4.201) of the classical penalty method. Alternatively, one may choose to enforce (4.207) weakly, resulting in

$$\hat{\boldsymbol{\theta}}^T \left[\mathbf{g}(\hat{\mathbf{u}}) - \frac{1}{\varepsilon}\hat{\boldsymbol{\Lambda}}\right] \;=\; 0\ , \tag{4.209}$$

which lead to the discrete equations

$$\hat{\boldsymbol{\Lambda}} \;=\; \varepsilon \mathbf{g}(\hat{\mathbf{u}})\ . \tag{4.210}$$

Depending on the interpolation of the multiplier field, it may be possible to efficiently determine $\hat{\boldsymbol{\Lambda}}$ at the element level. In such a case, the perturbed Lagrangian method would be an attractive alternative to the classical penalty method.

Finally, consider the augmented Lagrangian method, which may be thought of as a combination of the Lagrange multiplier and the classical penalty method. Here, the extremization of the functional in (4.198) leads to the equations

$$DG(\mathbf{u},\boldsymbol{\xi}) + \int_{\mathcal{C}_0} [D\mathbf{c}(\mathbf{u},\boldsymbol{\xi})] \cdot \boldsymbol{\Lambda}\, dV + \int_{\mathcal{C}_0} \varepsilon\, [D\mathbf{c}(\mathbf{u},\boldsymbol{\xi})] \cdot \mathbf{c}(\mathbf{u})\, dV \;=\; 0 \tag{4.211}$$

and

$$\int_{\mathcal{C}_0} \mathbf{c}(\mathbf{u},\boldsymbol{\xi}) \cdot \boldsymbol{\theta}\, dV \;=\; 0\ . \tag{4.212}$$

A common algorithmic implementation of the augmented Lagrangian method is the so-called *Uzawa algorithm*[12] as follows:

Algorithm 8: *Uzawa's algorithm for updated Lagrangian methods*

Data: state at time t_n, ε, ζ, *maxits*, *tol*

Set $k = 0$, $\mathbf{\Lambda}_0 = \mathbf{0}$ and $\mathbf{u}_0 = \mathbf{u}_n$;

while $k \leq maxit$ *and* $|\mathbf{c}(\mathbf{u}_k)| \geq tol$

  Solve discrete counterpart of (4.211) for $\Delta\mathbf{u}_k$;

  Set $\mathbf{u}_{k+1} = \mathbf{u}_k + \Delta\mathbf{u}_k$;

  Set $\mathbf{\Lambda}_{k+1} = \mathbf{\Lambda}_k + \zeta\mathbf{c}(\mathbf{u}_k)$;

  Set $k \leftarrow k + 1$

end

The above algorithm can be proven to converge to the desired solution given any ζ, such that $0 < \zeta < 2\varepsilon$, for a class of minimization problems with linear constraints.[13]

The augmented Lagrangian functional with the Uzawa algorithm requires the (repeated) solution of only N equations. However, in contrast to the classical penalty method, ill-conditioning of the tangent stiffness matrix is altogether avoided, since the penalty parameter ε is kept fixed at relatively small. In addition, the constraint equation is satisfied exactly despite the fixed value of the penalty parameter.

While the classical penalty method and its two variants are mathematically justified only for under the severe restriction of the existence of a variational problem for the momentum balance equations, they are used heuristically and with great success on a wide array of problems in computational mechanics.

A critical question in designing a robust finite element approximation of a continuum-mechanical problem in the presence of constraints is the choice of admissible displacement (or velocity) fields and of Lagrange multplier fields. To address this question, one may consider, for simplicity, a linearized counterpart of the extended system (4.189), in the form

$$\begin{bmatrix} \mathbf{K} & \mathbf{d} \\ \mathbf{d}^T & \mathbf{0} \end{bmatrix} \begin{bmatrix} \hat{\mathbf{u}} \\ \hat{\mathbf{\Lambda}} \end{bmatrix} = - \begin{bmatrix} \mathbf{f} \\ \mathbf{g} \end{bmatrix} , \tag{4.213}$$

where now $\mathbf{K}$, $\mathbf{d}$, $\mathbf{f}$, and $\mathbf{g}$ are constant arrays. It can be shown[14] that necessary and sufficient

[12] H. Uzawa, Iterative methods for concave programming. In K.J. Arrow,L. Hurwicz and H. Uzawa editors, **Studies in linear and nonlinear programming**, Stanford University Press, Palo Alto, (1958).

[13] See p. 48 of R. Glowinski and P. Le Tallec, **Augmented Lagrangian and Operator Splitting Methods in Non-linear Mechanics**, SIAM, Philadelphia, 1989.

[14] See Section 3 in F. Brezzi and K.-J. Bathe, A discourse on the stability conditions for mixed finite

conditions for the above system to be solvable are that: (i) $N \geq M$ and (ii) if $\mathbf{v} \in \ker \mathbf{d}$ and $\mathbf{w}^T\mathbf{K}\mathbf{v} = 0$ for all $\mathbf{w} \in \ker \mathbf{d}$, then $\mathbf{v} = \mathbf{0}$. These conditions ensure that the solution to (4.213) exists, but do not guarantee that it will be a convergent solution, say, in the sense of h-refinement. Regardless, condition (i) is an easy one to check when contemplating a dual method for the solution of a constrained problem.

Example 4.5.6: Constraint counts for incompressibility

Consider a square block meshed using $n \times n$ 4-node elements ($n > 1$) and assume that it is used to model an incompressible continuum (solid or fluid). Let the displacements or velocities be fully prescribed on the boundary (except for a single point). In this case, the number of uknowns displacement or velocity degrees of freedom is

$$N \;=\; 2(n-1)^2 - 2 \;. \tag{4.214}$$

Also, assume that the Lagrange multiplier field is piecewise constant in each element and free of specification (except for one point). In this case, the number of uknown Lagrange multiplier degrees of freedom is

$$M \;=\; n^2 - 1 \;. \tag{4.215}$$

Clearly, in this case $N > M$ so the preceding solvability condition (i) is met. Moreover, it is immediately clear from (4.214) and (4.216) that, under uniform h-refinement,

$$\lim_{n\to\infty} \frac{N}{M} \;=\; 2 \;. \tag{4.216}$$

This ratio is considered optimal, as it equals the ratio of linear momentum equations to constraint equations in the continuum problem.

element formulations, *Computer Methods in Applied Mechanics and Engineering*, 82:27–57, (1990).

Chapter 5

Constitutive Modeling of Deformable Continua

5.1 Incompressible Newtonian Viscous Fluid

In this problem, the balance of linear momentum is solved together with the condition of incompressibility, that is,

$$\begin{aligned} \operatorname{div}\mathbf{T} + \rho\mathbf{b} &= \rho\left(\frac{\partial\tilde{\mathbf{v}}}{\partial t} + \frac{\partial\tilde{\mathbf{v}}}{\partial\mathbf{x}}\mathbf{v}\right) \quad \text{in } \mathcal{R} \ , \\ \operatorname{div}\mathbf{v} &= 0 \quad \text{in } \mathcal{R} \ . \end{aligned} \tag{5.1}$$

These equations are subject to the boundary conditions

$$\begin{aligned} v_i &= \bar{v}_i \ \text{ on } \Gamma_{u_i} \\ T_{ij}n_j &= \bar{t}_i \ \text{ on } \Gamma_{q_i} \end{aligned} \tag{5.2}$$

where, $\Gamma_{u_i} \cap \Gamma_{q_i} = \emptyset$, $\Gamma_u = \bigcup_{i=1}^{3} \Gamma_{u_i}$, $\Gamma_q = \bigcup_{i=1}^{3} \Gamma_{q_i}$, and $\partial\mathcal{R} = \overline{\Gamma_u \cup \Gamma_q}$, as well as the initial condition

$$\mathbf{v}(\mathbf{x}, 0) = \mathbf{v}_0(\mathbf{x}) \ , \tag{5.3}$$

where $\operatorname{div}\mathbf{v}_0 = 0$. Note that if $\Gamma_q = \emptyset$, then the boundary velocity $\bar{\mathbf{v}}$ should satisfy

$$\int_{\partial\mathcal{R}} \bar{\mathbf{v}} \cdot \mathbf{n}\, da = \int_{\mathcal{R}} \operatorname{div}\mathbf{v}\, dv = 0 \ . \tag{5.4}$$

The Cauchy stress $\mathbf{T}$ is written as

$$\mathbf{T} = -p\mathbf{i} + 2\mu\mathbf{D} \ , \tag{5.5}$$

where, as argued in Section 4.5, p is the Lagrange multiplier which enforced the incompressibility condition $(5.1)_2$ and μ is the viscosity coefficient (assumed here to be constant). Given the preceding constitutive law, one may write

$$\operatorname{div}\mathbf{T} \;=\; \operatorname{div}(-p\mathbf{i}+2\mu\mathbf{D}) \;=\; -\operatorname{grad}p+2\mu\operatorname{div}\mathbf{D} \;=\; -\operatorname{grad}p+2\mu\operatorname{div}\left(\frac{\partial\tilde{\mathbf{v}}}{\partial\mathbf{x}}\right)^{s} . \tag{5.6}$$

Starting from the weak form of linear momentum balance in (3.184), rewrite the stress-divergence term as

$$\int_{\mathcal{R}}\left(\frac{\partial\tilde{\boldsymbol{\xi}}}{\partial\mathbf{x}}\right)^{s}\cdot\left[-p\mathbf{i}+2\mu\left(\frac{\partial\tilde{\mathbf{v}}}{\partial\mathbf{x}}\right)^{s}\right]dv \;=\; \int_{\mathcal{R}}\left[-p\operatorname{div}\boldsymbol{\xi}+\left(\frac{\partial\tilde{\boldsymbol{\xi}}}{\partial\mathbf{x}}\right)^{s}\cdot 2\mu\left(\frac{\partial\tilde{\mathbf{v}}}{\partial\mathbf{x}}\right)^{s}\right]dv . \tag{5.7}$$

Therefore, the weak form of linear momentum balance (3.184) takes the form

$$\int_{\mathcal{R}}\boldsymbol{\xi}\cdot\rho\left(\frac{\partial\tilde{\mathbf{v}}}{\partial t}+\frac{\partial\tilde{\mathbf{v}}}{\partial\mathbf{x}}\mathbf{v}\right)dv+\int_{\mathcal{R}}\left[-p\operatorname{div}\boldsymbol{\xi}+\left(\frac{\partial\tilde{\boldsymbol{\xi}}}{\partial\mathbf{x}}\right)^{s}\cdot 2\mu\left(\frac{\partial\tilde{\mathbf{v}}}{\partial\mathbf{x}}\right)^{s}\right]dv = \int_{\mathcal{R}}\boldsymbol{\xi}\cdot\rho\mathbf{b}\,dv+\int_{\Gamma_q}\boldsymbol{\xi}\cdot\bar{\mathbf{t}}\,da . \tag{5.8}$$

In addition, the weak form of the incompressibility condition may be expressed as

$$\int_{\mathcal{R}}\sigma(\operatorname{div}\mathbf{v})dv \;=\; 0 . \tag{5.9}$$

Before proceeding with the numerical approximation of the preceding weak forms, recall the *Helmholtz-Hodge decomposition*, according to which any vector field $\mathbf{v}:\mathcal{R}\to\mathcal{E}^3$ can be uniquely decomposed into a solenoidal and an irrotational part, that is,

$$\mathbf{v} \;=\; \mathbf{v}_{so}+\mathbf{v}_{ir} , \tag{5.10}$$

where $\mathbf{v}_{so}$ satisfies

$$\begin{aligned}\operatorname{div}\mathbf{v}_{sol} &= 0 \quad \text{in } \mathcal{R} ,\\ \mathbf{v}_{sol}\cdot\mathbf{n} &= 0 \quad \text{on } \mathcal{R} ,\end{aligned} \tag{5.11}$$

while for $\mathbf{v}_{ir}$ there exists a scalar function $\phi:\mathcal{R}\to\mathbb{R}$, such that

$$\mathbf{v}_{irr} \;=\; \operatorname{grad}\phi , \tag{5.12}$$

hence

$$\operatorname{curl}\mathbf{v}_{irr} \;=\; \operatorname{curl}\operatorname{grad}\phi \;=\; \mathbf{0} . \tag{5.13}$$

A proof of this result can be found elsewhere.[1]

A very efficient and straightforward method for solving the incompressible Navier-Stokes equation using finite elements is based on a classical work in the context of finite differences.[2] In order to appreciate this approach, it is introduced first using the strong forms. To this end, suppose that the velocity and pressure fields have already been determined to be $\mathbf{v}_n$ and p_n, respectively, at time t_n, respectively, and the same fields are to be determined at time $t_{n+1} = t_n + \Delta t_n$. Therefore, it is known that

$$\begin{aligned} \rho\left(\frac{\partial \tilde{\mathbf{v}}_n}{\partial t} + \frac{\partial \tilde{\mathbf{v}}_n}{\partial \mathbf{x}}\mathbf{v}_n\right) &= -\operatorname{grad} p_n + 2\mu \operatorname{div}\left(\frac{\partial \tilde{\mathbf{v}}_n}{\partial \mathbf{x}}\right)^s + \rho \mathbf{b}_n \ , \\ \operatorname{div} \mathbf{v}_n &= 0 \ , \end{aligned} \tag{5.14}$$

everywhere in $\mathcal{R}_n$. To advance the solution in time to t_{n+1}, first determine a predictor velocity $\mathbf{v}^*_{n+1}$, such that

$$\begin{aligned} \rho\left(\frac{\mathbf{v}^*_{n+1} - \mathbf{v}_n}{\Delta t_n} + \frac{\partial \tilde{\mathbf{v}}_n}{\partial \mathbf{x}}\mathbf{v}_n\right) &= 2\mu \operatorname{div}\left(\frac{\partial \tilde{\mathbf{v}}_n}{\partial \mathbf{x}}\right)^s + \rho \mathbf{b}_{n+1} \quad \text{in } \mathcal{R} \ , \\ \mathbf{v}^*_{n+1} &= \bar{\mathbf{v}}_{n+1} \qquad \text{on } \Gamma_u \ , \\ \mathbf{t}^*_{n+1} &= \mathbf{0} \qquad \text{on } \Gamma_q \ . \end{aligned} \tag{5.15}$$

Note that the predictor velocity ignores completely any forces due to change in the pressure, as well as any external tractions. As a result, it does not necessarily satisfy the incompressibility condition. Subsequently, a corrector step is applied to account for the pressure, as

$$\rho \frac{\mathbf{v}_{n+1} - \mathbf{v}^*_{n+1}}{\Delta t_n} = -\operatorname{grad} p_{n+1} \ . \tag{5.16}$$

Note that in the above equation, both $\mathbf{v}_{n+1}$ and p_{n+1} are unknown, so this equation cannot be solved directly. Equation (5.16) may be readily rewritten as

$$\mathbf{v}^*_{n+1} = \mathbf{v}_{n+1} + \frac{\Delta t_n}{\rho} \operatorname{grad} p_{n+1} \ . \tag{5.17}$$

If $\mathbf{v}_{n+1} \cdot \mathbf{n} = 0$ on $\partial\mathcal{R}$, then (5.17) represents precisely the Helmholtz-Hodge decomposition in (5.10–5.13). Hence, in this case, $\mathbf{v}_{n+1}$ and p_{n+1} are obtained by projecting $\mathbf{v}^*_{n+1}$ onto its solenoidal and irrotational parts. Even in the case of more general boundary conditions

[1] See, *e.g.*, Section 6.3.1 in P. Papadopoulos, Introduction to Continuum Mechanics, ME185 course notes, Berkeley, 2017.

[2] A. Chorin. Numerical solution of the Navier-Stokes equations. *Math. Comp.*, 22:745–762, (1968).

for $\mathbf{v}_{n+1}$, one may take the divergence of both sides of (5.17) and observe $(5.1)_2$ to deduce the Laplace equation

$$\operatorname{div} \mathbf{v}^*_{n+1} \;=\; \frac{\Delta t_n}{\rho} \operatorname{div}(\operatorname{grad} p_{n+1}) \quad \text{in } \mathcal{R}_{n+1} \;, \tag{5.18}$$

for p_{n+1}, subject to boundary conditions

$$\begin{aligned} \frac{\Delta t_n}{\rho} \operatorname{grad} p_{n+1} \cdot \mathbf{n} \;&= 0 \quad \text{on } \Gamma_u \;, \\ \left[-p_{n+1}\mathbf{i} + 2\mu \left(\frac{\partial \mathbf{v}_n}{\partial \mathbf{x}} \right)^s \right] \mathbf{n} \;&= \bar{\mathbf{t}}_{n+1} \quad \text{on } \Gamma_q \;. \end{aligned} \tag{5.19}$$

Note that $(5.19)_1$ by taking the normal projection of (5.17) and recalling $(5.15)_2$. Likewise, $(5.19)_2$ is obtained from (1.76) and (5.5), where the rate-of-deformation tensor is evaluated at $\mathbf{v} = \mathbf{v}_n$ (or, possibly, $\mathbf{v} = \mathbf{v}^*_{n+1}$) to avoid an implicit dependence on (the yet unknown) $\mathbf{v}_{n+1}$. It follows that $(5.19)_{1,2}$ are now respectively the Neumann and Dirichlet boundary conditions for the Laplace equation (5.18). After p_{n+1} is calculated from (5.18) and (5.19), the velocity $\mathbf{v}_{n+1}$ is determined from (5.16).

Turning to the Galerkin-based finite element interpretation,[3] this procedure translates to finding the predictor velocity $\mathbf{v}^*_{n+1}$ from

$$\int_{\mathcal{R}} \boldsymbol{\xi}_{n+1} \cdot \rho \left(\frac{\partial \tilde{\mathbf{v}}^*_{n+1}}{\partial t} + \frac{\partial \tilde{\mathbf{v}}_n}{\partial \mathbf{x}} \mathbf{v}_n \right) dv \;=\; \int_{\mathcal{R}} \left[- \left(\frac{\partial \tilde{\boldsymbol{\xi}}_{n+1}}{\partial \mathbf{x}} \right)^s \cdot 2\mu \left(\frac{\partial \tilde{\mathbf{v}}_n}{\partial \mathbf{x}} \right)^s + \boldsymbol{\xi}_{n+1} \cdot \rho \mathbf{b}_{n+1} \right] dv \;, \tag{5.20}$$

where $\frac{\partial \tilde{\mathbf{v}}^*_{n+1}}{\partial t} \doteq \frac{\mathbf{v}^*_{n+1} - \mathbf{v}_n}{\Delta t_n}$, with $\mathbf{v}^*_{n+1} = \bar{\mathbf{v}}_{n+1}$ on Γ_u and $\boldsymbol{\xi}_{n+1} = \mathbf{0}$ on Γ_u. Subsequently, solve the weak counterpart of (5.16) together with the incompressibility constraint $(5.1)_2$. Upon using the divergence theorem for the former, the system of equations may be expressed as

$$\begin{aligned} \int_{\mathcal{R}} \boldsymbol{\xi}_{n+1} \cdot \rho \frac{\mathbf{v}_{n+1} - \mathbf{v}^*_{n+1}}{\Delta t_n} \, dv \;&=\; \int_{\mathcal{R}} \operatorname{div} \boldsymbol{\xi}_{n+1} \cdot p_{n+1} \, dv + \int_{\Gamma_q} \boldsymbol{\xi}_{n+1} \cdot \bar{\mathbf{t}}_{n+1} \, dv \;, \\ \int_{\mathcal{R}} \sigma_{n+1} \operatorname{div} \mathbf{v}_{n+1} \, dv \;&=\; 0 \;, \end{aligned} \tag{5.21}$$

with $\mathbf{v}_{n+1} \cdot \mathbf{n} = \bar{\mathbf{v}}_{n+1} \cdot \mathbf{n}$ and $\boldsymbol{\xi}_{n+1} \cdot \mathbf{n} = 0$ on Γ_u. Note that the tangential component of the velocity does not affect incompressibility.

Neglecting the element representation for brevity, proceed with the global matrix form of this two-step algorithm. The predictor step is expressed as

$$\frac{1}{\Delta t_n} [\mathbf{M}] \left([\hat{\mathbf{v}}^*_{n+1}] - [\hat{\mathbf{v}}_n] \right) + [\mathbf{A}(\hat{\mathbf{v}}_n)] + [\mathbf{K}][\hat{\mathbf{v}}_n] \;=\; [\mathbf{F}^b_{n+1}] \;, \tag{5.22}$$

[3] J. Donea, S. Giuliani, H. Laval, and L. Quartapelle, Finite element solution of the unsteady Navier-Stokes equations by a fractional step method, *Comp. Meth. Appl. Mech. Engrg.*, 30:53–73, (1982).

subject to $[\hat{\mathbf{v}}^*_{n+1}] = [\hat{\bar{\mathbf{v}}}_{n+1}]$ on Γ_u. In (5.22), $[\mathbf{M}]$ is the global mass matrix (symmetric, positive-definite), $[\mathbf{A}(\hat{\mathbf{v}}_n)]$ is the global advection vector (a non-linear function of $\hat{\mathbf{v}}_n$), $[\mathbf{K}]$ is the global diffusion matrix (symmetric, positive-semidefinite), and $[\mathbf{F}^b_{n+1}]$ is the global external force due to prescribed body forces only. This system is now solved for $[\mathbf{v}^*_{n+1}]$. The solution becomes trivially simple to compute if $[\mathbf{M}]$ is rendered diagonal, as earlier. Either way, one may write

$$[\hat{\mathbf{v}}^*_{n+1}] = [\hat{\mathbf{v}}_n] - \Delta t_n [\mathbf{M}]^{-1} \left([\mathbf{A}(\hat{\mathbf{v}}_n)] + [\mathbf{K}][\mathbf{v}_n] \right) + \Delta t_n [\mathbf{M}]^{-1} [\mathbf{F}^b_{n+1}] \ . \tag{5.23}$$

For the corrector step, write the matrix counterpart of (5.21) as

$$\begin{aligned} \frac{1}{\Delta t_n} [\mathbf{M}] \left([\hat{\mathbf{v}}_{n+1}] - [\hat{\mathbf{v}}^*_{n+1}] \right) - [\mathbf{C}][\hat{\mathbf{p}}_{n+1}] &= [\mathbf{F}^t_{n+1}] \ , \\ [\mathbf{C}]^T [\hat{\mathbf{v}}_{n+1}] &= [\mathbf{G}_{n+1}] \ , \end{aligned} \tag{5.24}$$

where $[\mathbf{C}]$ is the matrix emanating from the divergence operator and $[\mathbf{F}^t_{n+1}]$ is the external force vector due to prescribed tractions only. Note that the right-hand side of $(5.24)_2$ becomes non-zero upon accounting for boundary conditions because it needs to account for the discrete counterpart of the boundary condition $\mathbf{v}_{n+1} \cdot \mathbf{n} = \bar{\mathbf{v}}_{n+1} \cdot \mathbf{n}$ on Γ_u.

The pressure $[\hat{\mathbf{p}}_{n+1}]$ may be determined from the system (5.24) as

$$[\mathbf{C}]^T [\mathbf{M}]^{-1} [\mathbf{C}][\hat{\mathbf{p}}_{n+1}] = \frac{1}{\Delta t_n} \left([\mathbf{G}_{n+1}] - [\mathbf{C}]^T [\hat{\mathbf{v}}^*_{n+1}] \right) - [\mathbf{C}]^T [\mathbf{M}]^{-1} [\mathbf{F}^t_{n+1}] \ , \tag{5.25}$$

where $[\mathbf{C}]^T [\mathbf{M}]^{-1} [\mathbf{C}]$ is symmetric and under sufficiently general conditions has the rank of $[\hat{\mathbf{p}}_{n+1}]$. Lastly, the velocity $[\hat{\mathbf{v}}_{n+1}]$ is determined as

$$[\hat{\mathbf{v}}_{n+1}] = [\hat{\mathbf{v}}^*_{n+1}] + \Delta t_n [\mathbf{M}]^{-1} \left([\mathbf{F}^t_{n+1}] + [\mathbf{C}][\hat{\mathbf{p}}_{n+1}] \right) \ . \tag{5.26}$$

Therefore, obtaining the new state vectors $[\hat{\mathbf{v}}_{n+1}]$ and $[\hat{\mathbf{p}}_{n+1}]$ requires the solution of a symmetric linear algebraic system for $[\hat{\mathbf{p}}_{n+1}]$ and performing two updates for $[\hat{\mathbf{v}}^*_{n+1}]$ and $[\hat{\mathbf{v}}_{n+1}]$.

5.2 Nonlinear Elasticity

Recall the mechanical energy balance equation (1.80), and admit the existence of a strain energy function $\hat{\psi}(\mathbf{F})$ per unit mass, such that

$$\int_{\mathcal{P}} \mathbf{T} \cdot \mathbf{D} \, dv = \int_{\mathcal{P}} \rho \dot{\psi} \, dv \ . \tag{5.27}$$

Recalling the result on work-conjugacy of stress and strain or deformation measures, one may also write

$$\int_{\mathcal{P}} \rho\dot{\psi}\, dv \;=\; \int_{\mathcal{P}_0} \rho_0\dot{\psi}\, dV \;=\; \int_{\mathcal{P}_0} \mathbf{P}\cdot\dot{\mathbf{F}}\, dV \;=\; \int_{\mathcal{P}_0} \mathbf{S}\cdot\dot{\mathbf{E}}\, dV \;. \tag{5.28}$$

It follows from (5.28) that

$$\int_{\mathcal{P}_0} \left(\rho_0\frac{\partial\hat{\psi}}{\partial\mathbf{F}} - \mathbf{P}\right)\cdot\dot{\mathbf{F}}\, dV \;=\; 0\;, \tag{5.29}$$

so that, using a standard argument,

$$\mathbf{P} \;=\; \rho_0\frac{\partial\hat{\psi}}{\partial\mathbf{F}}\;. \tag{5.30}$$

This constitutive law characterizes a general homogeneous *hyperelastic* (or *Green-elastic*) material.

The strain energy function is subject to invariance requirements under superposed rigid-body motions, namely

$$\psi \;=\; \hat{\psi}\,(\mathbf{F}) \;=\; \hat{\psi}\left(\mathbf{F}^{+}\right) \;=\; \hat{\psi}\,(\mathbf{QF})\;, \tag{5.31}$$

for all proper orthogonal $\mathbf{Q}$. It can be easily argued that this implies

$$\psi \;=\; \hat{\psi}\,(\mathbf{F}) \;=\; \hat{\psi}\,(\mathbf{U}) \;=\; \bar{\psi}\,(\mathbf{C}) \;=\; \tilde{\psi}\,(\mathbf{E})\;. \tag{5.32}$$

Therefore, one may conclude from $(5.28)_{2,4}$ that

$$\int_{\mathcal{P}_0} \left(2\rho_0\frac{\partial\bar{\psi}}{\partial\mathbf{C}} - \mathbf{S}\right)\cdot\dot{\mathbf{E}}\, dV \;=\; 0\;, \tag{5.33}$$

therefore,

$$\mathbf{S} \;=\; 2\rho_0\frac{\partial\bar{\psi}}{\partial\mathbf{C}} \;=\; \rho_0\frac{\partial\bar{\psi}}{\partial\mathbf{E}}\;. \tag{5.34}$$

If the stress response of the hyperelastic material is further assumed isotropic, then, given any orthogonal tensor $\mathbf{Q}$,

$$\psi \;=\; \hat{\psi}\,(\mathbf{F}) \;=\; \hat{\psi}\,(\mathbf{FQ}) \;=\; \bar{\psi}\,(\mathbf{C}) \;=\; \bar{\psi}\left(\mathbf{Q}^T\mathbf{CQ}\right)\;. \tag{5.35}$$

Recalling the standard representation theorem for isotropic scalar functions of a tensor variable, one may conclude that

$$\psi \;=\; \check{\psi}\,(I_{\mathbf{C}}, II_{\mathbf{C}}, III_{\mathbf{C}}) \tag{5.36}$$

where $I_{\mathbf{C}}$,$II_{\mathbf{C}}$, $III_{\mathbf{C}}$ are the three scalar invariants of $\mathbf{C}$. In view of $(5.34)_1$ and (5.36), one may conclude, with the aid of the chain rule, that

$$\mathbf{S} \;=\; 2\rho_0 \left[\frac{\partial \check{\psi}}{\partial I_{\mathbf{C}}} \frac{\partial I_{\mathbf{C}}}{\partial \mathbf{C}} + \frac{\partial \check{\psi}}{\partial II_{\mathbf{C}}} \frac{\partial II_{\mathbf{C}}}{\partial \mathbf{C}} + \frac{\partial \check{\psi}}{\partial III_{\mathbf{C}}} \frac{\partial III_{\mathbf{C}}}{\partial \mathbf{C}} \right] \,. \tag{5.37}$$

The identities

$$\begin{aligned} \frac{\partial I_{\mathbf{C}}}{\partial \mathbf{C}} \;&=\; \frac{\partial}{\partial \mathbf{C}} \left(\operatorname{tr} \mathbf{C} \right) \;=\; \mathbf{I} \,, \\ \frac{\partial II_{\mathbf{C}}}{\partial \mathbf{C}} \;&=\; \frac{\partial}{\partial \mathbf{C}} \left[\frac{1}{2} \left\{ (\operatorname{tr} \mathbf{C})^2 - \operatorname{tr} \mathbf{C}^2 \right\} \right] \;=\; I_{\mathbf{C}} \mathbf{I} - \mathbf{C} \,, \\ \frac{\partial III_{\mathbf{C}}}{\partial \mathbf{C}} \;&=\; III_{\mathbf{C}} \mathbf{C}^{-1} \,, \end{aligned} \tag{5.38}$$

can be shown to hold. Indeed, the first two may be confirmed by direct calculation, while the third one follows immediately from (2.55). In view of (5.38), the constitutive equation (5.37) takes the form

$$\mathbf{S} \;=\; 2\rho_0 \left[\left(\frac{\partial \check{\psi}}{\partial I_{\mathbf{C}}} + I_{\mathbf{C}} \frac{\partial \check{\psi}}{\partial II_{\mathbf{C}}} \right) \mathbf{I} - \frac{\partial \check{\psi}}{\partial II_{\mathbf{C}}} \mathbf{C} + \frac{\partial \check{\psi}}{\partial III_{\mathbf{C}}} III_{\mathbf{C}} \mathbf{C}^{-1} \right] \,. \tag{5.39}$$

Example 5.2.1: Kirchhoff-Saint Venant material
In this model, the classical stress-strain law of elasticity at infinitesimal strains is written in terms of the second Piola-Kirchhoff stress and the Lagrangian strain, that is,

$$\mathbf{S} \;=\; 2\mu \mathbf{E} + \lambda (\operatorname{tr} \mathbf{E}) \mathbf{I} \,, \tag{5.40}$$

where λ and μ are material constants. This is the *Kirchhoff-Saint Venant* (or *generalized Hookean*) law. The preceding law can be expressed equivalently as

$$\mathbf{S} \;=\; \mu (\mathbf{C} - \mathbf{I}) + \lambda \frac{1}{2} (I_{\mathbf{C}} - 3) \mathbf{I} \;=\; \left[\frac{1}{2} \lambda (I_{\mathbf{C}} - 3) - \mu \right] \mathbf{I} + \mu \mathbf{C} \,. \tag{5.41}$$

This constitutive law is derivable from a strain-energy function defined as

$$\rho_0 \check{\psi} (I_{\mathbf{C}}, II_{\mathbf{C}}, III_{\mathbf{C}}) \;=\; \frac{1}{8} \lambda (I_{\mathbf{C}} - 3)^2 + \; frac14 \mu \left(I_{\mathbf{C}}^2 - 2 I_{\mathbf{C}} - 2 II_{\mathbf{C}} \right) \,. \tag{5.42}$$

Recalling (1.86), it follows from (5.41) and (1.14) that

$$\mathbf{T} \;=\; \frac{1}{J} \left[\frac{1}{2} \lambda (I_{\mathbf{B}} - 3) - \mu \right] \mathbf{B} + \frac{1}{J} \mu \mathbf{B}^2 \,. \tag{5.43}$$

Clearly, the Kirchhoff-Saint Venant law reduces to the constitutive equations of isotropic linear elasticity for infinitesimal deformations.

The Kirchhoff-Saint Venant material law is used to describe materials that undergo a moderate amount of elastic deformation.

Example 5.2.2: Compressible neo-Hookean material
Here, the strain energy takes the form

$$\rho_0\check{\psi}(I_{\mathbf{C}}, II_{\mathbf{C}}, III_{\mathbf{C}}) \;=\; \frac{\mu}{2}(I_{\mathbf{C}}-3) - \mu\ln J + \frac{\lambda}{2}(J-1)^2 \;, \tag{5.44}$$

where λ and μ are material parameters. Taking into account (5.39) that

$$\mathbf{S} \;=\; \mu(\mathbf{I}-\mathbf{C}^{-1}) + \lambda J(J-1)\mathbf{C}^{-1} \;. \tag{5.45}$$

Pushing the preceding equation forward to the current configuration, it follows that

$$\mathbf{T} \;=\; \frac{1}{J}\mu(\mathbf{B}-\mathbf{i}) + \lambda(J-1)\mathbf{i} \;. \tag{5.46}$$

This constitutive law is consistent with linearized isotropic elasticity. Indeed, recalling (2.54) and (2.64), it can be shown that

$$\begin{aligned}\mathcal{L}\,[\mathbf{T};\mathbf{u}]_{\mathbf{X}} \;&=\; \boldsymbol{\sigma} \\ &=\; \mu D\mathbf{B}(\mathbf{X},\mathbf{u}) + \lambda DJ(\mathbf{X},\mathbf{u})\mathbf{I} \;=\; 2\mu\boldsymbol{\varepsilon} + \lambda(\operatorname{tr}\boldsymbol{\varepsilon})\mathbf{I} \;,\end{aligned} \tag{5.47}$$

as expected.

The compressible neo-Hookean material law is used to describe materials that may undergo large elastic deformations, such as rubber.

Under quasi-static conditions and under mild assumptions on the strain energy function Ψ, there exists a variational theorem for nonlinear elasticity, according to which the total potential functional $G(\mathbf{u})$, defined as

$$G(\mathbf{u}) \;=\; \int_{\mathcal{R}_0}\rho_0\Psi\,dV - \int_{\mathcal{R}_0}\mathbf{u}\cdot\rho_0\mathbf{b}\,dV - \int_{\Gamma_{q,0}}\mathbf{u}\cdot\bar{\mathbf{p}}\,dA \;, \tag{5.48}$$

attains a local minimum at $\mathbf{u}$ which satisfies equilibrium.[4]

Many nonlinearly elastic materials, such as dense rubber, are incompressible or nearly incompressible. Here, write the constraint of incompressibility as

$$c(\mathbf{F}) \;=\; \det\mathbf{F} - 1 \;=\; 0 \;. \tag{5.49}$$

To impose incompressibility, it is important to recognize that it is an internal constraint that affects the form of the strain energy function. In particular, in view of the discussion in Section 4.5, write the strain energy functional Ψ_c of the incompressible elastic material as

$$\rho_0\hat{\Psi}_c(\mathbf{F},p) \;=\; \rho_0\hat{\Psi}(\mathbf{F}) + pc(\mathbf{F}) \;, \tag{5.50}$$

[4]See Chapter 11 in M.E. Gurtin, Topics in Finite Elasticity, SIAM, Philadelphia, 1981.

where p is a Lagrange multplier, and proceed as usual to defining the stress starting with the definition

$$\int_{\mathcal{P}_0} \rho_0 \dot{\Psi}_c \, dV \;=\; \int_{\mathcal{P}_0} \mathbf{P} \cdot \dot{\mathbf{F}} \, dV \;. \tag{5.51}$$

Recalling that $c = 0$, this implies that

$$\int_{\mathcal{P}_0} \left[\rho_0 \left(\frac{\partial \Psi}{\partial \mathbf{F}} + \frac{p}{\rho_0} \frac{\partial c}{\partial \mathbf{F}} \right) - \mathbf{P} \right] \cdot \dot{\mathbf{F}} \, dV \;=\; 0 \;, \tag{5.52}$$

hence, in view of (2.55),

$$\mathbf{P} \;=\; \rho_0 \frac{\partial \hat{\Psi}}{\partial \mathbf{F}} + pJ\mathbf{F}^{-T} \;. \tag{5.53}$$

Taking into account (1.86) and (5.53), it follows that

$$\mathbf{S} \;=\; \rho_0 \mathbf{F}^{-1} \frac{\partial \hat{\Psi}}{\partial \mathbf{F}} + pJ\mathbf{C}^{-1} \tag{5.54}$$

and

$$\mathbf{T} \;=\; \rho \frac{\partial \hat{\Psi}}{\partial \mathbf{F}} \mathbf{F}^T + p\mathbf{i} \;. \tag{5.55}$$

The last equation demonstrates that the Lagrange multiplier is a pressure term on the Cauchy stress.

Example 5.2.3: Compressible neo-Hookean material

Start with the strain energy function of the compressible neo-Hookean model in (5.44) and assume incompressibility, which reduces the function to

$$\rho_0 \psi \;=\; \frac{\mu}{2} (I_{\mathbf{C}} - 3) \;. \tag{5.56}$$

Taking into account (5.53-5.55), one may write

$$\mathbf{P} \;=\; \frac{\mu}{2} \frac{\partial}{\partial \mathbf{F}} \left\{ \mathrm{tr} \left(\mathbf{F}^T \mathbf{F} \right) \right\} + pJ\mathbf{F}^{-T} \;=\; \mu \mathbf{F} + p\mathbf{F}^{-T} \;, \tag{5.57}$$

$$\mathbf{S} \;=\; \mathbf{F}^{-1}\mathbf{P} \;=\; \mu \mathbf{I} + p\mathbf{C}^{-1} \;, \tag{5.58}$$

and

$$\mathbf{T} \;=\; \mu \mathbf{B} + p\mathbf{i} \;, \tag{5.59}$$

subject to $c = 0$. Alternatively, one may start with the stress relations (5.45) and (5.46), and append the pressure term. For instance, for the Cauchy stress, one would deduce the expression

$$\mathbf{T} \;=\; \mu(\mathbf{B} - \mathbf{i}) + p\mathbf{i} \;=\; \mu \mathbf{B} + (p - \mu)\mathbf{i} \;, \tag{5.60}$$

which suggests that the same meaning of the pressure as in (5.59) to within a constant μ.

In the nearly incompressible case, one would use the original stain-energy function of (5.44), but view λ as a penalty parameter by letting it grow toward infinity to satisfy the constraint of incompressibility in approximate fashion.

From the standpoint of finite element implementation, it is important to observe that the material stiffness of the hyperelastic material model is symmetric. Indeed, starting from the term which is associated with the stress-divergence in linear momentum balance, recall that

$$D\left[\int_{\Omega_0^e} \frac{\partial \boldsymbol{\xi}}{\partial \mathbf{X}} \cdot (\mathbf{F}\mathbf{S})\, dV\right](\mathbf{u}, \Delta\mathbf{u}) \;=\; \underbrace{\int_{\Omega_0^e} \left(\frac{\partial \Delta\mathbf{u}}{\partial \mathbf{X}}\right)^T \frac{\partial \boldsymbol{\xi}}{\partial \mathbf{X}} \cdot \mathbf{S}\, dV}_{\text{geometric term}} + \underbrace{\int_{\Omega_0^e} \frac{\partial \boldsymbol{\xi}}{\partial \mathbf{X}} \cdot \mathbf{F} D\mathbf{S}(\mathbf{u}, \Delta\mathbf{u})\, dV}_{\text{material term}} \,. \tag{5.61}$$

As already argued in Section 4.3, the geometric term yields a symmetric stiffness provided $\boldsymbol{\xi}$ and $\Delta\mathbf{u}$ are interpolated by the same functions. For a hyperelastic solid, the material term also yields a symmetric stiffness. This is because, according to (5.34),

$$\frac{\partial \mathbf{S}}{\partial \mathbf{E}} \;=\; \rho_0 \frac{\partial^2 \tilde{\Psi}}{\partial \mathbf{E}^2} \tag{5.62}$$

hence, it is symmetric. Therefore, in light of (2.41),

$$\begin{aligned} \int_{\Omega_0^e} \frac{\partial \boldsymbol{\xi}}{\partial \mathbf{X}} \cdot \mathbf{F} D\mathbf{S}(\mathbf{u}, \Delta\mathbf{u})\, dV \;&=\; \int_{\Omega_0^e} \mathbf{F}^T \frac{\partial \boldsymbol{\xi}}{\partial \mathbf{X}} \cdot D\mathbf{S}(\mathbf{u}, \Delta\mathbf{u})\, dV \;= \\ &\int_{\Omega_0^e} \frac{1}{2}\left[\mathbf{F}^T \frac{\partial \boldsymbol{\xi}}{\partial \mathbf{X}} + \left(\frac{\partial \boldsymbol{\xi}}{\partial \mathbf{X}}\right)^T \mathbf{F}\right] \cdot \frac{\partial \mathbf{S}}{\partial \mathbf{E}} D\mathbf{E}(\mathbf{u}, \Delta\mathbf{u})\, dV \;= \\ &\int_{\Omega_0^e} \frac{1}{4}\left[\mathbf{F}^T \frac{\partial \boldsymbol{\xi}}{\partial \mathbf{X}} + \left(\frac{\partial \boldsymbol{\xi}}{\partial \mathbf{X}}\right)^T \mathbf{F}\right] \cdot \frac{\partial \mathbf{S}}{\partial \mathbf{E}} \left[\mathbf{F}^T \frac{\partial \Delta\mathbf{u}}{\partial \mathbf{X}} + \left(\frac{\partial \Delta\mathbf{u}}{\partial \mathbf{X}}\right)^T \mathbf{F}\right] dV \,, \end{aligned} \tag{5.63}$$

which proves the symmetry.

Index